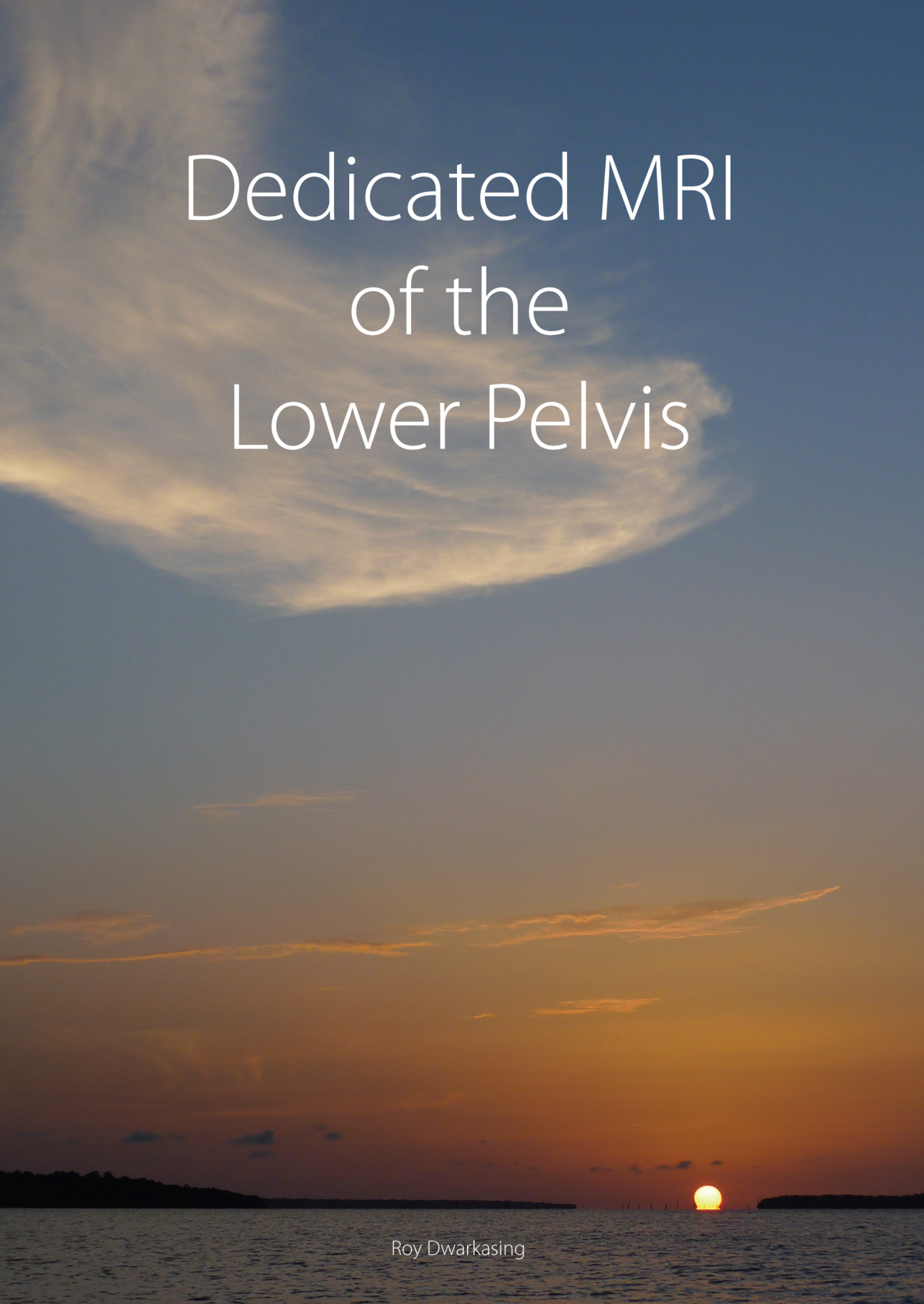

Dedicated MRI of the Lower Pelvis

Roy Dwarkasing

Dedicated MRI of the Lower Pelvis

MRI bij aandoeningen van het kleine bekken
en bekken bodem regio

Roy Soendersing Dwarkasing

Cover design: Ton Everaers
Cover photo: Roy Dwarkasing. View Suriname river, Paramaribo
Thesis layout: Ton Everaers
Printing: Print Partners Ipskamp

ISBN:

Dedicated MRI of the Lower Pelvis

MRI bij aandoeningen van het kleine bekken
en bekken bodem regio

Proefschrift

ter verkrijging van de graad van doctor aan de
Erasmus Universiteit Rotterdam
op gezag van de
rector magnificus

Prof.dr. H.A.P. Pols

en volgens besluit van het College voor Promoties.

De openbare verdediging zal plaatsvinden op
woensdag 17 februari 2016 om 13.30 uur

door

Roy Soendersing Dwarkasing

geboren te Paramaribo, Suriname

Erasmus University Rotterdam

Erasmus

PROMOTIECOMMISSIE

Promotor:	Prof.dr. G. P. Krestin
Overige leden:	Prof.dr. C.H. Bangma Prof.dr. C. Verhoef Prof.dr. J. Stoker
Copromotor:	Dr. R.W. Schouten

Erasmus University Rotterdam

For my boys: Timothy, Martijn & Pascal.

You make life a very busy place (far more than this thesis), but mostly enjoyable.

CONTENTS

MANUSCRIPTS BASED ON THIS THESIS

CHAPTER 2

Dwarkasing RS, Herman Flick, Krestin GP.
Endoluminal Receiver Coil for Intravaginal and Endoanal Application on 1.5 and 3.0 T. MRI Systems; Design, Technical Aspects and Clinical Value.
Submitted.

CHAPTER 3

Chapter 3.1

Dwarkasing RS, Hussain SM, Krestin GP. Magnetic Resonance Imaging of Perianal Fistulas. Seminars in Ultrasound CT and MR. 2005 Aug;26(4):247-58. Review

Chapter 3.2

Dwarkasing RS, Hussain SM, Hop WC, Krestin GP. Anovaginal Fistulas: Evaluation with Endoanal MR Imaging. Radiology. 2004 Apr;231(1):123-8.

Chapter 3.3

Mitalas LE, **Dwarkasing RS**, Verhaaren R, Zimmerman DD, Schouten WR. Is the Outcome of Transanal Advancement Flap Repair Affected by the Complexity of High Transsphincteric Fistulas? Diseases of the Colon & Rectum. 2011 Jul;54(7):857-62.

Chapter 3.4

Dwarkasing RS, Schouten WR, Geeraedts TE, Mitalas LE, Hop WC, Krestin GP. Chronic Anal and Perianal Pain Resolved with MRI. American Journal of Roentgenology. 2013 May;200(5):1034-41.

CHAPTER 4

Chapter 4.1

Dwarkasing RS, Verschuuren SI, Leenders GJ, Thomeer MG, Dohle GR, Krestin GP. Chronic Lower Urinary Tract Symptoms in Women: Classification of Abnormalities and Value of Dedicated MRI for Diagnosis. American Journal of Roentgenology. 2014 Jan;202(1):W59-66.

Chapter 4.2

Dwarkasing RS, Dinkelaar W, Hop WC, Steensma AB, Dohle GR, Krestin GP. MRI Evaluation of Urethral Diverticula and Differential Diagnosis in Symptomatic Women. American Journal of Roentgenology. 2011 Sep;197(3):676-82.

CHAPTER 5

Chapter 5.1

Dwarkasing RS, Ruben van Waardhuizen, Wijnand J. Alberda, Michael Doukas, Maria A.J. de Ridder, Joost J.M.E. Nuyttens, Cornelis Verhoef, François E. J. A. Willemssen
Value of MRI for Diagnosis and Local Staging of Recurrent Rectal Cancer: Correlation with Surgery and Histopathology of Resected Specimen.
Submitted.

Chapter 5.2

Dwarkasing RS, Verschuuren SI, Leenders GJ, Krestin GP, Schouten WR.
Primary Cystic Lesions of the Retrorectal Space: MRI evaluation, Histopathology Confirmation and Clinical assessment.
Submitted.

chapter 1

General Introduction

In the past decades MRI of the pelvis and pelvic floor has gained a lot of attention and development. For benign conditions and diseases dedicated MRI has demonstrated value for diagnosis and guiding appropriate treatment (1-5). In oncology multiparametric MRI has been the established method for detection and local staging of rectal cancer, prostate cancer and cervical cancer (6-9). It is of paramount importance to adapt imaging technique and MRI protocols to the clinical indication for imaging. Advances in medical technology and clinical insight enables to apply dedicated imaging tailored to the specific clinical problem. This leads not only to gain in diagnostic accuracy but has become an integral part of patient management. Our center, a tertiary referral center for diseases in both, the ventral and dorsal compartments of the pelvis, including the pelvic floor, has extensive experience with the application of pelvic phased array multicoils and endoluminal surface coils for the preoperative evaluation of perianal and female urethral and periurethral diseases. The endoluminal coils are of a rigid design and can be used repeatedly. They are custom built in collaboration with our technical staff and are regularly upgraded technically.

The purpose of this thesis was to investigate the value of dedicated MRI of the pelvis and pelvic floor in clinical patients referred to the radiology department with diseases in this anatomic region.

ENDOLUMINAL COIL VERSUS PELVIC PHASED ARRAY IMAGING

The value of endoluminal receiver coils for application in the pelvic area has been established with proven clinical value especially for perianal fistula imaging and prostate imaging. Recent studies have demonstrated valuable clinical potential for endovaginal application with visualization of urethral and periurethral pathology in woman. Our center, a tertiary referral center for diseases of the pelvis and pelvic floor, has solid experience with the use of rigid endoluminal receiver coils for endoanal, and endovaginal application on 1.5 T and 3.0 T MRI systems. With endoluminal MRI we aim to aquire accurate morphologic images. The endoluminal coil has been technically improved with the dualloop design with an increase in SNR and spatial resolution over the previous generation single loop coils. The dual loop endoluminal receiver coil may allow for better diagnosis through improved spatial resolution without increase in imaging time compared with the single loop coil. Practically, there are 2 main types of endocavitary receiver coils for use in the pelvic region: the inflatable and rigid design. The inflatable design has been more widely used especially for endorectal application with focus on prostate imaging. An adapted version has been used for intravaginal application. This inflatable version is of a disposable design with 1 coil application per examination. The rigid endocavitary coil has been initially designed for endoanal application. The same coil has also been used for endovaginal placement with satisfactory results (3, 5). This rigid type is reusable and provides unequaled image quality and conspicuity of numerous diseases of the ano-vaginal region and pelvic floor. Previous studies found the endoluminal coil to be superior to the phased array coil for demonstration of anal sphincter anatomy and perianal fistula disease (10, 11). Endoanal MRI is especially valuable for classification of the primary tract and identification of the internal ostium in cryptoglandular fistula's (11-14). Because of the limited field of view, the phased array was especially superior for demonstration of distant fistula extensions (15, 16).

Endoanal MRI is highly accurate in demonstrating lesions of the sphincter complex (17-19). Sphincter damage is especially seen in patients with chronic fistula and previous surgery and is important for surgical planning. For prostate cancer imaging, studies have shown superior image quality and improved reader confidence using an ERC in staging performance for prostate cancer at 3T when compared with pelvic phased array coil at 3T (20, 21). For female urethral diverticula, endoluminal coil demonstrated better subjective image quality with endovaginal placement when compared with endoanal placement or phased array coil imaging (3). All these studies were based on imaging with the single loop coil design. In addition, vaginal endoluminal coil imaging proved valuable for diagnosis and preoperative assessment of periurethral disease (5).

PERIANAL FISTULA DISEASE

Fistula-in-ano is an abnormal communication between the anal canal and the perianal skin. Perianal abscess is an acute manifestation of fistula-in-ano. (22). In the surgical literature, cryptoglandular fistulas and abscesses are distinguished from fistulas and abscesses due to an underlying disease such as Crohn's disease (14, 23). Fistulas resulting from an underlying disease are termed specific. Most cases of fistula-in-ano are nonspecific and result from inflammation of anal glands and crypts (cryptoglandular) (14, 24). The prevalence of this type of fistula is said to be approximately 10 per 100,000 of the general population. Perianal fistulas and abscesses are often diagnosed clinically, based on typical symptomatology and physical examination. The exact relationship between the fistula and the anorectum, in particular the anal sphincter complex, is often not evident at physical examination. The classification of cryptoglandular fistulas depends on the degree of involvement of the anal sphincter complex and determines the type of surgical treatment. MR imaging has become the standard imaging technique for demonstration and classification of perianal fistulas and abscesses (14). This modality provides multiplanar images with high inherent contrast resolution and high spatial resolution of the anal canal, rectum, rectovaginal septum, and vagina (1-5). At MR imaging, the identification and localization of the entire fistula, including the external opening, the primary tract, secondary tracts, abscesses, and the internal opening, are essential for fistula classification and treatment. Fistulas with unrecognized components may cause problems during surgery and are more likely to recur (14, 25, 26). Studies have shown that preoperative MR imaging revealed important additional information compared with surgery alone and better predicts clinical outcome of patients with fistula-in ano than initial surgical exploration (6, 27).

Anovaginal fistula is considered a special type of perianal fistula with typical symptoms of recurrent vaginal infections with vaginal flatus and vaginal defecation and can clearly be depicted with MR imaging using an endoanal coil (1). At our institution, endoanal MR imaging is routinely performed in the assessment of perianal fistulas, including anovaginal fistula. In particular, T2weighted MR imaging sequences can demonstrate fistulas and abscesses, as high signal intensity lesions.

The treatment of these fistulas is mainly surgical, with a number of options. For low transsphincteric andintersphincteric fistulas fistulotomy is the treatment of choice.

Transanal advancement flap repair has been advocated as the treatment of choice for transsphincteric fistulas passing through the upper and middle third of the external anal sphinc-

ter. This procedure enables healing of the fistula in 2 out of 3 patients without consequent sphincter damage.

CHRONIC ANAL PAIN

Chronic anal and perianal pain (CAP) is a common problem in the gastroenterological practice (28, 29). CAP is defined as recurrent or persistent pain in the anal canal, usually deep and severe, with a variable radiation and of more than 3 months duration (29). CAP is thought to be present as a major symptom in up to 6% of U.S. citizens (28). Patients generally present with a combination of symptoms, including pain, soiling, loss of blood or pus from the anus, faecal incontinence or a palpable mass in and around the anus. A combination of symptoms may lead to clinically suspected disease and a clinical examination will assess local anal pathology including complicated hemorrhoids, hypertrophied anal papillas, anal fissure and perianal suppurative conditions. When the only presentation is pain in the anal region and no local pathology is found at initial clinical evaluation, the clinician is faced with a major challenge. It has been speculated that patients without a clinically confirmed physical explanation may have an underlying functional disorder or that CAP may result from a significant psychological overlay (19, 20). The aim of further investigations, including imaging, must be to identify causes of pain not initially detected at clinical evaluation. Only few ultrasoundbased studies were published in a patient cohort with CAP (30).

MRI IN CHRONIC LOWER URINARY TRACT SYMPTOMS IN WOMEN

Chronic lower urinary tract symptoms are common in women. Lower urinary tract symptoms are a group of symptoms with abnormalities that may be categorized into seven groups: storage problems, voiding problems, postmicturition symptoms, symptoms associated with sexual intercourse or pelvic organ prolapse, lower urinary tract pain, and lower urinary tract dysfunction syndrome (31). New insights suggest that lower urinary tract symptoms are a non-organ-specific group of symptoms, which are sometimes age related and progressive, affecting up to 26% of women 40 years and older (32, 33). The presentation of symptoms can be diverse and the differential diagnoses extensive. It is of importance to differentiate morphologic abnormalities from dysfunctional conditions that are responsible for a patient's complaints. Dedicated MRI and urodynamic studies are important tools in this respect (3). With its excellent soft-tissue contrast and multiplanar acquisition, MRI has become the imaging modality of choice for diagnosis and preoperative evaluation in female patients with urethral and periurethral disease. Previously, pelvic phasedarray coils were applied for female pelvic imaging, including imaging of the urethra and periurethral region. Subsequently, intracavitary MRI coil design (for endovaginal and endorectal placement) made imaging with increased spatial resolution and high signal-to-noise ratio of this anatomic region possible (3, 34, 35).

MRI OF FEMALE URETHRAL DIVERTICULA

Female urethral diverticulum is often overlooked and frequently misdiagnosed because of unawareness of the condition. Urethral diverticula are estimated to occur in 1–6% of women. Although usually diagnosed between the third and fifth decade of life, it can affect all age groups (36-38). Usually, an array of nonspecific genitourinary symptoms predominate. This condition should always be considered in women with unexplained lower urinary tract symptoms. In addition to interstitial cystitis, urethral syndrome, and urgencyfrequency syndrome, the clinician should include urethral diverticula in the differential diagnosis (39). Appropriate investigations play an important role in the diagnosis of urethral diverticula and ideally should provide the surgeon with information regarding location, number, size, configuration, and communication of the urethral diverticula (40). MRI has now become the imaging study of choice (40).

MRI OF LOCALLY RECURRENT RECTAL CANCER (LRRC)

Colorectal cancer is a common malignancy and rectal cancer accounts for approximately one third of the colorectal malignancies (41). Developments in the treatment of rectal cancer, such as neo-adjuvant (chemo) radiotherapy and total mesorectal excision, have significantly reduced local recurrence rate over the last decades. Currently, the local recurrence rate after rectal surgery amounts 5-10 % (42). Locally recurrent rectal cancer (LRRC) often occurs within the first 2 years after treatment of the primary tumor and has often disabling and difficult to treat symptoms, such as severe pain, fistulating and bleeding tumors (43, 44). Radical surgical resection of the local recurrence offers the highest chance of cure and leads to survival rates ranging between 14 % and 30 % (45, 46). On the contrary, without surgical intervention LRRC is associated with a dismal 5-year survival rate of less than 4% (4). Early detection of LRRC may facilitate radical resection and thus achieve a better survival (46, 47). Magnetic Resonance imaging (MRI) is widely used for diagnosis and surgical planning of LRRC (48). The diagnosis is challenging due to difficulty of differentiating actual recurrent disease from fibrosis and scarring (44, 47, 48). This hinders the detection of local recurrences and also poses a problem in defining the exact tumor extent (48). In addition to conventional MRI sequences (T1and T2weighted MRI), contrast enhanced (CE) MRI has the potential to increase lesion visibility and conspicuity and thus may be of additional value in distinguishing malignant from non-malignant tissue. (47, 49, 50).

PRIMARY CYSTIC LESIONS OF THE RETRORECTAL SPACE

The retrorectal space, which is also known as the presacral space, is a space bounded by the rectum anteriorly, presacral fascia posteriorly, and the endopelvic fascia laterally. The superior border is formed by the posterior peritoneal reflection of the rectum with the inferior border being the superior fascia of the pelvic diaphragm. This space contains remnants derived from embryonic neuroectoderm, notochord, and hindgut, and hence may result in a wide variety of congenital lesions herein. Malignancy is more common in the pediatric population, and solid lesions are more likely to be malignant than are cystic lesions (51).

Retrorectal cystic lesions (RRCL) in adults are rare with little literature available and an unknown prevalence. Often the basic clinical problem is whether a RCL lesion should be considered a malignant lesion.

AIM OF THIS THESIS

The aim of this thesis was to determine the value of dedicated MRI with high spatial and contrast resolution in different diseases of the lower pelvis and pelvic floor.

OUTLINE OF THIS THESIS

Chapter 2 focuses on applied physics and design of the current rigid endoluminal surface coils for pelvic imaging, including translation to state of the art imaging of the perianal and periurethral (female) anatomic regions. These coils were applied in some of the studies described in this thesis.

In **Chapter 3,** the focus is on MRI of perianal fistula disease and chronic anal pain. **Chapter 3.1** relate to a review study on MRI of perianal fistula disease. In **Chapter 3.2**, I present the results of a study with endoanal MRI of anovaginal fistulas. In many institutions, the clinical diagnosis or suspicion of an anovaginal fistula is confirmed with imaging studies especially conventional fistulography and and anal endosonography. Conventional fistulography may not be possible in many patients because the internal openings of the fistulas may not be visible at physical examination. Endoanal ultrasonography (US) is often inaccurate in the depiction of anovaginal fistulas, mainly because endoanal US has inherent low soft-tissue contrast. We evaluated the role of endoanal MR imaging in the assessment of anovaginal fistulas and associated findings. In **Chapter 3.3**, a clinical study on surgical outcome of complex high transshpincteric fistulas is described. Transanal advancement flap repair for the treatment of high transsphincteric fistulas fails in 1 out of 3 patients. The present study was conducted to determine the prevalence of horseshoe extensions in posterior and anterior high transsphincteric fistulas with the use of endoanal MR imaging and to investigate whether the more complex fistulas, such as those with horseshoe extensions and associated abscesses, have a less favorable outcome. In **Chapter 3.4**, a study is presented on dedicated MRI in patients with clinical occult chronic analand perianal pain (CAP). Although CAP is a relatively common problem in the general population, few studies have focused on this problem. These ultrasound-based studies showed a common weakness in that a clear clinical reference standard for the reported ultrasound findings was lacking. In addition, the nature of ultrasound as an operator-dependent imaging modality leads to limitations in the reproducibility of findings. Our study is the first with use of MRI in a cohort of patients with CAP. Imaging findings were correlated with surgery and clinical follow up data.

Chapter 4 focuses on the value of dedicated MRI in female patients with chronic lower urinary tract symptoms (LUTS). In **Chapter 4.1**, I describe and illustrate our experiences with state of the art MRI of female patients with chronic lower urinary tract symptoms (LUTS) in a clinical perspective paper. The presentation of LUTS can be diverse and the differential diagnoses extensive. This article presents a classification of morphologic or functional abnormalities that can be considered in the differential diagnoses of women with LUTS.

This classification is based on common and less-common causes for lower urinary tract symptoms according to the literature and our experience at a tertiary referral center for female genitourinary symptoms and dedicated MRI of the pelvis and pelvic floor. In **Chapter 4.2**, I investigate a cohort of female patients referred for MRI with clinical suspicion of urethral diverticula. Accurate imaging plays an important role in the diagnosis and differential diagnosis of urethral diverticula and ideally should provide the surgeon with information regarding location, number, size, configuration, and communication of the urethral diverticulum.

Chapter 5 focuses on the value of dedicated MRI for diagnosis and local staging of malignancies in the dorsal compartment of the pelvis. In **Chapter 5.1**, I present a study on staging of locally recurrent rectal cancer (LRRC) with MRI, with focus on the added value of contrast enhanced MRI, to predict accuracy of tumor size and surgical resection margins (radical or incomplete). The diagnosis of LRRC is challenging due to difficulty of differentiating actual recurrent disease from fibrosis and scarring. In addition to conventional MRI sequences (T1and T2weighted MRI), contrast enhancement (CE) MRI has the potential to increase lesion visibility and conspicuity and thus may be of additional value in distinguishing malignant from non-malignant tissue. In **Chapter 5.2**, I describe the retrorectal space (RRS) and present a study of primary cystic lesions of the RRS, using MRI to assess malignancy. Often the basic clinical problem is whether a retrorectal cystic lesion should be considered a malignant lesion. Based on our analysis, we assessed the a priori chance that a RRCL is malignant and we tried to identify MR imaging characteristics which may be indicative of malignancy.

Chapter 6, Interlude. These images were captured during one of my favourite activities, travel. Finally, in **Chapter 7**, I conclude with a review of my main findings in the context of present knowledge and indicate the importance for patient management.

1

REFERENCES

1. Dwarkasing S, Hussain SM, Hop WC, Krestin GP. Anovaginal fistulas: evaluation with endoanal MR imaging. Radiology 2004; 231:123-128.
2. Dwarkasing S, Hussain SM, Krestin GP. Magnetic resonance imaging of perianal fistulas. Semin Ultrasound CT MR 2005; 26:247-258.
3. Dwarkasing RS, Dinkelaar W, Hop WC, Steensma AB, Dohle GR, Krestin GP. MRI evaluation of urethral diverticula and differential diagnosis in symptomatic women. AJR Am J Roentgenol 2011; 197:676-682.
4. Dwarkasing RS, Schouten WR, Geeraedts TE, Mitalas LE, Hop WC, Krestin GP. Chronic anal and perianal pain resolved with MRI. AJR Am J Roentgenol 2013; 200:1034-1041.
5. Dwarkasing RS, Verschuuren SI, Leenders GJ, Thomeer MG, Dohle GR, Krestin GP. Chronic lower urinary tract symptoms in women: classification of abnormalities and value of dedicated MRI for diagnosis. AJR Am J Roentgenol 2014; 202:W59-66.
6. Beets-Tan RG, Beets GL, van der Hoop AG, et al. Preoperative MR imaging of anal fistulas: Does it really help the surgeon? Radiology 2001; 218:75-84.
7. Beets-Tan RG, Beets GL, Vliegen RF, et al. Accuracy of magnetic resonance imaging in prediction of tumour-free resection margin in rectal cancer surgery. Lancet 2001; 357:497-504.
8. Engelbrecht MR, Huisman HJ, Laheij RJ, et al. Discrimination of prostate cancer from normal peripheral zone and central gland tissue by using dynamic contrast-enhanced MR imaging. Radiology 2003; 229:248-254.
9. Thomeer MG, Gerestein C, Spronk S, van Doorn HC, van der Ham E, Hunink MG. Clinical examination versus magnetic resonance imaging in the pretreatment staging of cervical carcinoma: systematic review and meta-analysis. Eur Radiol 2013; 23:2005-2018.
10. Hussain SM, Stoker J, Lameris JS. Anal sphincter complex: endoanal MR imaging of normal anatomy. Radiology 1995; 197:671-677.
11. Stoker J, Hussain SM, van Kempen D, Elevelt AJ, Lameris JS. Endoanal coil in MR imaging of anal fistulas. AJR Am J Roentgenol 1996; 166:360-362.
12. Halligan S, Bartram CI. MR imaging of fistula in ano: are endoanal coils the gold standard? AJR Am J Roentgenol 1998; 171:407-412.
13. deSouza NM, Puni R, Kmiot WA, Bartram CI, Hall AS, Bydder GM. MRI of the anal sphincter. J Comput Assist Tomogr 1995; 19:745-751.
14. Hussain SM, Stoker J, Schouten WR, Hop WC, Lameris JS. Fistula in ano: endoanal sonography versus endoanal MR imaging in classification. Radiology 1996; 200:475-481.
15. deSouza NM, Gilderdale DJ, Coutts GA, Puni R, Steiner RE. MRI of fistula-in-ano: a comparison of endoanal coil with external phased array coil techniques. J Comput Assist Tomogr 1998; 22:357-363.
16. Stoker J, Lameris JS. MR imaging of perianal fistulas using body and endoanal coils. AJR Am J Roentgenol 1999; 172:1139-1140.
17. deSouza NM, Hall AS, Puni R, Gilderdale DJ, Young IR, Kmiot WA. High resolution magnetic resonance imaging of the anal sphincter using a dedicated endoanal coil. Comparison of magnetic resonance imaging with surgical findings. Dis Colon Rectum 1996; 39:926-934.
18. deSouza NM, Puni R, Gilderdale DJ, Bydder GM. Magnetic resonance imaging of the anal sphincter using an internal coil. Magn Reson Q 1995; 11:45-56.
19. Rociu E, Stoker J, Eijkemans MJ, Schouten WR, Lameris JS. Fecal incontinence: endoanal US versus endoanal MR imaging. Radiology 1999; 212:453-458.
20. Heijmink SW, Futterer JJ, Hambrock T, et al. Prostate cancer: body-array versus endorectal coil MR imaging at 3 T--comparison of image quality, localization, and staging performance. Radiology 2007; 244:184-195.
21. Futterer JJ, Engelbrecht MR, Jager GJ, et al. Prostate cancer: comparison of local staging accuracy of pelvic phased-array coil alone versus integrated endorectal-pelvic phased-array coils. Local staging accuracy of prostate cancer using endorectal coil MR imaging. Eur Radiol 2007; 17:1055-1065.
22. Hussain SM, Stoker J, Schutte HE, Lameris JS. Imaging of the anorectal region. Eur J Radiol 1996; 22:116-122.

23. Shouler PJ, Grimley RP, Keighley MR, Alexander-Williams J. Fistula-in-ano is usually simple to manage surgically. Int J Colorectal Dis 1986; 1:113-115.
24. O'Donovan AN, Somers S, Farrow R, Mernagh JR, Sridhar S. MR imaging of anorectal Crohn disease: a pictorial essay. Radiographics 1997; 17:101-107.
25. Keighley MR, Allan RN. Current status and influence of operation on perianal Crohn's disease. Int J Colorectal Dis 1986; 1:104-107.
26. Hussain SM, Outwater EK, Joekes EC, et al. Clinical and MR imaging features of cryptoglandular and Crohn's fistulas and abscesses. Abdom Imaging 2000; 25:67-74.
27. Chapple KS, Spencer JA, Windsor AC, Wilson D, Ward J, Ambrose NS. Prognostic value of magnetic resonance imaging in the management of fistula-in-ano. Dis Colon Rectum 2000; 43:511-516.
28. Drossman DA, Li Z, Andruzzi E, et al. U.S. householder survey of functional gastrointestinal disorders. Prevalence, sociodemography, and health impact. Dig Dis Sci 1993; 38:1569-1580.
29. Whitehead WE, Wald A, Diamant NE, Enck P, Pemberton JH, Rao SS. Functional disorders of the anus and rectum. Gut 1999; 45 Suppl 2:II55-59.
30. Beer-Gabel M, Carter D, Venturero M, Zmora O, Zbar AP. Ultrasonographic assessment of patients referred with chronic anal pain to a tertiary referral centre. Tech Coloproctol 2010; 14:107-112.
31. Al-Hayek S, Abrams P. Women's lower urinary tract function and dysfunction: definitions and epidemiology. Minerva Ginecol 2004; 56:311-325.
32. Chapple CR, Wein AJ, Abrams P, et al. Lower urinary tract symptoms revisited: a broader clinical perspective. Eur Urol 2008; 54:563-569.
33. Coyne KS, Sexton CC, Thompson CL, et al. The prevalence of lower urinary tract symptoms (LUTS) in the USA, the UK and Sweden: results from the Epidemiology of LUTS (EpiLUTS) study. BJU Int 2009; 104:352-360.
34. Elsayes KM, Mukundan G, Narra VR, Abou El Abbass HA, Prasad SR, Brown JJ. Endovaginal magnetic resonance imaging of the female urethra. J Comput Assist Tomogr 2006; 30:1-6.
35. Lorenzo AJ, Zimmern P, Lemack GE, Nurenberg P. Endorectal coil magnetic resonance imaging for diagnosis of urethral and periurethral pathologic findings in women. Urology 2003; 61:1129-1133; discussion 1133-1124.
36. Davis BL, Robinson DG. Diverticula of the female urethra: assay of 120 cases. J Urol 1970; 104:850-853.
37. Foster RT, Amundsen CL, Webster GD. The utility of magnetic resonance imaging for diagnosis and surgical planning before transvaginal periurethral diverticulectomy in women. Int Urogynecol J Pelvic Floor Dysfunct 2007; 18:315-319.
38. Rufford J, Cardozo L. Urethral diverticula: a diagnostic dilemma. BJU Int 2004; 94:1044-1047.
39. Aspera AM, Rackley RR, Vasavada SP. Contemporary evaluation and management of the female urethral diverticulum. Urol Clin North Am 2002; 29:617-624.
40. Patel AK, Chapple CR. Female urethral diverticula. Curr Opin Urol 2006; 16:248-254.
41. Jemal A, Siegel R, Xu J, Ward E. Cancer statistics, 2010. CA Cancer J Clin 2010; 60:277-300.
42. Bakx R, Visser O, Josso J, Meijer S, Slors JF, van Lanschot JJ. Management of recurrent rectal cancer: a population based study in greater Amsterdam. World J Gastroenterol 2008; 14:6018-6023.
43. Kusters M, Marijnen CA, van de Velde CJ, et al. Patterns of local recurrence in rectal cancer; a study of the Dutch TME trial. Eur J Surg Oncol 2010; 36:470-476.
44. Messiou C, Chalmers A, Boyle K, Sagar P. Surgery for recurrent rectal carcinoma: The role of preoperative magnetic resonance imaging. Clin Radiol 2006; 61:250-258.
45. Shoup M, Guillem JG, Alektiar KM, et al. Predictors of survival in recurrent rectal cancer after resection and intraoperative radiotherapy. Dis Colon Rectum 2002; 45:585-592.
46. Hahnloser D, Haddock MG, Nelson H. Intraoperative radiotherapy in the multimodality approach to colorectal cancer. Surg Oncol Clin N Am; 12:993-1013.
47. Krestin GP, Steinbrich W, Friedmann G. Recurrent rectal cancer: diagnosis with MR imaging versus CT. Radiology 1988; 168:307-311.
48. Dresen RC, Kusters M, Daniels-Gooszen AW, et al. Absence of tumor invasion into pelvic structures in locally recurrent rectal cancer: prediction with preoperative MR imaging. Radiology 2010; 256:143-150.

49. Muller-Schimpfle M, Brix G, Layer G, et al. Recurrent rectal cancer: diagnosis with dynamic MR imaging. Radiology 1993; 189:881-889.
50. Goh V, Padhani AR, Rasheed S. Functional imaging of colorectal cancer angiogenesis. Lancet Oncol 2007; 8:245-255.
51. Bullard Dunn K. Retrorectal tumors. Surg Clin North Am 2010; 90:163-171, Table of Contents.

chapter 2

Endoluminal Receiver Coil for Endoanal and Intravaginal Application on 1.5 and 3.0 T MRI Systems; Technical Aspects, Design and Clinical Value

Roy S. Dwarkasing
Herman Flick
Gabriel P. Krestin

Submitted

ABSTRACT

There are two main types of endocavitary MRI coils (eCoils) for use in the pelvic region: the inflatable and rigid type. The inflatable type has been more widely used especially for prostate imaging with endorectal application. This inflatable version is meant for use of one disposable coil per examination. The rigid eCoil has been designed initially for endoanal application with proved value for classification of the primary tract and identification of the internal ostium in cryptoglandular fistulas. The same coil has also been used for endovaginal assessment of female urethral diverticula and periurethral disease. This rigid coil is reusable. Both coil types were technically improved recently with the dual loop design, including an increase in SNR and improved image quality. The dual loop eCoil may allow for better diagnosis through improved spatial resolution without increase in imaging time when compared with the single loop coil. In this article we describe and illustrate our experiences with the use of the rigid eCoils for endoanal and endovaginal application, including added value over the pelvic phased array multicoils as well as pitfalls in using these coils.

INTRODUCTION

The value of endoluminal receiver coils (eCoils) for application in the pelvic area has been established with proven clinical value especially for perianal fistula imaging and prostate imaging (1-3). Recent studies have proven valuable clinical potential for endovaginal application with demonstration of urethral and periurethral pathology. Our center, a tertiary referral center for diseases of the pelvis and pelvic floor, has solid experience with the use of rigid eCoils for endoanal and endovaginal application on both, 1.5 T and 3.0 T MRI systems. In this article we describe our experience with the use of these coils, including added value over the pelvic phased array multicoils as well as pitfalls in using these coils.

Endoluminal receiver coils for use in the pelvic region

There are 2 main types of eCoils for use in the pelvic region: the inflatable and rigid type. The inflatable design has been more widely used especially for endorectal application with focus on prostate imaging. This inflatable version is meant for use of one disposable coil per examination. The rigid eCoil has been initially designed for endoanal application. The same coil has also been used for endovaginal placement with satisfactory results (4, 5). This rigid coil type is reusable. Due to its versatile use, this paper will further focus on the rigid eCoils.

Design of a rigid MRI coil with a cylindrical reception field profile

Given the anatomy of the anal canal, a homogeneous cylindrical radiofrequency (rf) field profile of the receiving coil is required. A single loop coil generates a dipole H_1 field that can be described by using Biot Savart's law for a quasi- static H_1 field. Calculation of the H_1 field demonstrates the rf field in the axial plane around two wires separated by 12 mm (Fig 1). Note that the field has an elliptic profile close to the coil. To correct for this a second loop coil, placed orthogonally to the first loop, was introduced.

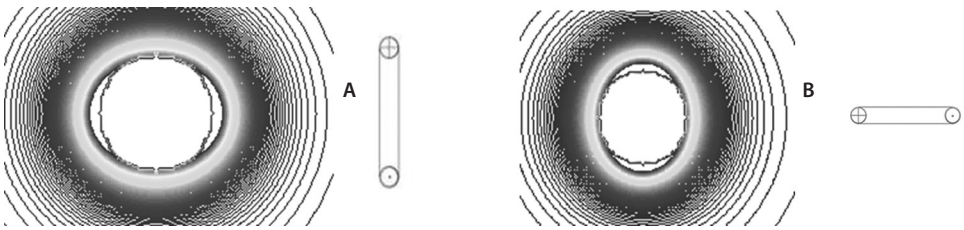

Figure 1. Calculations of the H_1field profile of two wires separated by 12 mm in vertical A) and horizontal (B) orientation. Calculations were performed using the mathematical program MatLab®.

By combining the signals of both coils in an array a cylindrical field is expected. The sensitivity of both coils combined can be described by the following equation:

$$SI \sim \frac{a}{\sqrt{(r^2+a^2)^2-4r^2a^2sin^2(\alpha)}} + \frac{a}{\sqrt{(r^2+a^2)^2-4r^2a^2cos^2(\alpha)}}$$

where a is the radius of the coil, r is the distance between a voxel and the center of the coil and is the voxel orientation with respect to the four wires. Based on above equation, following H1 field was expected for the dual loop design (Fig 2).

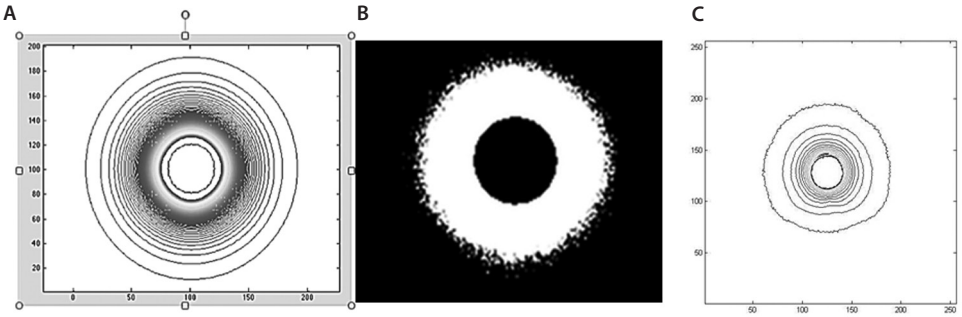

Figure 2. Dual loop design: Calculations of the H1 field profile (A), axial MRI image on phantom containing 0.9% NaCl and 20mMol CuSO4 (B) and associated iso- contour plot (C) show the circular field profile which is in accordance to the calculated profile. Calculations were performed using the mathematical program MatLab®.

Differences in SNR data derived from the single loop- and dual loop coils are displayed in Table I. Signal intensities were measured over an area of 14 mm^2 radially to a length of 50 mm from the coil center in two orthogonal directions.

Table I. SNR measured from the single- and dual loop design rigid endoluminal coil on 3T MR system.

r (mm)	SNR single loop at 0^0	SNR single loop at 90^0	SNR dual loop at 0^0	SNR dual loop at 90^0
11	414	370	587	569
15	257	206	334	348
19	167	118	244	242
23	119	76	161	156
27	90	42	98	98
31	70	39	72	87
35	53	31	55	56
39	42	27	44	53
43	34	23	36	42
47	26	20	32	29

r (mm): distance from the center of the coil measured in mm.
SNR single loop: measurements in two orthogonal directions.
SNR dual loop: measurements in two orthogonal directions.

The SNR of the dual coil array exceeds that of the single loop coil at any distance, with an average increase of 35 % at 20 mm.

Coil construction and specifications

Coil specifications

Coil former	: Delrin®
Coil former	: Length 70 mm; diameter 15 mm.
Coil housing	: Length 20 mm, diameter: 18 mm
Preamplifier	: MWT®, MSM128281C
All capacitors	: ATC®
RF inductors	: Coilcraft®
All diodes	: Macom®

To ensure mechanical stability in the dual loop design, both coils were winded on a cylindrical former with groves to secure the loop coils. Circuitry was built on pcb which connect directly to the coils. To minimize transmission losses, the preamplifiers were integrated on the PCB, which holds the tuning and matching circuits. The crosstalk between the coils is reduced to -30 dB by proper mechanical adjustment of the orthogonal position. The loop wires are isolated from each other by using classical decoupling with preamplifiers built directly onto the coils. The isolation resulting from the preamplifier decoupling is 17dB. The T/R (coil decoupling during transmit) switch is built in a classical way by inserting an inductor in a parallel fashion over one of the coil capacitors. Decoupling is realized by enabling a PIN diode (MA4P7461F). The off-gating detunes the coil by another 23 dB. Figure 3 shows the pcb assembly (A) and coil complete with housing (B).

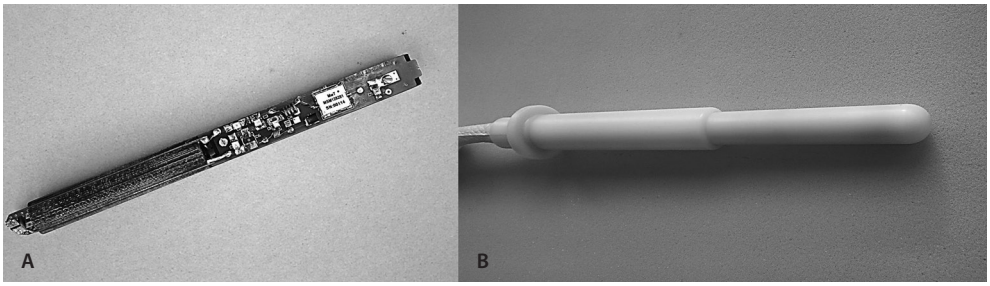

Figure 3. The current rigid endoluminal coil on 3T. A) PCB assembly, B) Complete with housing.

According to Faraday's law, rf electromagnetic fields may result in induced currents in the transmission line of the coil, which may interfere with the local excitation field and cause artifacts (Fig 4A). To minimize these braiding currents rf- traps have been installed at every 1/8 λ (=23 cm) with a high impedance factor and an attenuation of 20 dB per trap (Fig 4B). The final result is a homogenous cylindrical H_1 field over the total length of the coil (Fig 5).

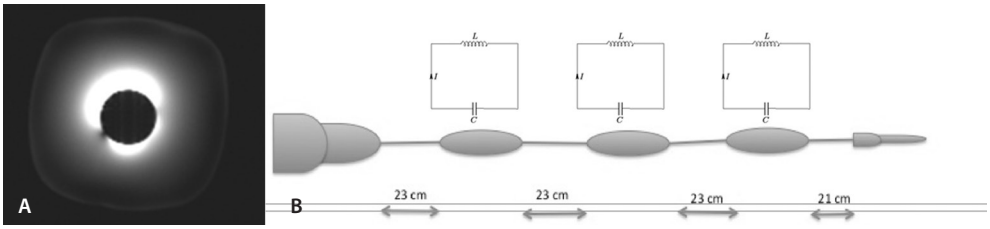

Figure 4. A) Phantom image acquired with the endoluminal coil showing an artefact caused by standing waves on the transmission line. B) Schematic display of rf- traps installed along the transmission line to minimize braiding currents.

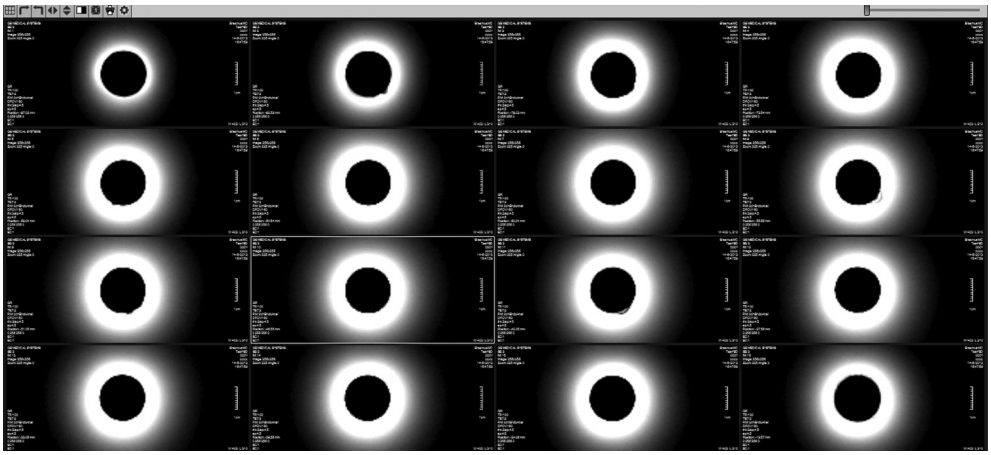

Figure 5. Test MR images (3T) on phantom (containing an aqueous solution of 0.9% NaCl and 20mMol CuSO4) on 3T with a homogenous H_1field on consecutive axial slices resulting in an almost perfect cylindrical field produced by the dual coil array.

CLINICAL APPLICATION

Preparation for use in patients

The coil should be cleaned conform procedures for Ultrasound endocavitary probes. Cleaning the coil with 70% medical alcohol is sufficient. The device is covered with a condom before application. For each patient a new condom must be used. In case of rupture or damage of the condom above cleaning procedure is not sufficient and sterilization is mandatory. Patient needs to be positioned head-first in the MRI scanner. Before insertion a lubricant over the condom is applied. We use a thin layer of hydrophile ultrasound gel for this purpose. For endoanal insertion the patients is positioned in the left lateral decubitus position after which the patient needs to be carefully positioned in the prone position. For endovaginal insertion, the patient is asked to insert the device herself. On coronal and sagittal survey images, the right postion of the coil is confirmed or adjusted and scan planes are planned.

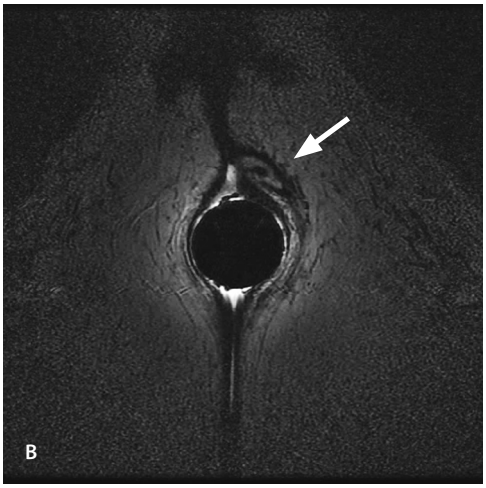

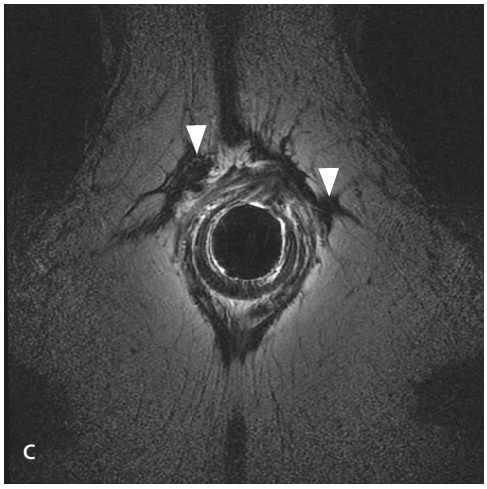

Pelvic phased array versus endoanal coil imaging

Figure 6. 48-year-old woman with MRI after surgery (incision and drainage perianal abcess, including seton drain placement in fistula). On the external phased array image (A) no obvious lesions are seen; conversion with the endoanal coil (1.5 T) demonstrates a subsphincteric fistula with drain in situ (arrow) (B), including the patent ostia of two fistula tracks (12 and 1 o'clock position). Arrowheads indicate scar tissue. Axial T2W TSE with fat saturation (A) and without (B,C).

Endoluminal coil versus pelvic phased array imaging

Previous studies found the eCoil to be superior to the phased array coil for demonstration of anal sphincter anatomy and perianal fistula disease (6, 7). Endoanal MRI is especially valuable for classification of the primary tract and identification of the internal ostium (Fig. 6) in cryptoglandular fistula's (7-10). Because of the limited field of view, the phased array was especially superior for demonstration of distant fistula extensions (11, 12).

Endoanal MRI is highly accurate in demonstrating lesions of the sphincter complex (Fig. 7) (13-15). Sphincter damage is especially seen in patients with chronic fistula and previous surgery and is important for surgical planning (Fig. 8). For prostate cancer imaging, studies have shown superior image quality and improved reader confidence using an ERC in staging performance for prostate cancer at 3T when compared with pelvic phased array coil at 3T (2, 3). For female urethral diverticula, endoluminal coil demonstrated better subjective image quality with endovaginal placement when compared with endoanal placement or

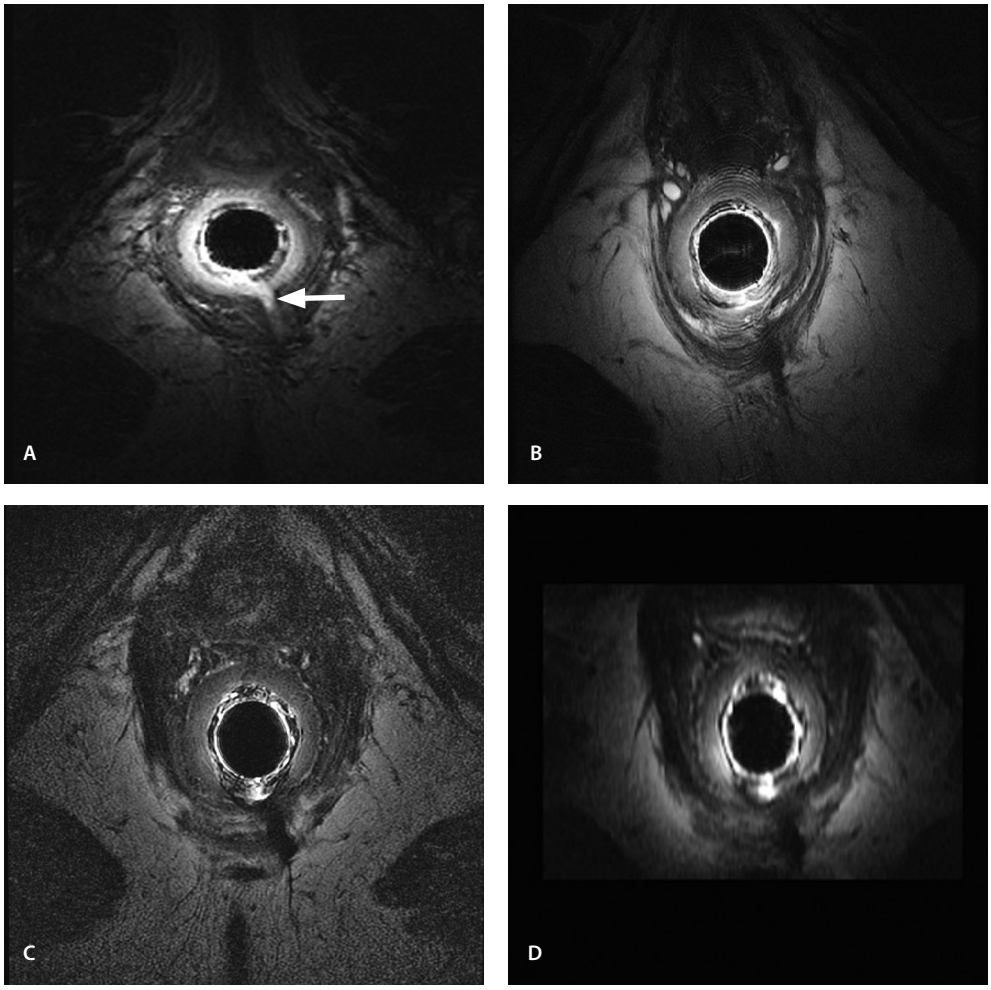

Dedicated endoanal imaging correlated with symptoms

Figure 7. A) 47- year-old woman with active transsphincteric fistula (arrow) in 2007. B) Post- surgery MRI in 2009 because of persistent anal pain demonstrates fibrosis in the old fistula tract (dashed arrow) and no evidence of active disease. C) Repeat MRI in 2013 because of increased pain, soiling, including bloody content, and no obvious abnormalities found at initial clinical examination. Small submucosal abscess is noted at the level of the original internal ostium. All images: axial: T2W TSE on 1.5 T. D) Axial reconstructed sagittal T2W cube image affirms the small submucosal abscess which was surgically confirmed.

phased array coil imaging (Fig. 9)(4). All these studies were based on imaging with the single loop coil design. In addition, vaginal endocoil imaging proved valuable for diagnosis and preoperative assessment of periurethral disease (Fig. 10)(5).

Dual loop versus single loop design

We found two clinical publications on the dual loop design of an endoluminal pelvic coil; both were applied for prostate imaging. An investigational dual-channel next-generation endorectal coil (NG-ERC) was compared with the current clinically available single-loop endorectal coil (ERC) at both 1.5 and 3 T (16). The authors found that the SNR was higher for the NG-ERC compared with the ECR. Overall, T2-weighted image quality was considered better for NG-ERC at both field strengths. In addition, a two-channel solid reusable phased array endorectal receiver coil (SPAC) was compared with a single-channel inflatable endorectal balloon coil on 1.5 T MRI (17). SNR of the SPAC was significantly better compared

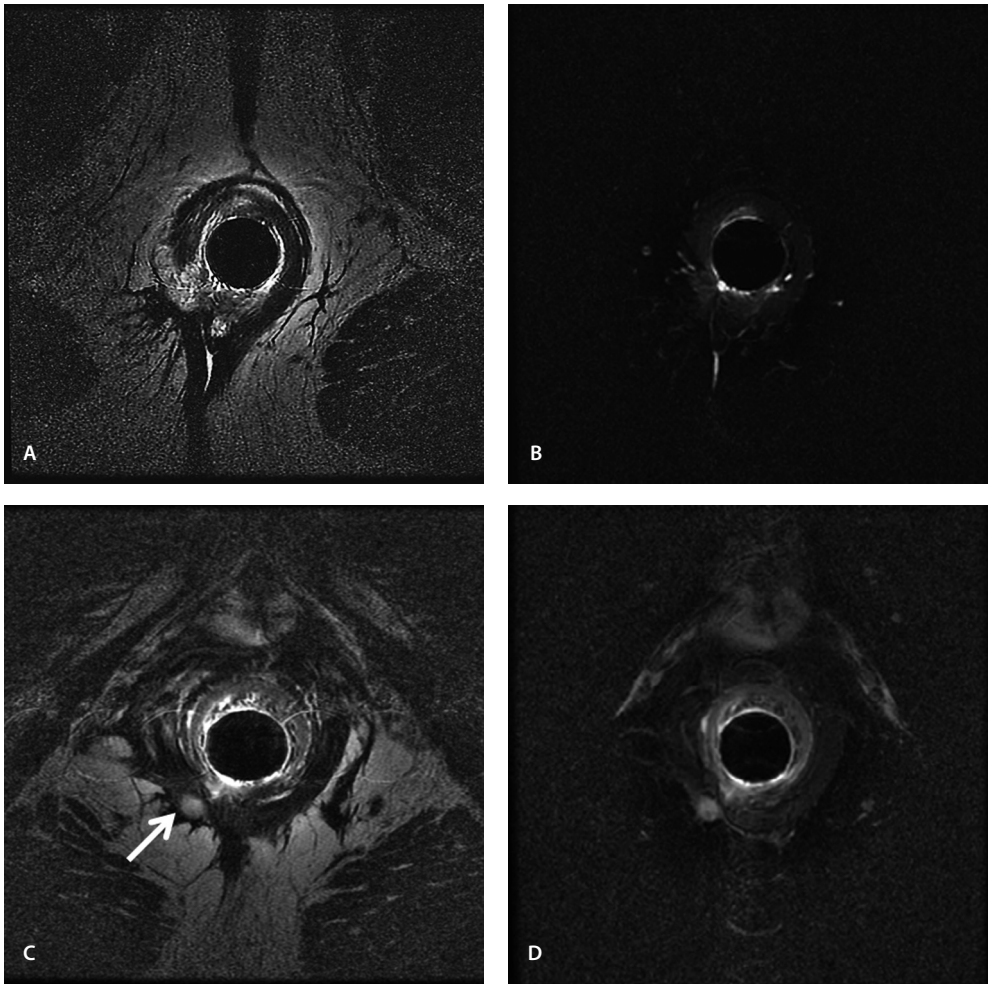

Sphincter damage with focal fat versus active fistula

Figure 8. 34-year-old man with chronic perianal fistula, including sphincter damage. A) Axial T2W TSE image with a local defect of the external sphincter, including fatty tissue deposition on the right which is evident on the T2W image with fat saturation in B) depressed signal intensity (SI). At the level of the puborectalis muscle an active fistula (arrow) is seen with high SI on both, the axial T2W TSE image without (C) and with fat saturation (D).

Female urethral diverticulum

Figure 9. 53-year-old woman with an uncertain periurethral lesion (arrow) on screening CT for persistent retropubic pain. A) Subsequent MRI with the endoluminal coil in de vagina on 3T demonstrates a semicircular urethral diverticulum, including level of the internal ostium (arrow) in B) and diverticular neck (arrow) in C. B,C: Axial T2W TSE images.

with that of the balloon coil. Both SNR and image quality were significantly improved with use of the SPAC at 1.5 T compared with the single-channel inflatable endorectal balloon coil. In addition, both studies showed that the dual loop design can reduce patient imaging time without loss in image quality compared with that of a single-channel balloon endorectal coil. The increase in SNR can be used to increase the spatial resolution (Fig. 11). To our knowledge, no studies were performed that directly compare image quality in the same patient cohort with similar setups at the two field strengths. Because of the increase in spatial resolution at 3 T it is expected that images will be of higher quality when compared with 1.5 T (Fig. 12).

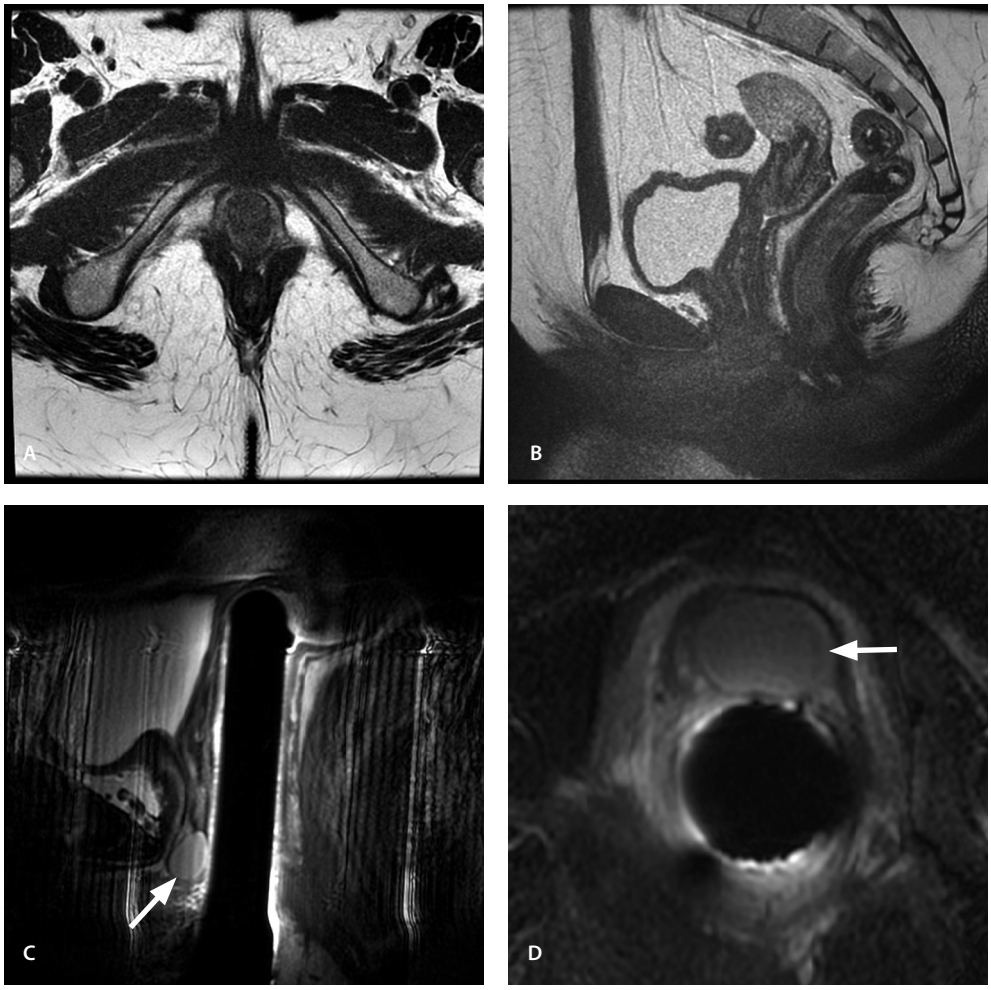

Cyst of Skene, pelvic phased array versus endoluminal coil imaging

Figure 10. 23- year-old woman with dysuria and palpable periurethral mass. A, B) On initial MRI with the phased array coil on 3T, the lesion is hard to discern on axial (A) and sagittal (B) T2WTSE image. C, D) Repeat examination with the endovaginal coil on 3T demonstrates a cyst (arrow) in the left periurethral region which is consistent with a cyst of Skene (surgery and pathology confirmed). The displaced urethra can be identified on the right (D).

Patient tolerance of the endoluminal coil

The use of endoluminal coils may be impossible in case of anal stenosis or severe local pain . Studies found that the endoanal coil could not be inserted in 3-17 % of patients respectively (8, 18). In a study of MRI in patients with clinical occult anal and perianal pain 7% of cases the endoluminal coil could not be used because of severe pain or patient preferance for the phased array pelvic coil (19). A prospective comparison of an inflatable endorectal coil with a rigid endorectal coil for prostate imaging proved significant increased patient discomfort with the inflatable design (20).

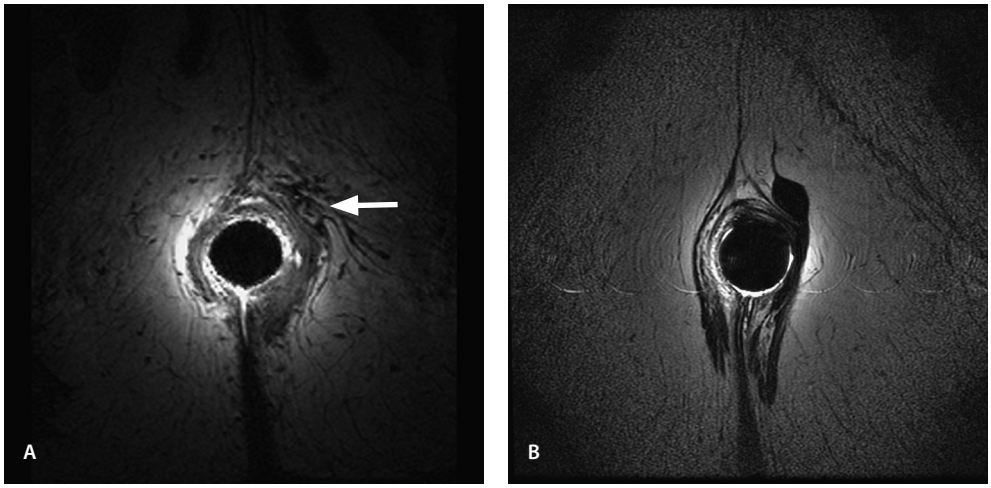

Single loop versus dual loop endoluminal coil design on 1.5 T

Figure 11. A) 68-year-old man with low transshpincteric fistula (arrow) after insertion of a seton drain in 2005. B) Repeat MRI in 2013 after successful treatment with a fistula plug. Note the better detailed image including, homogeneous signal intensity with no signal voids with the current endoluminal coil (dual loop design) on 1.5 T when compared with the old single loop design in (A).

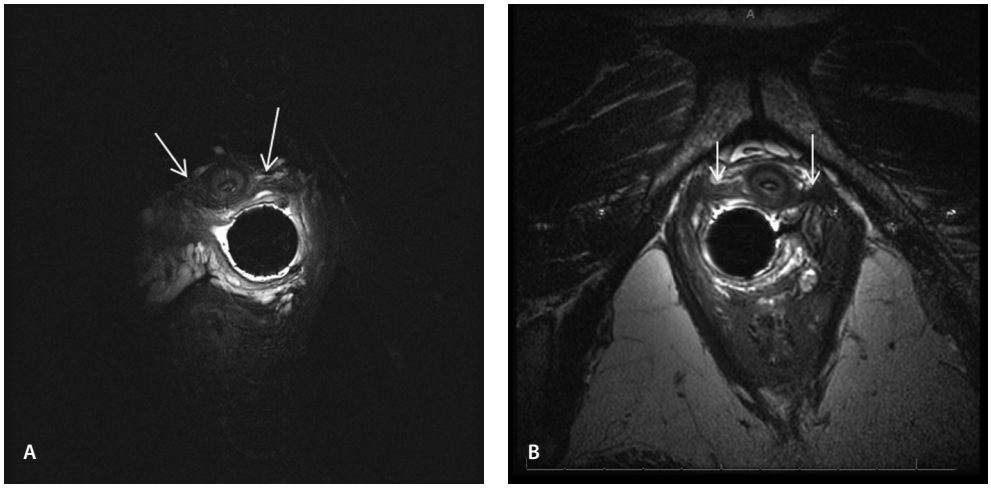

Improved SRN on 3T versus 1.5 T

Figure 12. 43-year-old woman A) 1.5 T in 2009, B) 3.0 T in 2011. Patient underwent MRI for evaluation of urethra diverticulum (not shown) in 2009 and follow up MRI after surgery in 2011. Endoluminal coil in the vagina. Better image quality due to increase in SNR and larger field of view can be noted on 3T. Both, axial T2W TSE images. Arrows demonstrate the periurethral ligaments which are more clearly observed in B.

MRI protocol

With endoluminal MRI we aim to aquire accurate morphologic images. Image volume encompasses the entire sensitive region of the coil with recommended field of view of 120

Pitfall: technical artefact

Figure 13. 32-year-old man with active intersphincteric fistula on the left (arrow) on axial T2W TSE image. Two regions of signal voids are noted on the right. These are technical artifact because of a dysfunctional rf- traps and may be misinterpreted as focal fibrosis. The blooming nature suggests an artefact.

mm, matrix: 256x256 – 256x384, slice thickness/gap 2/0.2- 2.5/0.3 mm. For perianal fistula imaging T2-weighted (T2W) turbo spin-echo (TSE) sequences in three planes (axial, coronal, and sagittal), including axial T2W with fat saturation (fat sat) imaging is recommended. For female urethral and periurethral imaging: T2W TSE in three planes (axial, coronal, and sagittal), including axial T2W fat sat and T1W is recommended. With this concise protocol, scan times may be limited to an average of 20 minutes per patient.

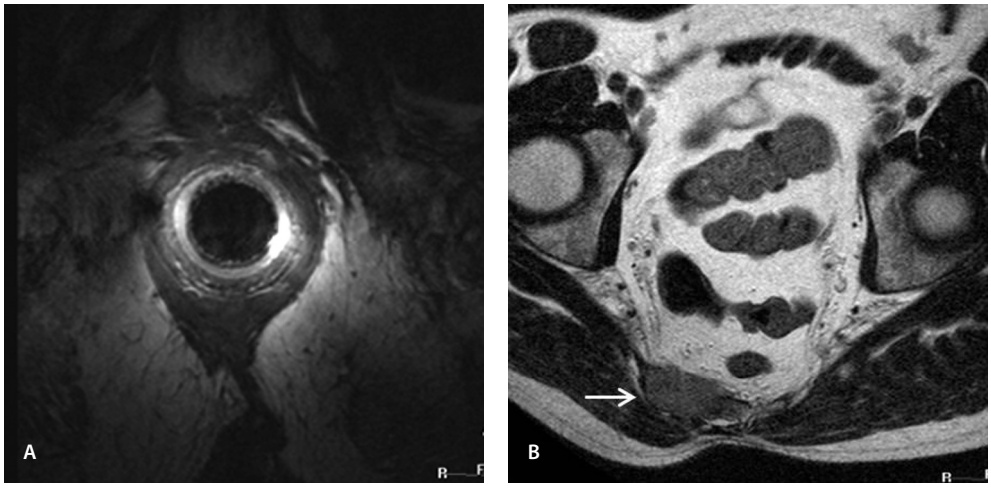

Pitfall: MR imaging of perianal pain.

Figure 14. 40-year-old man, seventeen years after surgical drainage of perianal abscess with persistent and increasing anal and perianal pain for almost a year. A, Endoanal MRI revealed only a thickened anococcygeus ligament. B, Whole pelvic imaging with the pelvic coil (axial T2W TSE) demonstrates a tumor at the sacrococcygeus joint (arrow) which was confirmed as an adenocarcinoma of unknown primary. For screening studies in patients with pelvic pain whole field imaging of the pelvis is recommended.

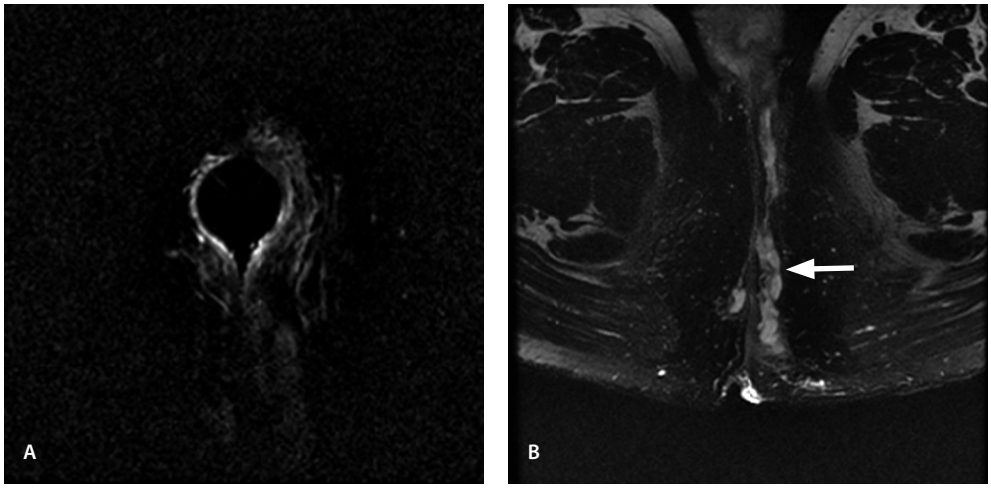

Pitfall: MR imaging of superficial extended fistulas
Figure 15. 69-year-old man with extensive superficial fistulas in the left nates. In A) the lesion is hard to discern on the lower slice (T2W image with fat saturation) with the endoluminal coil. B) Conversion with the pelvic phased array coil demonstrates the fistula (arrow) on the left in full extent from buttocks to scrotum. In addition, a small fistula is seen on the right (Axial T2WTSE with fat saturation) It is recommended to confirm that the field of view is sufficient before regarding the examination as complete.

For extensive fistula disease (e.g. Crohn's disease), perianal or periurethral pain, evaluation of prolapse or malignancy, imaging of the entire pelvis with the phased array multicoils is needed. To evaluate for prolapse, a dynamic true fast imaging with steady-state free precession (true FISP) or HASTE sequence in the midsagittal plane may be performed. When malignancy is suspected, lesion detection and characterization may be enhanced with diffusion-weighted imaging and dynamic contrast enhanced series after iv Gadolinium chelates.

Pitfalls in endoluminal coil MR imaging

Pitfalls in imaging using the endoluminal coil can be categorized in technical artefacts (Fig. 13) which may be confused for pathology and the limited field of view of the coil with failure to capture lesions outside the sensitive region of the coil (Fig. 14, 15). Especially in obese patients upper anal canal and anorectal region may fall outside the field of view. In these cases endoluminal coil imaging is not sufficient and application of the pelvic phased array coil is advised. It is therefore recommended to view the examination for completeness before the patient is dismissed.

Future perspective

Theoretically, an increase in SNR may be achieved by applying four loops rather than two like in the current approach. By arranging the four elements two by two in series the SNR could be increased without suffering loss of field homogeneity in the radial direction. Less decrease in SNR at increasing distance from the coil could also be expected when compared to the dual loop configuration. An obstacle though, will be the limited space for

installation of all components within current coil housing. Currently a version is being studied for endorectal application, including use of flexible material to adjust for the anorectal angle. Coupling of the endoluminal coil to an external receiver coil array may further increase the volume to be imaged. For this configuration proper matching and tuning of all components (endoluminal-, external coil and MR system) is required. For prostate imaging this configuration, using a single loop coil, resulted in significant improvement of anatomic details, extracapsular extension accuracy and specificity (2). We believe that stepwise technical improvements should be pursued based on clinical need.

CONCLUSION

The endoluminal coil has been technically improved with the dual- loop design, including an increase in SNR over the previous generation single loop coils. The dual loop endoluminal receiver coil may allow for better diagnosis through improved spatial resolution without increase in imaging time compared with the single loop coil.

REFERENCES

1. Halligan S, Stoker J. Imaging of fistula in ano. Radiology 2006; 239:18-33.
2. Futterer JJ, Engelbrecht MR, Jager GJ, et al. Prostate cancer: comparison of local staging accuracy of pelvic phased-array coil alone versus integrated endorectal-pelvic phased-array coils. Local staging accuracy of prostate cancer using endorectal coil MR imaging. Eur Radiol 2007; 17:1055-1065.
3. Heijmink SW, Futterer JJ, Hambrock T, et al. Prostate cancer: body-array versus endorectal coil MR imaging at 3 T--comparison of image quality, localization, and staging performance. Radiology 2007; 244:184-195.
4. Dwarkasing RS, Dinkelaar W, Hop WC, Steensma AB, Dohle GR, Krestin GP. MRI evaluation of urethral diverticula and differential diagnosis in symptomatic women. AJR Am J Roentgenol 2011; 197:676-682.
5. Dwarkasing RS, Verschuuren SI, Leenders GJ, Thomeer MG, Dohle GR, Krestin GP. Chronic lower urinary tract symptoms in women: classification of abnormalities and value of dedicated MRI for diagnosis. AJR Am J Roentgenol 2014; 202:W59-66.
6. Hussain SM, Stoker J, Lameris JS. Anal sphincter complex: endoanal MR imaging of normal anatomy. Radiology 1995; 197:671-677.
7. Stoker J, Hussain SM, van Kempen D, Elevelt AJ, Lameris JS. Endoanal coil in MR imaging of anal fistulas. AJR Am J Roentgenol 1996; 166:360-362.
8. Halligan S, Bartram CI. MR imaging of fistula in ano: are endoanal coils the gold standard? AJR Am J Roentgenol 1998; 171:407-412.
9. deSouza NM, Puni R, Kmiot WA, Bartram CI, Hall AS, Bydder GM. MRI of the anal sphincter. J Comput Assist Tomogr 1995; 19:745-751.
10. Hussain SM, Stoker J, Schouten WR, Hop WC, Lameris JS. Fistula in ano: endoanal sonography versus endoanal MR imaging in classification. Radiology 1996; 200:475-481.
11. deSouza NM, Gilderdale DJ, Coutts GA, Puni R, Steiner RE. MRI of fistula-in-ano: a comparison of endoanal coil with external phased array coil techniques. J Comput Assist Tomogr 1998; 22:357-363.
12. Stoker J, Lameris JS. MR imaging of perianal fistulas using body and endoanal coils. AJR Am J Roentgenol 1999; 172:1139-1140.
13. deSouza NM, Hall AS, Puni R, Gilderdale DJ, Young IR, Kmiot WA. High resolution magnetic resonance imaging of the anal sphincter using a dedicated endoanal coil. Comparison of magnetic resonance imaging with surgical findings. Dis Colon Rectum 1996; 39:926-934.
14. deSouza NM, Puni R, Gilderdale DJ, Bydder GM. Magnetic resonance imaging of the anal sphincter using an internal coil. Magn Reson Q 1995; 11:45-56.
15. Rociu E, Stoker J, Eijkemans MJ, Schouten WR, Lameris JS. Fecal incontinence: endoanal US versus endoanal MR imaging. Radiology 1999; 212:453-458.
16. Vos EK, Sambandamurthy S, Kamel M, et al. Clinical comparison between a currently available single-loop and an investigational dual-channel endorectal receive coil for prostate magnetic resonance imaging: a feasibility study at 1.5 and 3 T. Invest Radiol 2014; 49:15-22.
17. Haider MA, Krieger A, Elliott C, Da Rosa MR, Milot L. Prostate imaging: evaluation of a reusable two-channel endorectal receiver coil for MR imaging at 1.5 T. Radiology 2014; 270:556-565.
18. Stoker J, Rociu E, Zwamborn AW, Schouten WR, Lameris JS. Endoluminal MR imaging of the rectum and anus: technique, applications, and pitfalls. Radiographics 1999; 19:383-398.
19. Dwarkasing RS, Schouten WR, Geeraedts TE, Mitalas LE, Hop WC, Krestin GP. Chronic anal and perianal pain resolved with MRI. AJR Am J Roentgenol 2013; 200:1034-1041.
20. Powell DK, Kodsi KL, Levin G, Yim A, Nicholson D, Kagen AC. Comparison of comfort and image quality with two endorectal coils in MRI of the prostate. J Magn Reson Imaging 2014; 39:419-426.

chapter 3

chapter 3.1

Magnetic Resonance Imaging of Perianal Fistulas

Roy S. Dwarkasing
Shahid M. Hussain
Gabriel P. Krestin

Seminars in Ultrasound CT and MR. 2005 Aug;26(4):247-58. Review

ABSTRACT

Most cases of fistula-in-ano are nonspecific and result from inflammation of anal glands and crypts (cryptoglandular). The classification of cryptoglandular fistulas depends on the degree of involvement of the anal sphincter complex and determines the type of treatment. Studies have shown that preoperative MR imaging revealed important additional information compared with surgery alone and better predicts clinical outcome of patients with fistula-in-ano than initial surgical exploration. With the emergence of novel surgical treatments like MRI-guided surgery, laser, and adhesive treatments, MR imaging is a mainstay for pre-procedural and intra-operative evaluation to ensure the adequacy of the procedure.

INTRODUCTION

Fistula-in-ano is an abnormal communication between the anal canal and the perianal skin. Perianal abscess is an acute manifestation and fistula-in-ano a chronic condition of the same disease (1). In the surgical literature, cryptoglandular fistulas and abscesses are distinguished from fistulas and abscesses due to an underlying disease such as Crohn's disease (2). Fistulas resulting from an underlying disease are termed specific. Most cases of fistula-in-ano are nonspecific and result from inflammation of anal glands and crypts (cryptoglandular) (3,4). Anal glands, slightly more numerous in men than in women, are located at the level of the dentate line of the anal canal and sometimes penetrate through the internal anal sphincter and intersphincteric space into the ischioanal space (3). Infection of these glands due to predisposing factors such as an acute episode of diarrhea or trauma plays an essential role in the development of cryptoglandular fistulas (5,6) (Fig 1). The preva-

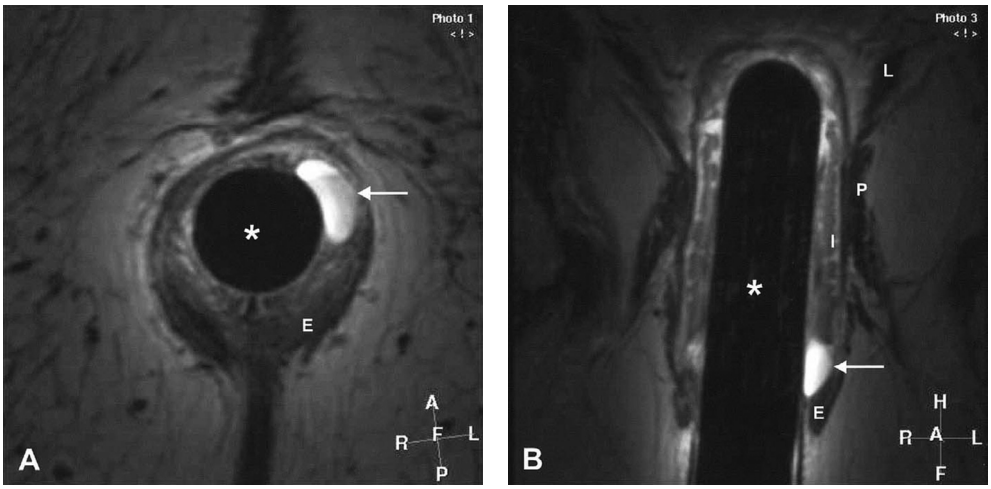

Figure 1. Anal sinus (pre-fistula stage). An anal sinus is a localized infection of the anal glands and crypts. (A) Axial T2-weighted fast spin-echo (FSE) endoanal MR image (TR/TE = 2000/150 ms). (B) Coronal T2-weighted FSE image (TR/TE = 2136/120 ms). A well-circumscribed lesion with high signal intensity on T2W images (arrow) can be seen submucosally. There are no additional fistula tracts. An anal sinus can heal completely or progress into a fistula. This patient had complaints of perianal pain in the last month, especially during defecation, without perianal discharge. E, external anal sphincter; I, internal anal sphincter; P, puborectalis muscle; L, levator ani muscle; Endoanal coil (*).

lence of this type of fistula is said to be approximately 10 per 100,000 of the general population (5). Specific or Crohn's fistulas and abscesses result from transmural spread of chronic granulomatous inflammation (3,6). The prevalence of Crohn's disease varies between 3 and 7 per 100,000 of the general population (3,6). Approximately 36% of Crohn's patients have perirectal disease, which results in the specific type of pelvic fistulas and abscesses (3,6). Perianal fistulas may also be caused by other conditions and events, including tuberculosis, trauma during childbirth, pelvic infection, pelvic malignancy, and radiation therapy.

This report describes the current views on diagnosis and treatment of perianal fistula disease. Recent developments in preoperative imaging with emphasis on magnetic resonance imaging (MRI) and pitfalls on MRI will be described and illustrated.

DIAGNOSIS AND CLASSIFICATION

3.1

Perianal fistulas and abscesses are often diagnosed clinically, based on typical symptomatology and physical examination (5). The exact relationship between the fistula and the anorectum, in particular the anal sphincter complex, is often not evident at physical examination. The classification of cryptoglandular fistulas depends on the degree of involvement of the anal sphincter complex and determines the type of surgical treatment. In addition to digital examination, rectosigmoidoscopy with or without mucosal biopsies and careful cannulation of the external opening with fistulography are traditional techniques for fistula evaluation. Fistulography, however, is an unreliable technique because the sphincter complex is not directly visualized, and the level of the internal opening in the anal canal is difficult to visualize because of the absence of precise anatomic landmarks. In addition, secondary fistulous tracks often fail to fill with contrast material (7,8). Cross-sectional imaging modalities, such as computed tomography, ultrasound, and MR imaging, have become standard imaging techniques for classification of perianal fistulas and abscesses. Computed tomography, performed with rectally and intravenously administered contrast media,

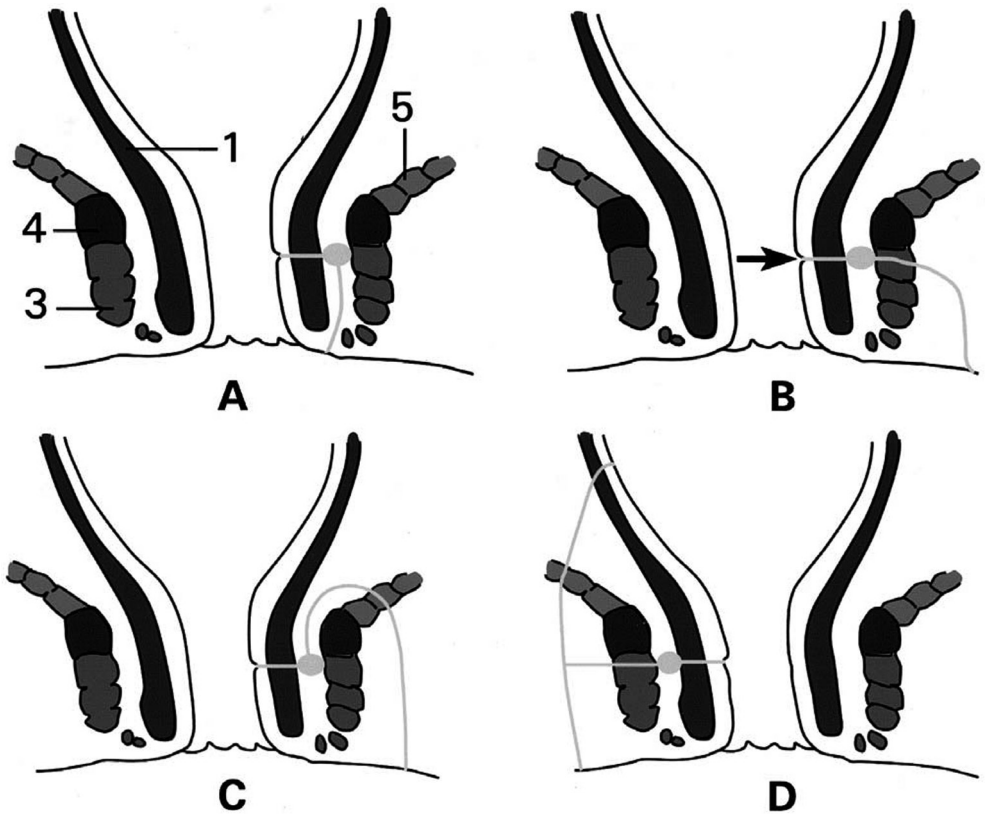

Figure 2. Classification of perianal fistulas according to Parks et al.14 (A) Intersphincteric fistula located between the internal (1) and external anal sphincter (3). (B) Trans-sphincteric fistulas (arrow) cross these muscles and run in the ischioanal space. (C) Suprasphincteric and (D) extrasphincteric fistulas are rare and show a complex course. Puborectalis muscle (4) and levator ani muscle (5). (Modified from Parks et al. (14))

showed some early promise (9,10). However, the attenuation values for the sphincters, levator ani, fibrotic fistulous tracks, and active fistulas are so similar that it is difficult to characterize these structures accurately, unless the track contains gas or leaked contrast material. Anal endosonography (AES), though also promising, has proved inferior to expert clinical assessment (11). The external sphincter can be difficult to assess in some individuals. In addition, infection cannot be distinguished from fibrosis with this technique, and insufficient depth penetration results in a failure to identify secondary fistulous extensions in some cases (4,11).

Contrast-enhanced (with hydrogen peroxide) AES appears to be superior to non-contrast AES in the preoperative assessment of anal and anovaginal fistulas and in demonstrating and locating their internal openings (12). West et al. showed good agreement between hydrogen peroxide-enhanced three-dimensional AES and endoanal magnetic resonance imaging especially for classification of the primary fistula track and location of the internal opening compared with surgical findings in patients with a visible external opening of perianal fistulas. However, there is no place for contrast enhanced EAS when an external opening is not visible or cannulation of the external opening is not possible (13).

Due to the multiplanar capability and high inherent soft tissue contrast, MR imaging has been suggested as the modality of choice for classification of perianal fistulas and abscesses (4,5). Cryptoglandular fistulas, predominantly located at the level of the anal canal and direct surroundings, can be classified according to the classification by Parks et al (14) (Figs 1 and 2). This classification is used most often. Recently Morris et al presented a classification of five MR imaging- based grades. If the ischioanal and ischiorectal fossae are unaffected, disease is likely confined to the sphincter complex (Grade 1, simple linear intersphincteric fistula; Grade 2, intersphincteric fistula with abscess or secondary track), and outcome following simple surgical management is favorable. Involvement of the ischioanal or ischiorectal fossa by a fistulous track or abscess indicates complex disease related to trans-sphincteric or suprasphincteric disease (Grade 3, trans-sphincteric fistula; Grade 4, trans-sphincteric fistula with abscess or secondary track within the ischiorectal fossa) (15). Correspondingly, more complex surgery may be required that may threaten continence or may require colostomy to allow healing. If the track traverses the levator plate, a translevator fistula is present (Grade 5, supralevator and translevator disease), and a source of pelvic sepsis should be sought. Studies have shown that preoperative MR imaging revealed important additional information compared with surgery alone and better predicts clinical outcome of patients with fistula-in-ano than initial surgical exploration (16,17).

TREATMENT

The treatment of cryptoglandular fistulas is mainly surgical, with a number of options. To understand the surgical options for treating fistulous disease, one must first consider the anatomy and function of the anal sphincters and the causes of perianal fistulas. The internal sphincter is involuntary and is composed of smooth muscle continuous with the circular smooth muscle of the rectum. It is responsible for 85% of resting anal tone. In most individuals, it can be divided without causing a loss of continence. The external sphincter is composed of striated muscle and is continuous superiorly with the puborectalis and levator ani muscles. It contributes only 15% of resting anal tone, but its strong voluntary contractions resist defecation (15). A division of the external sphincter can lead to incontinence. Preser-

vation of fecal continence is a paramount consideration, and treatment strategies aim to preserve the integrity of the external sphincter. Fistulotomy, fistulectomy, drain placement, advancement flap closure, and fecal deviating colostomy are traditional techniques for fistula surgery (2,6). Fistulotomy, which denotes only the unroofing of a fistula, is preferred to fistulectomy, which involves the unroofing and coring out of a fistula in combination with excision of the sphincter muscle below the level of the internal opening. In general, intersphincteric and low trans-sphincteric fistulas are preferably treated with fistulotomy, whereas other types of fistulas require stepwise or modified procedures. The treatment of perianal abscesses, due either to cryptoglandular disease or Crohn's disease, is incision and drainage (2,6,18). Fecal deviating colostomy is reserved for patients with uncontrollable extensive perianal fistulous disease and severe clinical symptoms, which usually is associated with Crohn's proctitis (6). Novel surgical treatments include laser and adhesive treatments. The use of laser ablation or fibrin glue to treat fistula seems attractive, especially in more complex fistulas (19,20). There are promising reports of human granulocyte colony stimulating factor, as an alternative to fibrin glue in the treatment of perianal Crohn's fistula (21). MRI-guided surgery for anal fistula is feasible. Pre-procedural and intraoperative MRI techniques can be used to identify the extent of the fistula tracts and septic foci and to ensure the adequacy of the surgical procedure. It can thus prevent an incomplete procedure and the potential requirement for a second operation. It may become particularly useful in surgery for recurrent and complex anal fistulas and may lead to fewer recurrences (22).

MRI OF PERIANAL FISTULA DISEASE

Cryptoglandular Fistulas

A typical cryptoglandular fistula has an internal opening at the level of the anal canal, a primary tract, and an external opening (5). Occasionally, cryptoglandular fistulas have a secondary tract, a horseshoe shaped spread, an abscess, and more than one external opening.

At T2-weighted MR images, fistulas have a distinct appearance, with a central high signal intensity tract that is surrounded by a relatively low signal intensity wall (5). Presumably, the inner high signal intensity region of fistulas consists of the true lumen and granulation tissue, and the outer part of fistulas with lower signal intensity is comprised of fibrotic tissue. The ratio of high and low signal intensity areas is expected to decrease as a fistula becomes more chronic, which is consistent with the development of an increasing amount of fibrotic tissue (4,5). Most of the MR images of cryptoglandular fistulas shown in the present review were acquired by using an endoanal coil at a 1.5 T MR imager (Gyroscan NT Intera 1.5; Philips Medical Systems, Best, the Netherlands). The endoanal coil is commercially available (Philips Medical Systems) and consists of a fixed, rectangular, 60 mm long rigid receiver with a width of 16 mm. The coil is contained within an 80 mm long cylindrical coil holder with a diameter of 19 mm. Before the introduction of the coil into the anal canal, a condom was placed over the coil and ultrasound gel was used as a lubricant. The coil was introduced while the patient was lying in the left lateral position. After the coil was introduced, each patient carefully turned onto his or her back, and the position of the coil was rechecked. For MR imaging sequences, the following parameters are suggested: axial three dimensional turbo spin echo images [repetition time (TR) = 2000 ms, effective echo time (TE) = 150-170 ms, field of view = 140 mm, matrix = 68 x 256, slice thickness = 2 mm without gaps, 60 slices], coronal, and sagittal two-dimensional turbo spin-echo images (TR = 2100 ms, effective TE = 120 ms, field of view = 120 mm, matrix = 205 x 256, slice thickness = 4 mm/0.4 mm).

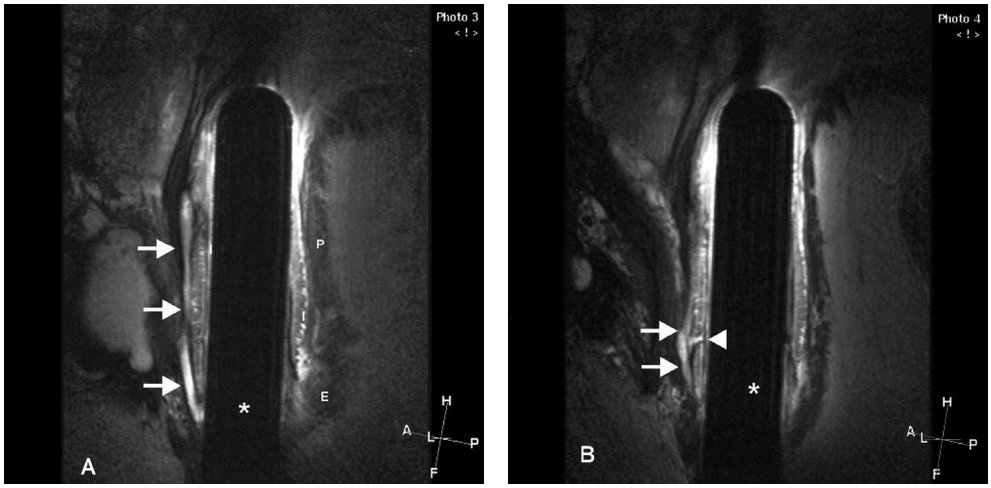

Figure 3. Intersphincteric fistula. (A) Sagittal T2-weighted fast spin-echo endoanal MR image (TR/TE = 2443/100 ms) with an intersphincteric fistula (arrows) displayed in full extent. (B) Sagittal slice next to (A) shows an internal opening (arrowhead) in the lower part of the fistula. I, internal anal sphincter; E, external anal sphincter; P, puborectalis muscle; endoanal coil (*). Compare with Fig. 1, which illustrates the classification of perianal fistulas according to Parks et al.14

At MR imaging, the identification and localization of the entire cryptoglandular fistula, including the external opening, the primary tract, secondary tracts, abscesses, and the internal opening, are essential for fistula classification and treatment. Fistulas with unrecognized

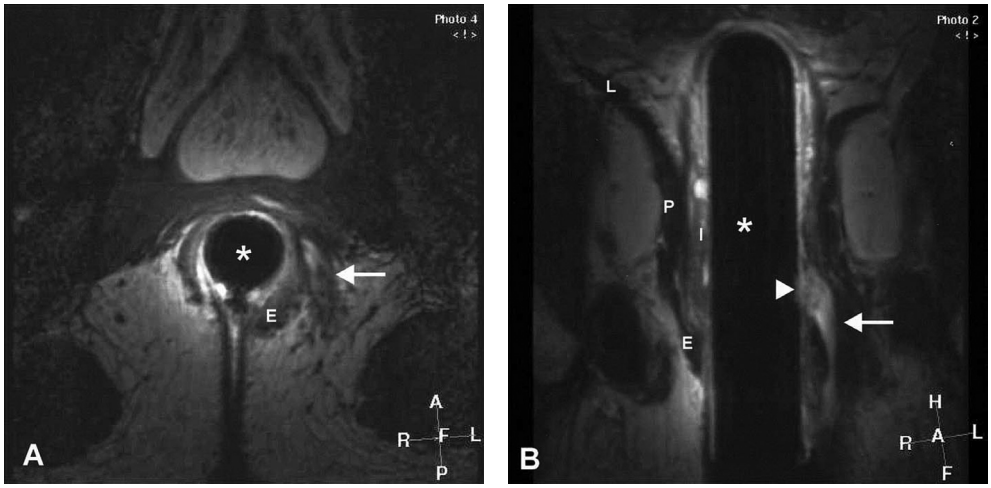

Figure 4. Low trans-sphincteric fistula. (A) Axial T2-weighted fast spin-echo (FSE) endoanal MR image (TR/TE = 2000/170 ms). An active fistula with high signal intensity (arrow) is seen tracking through the external sphincter muscle (E) on the left. Endoanal coil (*). (B) Coronal T2-weighted FSE image
(TR/TE = 2136/150 ms). The fistula (arrow) is displayed almost to full extent tracking through the lower half of the external anal sphincter. The internal opening of the fistula in the anal canal (arrowhead) is clearly demonstrated. E, external anal sphincter; I, internal anal sphincter; P, puborectalis muscle; L, levator ani muscle; endoanal coil (*).

3.1

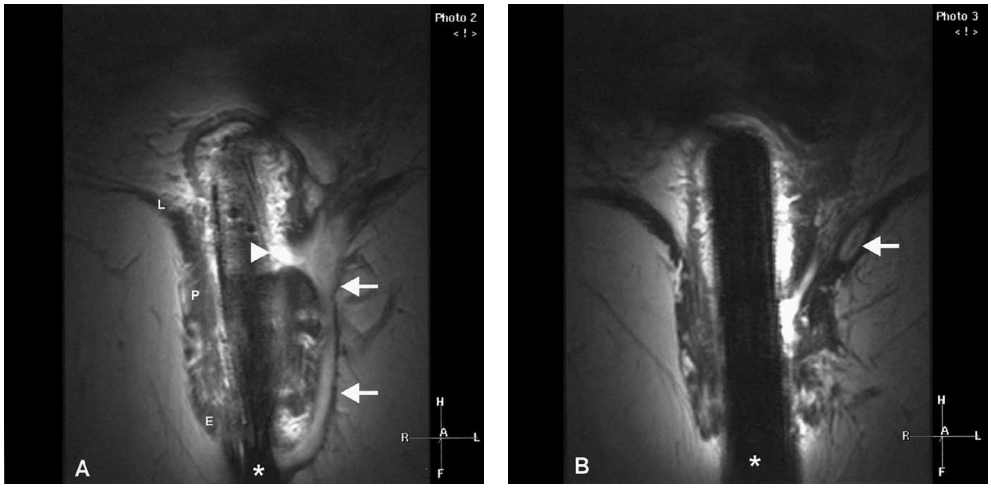

Figure5. High trans-sphincteric fistula with secondary extension. (A) Coronal T2-weighted fast spin-echo endoanal MR image (TR/TE = 2443/100 ms) shows a high trans-sphincteric fistula (arrows) with the internal opening (arrowhead) at the level of the junction of the puborectal muscle (P) and the levator plate (L). E, external anal sphincter; endoanal coil (*). (B) On the next coronal slice one can see an extension of fistula (arrow) within the left sided levator ani muscle causing local thickening (compare with the right sided levator ani muscle). Endoanal coil (*).

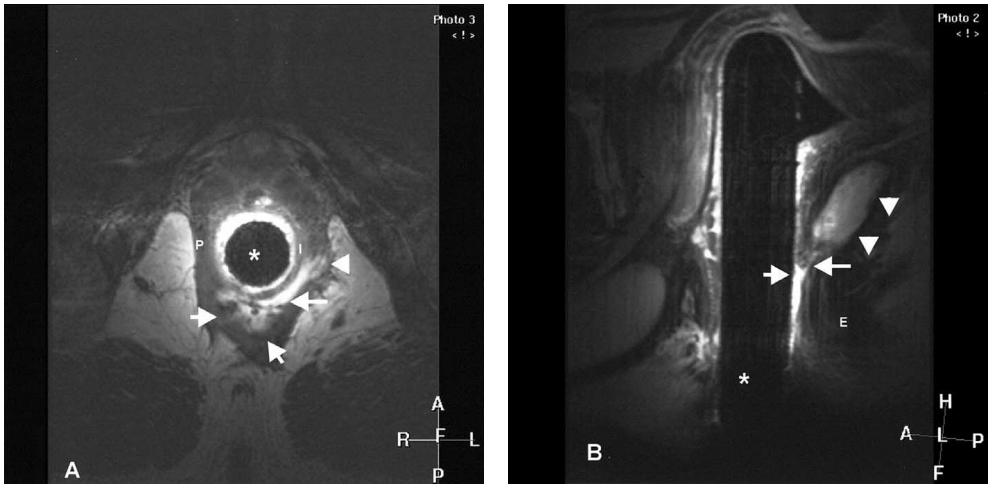

Figure 6. Intersphincteric abscess. (A) Axial T2-weighted fast spin echo (FSE) endoanal MR image (TR/TE = 2500/100 ms). Circumferential spread of fistula to the left (long arrow) predominantly within the intersphincteric space; also small extension of fistula is seen within the puborectalis muscle (arrowhead). In the midline posteriorly, local widening of the fistula (arrows) can be seen in the intersphincteric space, indicative of an abscess. I, internal anal sphincter; P, puborectalis muscle. (B) On the mid-sagittal T2-weighted FSE
(TR/TE = 2454/100 ms) image the abscess can clearly be demonstrated (arrowheads). Note that part of the fistula (arrow) with an internal opening in the anal canal (small arrow) can also be seen on this slice. E, external anal sphincter; endoanal coil (*).

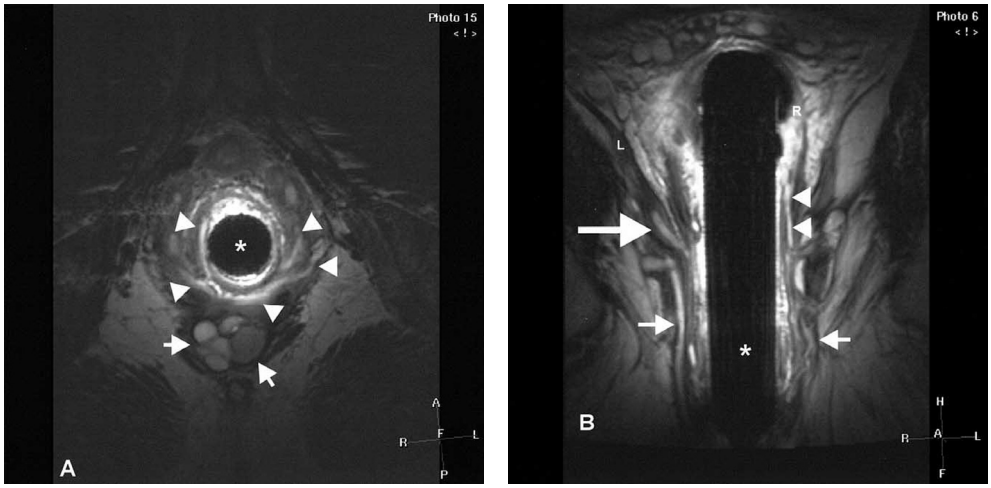

Figure 7. Horseshoe-type fistula with fluid collection. (A) Axial T2-weighted fast spin-echo (FSE) endoanal image (TR/TE = 2500/100 ms). Multiple circumferential spread of fistula tracks within the sphincter complex (arrowheads) with a fluid collection in the ischioanal space posteriorly (arrows). Please note the multiloculated aspect of the fluid collection with slightly different signal intensity within, suggestive of a chronic abscess. Endoanal coil (*). (B) On the coronal T2-weighted FSE image (TR/TE = 2443/100 ms) fistula extensions are also seen cranially within the external sphincter and puborectalis muscles (small arrows) and in the levator ani muscle (L) on the right (thick arrow). On the left cranial extension of a fistula track is seen into the rectal wall (arrowheads). R, rectum; endoanal coil (*).

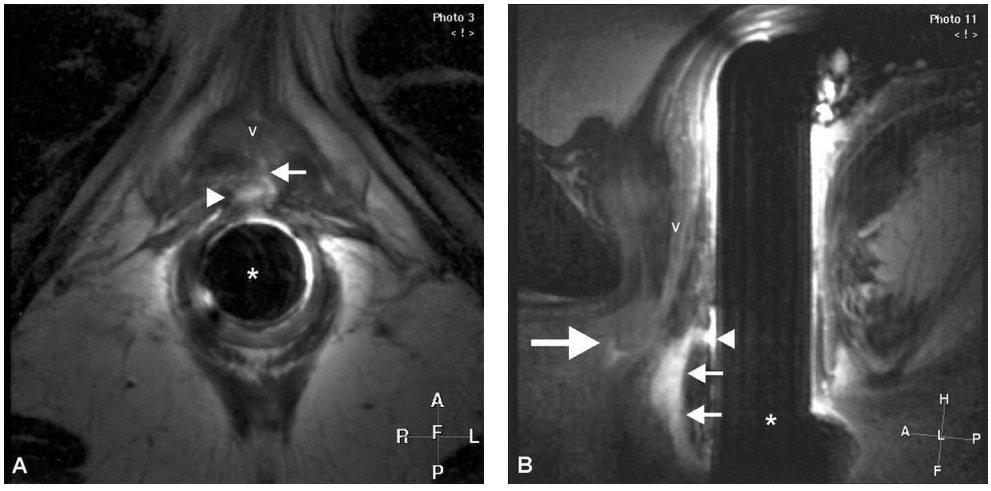

Figure 8. Concurrent perianal and anovaginal fistula. (A) Axial T2-weighted fast spin-echo (FSE) endoanal MR image (TR/TE = 2454/100 ms) with a perianal fistula (arrow) anteriorly extending from the anal canal to the lower part of the vagina. Local widening of the fistula tract (arrowheads) at the level of the rectovaginal septum can be seen, indicative of a small abscess. V, vagina; endoanal coil (*). (B) On the mid sagittal T2-weighted FSE image (TR/TE = 2443/100 ms), the anovaginal fistula track is demonstrated with the internal opening in the anal canal (arrowhead) and the internal opening in the vagina (thick arrow). The perianal fistula track (small arrows) is also demonstrated on this slice. V, vagina; endoanal coil (*).

3.1

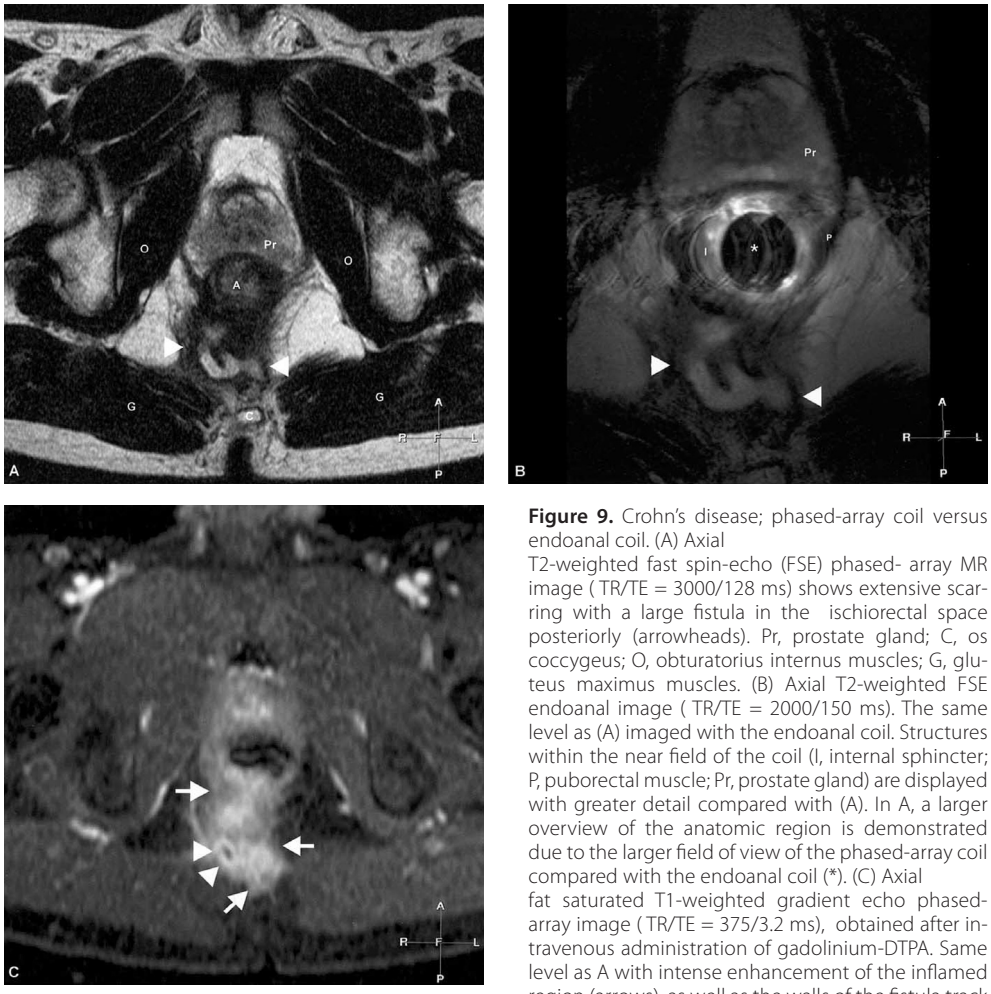

Figure 9. Crohn's disease; phased-array coil versus endoanal coil. (A) Axial T2-weighted fast spin-echo (FSE) phased- array MR image (TR/TE = 3000/128 ms) shows extensive scarring with a large fistula in the ischiorectal space posteriorly (arrowheads). Pr, prostate gland; C, os coccygeus; O, obturatorius internus muscles; G, gluteus maximus muscles. (B) Axial T2-weighted FSE endoanal image (TR/TE = 2000/150 ms). The same level as (A) imaged with the endoanal coil. Structures within the near field of the coil (I, internal sphincter; P, puborectal muscle; Pr, prostate gland) are displayed with greater detail compared with (A). In A, a larger overview of the anatomic region is demonstrated due to the larger field of view of the phased-array coil compared with the endoanal coil (*). (C) Axial fat saturated T1-weighted gradient echo phased-array image (TR/TE = 375/3.2 ms), obtained after intravenous administration of gadolinium-DTPA. Same level as A with intense enhancement of the inflamed region (arrows), as well as the walls of the fistula track (arrowheads). Extensive disease can favor the use of surface coils to obtain as much information as possible with the larger field of view compared to the endoluminal coils. Also the use of intravenous gadolinium in combination with fat suppression techniques may increase the conspicuity of the lesions, allowing the diagnosis to be made with confidence.

components may cause problems during surgery and are more likely to recur (2,4,6). Cryptoglandular fistulas are often relatively small and are located close to the anal sphincter complex (4,6). MR imaging with an endoanal surface coil provides high resolution images of the anal sphincter complex and is also accurate in the depiction and classification of cryptoglandular fistulous disease (4). If one considers the anatomic knowledge obtained by using the endoanal coil, MR imaging with a phased array coil may also be sufficient for classification of cryptoglandular fistulas (23,24). Localization of the internal opening with respect to the anal verge and anal sphincter complex is the first and most important step for the classification of the cryptoglandular fistulas (6). After identification of the primary tract, the distinction between an intersphincteric (Fig 3) and a trans-sphincteric (Figs 4 and 5) tract

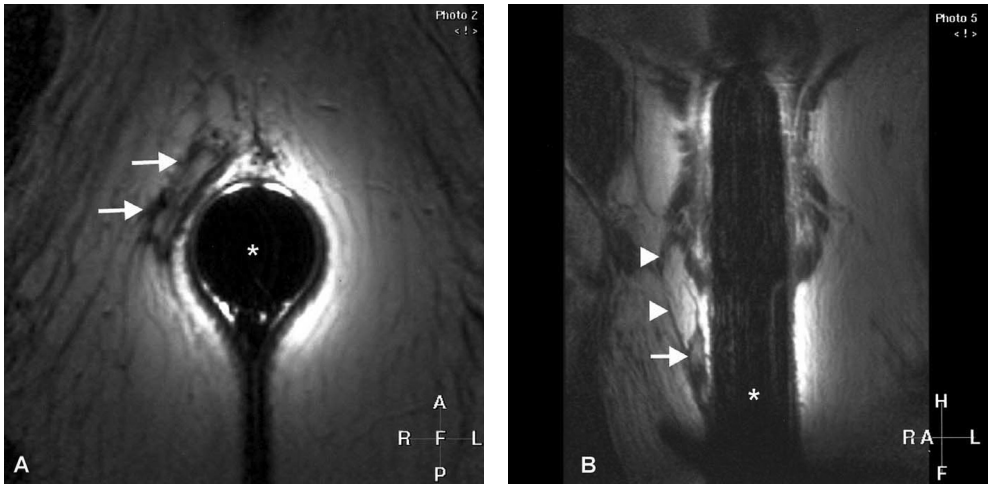

Figure 10. Subsphincteric fistula. Small fistula track is seen on the right (arrows). (A) Axial T2-weighted fast spin- echo (FSE) endoanal MR image (TR/TE = 2500/100 ms). (B) Coronal T2-weighted FSE image (TR/TE = 2443/100 ms). (B) Thin fibrous strand (arrowheads) is seen extending from the fistula to the sphincter muscles. Endoanal coil (*).

is often a challenge. Typically, an intersphincteric tract runs in a straight or a spiral path between the internal and the external anal sphincters within the intersphincteric space (Fig 3). A typical trans-sphincteric tract runs through the external anal sphincter into the ischioanal space (Fig 4 and 5). The distance between a trans-sphincteric tract and the external anal sphincter may differ; some tracts run directly outside the external anal sphincter, whereas others are located a few centimeters from it. Secondary tracts are the side branches of a primary tract (Figs 5 and 6). In 5% to 15% of patients with cryptoglandular fistula disease, secondary extensions outside the anal sphincter are present (2,25). If present, secondary tracts are relatively small, and abscesses may or may not be present (Figs 6 and 7).

Any widening of the primary or the secondary tract is considered a fistulous abscess (1). MR imaging enables direct multiplanar visualization of the anatomic structures and spaces, which facilitates the detection and localization of secondary tracts and abscesses. The presence, size, and exact location of a secondary tract and abscess should be described. Cryptoglandular horseshoe shaped fistulas (Fig 7) can accurately be assessed with MR imaging (4,5,26). Any type of fistula may show a circumferential spread, but a typical horseshoe shaped fistula has two fistula tracks within the ischioanal space and one internal opening, often in the midline posteriorly at the level of the inferior border of the puborectalis muscle. Horseshoe shaped fistulas should be distinguished especially from trans-sphincteric fistulas. Sometimes one leg of a horseshoe shaped fistula may be shorter than the other, with only one external opening. Such a fistula could be misclassified as a simple trans-sphincteric fistula during surgical assessment (4). Anovaginal fistulas with typical symptoms of recurrent vaginal infections with vaginal flatus and vaginal defecation can clearly be depicted with MR imaging using an endoanal coil (27) (Fig 8).

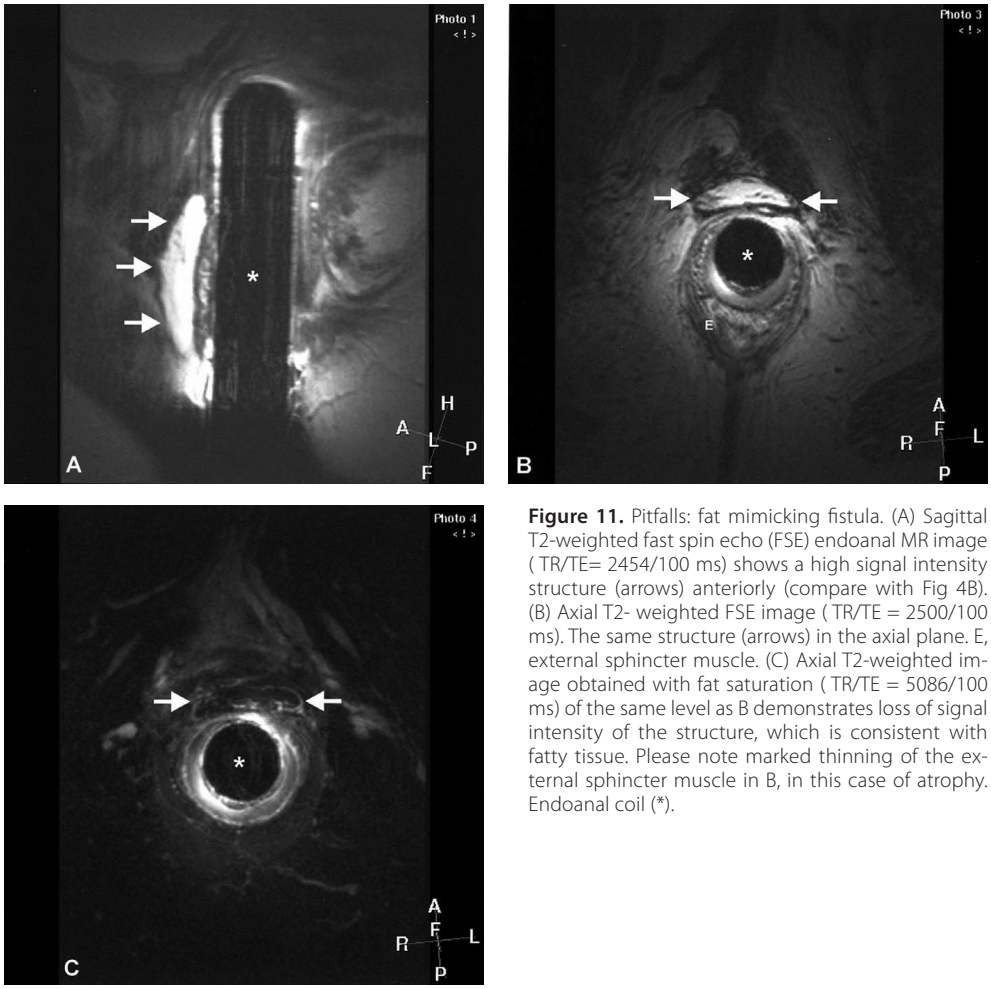

Figure 11. Pitfalls: fat mimicking fistula. (A) Sagittal T2-weighted fast spin echo (FSE) endoanal MR image (TR/TE= 2454/100 ms) shows a high signal intensity structure (arrows) anteriorly (compare with Fig 4B). (B) Axial T2- weighted FSE image (TR/TE = 2500/100 ms). The same structure (arrows) in the axial plane. E, external sphincter muscle. (C) Axial T2-weighted image obtained with fat saturation (TR/TE = 5086/100 ms) of the same level as B demonstrates loss of signal intensity of the structure, which is consistent with fatty tissue. Please note marked thinning of the external sphincter muscle in B, in this case of atrophy. Endoanal coil (*).

Crohn's Fistulas

Typical Crohn's fistulas consist of multiple tracks and abscesses.

A well-defined primary fistula track is often not recognizable (6). The tracks tend to be relatively large, often with circumferential or horseshoe shaped spread and intramuscular spread (Fig 9). In addition to the anal canal, the tracts may involve the rectum, sigmoid colon, small bowel loops, and other pelvic organs such as bladder and vagina (6). The fistulas and abscesses can be located below, within, or above the level of the levator ani muscle. There may not be an internal opening at the level of the anal canal. An external opening in the perineum may be absent, or there may be several external openings. The use of an intraluminal coil can be avoided in favor of phased array multicoils to obtain as much information as possible with the larger field of view compared to endoanal coil (3,6). Also the use of gadolinium in combination with fat suppression techniques may increase the conspicuity of the lesions, allowing the diagnosis to be made with confidence (3,6) (Fig 9).

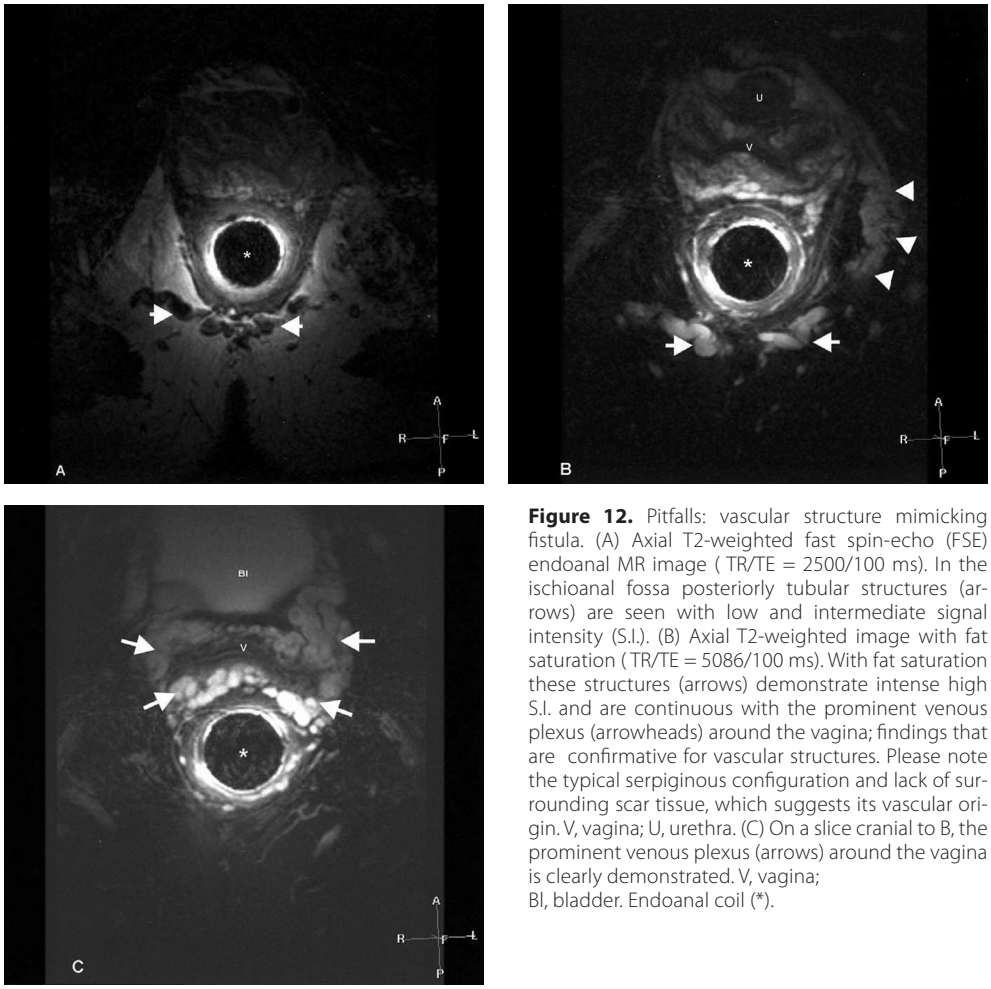

Figure 12. Pitfalls: vascular structure mimicking fistula. (A) Axial T2-weighted fast spin-echo (FSE) endoanal MR image (TR/TE = 2500/100 ms). In the ischioanal fossa posteriorly tubular structures (arrows) are seen with low and intermediate signal intensity (S.I.). (B) Axial T2-weighted image with fat saturation (TR/TE = 5086/100 ms). With fat saturation these structures (arrows) demonstrate intense high S.I. and are continuous with the prominent venous plexus (arrowheads) around the vagina; findings that are confirmative for vascular structures. Please note the typical serpiginous configuration and lack of surrounding scar tissue, which suggests its vascular origin. V, vagina; U, urethra. (C) On a slice cranial to B, the prominent venous plexus (arrows) around the vagina is clearly demonstrated. V, vagina;
Bl, bladder. Endoanal coil (*).

Pitfalls

Medical history, clinical examination, and findings from other investigations may help to avoid pitfalls during MR imaging of pelvic fistulas. Small fistulas confined to the subcutaneous fatty tissue (sub-sphincteric) (Fig 10) may fall outside the imaging field. Confirmation that the region of interest is within the field of view is essential. Fatty tissue may show a configuration that mimic a fistula track (Fig 11). This is often seen in cases of atrophy of the sphincter muscles where muscle fibers are replaced by fatty tissue. In these cases a fistula track can be excluded with confidence on the fat saturated images. Vascular structures can sometimes be prominent in the ischioanal fossa (Fig 12). The typical tubular configuration, which is continuous with the normal vascular channels (e.g., venous plexus from vagina or prostate), helps to make the differentiation from fistulas. Hemorrhoids can resemble small submucosal fluid collections on MR images. Fistulas located at the anterior aspect of the anorectum may simulate rectovaginal, recto-urethral, or rectovesical fistulas (27).

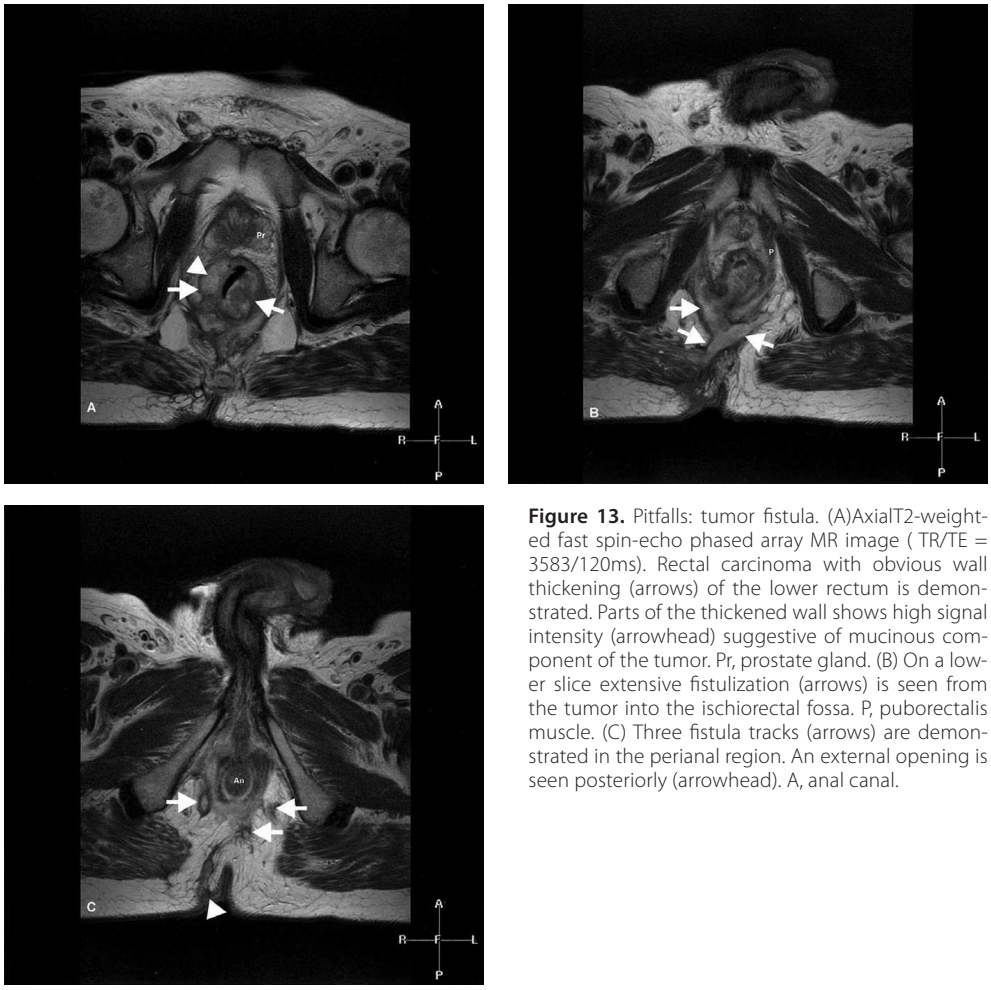

Figure 13. Pitfalls: tumor fistula. (A)AxialT2-weighted fast spin-echo phased array MR image (TR/TE = 3583/120ms). Rectal carcinoma with obvious wall thickening (arrows) of the lower rectum is demonstrated. Parts of the thickened wall shows high signal intensity (arrowhead) suggestive of mucinous component of the tumor. Pr, prostate gland. (B) On a lower slice extensive fistulization (arrows) is seen from the tumor into the ischiorectal fossa. P, puborectalis muscle. (C) Three fistula tracks (arrows) are demonstrated in the perianal region. An external opening is seen posteriorly (arrowhead). A, anal canal.

Clinical correlation is essential. At MR imaging, old inactive fibrotic tissue in the perianal region, which sometimes produces perianal pain and simulates a recurrent fistula, may be difficult to distinguish from a recurrent or a longstanding active fistula. Imaging during a period with clinically evident symptoms, preferably with perianal inflammation and fluid discharge, may be helpful. Pelvic abscesses with perianal fistulous tracts may occur in Crohn's disease, AIDS, tuberculous or ulcerative colitis, or amoebiasis or may occur secondary to trauma, irradiation, and previous pelvic surgery (4,6). Perianal fistulous tracts with fluid collection in the ischioanal fossa may be due to malignant disease, for example, rectal mucinous adenocarcinoma (Fig 13). Medical history, symptomatology, and clinical examination, as well as contrast-enhanced MR imaging are essential to make the differentiation from benign fluid collections.

CONCLUSION

The present review illustrates that imaging in the preoperative workup of perianal fistula disease is essential. Studies have shown that preoperative MR imaging revealed important additional information compared with surgery alone and better predicts clinical outcome of patients with fistula-in-ano than initial surgical exploration. With the emergence of novel surgical treatments like MRI guided surgery, laser, and adhesive treatments, MR imaging is a mainstay for pre-procedural and intraoperative evaluation to ensure the adequacy of the procedure. MRI can thus prevent an incomplete procedure and the potential requirement for a second operation. In addition, it can also be used as a tool to follow up disease activity.

REFERENCES

1. Hussain SM, Stoker J, Schutte HE, et al: Imaging of the anorectal region. Eur J Radiol 22:116-122, 1996.
2. Shouler PJ, Grimley RP, Keighley MR, et al: Fistula in ano is usually simple to manage surgically. Int J Colorectal Dis 1:113-115, 1986.
3. O'Donovan AN, Somers S, Farrow R, et al: MR imaging of anorectal Crohn's disease: A pictorial essay. Radio graphics 17:101-107, 1997.
4. Hussain SM, Stoker J, Schouten WR, et al: Fistula in ano: Endoanal sonography versus endoanal MR imaging in classification. Radiology 200:475-481, 1996.
5. Hussain SM: Anal fistulae, in Hussain SM, ed: Imaging of Anorectal Diseases. London, Greenwich Medical Media, 1998:55–73.
6. Hussain SM, Outwater EK, Joekes EC, et al: Clinical and MR imaging features of cryptoglandular and Crohn's fistulas and abscesses. Abdom Imaging 25:67-74, 2000.
7. Kuijpers HC, Schulpen T: Fistulography for fistula in ano: Is it useful? Dis Colon Rectum 28:103-104, 1985.
8. Weisman RI, Orsay CP, Pearl RK, et al.: The role of fistulography in fistula in ano: Report of 5 cases. Dis Colon Rectum 34:181-184, 1991 9.
9. Guillaumin E, Jeffrey RB, Shea WJ, et al: Perirectal inflammatory disease: CT findings. Radiology 161:153-157, 1986.
10. Yousem DM, Fishman EK, Jones B: Crohn disease: Perirectal and perianal findings at CT. Radiology 167:331-334, 1988.
11. Choen S, Burnett S, Bartram CI, et al: Comparison between anal endosonography and digital examination in the evaluation of anal fistulae. Br J Surg 78:445-447, 1991.
12. Sudol-Szopinska I, Jakubowski W, Szczepkowski M: Contrast enhanced endosonography for the diagnosis of anal and anovaginal fistulas. J Clin Ultrasound 30:145-50, 2002.
13. West RL, Zimmerman DD, Dwarkasing S, et al: Prospective comparison of hydrogen peroxide-enhanced three dimensional endoanal ultrasonography and endoanal magnetic resonance imaging of perianal fistulas. Dis Colon Rectum 46:1407-1415, 2003.
14. Parks AG, Gordon PH, Hardcastle JD: a Classification of anal fistula. Br J Surg 63:1- 2, 1976.
15. Morris J, Spencer JA, Ambrose NS: MR imaging classification of perianal fistulas and its implications for patient management. Radiographics 20:623-37, 2000.
16. Chapple KS, Spencer JA, Windsor AC, et al: Prognostic value of magnetic resonance imaging in the management of fistula in ano. Dis Colon Rectum 43:511-516, 2000.
17. Beets-Tan RG, Beets GL, van der Hoop AG, et al: Preoperative MR imaging of anal fistulas: Does it really help the surgeon? Radiology 218:75-84, 2001.
18. Ascher SM, Semelka RC: Peritoneal cavity, in Semelka RC, Ascher SM, Reinhold C: MRI of the Abdomen and Pelvis. A Text-Atlas. New York, Wiley-Liss, 1997:329-353.
19. Bodzin JH: Laser ablation of complex perianal fistulas preserves continence and is a rectum sparing alternative in Crohn's disease patients. Am Surg 64:627-631, 1998.
20. Lindsey I, Smilgin-Humphreys MM, Cunningham C, et al: A randomized, controlled trial of fibrin glue vs. conventional treatment for anal fistula. Dis Colon Rectum 45:1608-1615, 2002.
21. Vaughan D, Drumm B: Treatment of fistulas with granulocyte colony-stimulating factor in a patient with Crohn's disease. N Engl J Med 340:239-240, 1999.
22. Gould SW, Martin S, Agarwal T, et al: Image guided surgery for anal fistula in a 0.5T interventional MRI unit. J Magn Reson Imaging 16: 267-276, 2002.
23. Halligan S, Bartram CI: MR imaging of fistula in ano: Are endoanal coils the gold standard? AJR Am J Roentgenol 171:407-412, 1998.
24. Beets-Tan RG, Beets GL, van der Hoop AG, et al: High resolution magnetic resonance imaging of the anorectal region without an endocoil. Abdom Imaging 24:576-581, 1999.
25. Seow-Choen F, Phillips RK: Insights gained from the management of problematical anal fistulae at St. Mark's Hospital: Br J Surg 78:539-541, 1991.

26. Barker PG, Lunniss PJ, Armstrong P, et al: Magnetic resonance imaging of anal fistula: Technique, interpretation and accuracy. Clin Radiol 49:7-13, 1994.
27. Dwarkasing S, Hussain SM, Hop WC, et al: Anovaginal fistulas: Evaluation endoanal MR imaging. Radiology 231:123-128, 2004.

chapter 3.2

Anovaginal Fistulas: Evaluation with Endoanal MR Imaging

Roy S. Dwarkasing
Shahid M. Hussain
Wim C. J. Hop
Gabriel P. Krestin

Radiology. 2004 Apr;231(1):123-8.

ABSTRACT

Purpose To evaluate endoanal magnetic resonance (MR) imaging in the assessment of anovaginal fistulas and associated findings.

Material and methods In a retrospective descriptive study, two radiologists systematically reviewed MR findings in 20 patients with a clinically proved anovaginal fistula and looked for the main fistula tract, the internal opening in the anal canal and/or vagina, secondary fistula tracts, abscesses within the rectovaginal septum, and sphincter damage. Interobserver variability was calculated, and clinical records were searched for possible underlying causes that could explain the complexity of anovaginal fistulas. The κ value was calculated. Patients with or without a complex anovaginal fistula were compared in regard to the presence of any underlying disease or condition. Statistical significance was calculated with the Fisher exact test.

Results In all 20 patients, anovaginal fistulas were identified on T2-weighted MR images as predominantly high signal intensity linear abnormalities extending between the anal canal and the vagina. In all patients, the fistulas were typically located in the sagittal plane, and the mean distance from the anal verge to the fistula was 25.0 mm (range, 13–32 mm). The internal opening in the anal canal was detected in all patients. The internal opening in the vagina was detected in 19 (95%) patients. In seven (35%) patients, an anovaginal fistula with an additional abnormality was found and included an abscess within the rectovaginal septum (n= 1), a perianal fistula (n= 3), and a perianal fistula in combination with an abscess (n= 3). Defects of the external anal sphincter were present in three (15%) patients. There was complete agreement between observers for all items on endoanal MR images, except for the presence of secondary fistula extensions (agreement, 90%; κ, 0.74). History of obstetric trauma, pelvic floor surgery, or Crohn disease was present in 10 (50%) patients. Of these patients, six (60%) had a complex anovaginal fistula and four (40%) had a simple anovaginal fistula. In the remaining 10 patients without relevant medical history, one (10%) had a complex anovaginal fistula. This difference tended toward statistical significance (P= .057).

Conclusions Endoanal MR imaging allows evaluation of anovaginal fistulas and additional abnormalities, such as abscesses within the rectovaginal septum, secondary perianal fistula tracts, and sphincter damage.

INTRODUCTION

Anovaginal fistula is a socially disabling disease, in which patients pass gas and feces through the vagina and experience recurrent vaginal infections. In 5%–15% of patients with perianal fistula disease, secondary extensions outside the anal sphincter are present (1,2). Previous studies have shown anal sphincter defects to be an associated finding in patients with anovaginal or rectovaginal fistulas (3,4). To our knowledge, however, a comprehensive evaluation of anovaginal fistulas and a number of associated abnormalities suchc as edema and abscesses within the rectovaginal septum, additional fistula extensions, perianal fistulas, and concomitant sphincter damage with magnetic resonance (MR) imaging or another imaging modality has not been described. Accurate and comprehensive preoperative assessment with imaging of the course of the primary anovaginal fistula and possible secondary extensions or abscesses may improve surgical treatment of these fistulas.

Currently, an anovaginal fistula is diagnosed on the basis of typical clinical symptoms, such as recurrent vaginal infection with vaginal flatus and vaginal defecation, and a gynecologic or surgical examination performed with general anesthesia. In many institutions, the clinical diagnosis or suspicion of an anovaginal fistula is confirmed with imaging studies (5). These studies may include conventional fistulography and anal endosonography (6,7). Conventional fistulography may not be possible in many patients because the internal openings of the fistulas may not be visible at physical examination. Mainly because of this problem, fistulographic findings are reported to be correct in only 16% of patients with anal fistulas (6). Endoanal ultrasonography (US) is often inaccurate in the depiction of anovaginal fistulas, mainly because endoanal US has inherent low soft tissue contrast (7,8).

At our institution, endoanal MR imaging is routinely performed in the assessment of perianal fistulas. The role of endoanal MR imaging in the detection and classification of perianal fistulas is well established (7). Endoanal MR imaging has proved to be an excellent imaging modality in the assessment of anal sphincter anatomy, anal sphincter damage, and perianal fistulas (7,9). This modality provides multiplanar images with high inherent contrast resolution and high spatial contrast resolution of the anal canal, rectum, rectovaginal septum, and vagina (5,9). In particular, T2- weighted MR imaging sequences can depict lesions, such as fistulas and fluid collections, with high signal intensity (10). For surgical planning, the exact location of the main fistula and possible secondary extensions or abscesses must be established, and sphincter damage must be assessed. Thus, the purpose of this study was to evaluate endoanal MR imaging in the assessment of anovaginal fistulas and associated findings.

MATERIALS AND METHODS

Patients

We retrospectively reviewed all reports of endoanal MR imaging examinations of female patients that were performed between January 1997 and June 2000. During this period, 443 female patients were referred to the MR imaging section at our institution for work up of suspected anorectal abnormalities. The MR imaging reports were cross-referenced with the clinical records and follow-up data. Our Medical Ethics Committee did not require its approval or patient informed consent for this study.

We found 36 consecutive patients who were referred because of suspected or proved anovaginal fistula. Patients were included in this study if they had either (a) evidence of anovaginal fistula at exploratory surgery or at examination by the surgeon or gynecologist with anorectoscopy and/or colposcopy or (b) persistent clinical symptoms of recurrent vaginal infections combined with the passage of gas, feces, or both through the vagina. Symptoms were present for more than 3 months.

Sixteen patients were excluded from the study because (a) no information was available concerning any of the inclusion criteria because patients were referred from other institutions (n = 9), (b) MR imaging revealed a perianal fistula instead of an anovaginal fistula that was subsequently confirmed at surgery (n = 5), or (c) anovaginal fistulas could not be confirmed with a gynecologic examination and anosigmoidoscopy (n = 1) or with a barium enema examination and general anesthesia (n = 1). Thus, the remaining 20 patients formed the study group.

In all 407 patients with endoanal MR imaging reports that were negative for anovaginal fistula, a careful search of clinical findings was performed by two authors (S.D., S.M.H.). The follow-up period was 2–5 years. In this survey, we were unable to detect any instances of anovaginal fistulas that were not mentioned initially on the MR imaging report but were subsequently mentioned in the clinical records or proved to exist, either with endoscopic or gynecologic examinations or at surgery or follow-up MR imaging.

The mean age of patients in the study group (n = 20) was 36 years (range, 20–55 years). All patients had anovaginal fistulas that were proved with exploratory surgery (n = 12), persistent clinical symptoms of the passage of gas and feces through the vagina with recurrent vaginal infections (n= 5), or surgery and/or gynecologic consultation and examination (n= 3). Two authors (S.D., S.M.H.) compared MR findings with the detailed descriptions of surgical findings in patient records, and patient follow-up status was assessed with clinical records and follow-up data available in the hospital information system.

MR Imaging

All MR imaging examinations were performed by using an endoanal coil with a 1.5-T MR imager (Gyroscan NT Intera 1.5; Philips Medical Systems, Best, the Netherlands). The endoanal coil is commercially available (Philips Medical Systems) and consisted of a fixed, rectangular, 60-mm long rigid receiver coil with a width of 16 mm. The coil is contained within an 80-mm long cylindrical coil holder with a diameter of 19 mm. Before the introduction of the coil into the anal canal, a condom was placed over the coil and US gel was used as a lubricant. The coil was introduced while the patient was lying in the left lateral position. After the coil was introduced, each patient carefully turned onto her back, and the position of the coil was rechecked.

In each patient, the following three sequences were used. Transverse T2-weighted contrast-enhanced fast field echo imaging was performed (repetition time msec/echo time msec, 23/14; acquisition time, 5 minutes 39 seconds; matrix, 205 x 256; flip angle, 60°; field of view, 140 mm; section thickness, 2 mm with no gaps; and two signals acquired). Contrast-enhanced fast field echo is a term used by Philips Medical Systems and does not indicate contrast material administration. Transverse T2-weighted fast spin echo [SE] MR imaging was performed with and without fat saturation (5,086/100; acquisition time, 2 minutes 23

seconds; matrix, 186 x 256; flip angle, 90°; field of view, 120 mm; section thickness, 4 mm with a 0.4-mm gap; and three signals acquired). Coronal and sagittal T2-weighted SE MR imaging was performed without fat saturation (2,454/ 100; acquisition time, 2 minutes 34 seconds; matrix, 186 x 256; flip angle, 90°; field of view, 120 mm; section thickness, 4 mm with a 0.4-mm gap; and four signals acquired).

Image Review

All MR images were transported from local digital media to a viewing station and were systematically and independently reviewed by two radiologists. Interobserver variability was calculated on the basis of the κ statistics. After calculating the κ value, images with disagreement were reevaluated with both observers working together, and consensus was reached. One radiologist (S.D.) had 1 year of experience in abdominal imaging, which included MR imaging of the pelvic floor, and the other (S.M.H.) had practiced abdominal imaging for 6 years, with scientific interest in MR imaging of abdominal and anorectal diseases. All MR images were assessed for the following items: (a) the presence of ano- vaginal fistulas, (b) the localization of anovaginal fistulas, (c) the distance of anovaginal fistulas from the anal verge in the sagittal plane, (d) the internal opening of anovaginal fistulas in the anal canal, (e) the internal opening of anovaginal fistulas in the vagina, (f) the presence of edema or abscesses in the rectovaginal septum, (g) the presence of secondary perianal or other extensions, and (h) internal and external anal sphincter damage. An abscess within the rectovaginal septum was defined as a localized and well circumscribed dilatation of the main fistula or secondary extension with high signal intensity on the T2-weighted images, while edema was indicated by an ill-defined area of intermediate to high signal intensity around the area of the anovaginal fistula. Sphincter damage was identified as a local area of low signal intensity on the T2-weighted images, which indicated scarring or discontinuity of the internal or external anal sphincters. In addition, clinical records were searched by two authors (S.D., S.M.H.) for possible underlying conditions or diseases, such as obstetric trauma, pelvic floor surgery, or Crohn disease, that could explain the presence of simple or complex anovaginal fistulas. According to the literature (5), anovaginal fistulas were considered to be simple if only one fistulous tract was depicted that extended between the anal canal and the vagina. Anovaginal fistulas associated with any additional fistulous tracts or abscesses were considered to be complex (11,12).

Statistical analysis

All MR images were systematically and independently reviewed by two radiologists (S.D., S.M.H.). Interobserver variability was calculated on the basis of the κ statistics. After calculating the κ value, the same two observers reevaluated the images with disagreement together, and consensus was reached. The number of patients with a complex anovaginal fistula and the number of patients without were compared with regard to the presence of any underlying disease or condition, and the significance was evaluated by using the Fisher exact test. A P- value less than or equal to .05 was considered to indicate a statistically significant difference.

RESULTS

There was complete agreement between the observers for all items on the evaluated MR images, except for the presence of secondary perianal fistulas or other extensions (agreement, 90%; κ, 0.74).

The main anovaginal fistulas could be identified in all patients on T2-weighted images as predominantly high signal intensity linear abnormalities extending between the anal canal and the vagina. The fistulas were typically located in the mid- or parasagittal plane, just superior to the external anal sphincter (Fig 1). The mean distance from the anal verge to the fistula was 25.0 mm (range, 13–32 mm). In all 20 patients (100%), the internal opening of the main fistula tract in the anal canal was clearly identified. In 19 patients (95%), the internal opening in the posterior wall of the vagina could be seen. One patient had extensive edema within the rectovaginal septum, which caused difficulties in the identification of the internal opening in the vagina.

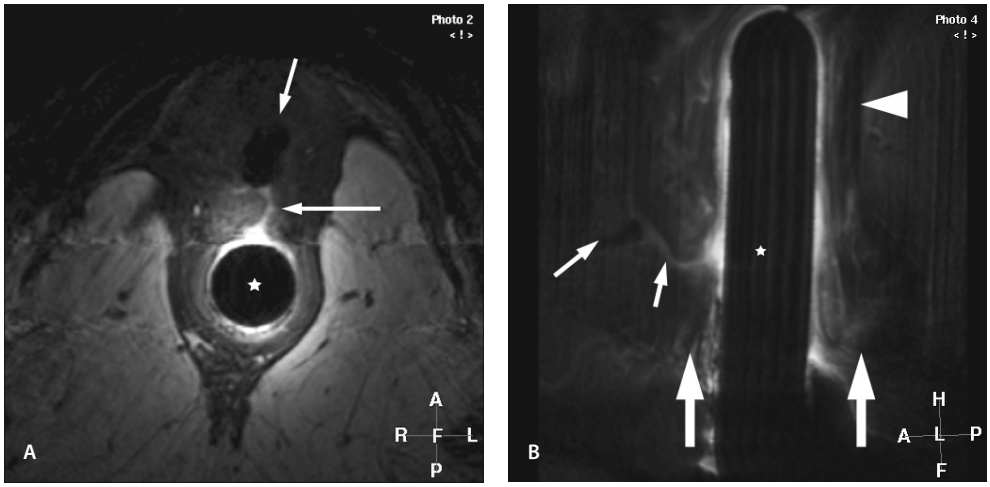

Figure 1. Simple anovaginal fistula. (a) Transverse T2-weighted fast Spin Echo (SE) MR image (2,500/100) shows an anovaginal fistula (straight arrow) as a high signal intensity linear abnormality, with direct depiction of the internal openings with the anal canal containing the endoanal coil (★) and the vagina containing some air (upper arrow). (b) Sagittal T2-weighted fast SE MR image (2,443/100) confirms the findings of transverse MR imaging and shows the relationship of the anovaginal fistula (thin straight arrow) to the lower edge of the anal sphincter complex (thick straight arrows) that clinically indicates the position of the anal verge. The vagina (left arrow), puborectal muscle (arrowhead), and endoanal coil (★) are also shown.

In seven patients (35%), the main anovaginal fistula was associated with one or more additional perianal abnormalities. In six of these seven patients, the anovaginal fistulas had an additional extension with a separate external opening located at the level of the perineum (Fig 2). Among these six patients, one had a perianal intersphincteric fistula (Fig 3). Four of these seven patients also had one or more small abscesses located close to the main anovaginal fistulas within the rectovaginal septum (Fig 4). Patients without any abscesses in the rectovaginal septum showed edema of the septum. In three patients (15%), the external anal sphincter had defects (Fig 5). Clinical data indicated that among our patients, 10 (50%) had underlying Crohn disease, a history of obstetric trauma, or pelvic floor surgery.

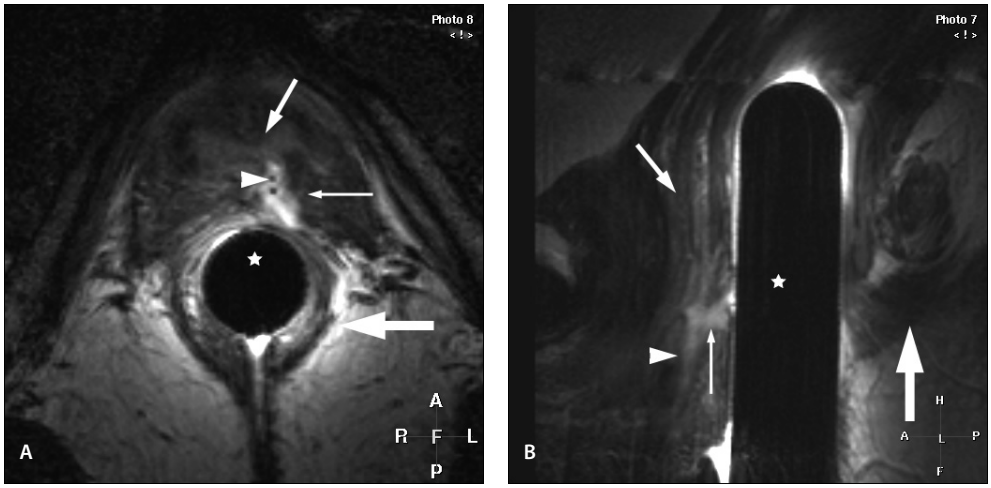

Figure 2. Anovaginal fistula with an additional extension between the anus and the vagina. (a) Transverse T2-weighted fast SE image (2,500/100) shows a high-signal-intensity anovaginal fistula (thin straight arrow) containing low-signal-intensity air bubbles (arrowhead). The vagina (upper arrow), external anal sphincter (thick straight arrow), and endoanal coil (★) are also seen. (b) Midsagittal T2-weighted fast SE image (2,443/100) shows the anovaginal fistula (thin straight arrow) and a part of an additional caudal extension (arrowhead). The vagina (upper arrow), external anal sphincter (thick straight arrow), and endoanal coil (★) are also shown.

The remaining 10 patients had no particular disease or condition that could explain the presence of anovaginal fistulas. In the 10 patients with an underlying cause, four (40%) had a simple anovaginal fistula and six (60%) had a complex anovaginal fistula. All six patients with a complex anovaginal fistula had a second perianal fistula, and three of these had an additional abscess in the rectovaginal septum. Of the 10 patients without any underlying disease or condition, only one (10%) had a complex anovaginal fistula with an abscess in the rectovaginal septum. The remaining nine patients (90%) had simple anovaginal fistulas (Table). Compared with the simple fistulas, the complex anovaginal fistulas tended to be associated with an underlying disease or condition, although the difference was not significant (P = .057).

Table 1. Anovaginal Fistulas in Relation to the Underlying Disease or Condition

Underlying Disease or Condition*	Anovaginal Fistula		
	Simple	Complex	Total
Present	4	6†	10
Absent	9	1†	10
Total	13	7	20

Note.—Data are numbers of patients.

* Crohn disease, previous obstetric trauma, or pelvic floor surgery.

† Comparison performed with the Fisher exact test. P = .057.

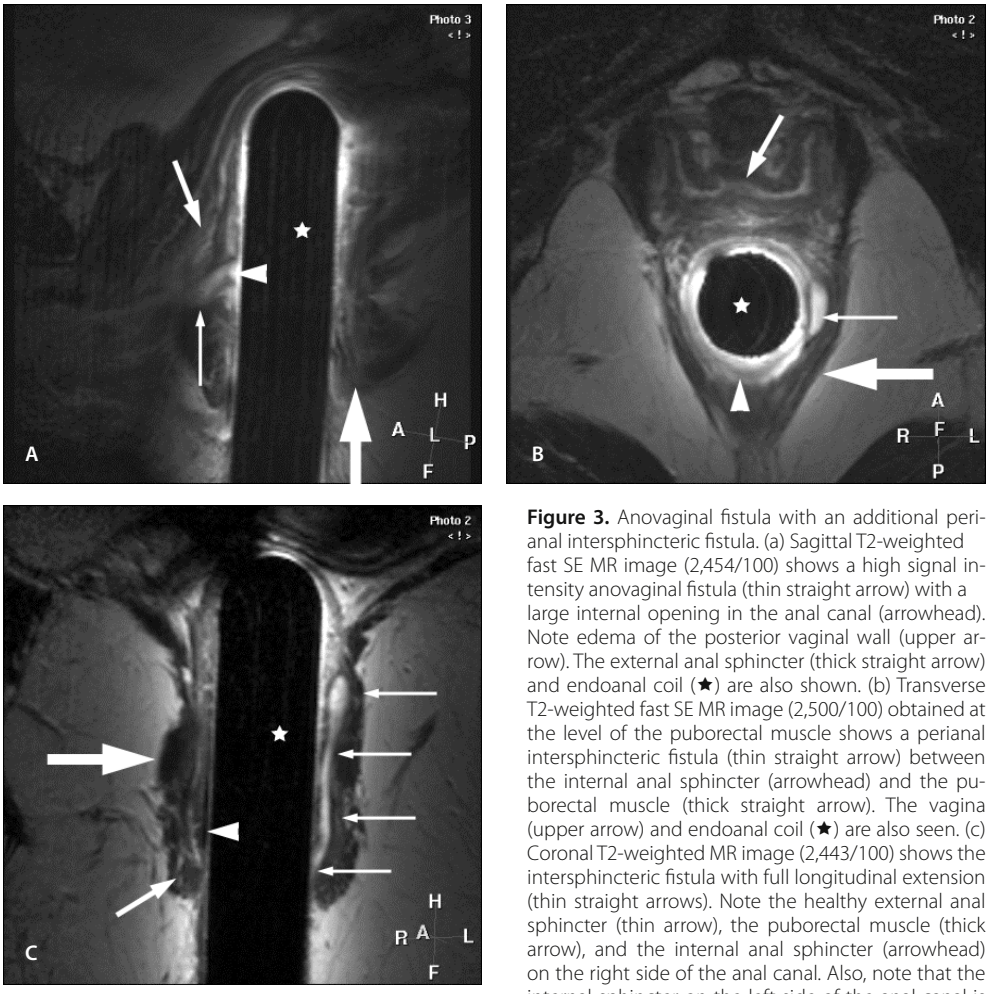

Figure 3. Anovaginal fistula with an additional perianal intersphincteric fistula. (a) Sagittal T2-weighted fast SE MR image (2,454/100) shows a high signal intensity anovaginal fistula (thin straight arrow) with a large internal opening in the anal canal (arrowhead). Note edema of the posterior vaginal wall (upper arrow). The external anal sphincter (thick straight arrow) and endoanal coil (★) are also shown. (b) Transverse T2-weighted fast SE MR image (2,500/100) obtained at the level of the puborectal muscle shows a perianal intersphincteric fistula (thin straight arrow) between the internal anal sphincter (arrowhead) and the puborectal muscle (thick straight arrow). The vagina (upper arrow) and endoanal coil (★) are also seen. (c) Coronal T2-weighted MR image (2,443/100) shows the intersphincteric fistula with full longitudinal extension (thin straight arrows). Note the healthy external anal sphincter (thin arrow), the puborectal muscle (thick arrow), and the internal anal sphincter (arrowhead) on the right side of the anal canal. Also, note that the internal sphincter on the left side of the anal canal is barely visible, which is mainly due to thinning. The endoanal coil (★) is also shown.

DISCUSSION

Our results indicate that endoanal MR imaging is suitable for use in the diagnostic work up of anovaginal fistulas. In this study, endoanal MR imaging was able to demonstrate the location and course of the main anovaginal fistulas in all patients. In addition, endoanal MR imaging showed a number of associated abnormalities, such as secondary fistula extensions, perianal fistulas, concomitant anal sphincter damage, and edema and abscesses within the rectovaginal septum. To our knowledge and with the exception of anal sphincter damage, such associated abnormalities have not been depicted with MR imaging or other imaging modalities in patients with anovaginal fistulas. It is important to establish the exact location and course of the main fistulas and the presence of additional findings for proper surgical management (13).

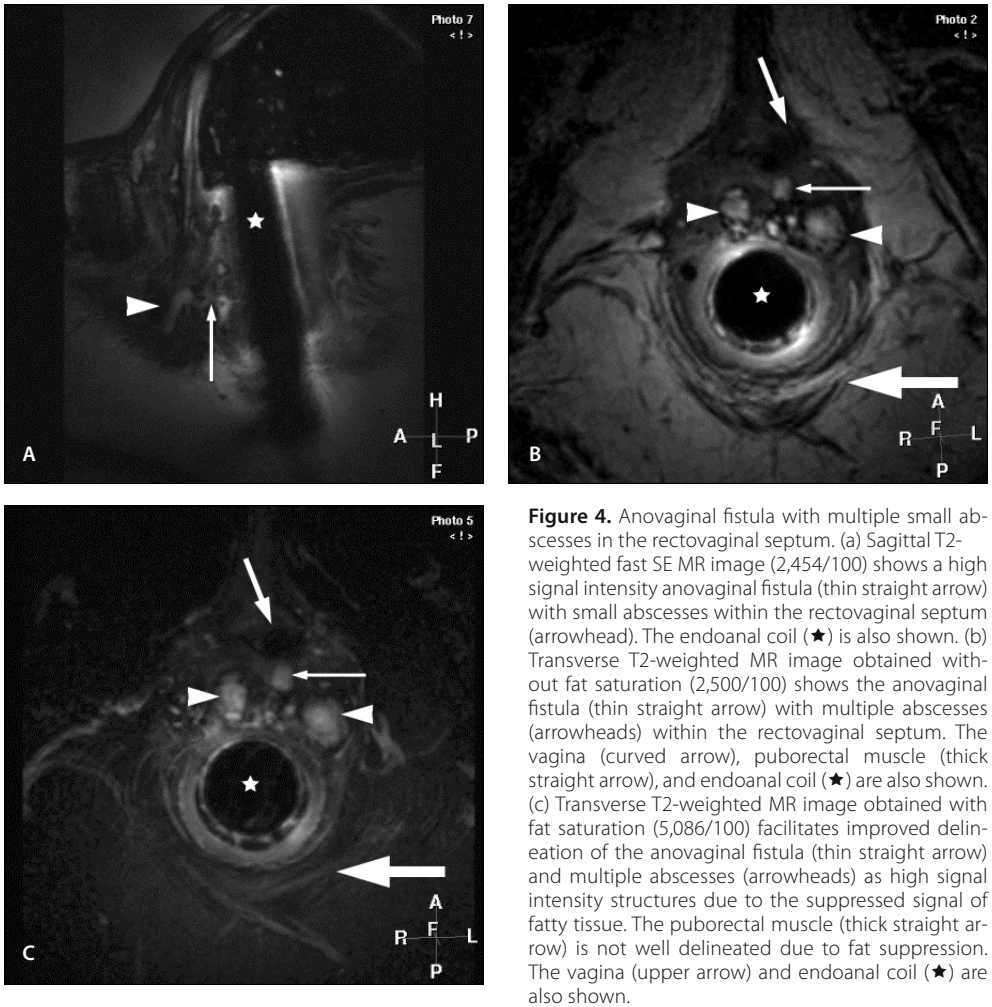

Figure 4. Anovaginal fistula with multiple small abscesses in the rectovaginal septum. (a) Sagittal T2-weighted fast SE MR image (2,454/100) shows a high signal intensity anovaginal fistula (thin straight arrow) with small abscesses within the rectovaginal septum (arrowhead). The endoanal coil (★) is also shown. (b) Transverse T2-weighted MR image obtained without fat saturation (2,500/100) shows the anovaginal fistula (thin straight arrow) with multiple abscesses (arrowheads) within the rectovaginal septum. The vagina (curved arrow), puborectal muscle (thick straight arrow), and endoanal coil (★) are also shown. (c) Transverse T2-weighted MR image obtained with fat saturation (5,086/100) facilitates improved delineation of the anovaginal fistula (thin straight arrow) and multiple abscesses (arrowheads) as high signal intensity structures due to the suppressed signal of fatty tissue. The puborectal muscle (thick straight arrow) is not well delineated due to fat suppression. The vagina (upper arrow) and endoanal coil (★) are also shown.

Anovaginal fistulas have a relatively thin low signal intensity fibrous wall, with a small amount of fluid or air present in the tract (7,14). At MR imaging, anovaginal fistulas appear as areas of high signal intensity on the T2-weighted images and often contain low signal intensity bubbles of air (5,7,14,15). A thin rim of low signal intensity surrounding the fistula tract illustrates the fibrous wall (7,14,15). Relatively less active tracts that contain less fluid and more scar tissue may appear as linear abnormalities with predominantly low signal intensity (7,14,15). Previously, a number of other imaging modalities, including fistulography and transrectal and endoanal US, have been used in the work up of patients with anovaginal fistula (10). In our experience, fistulography is often an inadequate procedure, because the internal opening of the fistulas in the anal canal and vagina are not always visible at physical examination (6). This makes cannulation for fistulography impossible. Also, this

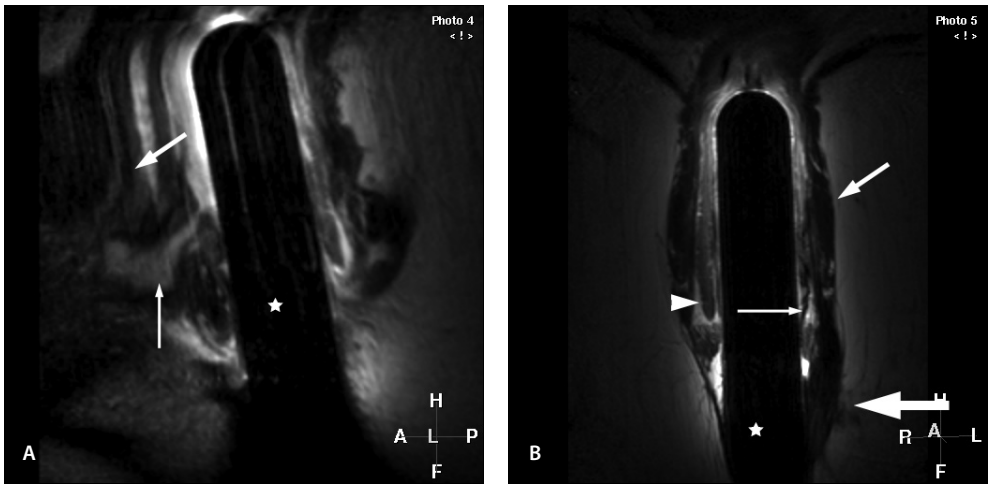

Figure 5. Anovaginal fistula with sphincter damage. (a) Sagittal T2-weighted fast SE MR image (2,443/100) shows high signal intensity anovaginal fistula (thin straight arrow) between the anal canal and the posterior wall of the vagina (curved arrow). The endoanal coil (★) is also shown. (b) Coronal T2-weighted fast SE MR image (2,443/100) shows thickening and scarring of the external anal sphincter (thick straight arrow) on the left side. The internal sphincter shows thinning on the left side (thin straight arrow), whereas the sphincter remains healthy on the right side (arrowhead). The puborectal muscle (curved arrow) and endoanal coil (★) are also shown.

technique does not allow depiction of the anal sphincter, so the fistula cannot be imaged in relation to the anal sphincter complex. It is reported that a correct diagnosis is made with fistulography in only 16% of patients with anal fistulas (6). Almost 20 years ago, transrectal and endoanal US were introduced and resulted in improved imaging and classification of anal fistulous disease (10,13). Yee et al (3) described a retrospective review of records of 25 female patients who underwent endoanal US before rectovaginal fistula repair. They concluded that transrectal US is not useful for imaging rectovaginal fistulas and cannot be recommended as a diagnostic or screening tool in the identification of rectovaginal fistulas. They did, however, recommend that transrectal US be performed before surgery in all patients with a known rectovaginal fistula to help identify and map occult sphincter defects (3). A comparative study of endoluminal US and endoluminal MR imaging in 28 patients revealed that classification is better with endoluminal MR imaging (7). Currently, MR imaging has become a promising modality for imaging of the complex anatomy of the pelvic floor and related structures. MR imaging has an excellent soft tissue contrast resolution and multiplanar imaging capability, without the need for ionizing radiation (9,10). In our experience, however, the limited spatial resolution of the body coil and other external surface coils prevents identification of small fistula tracts and their relation to the normal anatomic structures (10,14). Developments in coil technology have resulted in phased array coils, which provide higher signal to noise ratios and can be used to improve the spatial resolution (16). Blomqvist et al (17) demonstrated that use of an endorectal coil results in a more detailed depiction of the rectal wall than does use of phased array coils. Endoluminal MR imaging further improves the signal to noise ratio in combination with relatively smaller fields of view (9). This provides exquisite images of the rectum, anal canal, rectovaginal septum, and vagina, with much higher spatial resolution compared with the external surface coils (5,7).

The role of endoanal MR imaging in the detection and classification of perianal fistulas has been reported previously (7). Our results show that endoanal MR imaging can depict anovaginal fistulas, as well as a number of associated abnormalities that are important for surgical management. The disadvantages of endoanal MR imaging include mild discomfort at introduction of the coil and a limited field of view due to signal drop off at some distance from the coil (9). In our study, however, the field of view limitations did not pose any problems. In all patients, the anovaginal fistulas were depicted to their full extent. Larger complex fistulas may extend outside the sensitive region of the endoanal coil. In these patients, additional sequences can be performed with body or phased array coils for complete depiction of the fistulas.

Recently, the value of phased array coil MR imaging in the identification and classification of anal fistula disease has been reported (16). The use of phased array coils is advantageous because there is no need to introduce the coil into the anal canal or the rectum, whereas the larger field of view can provide images of the entire lower pelvic region. In our opinion, MR imaging with a phased array coil may identify most of the larger fistula tracts. The depiction of smaller primary and secondary tracts and anatomy may be problematic with phased array coils. Endoanal MR imaging proved to be superior to endoanal US and MR imaging with body coils in the detection and classification of anal fistula disease (7).

In our experience, T2-weighted MR imaging sequences are sufficient for depiction of fistulas and the surrounding anatomy. At our institution, we do not routinely use contrast material with MR imaging in the evaluation of patients with fistula disease, as doing so would lengthen the examination time and increase the cost. Our results indicate that complex anovaginal fistulas are more often seen in patients with a known underlying disease or condition, namely, Crohn disease, previous obstetric trauma, or pelvic floor surgery, which could explain the presence of the fistulas. This difference is not statistically significant, however, and is probably due to the small sample size.

Previously, Senatore (18) stated that obstetric injury is the most common cause of anovaginal fistula. Hull and Fazio (11) found that 48 (55%) of all patients who underwent surgery for anovaginal fistula had Crohn disease. Both can be considered important causes of complex anal fistula disease. The results of our study indicate that it is important to comprehensively evaluate patients before surgery. Complete mapping of the fistula with extensions, abscesses, and sphincter damage is important in the preoperative work up of the patient and may improve treatment (15,20). Scholefield et al. found that preoperative MR imaging was of little use in the surgical treatment of perianal fistulas (19). Beets-Tan et al. however, found that the largest additional value of preoperative MR imaging with the phased array coil was obtained in patients with complex fistulas associated with Crohn disease and recurrent perianal fistula (20). Lunniss et al. suggested that MR imaging could depict more extensions than surgical exploration (15).

Preoperative evaluation can help reduce the risk of procedure dependent complications. This could eventually lead to a reduction in the recurrence of fistulas and the occurrence of postoperative fecal incontinence. In our preliminary review, we also found five patients who were referred for MR imaging in whom an anovaginal fistula was suspected. In these patients, MR imaging showed a perianal fistula instead of an anovaginal fistula, a finding that was subsequently confirmed at surgery. It is likely that the additional information obtained with MR imaging will improve the surgical results in patients with complex fistulas, although this can be reliably

established only with a prospective randomized trial of patients who undergo surgery after undergoing preoperative MR imaging and those who undergo surgery without undergoing preoperative MR imaging (20).

Limitations of our study are its retrospective design, the small number of patients, and the lack of a single uniform standard of reference. The observers may have known some of the findings at MR imaging; however, this could not be avoided due to the retrospective nature of our study. We believe the standard of reference should be exploratory surgery, because this is the only clinical technique that may be used to determine the internal structure of the fistula. Not all patients in our study group underwent surgery within the review period. Despite these limitations, we believe our results indicate that endoanal MR imaging has sufficient value in the evaluation of primary anovaginal fistulas and additional abnormalities.

REFERENCES

1. Shouler PJ, Grimley RP, Keighley MR, Alexander-Williams J. Fistula in ano is usually simple to manage surgically. Int J Colorectal Dis 1986; 1:113–115.
2. Seow-Choen, Phillips RK. Insights gained from the management of problematical anal fistulae at St. Mark's Hospital: 1984 – 88. Br J Surg 1991; 78:539–541.
3. Yee LF, Birnbaum EH, Read TE, Kodner IJ, Fleshman JW. Use of endoanal ultrasound in patients with rectovaginal fistulas. Dis Colon Rectum 1999; 42:1057– 1064.
4. Stoker J, Rociu E, Schouten WR, Laméris JS. Anovaginal and rectovaginal fistulas: endoluminal sonography versus endoluminal MR imaging. AJR Am J Roentgenol 2002; 178:737–741.
5. Hussain SM, Stoker J, Schutte HE, Laméris JS. Imaging of the anorectal region. Eur J Radiol 1996; 22:116 –122.
6. Kuijpers HC, Schulpen T. Fistulography for fistula in ano: is it useful? Dis Colon Rectum 1985; 28:103–104.
7. Hussain SM, Stoker J, Schouten WR, Hop WC, Lameris JS. Fistula in ano: endoanal sonography versus endoanal MRI in classification. Radiology 1996; 200:475–481.
8. Baig MK, Zhao RH, Yuen CH, et al. Simple rectovaginal fistulas. Int J Colorectal Dis 2000; 15:323–327.
9. Hussain SM, Stoker J, Laméris JS. Anal sphincter complex: endoanal MR imaging for normal anatomy. Radiology 1995; 197:671– 677.
10. Hussain SM. Imaging of anorectal diseases. London, England: Greenwich Medical Media, 1998.
11. Hull TL, Fazio VW. Surgical approaches to low anovaginal fistula in Crohn disease. Am J Surg 1997; 173:95–98.
12. Radcliffe AG, Ritchie JK, Hawley PR, Lennard-Jones JE, Northover JM. Anovaginal and rectovaginal fistulas in Crohn's disease. Dis Colon Rectum 1988; 31:94–99.
13. Choen S, Burnett S, Bartram CI, Nicholls RJ. Comparison between anal and endosonography and digital examination in anal fistulae. Br J Surg 1991; 78:445–447.
14. Stoker J, Hussain SM, van Kempen D, Elevelt AJ, Laméris JS. Endoluminal coil in MR imaging of anal fistulas. AJR Am J Roentgenol 1996; 166:360–362.
15. Lunniss PJ, Armstrong P, Barker PG, Reznet RH, Phillips RK. Magnetic resonance imaging of anal fistulae. Lancet 1992; 340:394 –396.
16. Beets-Tan RG, Beets GL, van der Hoop AG, et al. High resolution magnetic resonance imaging of the anorectal region without an endocoil. Abdom Imaging 1999; 24:576–581.
17. Blomqvist L, Holm T, Rubio C, Hindmarsch T. Rectal tumours: MR imaging with endorectal and/or phased array coils and histopahologic staging on giant sections. Acta Radiol 1997; 38:437–444.
18. Senatore PJ Jr. Anovaginal fistulae. Surg Clin North Am 1994; 74:1361–1375.
19. Scholefield JH, Berry DP, Armitage NC, Wastie ML. Magnetic resonance imaging in the management of fistula in ano. Int J Colorectal Dis 1997; 12:276–279.
20. Beets-Tan RG, Beets GL, van der Hoop AG, et al. Preoperative MR of anal fistulas: does it really help the surgeon? Radiology 2001; 218:75–84.

chapter 3.3

Is the Outcome of Transanal Advancement Flap Repair Affected by the Complexity of High Transsphincteric Fistulas?

Litza E. Mitalas
Roy S. Dwarkasing
Rob Verhaaren
David D. E. Zimmerman
W. Rudolph Schouten

Dis Colon Rectum. 2011 Jul;54(7):857-62.

ABSTRACT

Background Transanal advancement flap repair for the treatment of high transsphincteric fistulas fails in 1 of every 3 patients. Until now no definite risk factors for failure have been identified. The question is whether the more complex fistulas, such as those with horseshoe extensions and associated abscesses, have a less favorable outcome.

Objective Aim of the present study was to indentify whether more complex fistulas have a less favorable outcome.

Material and methods This study is a retrospective case series. Between 1995 and 2007 a series of 162 patients underwent endoanal MR imaging before transanal advancement flap repair. Two investigators, without prior knowledge of the surgical findings, reviewed all MR images.

Results Lateral fistulas were identified in 5 patients. Because of the small number, these patients were excluded from further analysis. Posterior fistulas were identified in 119 patients (76%). These fistulas had 3 types of extensions: a direct course (36%), a classic horseshoe extension (23%), or an intersphincteric horseshoe extension (41%). The corresponding healing rates were 37%, 81%, and 73%. Anterior fistulas were observed in 23% of the patients. These fistulas had 2 types of extensions: a direct course (61%) or a classic horseshoe extension (39%). The corresponding healing rates were 60% and 52%. The healing rate of fistulas with a direct course was significantly lower than the healing rate of fistulas with a classic or intersphincteric horseshoe extension. Associated abscesses were found in 47% of the posterior fistulas and 5% of the anterior fistulas. Once adequately drained, these abscesses did not affect the outcome of transanal advancement flap repair.

Conclusion The complexity of high transsphincteric fistulas does not affect the outcome of transanal advancement flap repair.

INTRODUCTION

Transanal advancement flap repair has been advocated as the treatment of choice for transsphincteric fistulas passing through the upper and middle third of the external anal sphincter. This procedure enables healing of the fistula in 2 of every 3 patients without consequent sphincter damage. Several authors have tried to identify factors affecting the outcome of transanal advancement flap repair (1-4). However, until now, no definite predictive factors for failure have been identified. The question is whether the complexity of high transsphincteric fistulas affects the outcome of transanal advancement flap repair. Most of these fistulas have their internal opening at the posterior or anterior midline. From this point they can extend in different ways. Some fistulas have a direct course from the internal to the external opening, whereas others extend in a more complex horseshoe manner. Associated abscesses are not an uncommon finding in patients with a high transsphincteric fistula. It is not known whether high transsphincteric fistulas with an associated abscess and those with a more complex course have a lower tendency to heal.

The classic way in which horseshoe fistulas develop has been described in detail and mainly involves the horseshoe extension of posterior fistulas (5-10). When such a fistula penetrates the external anal sphincter it enters the deep postanal space, which is bounded by the levator ani muscle, the anococcygeal ligament, the coccyx, and the anal canal. This anatomical space communicates on both sides with the ischioanal spaces. The easiest way to extend from the deep postanal space is to either one or both of these ischioanal spaces, thereby forming a classic horseshoe extension. However, it has been reported that the circumferential spread may also occur in the intersphincteric plane, forming an intersphincteric horseshoe extension (11). In 1900 Goodsall described in which way a fistula is most likely to traverse, based on the location of the external opening. His observations have been almost universally accepted and are commonly known as Goodsall's rule. According to Goodsall's rule, the majority of posterior fistulas should form a horseshoe extension, but anterior fistulas should have a direct course (12). The aim of the present study was to determine the exact prevalence of horseshoe extensions in posterior and anterior high transsphincteric fistulas with the use of endoanal MR imaging. The present study was also conducted to answer the question of whether the more complex fistulas, such as those with horseshoe extensions and associated abscesses, have a less favorable outcome. The primary aim of the study was to assess whether the complexity of the fistula influences healing. A secondary aim was to determine the exact prevalence of horseshoe extensions in posterior and anterior high transsphincteric fistulas with the use of endoanal MR imaging.

MATERIALS AND METHODS

Between June 1995 and December 2007 a consecutive series of 178 patients with a cryptoglandular, transsphincteric fistula, passing through the upper or middle third of the external anal sphincter, underwent transanal advancement flap repair. In 162 of these patients MR imaging was performed before this procedure. Patients in whom no MR imaging was performed were excluded. Median age at time of repair was 47 (range, 21–73) years. Healing of the fistula was defined as complete wound healing and closure of all external openings in combination with the absence of symptoms. Follow-up was at least 12 months.

Exclusion criteria

Patients with a rectovaginal fistula or a fistula caused by Crohn's disease were excluded from the present series.

MR Imaging

Before transanal advancement flap repair was performed all patients underwent endoanal MR imaging. All MR imaging examinations were performed with the use of an endoanal coil with a 1.5-T MR imager (Gyroscan NT Intera 1.5; Philips Medical Systems, Best, the Netherlands). The endoanal coil (Philips Medical Systems) consisted of a fixed, rectangular, 60-mm-long rigid receiver coil with a width of 16 mm. The coil is contained within an 80-mm- long cylindrical coil holder with a diameter of 19 mm. Before the introduction of the coil into the anal canal, a condom was placed over the coil and ultrasound gel was used as a lubricant. The coil was introduced while the patient was lying in the left lateral position. After the coil was introduced, patients were carefully turned onto their back, and the position of the coil was rechecked.

In each patient, the following 3 sequences were used. Transverse T2-weighted contrast-enhanced fast field-echo imaging was performed (repetition time/echo time, 23 ms/14 ms; acquisition time, 5 minutes 39 seconds; matrix, 205 x 256; flip angle, 60°; field of view, 140 mm; section thickness, 2 mm with no gaps; and 2 signals acquired). Contrast-enhanced fast field-echo is a term used by Philips Medical Systems and does not indicate contrast material administration. Transverse T2-weighted fast spin-echo [SE] MR imaging was performed with and without fat saturation (5086/100; acquisition time, 2 minutes 23 seconds; matrix, 186 x 256; flip angle, 90°; field of view, 120 mm; section thickness, 4 mm with a 0.4-mm gap; and 3 signals acquired). Coronal and sagittal T2-weighted SE MR imaging was performed without fat saturation (2454/100; acquisition time, 2 minutes 34 seconds; matrix, 186 x 256; flip angle, 90°; field of view, 120 mm; section thickness, 4 mm with a 0.4-mm gap; and 4 signals acquired).

Two investigators, without prior knowledge of the surgical findings, independently reviewed all MR images. Images with disagreement were reevaluated with both observers working together, and consensus was reached.

Surgical technique

Patients underwent complete mechanical bowel preparation (polyethylene glycol: Kleanprep Helsinn Birex Pharmaceuticals, Dublin, Ireland). After induction of general endotracheal anesthesia, metronidazole (500 mg) together with cefuroxime (1500 mg) was administered intravenously. With the patient in a prone jackknife position, the external opening was enlarged and the fistulous tract was excised as far as possible. The internal opening of the fistula was exposed using a Lone Star retractor (Lone Star Retractor System, Lone Star Medical Products, Inc. Houston, TX). The cryptbearing tissue around the internal opening and the overlying anodermis were then excised. The fistulous tract was cored out of the sphincters. The defect in the internal anal sphincter was closed with absorbable sutures. A flap consisting of mucosa, submucosa, and some of the most superficial fibers of the internal anal sphincter, was raised from the level of the dentate line and mobilized over a distance of 4 to 6 cm proximally. The flap was advanced and sutured to the neodentate line with absorbable sutures. One surgeon performed all operations (W.R.S.).

Drainage of associated abscesses

At the same time flap repair was performed, all associated abscesses, detected with MR imaging, were drained with a 4-winged malecot catheter. A separate elliptical incision was made to gain access to the abscess cavity. Through another small incision the drain was inserted, tunneled subcutaneously, and positioned into the abscess cavity. The abscess cavity was irrigated 6 times daily with saline for 10 days.

Postoperative care

All patients were immobilized for 5 days. All patients received a clear liquid diet for 5 days. During this time period metronidazole and cefuroxime were administered intravenously 3 times daily.

RESULTS

Of the 162 patients who underwent endoanal MR imaging before the flap repair the internal opening of the fistula was located posterior in 119 patients, anterior in 38 patients, and at the lateral side of the anal canal in 5 patients. Because of the small number, patients with a lateral fistula were excluded from further analysis. Posterior fistulas were identified in 76% of the patients (Table 1). In 36% of these patients endoanal MRI revealed a direct course of the fistula, running from the internal to the external opening in the dorsal quadrant. Associated abscesses were found in 51% of these patients. The healing rate among patients with this fistula type was 37%. A classic horseshoe extension was found in 23% of the patients with a posterior fistula. In these patients, the fistula passed through the external anal sphincter in the posterior midline, extending from that point in a horseshoe manner to either one or both sides (Fig. 1). In 33% of these patients an associated abscess was detected. The healing rate was 81%. In 41% of the patients, the posterior fistula extended circumferentially in the

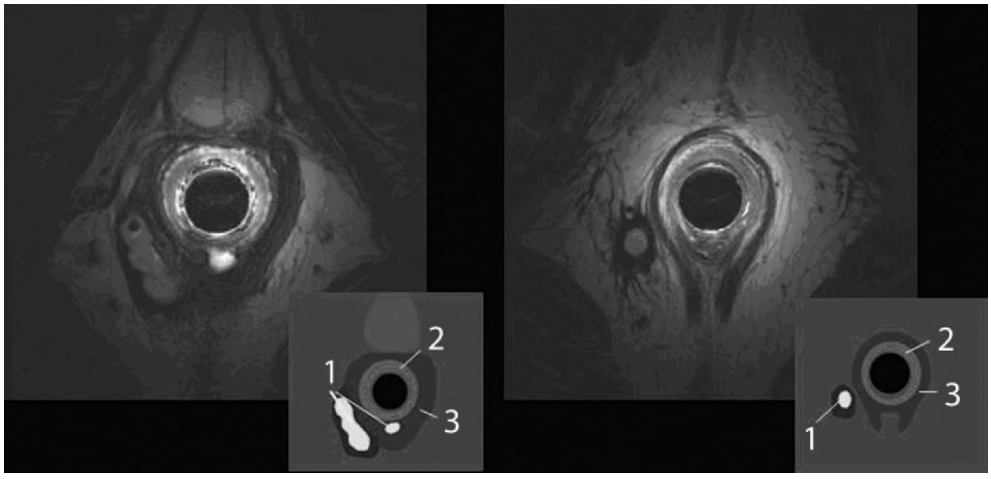

Figure 1. MRimagesofclassichorseshoefistula.1=fistula;2= internal anal sphincter; 3 = external anal sphincter.

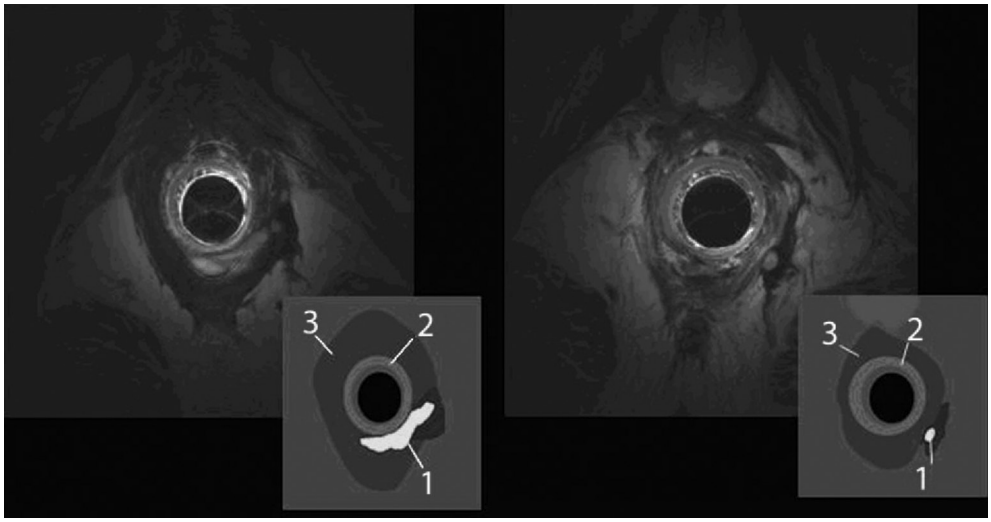

Figure 2. MRimagesofintersphincterichorseshoefistula.1= fistula; 2 = internal anal sphincter; 3 = external anal sphincter.

intersphincteric plane, passing through the external anal sphincter at either one or both lateral sides (Fig. 2). This fistula type was associated with an abscess in 47% of the cases. The healing rate was 73%. The healing rate of posterior fistulas with a direct course was significantly lower than the healing rate of fistulas with a classic or intersphincteric horseshoe extension (P = .001). Regarding the healing rate, no significant difference was observed between patients with a classic and those with an intersphincteric horseshoe extension.

Anterior fistulas were identified in 23% of the patients (Table 2). Endoanal MRI revealed 2 types of anterior fistulas. The first type includes the fistulas with a direct course between the internal opening and the external opening in the anterior quadrant. This fistula type was found in 23 (61%) of the patients with an internal opening at the anterior midline. The healing rate in these patients was 52%. In only one (4%) of these patients was an associated abscess detected. The second type was characterized by a classic horseshoe extension, observed in 15 (39%) of the patients. The healing rate among these patients was 60%. These fistulas were associated with an abscess in 6% of the cases. Anterior fistulas showed no intersphincteric extensions. The healing rate of anterior fistulas did not significantly differ from the healing rate of posterior fistulas.

Table 1. Healing rates and prevalence of associated abscesses in high transsphincteric posterior fistulas

Internal opening	Fistula type	n (%)	Associated abscesses n (%)	Healing rate n (%)
Posterior (76%)	Classic horseshoe	27 (23)	9 (33)	22 (81)
	Intersphincteric horseshoe	49 (41)	23 (47)	36 (73)
	Direct course	43 (36)	22 (51)	16 (37)
Total		119 (100)	56 (47)	74 (62)

Table 2. Healing rates and prevalence of associated abscesses in high transsphincteric anterior fistulas

Internal opening	Fistula type	n (%)	Associated abscesses n (%)	Healing rate n (%)
Anterior (23%)	Classic horseshoe	15 (39)	1 (7)	9 (60)
	Direct course	23 (61)	1 (4)	12 (52)
Total		38 (100)	2 (5)	21 (55)

Endoanal MR imaging revealed associated abscesses in 47% of the patients with a posterior fistula and in 5% of the patients with an anterior fistula. These abscesses were classified as intersphincteric (18%), infralevator (13%), intralevator (51%), supralevator (11%), and translevator (7%)

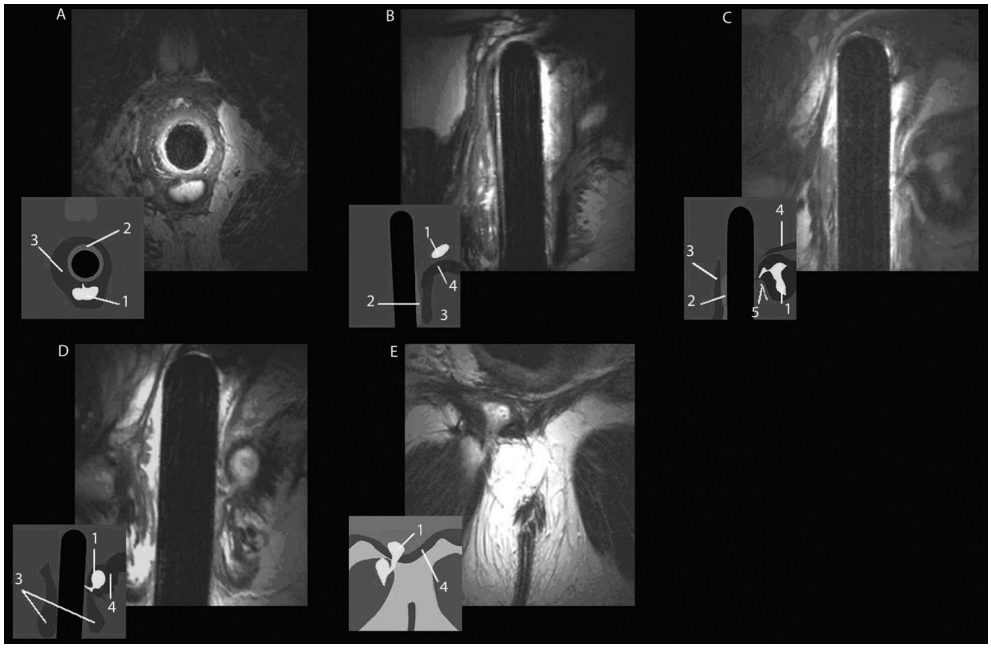

Figure 3. MRimagesofabscesses.A,Intersphincterica bscess.B,Supralevatorabscess.C,Infralevatorabscess.D,Intralevatorabscess.E, Translevator abscess. 1 = abscess; 2 = internal anal sphincter; 3 = external anal sphincter; 4 = levator muscle; 5 = fistulous tract.

(Fig. 3). Intersphincteric abscesses are located in the plane between the internal and external anal sphincter. Infralevator abscesses are located below the levator muscle and are commonly known as deep postanal space abscesses. Intralevator abscesses are located in the levator muscle itself. Abscesses above the pelvic floor are referred to as supralevator abscesses. Some abscesses are located below the levator muscle and from there on penetrate the pelvic floor to extend above the levator muscle. These hourglass-shaped abscesses are referred to as translevator abscesses.

Associated abscesses were significantly more often present in posterior fistulas than in anterior fistulas. Posterior fistulas with a direct course were significantly less often associated with an abscess than fistulas with either a classic or intersphincteric horseshoe extension. In a comparison of patients with and without an associated abscess, the healing rate was found to be 57% and 62%. This difference did not reach statistical significance. All abscesses were drained as previously described. Once adequately drained, abscesses did not affect the outcome of transanal advancement flap repair.

DISCUSSION

Perianal fistulas passing through the upper or middle third of the external anal sphincter present a challenge to many surgeons. Transanal advancement flap repair provides a useful tool in the treatment of these fistulas. It enables the healing of the fistula without damage of the external sphincter and consequent fecal incontinence. Initially, the reported healing rates varied between 84 and 100% (13-16). However, during the past decade it has become clear that transanal advancement flap repair fails in 1 of 3 patients (1-14,18). The majority of high transsphincteric fistulas, examined in the present study, had their internal opening at the posterior midline. These posterior fistulas showed 3 different ways of extension: a direct course, a classic horseshoe extension, and, the most common one, an intersphincteric horseshoe extension. Anterior fistulas extended in 2 different ways: a direct course and a classic horseshoe course. The healing rate of fistulas with a direct course was significantly lower than the healing rate of fistulas with a classic or intersphincteric horseshoe extension. Associated abscesses were found in 47% of the posterior fistulas and in 5% of the anterior fistulas. Once adequately drained, these abscesses did not affect the outcome of transanal advancement flap repair. Concordance between surgical findings and MR images was very high. However, the surgeon was aware of the MR images, so an objective correlation between MRI and surgical findings cannot be given based on these data. The most striking finding of the present study is the poor outcome after flap repair in patients with a high transsphincteric fistula, traversing the external anal sphincter in a direct course to the external opening. This finding is difficult to explain and has not been described before. In our opinion it might be possible that both anterior and posterior fistulas with a direct course represent a more aggressive form of perianal fistulous disease.

Another finding of the present study is the high prevalence of associated abscesses, especially in high transsphincteric fistulas with their internal opening at the posterior midline. Most of these abscesses could not be detected by physical examination. Although some of these abscesses presented a rather complex and bizarre course above the pelvic floor, they all could be detected and drained because of preoperative MR imaging.

Endoanal MR imaging provides a useful tool for the visualization of these abscesses, enabling adequate drainage. The abscess cavity was deroofed, drained, and irrigated for 10 days with a malecot catheter. This might explain why these abscesses in themselves had no detrimental effect on the outcome. Because the present study was not aimed at comparing flap repair with and without drainage of associated abscesses, it is not known what the outcome would have been had these abscesses been overlooked and not drained. In most studies, no distinction is made between classic and intersphincteric horseshoe extensions. Furthermore, the exact prevalence of these extensions is not known. MR imaging with an endoanal coil, used in the present study, has revealed that horseshoe extensions of posteri-

or fistulas most frequently occur in the intersphincteric plane. This finding has not been described before. Distinction between the 2 different types of horseshoe extensions is difficult without preoperative MR imaging. During flap repair, the fistulous tract is excised as far as possible, from the external opening to the exterior of the external anal sphincter. In a fistula with a classic horseshoe extension, a large part of the fistulous tract can be excised without damaging the external anal sphincter. While treating fistulas with an intersphincteric horseshoe extension one should be aware that the fistulous tract penetrates the external anal sphincter closer to the external opening. In this instance, only a limited part of the fistulous tract can be removed. Based on these considerations, it seems likely that preoperative imaging decreases the risk of sphincter damage in patients with horseshoe extensions. High transsphincteric fistulas with horseshoe extensions and associated abscesses are considered as complex fistulas (17). The present study shows that the complexity of these fistulas does not affect the healing rate of transanal advancement flap repair. In contrast to our expectations, the more simple fistulas with a direct course had a worse outcome. This finding is hard to explain. One of our hypotheses regarding this unexpected finding might be the possibility that the course of the fistula depends on the severity of the fistulous disease. The more fulminant the fistulous disease, the more straightforward the fistula might traverse the anal sphincter muscles, resulting in a direct course to the external anal

opening. Whether a fistula develops after incision and drainage of a perianal abscess might also depend on the severity of the fistulous disease. Further research is warranted to investigate this possibility. Another reason for this finding might be the fact that more complex fistulas are referred earlier to our hospital. We are a tertiary referral center and a substantial number of our patients are referred from other hospitals. It is possible that the direct fistulas represent a group of persistent fistulas that are only referred when prior surgery has failed. Because we did not have complete data of prior treatment elsewhere, we did not analyze this possibility. For several years, it has been our policy to offer patients a repeat flap repair if the first attempt has failed. In all patients who underwent a second procedure, complete healing of the flap was observed, with the exception of the site of the original internal opening (18). This remarkable clinical finding suggests that the persistence of fistulas might be caused by ongoing disease within the remaining fistulous tract. Further research is warranted regarding this possibility to control this ongoing disease, thereby increasing the healing rate.

CONCLUSION

The complexity of high transsphincteric fistulas characterized by horseshoe extensions and associated abscesses does not affect the outcome of transanal advancement flap repair. Horseshoe extensions occur in 2 of every 3 patients with a posterior fistula. Extension in the intersphincteric plane is the most frequent one. In patients with an anterior fistula, only classic extensions are observed. Fistulas with a horseshoe extension have a significantly better outcome than the more simple fistulas with a direct course.

REFERENCES

1. Sonoda T, Hull T, Piedmonte MR, Fazio VW. Outcomes of primary repair of anorectal and rectovaginal fistulas using the endorectal advancement flap. Dis Colon Rectum. 2002;45:1622– 1628.
2. Mizrahi N, Wexner SD, Zmora O, et al. Endorectal advancement flap: are there predictors of failure? Dis Colon Rectum. 2002;45:1616 –1621.
3. van Koperen PJ, Wind J, Bemelman WA, Bakx R, Reitsma JB, Slors JF. Long-term functional outcome and risk factors for recurrence after surgical treatment for low and high perianal fistulas of cryptoglandular origin. Dis Colon Rectum. 2008;51: 1475–1481.
4. Zimmerman DD, Delemarre JB, Gosselink MP, Hop WC, Briel JW, Schouten WR. Smoking affects the outcome of transanal mucosal advancement flap repair of trans-sphincteric fistulas. Br J Surg. 2003;90:351–354.
5. Courtney H. The posterior subsphincteric space: its relation to posterior horseshoe fistula. Dis Colon Rectum. 1949;89:222–226.
6. Hamilton CH. Anorectal problems: the deep postanal space surgical significance in horseshoe fistula and abscess. Dis Colon Rectum. 1975;18:642– 645.
7. Hanley PH. Conservative surgical correction of horseshoe abscess and fistula. Dis Colon Rectum. 1965;8:364–368.
8. Held D, Khubchandani I, Sheets J, Stasik J, Rosen L, Riether R. Management of anorectal horseshoe abscess and fistula. Dis Colon Rectum. 1986;29:793–797.
9. RosenSA, Colquhoun P, Efron J,et al. Horseshoe abscesses and fistulas: how are we doing? Surg Innov. 2006;13:17–21.
10. Ustynoski K, Rosen L, Stasik J, Riether R, Sheets J, Khubchandani IT. Horseshoe abscess fistula: seton treatment. Dis Colon Rectum. 1990;33:602– 605.
11. Gordon PH, Nivatvongs S. Principles and Practice of Surgery of Colon, Rectum, and Anus. 3rd ed. New York: Informa Healthcare; 2006.
12. Goodsall DH, Miles WE. Diseases of the Anus and Rectum. London: Longmans, Green and Co.; 1900.
13. Wedell J, Meier zu Eissen P, Banzhaf G, Kleine L. Sliding flap advancement for the treatment of high level fistulae. Br J Surg. 1987;74:390 –391.
14. Oh C. Management of high recurrent anal fistula. Surgery. 1983; 93:330 –332.
15. Kodner IJ, Mazor A, Shemesh EI, Fry RD, Fleshman JW, Birnbaum EH. Endorectal advancement flap repair of rectovaginal and other complicated anorectal fistulas. Surgery. 114:682– 690.
16. Aguilar PS, Plasencia G, Hardy TG Jr, Hartmann RF, Stewart WR. Mucosal advancement in the treatment of anal fistula. Dis Colon Rectum. 1985;28:496 – 498.
17. Williams JG, Farrands PA, Williams AB, et al. The treatment of anal fistula: ACPGBI position statement. Colorectal Dis. 2007; 9(suppl 4):18 –50.
18. Mitalas LE, Gosselink MP, Zimmerman DD, Schouten WR. Repeat transanal advancement flap repair: impact on the overall healing rate of high transsphincteric fistulas and on fecal continence. Dis Colon Rectum. 2007;50:1508 –1511.

chapter 3.4

Chronic Anal and Perianal Pain Resolved with MRI

Roy S. Dwarkasing
W. Rudolf Schouten
Tychon E. A. Geeraedts
Litza E. Mitalas
Wim C. J. Hop
Gabriel P. Krestin

AJR Am J Roentgenol. 2013 May;200(5):1034-41.

ABSTRACT

Objective. The purpose of this study was to assess the diagnostic value of anorectal MRI in the care of patients with chronic anal and perianal pain but without findings of abnormalities in the clinical workup.

Materials and Methods. Patients referred from a tertiary department of colorectal surgery to the MRI unit with clinically occult chronic anal and perianal pain were included. MRI of the anorectum was performed with an endoanal or pelvic phased array coil. The images from all examinations were read by two radiologists. MRI findings were correlated with clinical follow-up data.

Results. The study group (103 patients) was stratified into patients with no history of anorectal disease (n = 60) and those who had a history of surgery for anorectal disease (n = 43). MRI findings suggested the final diagnoses in 40 patients (39%). These diagnoses were 28 cases of suppurative lesions (27%), 11 cases of painful scarring of the anus (11%), and one case of metastasis to the sacrum (1%). Suppurative lesions were surgically proved with marked relief of pain after surgery. In the other patients the final diagnoses were 37 cases of levator ani syndrome (36%) and 26 cases of unspecified functional anorectal pain (25%). No MRI abnormalities were found in 33 of the patients with levator ani syndrome and 26 of the patients with unspecified anorectal pain. The two readers had very good agreement (κ= 0.92). The patients with a history of anorectal disease had significantly more MRI findings of abnormalities (60%) than did patients without a history of anorectal disease (23%). The positive predictive value of MRI was 91%, and the negative predictive value was 100%.

Conclusion. In 39% of patients, MRI showed abnormalities that were clinically confirmed as the final diagnosis. Surgical treatment will especially benefit patients with suppurative lesions, resulting in relief of pain.

INTRODUCTION

Chronic anal and perianal pain is a common problem in gastroenterologic practice (1,2). It is defined as recurrent or persistent pain in the anal canal, usually deep and severe, that lasts more than 3 months and has variable radiation (2). Chronic anal and perianal pain is thought to be present as a major symptom in as many as 6% of U.S. residents (1). Patients generally present with a combination of symptoms that can include pain, soiling, loss of blood or pus from the anus, fecal incontinence, and a palpable mass in and around the anus. The combination of symptoms suggests the presence of disease, and a clinical examination is performed to assess local anal abnormalities, including complicated hemorrhoids, hypertrophied anal papillae, anal fissure, and perianal suppurative conditions.

When the only presentation is pain in the anal region and no local abnormality is found at initial clinical evaluation, the clinician is faced with a challenge. It has been speculated that patients without a clinically confirmed physical explanation for the pain may have an underlying functional disorder or that chronic anal and perianal pain may result from a psychologic overlay (3-5). The aim of further investigations, including imaging, must be to identify causes of pain not initially detected at clinical examination (6). The purpose of this study was to evaluate the diagnostic role of anorectal MRI in the care of these patients.

MATERIALS AND METHODS

This study was performed without financial support, and the authors had exclusive control of the data and information presented.

Patient selection, clinical workup, and reference standard

Institutional review board approval was obtained for this retrospective study, and the requirement for informed consent was waived. The records of all patients referred to the MRI unit from a tertiary department of colorectal surgery between January 1999 and

December 2007 were reviewed with regard to symptoms and indication for MRI. The cases were selected from databases in the departments of radiology and surgery, and a patient was included in the study population when chronic anal and perianal pain was the only symptom. In cases in which the patient had been previously treated for anorectal disease, a disease-free period of at least 1 year was required for inclusion.

The clinical workup included evaluation and registration of symptoms in the patient record, anal inspection, and digital rectal examination by an experienced colorectal surgeon (the principal investigator). The findings at this initial workup guided a clinical decision to proceed with either proctoscopy or examination under general anesthesia performed by the principal investigator. All patients underwent a complete clinical work-up, including proctoscopy (n = 29) and examination under general anesthesia (n = 103), with no physical cause detected before admittance to the MRI unit (Fig. 1). After MRI, all patients underwent clinical reevaluation within 3 months. This sequence of patient evaluation and use of MRI is standard practice at our institution.

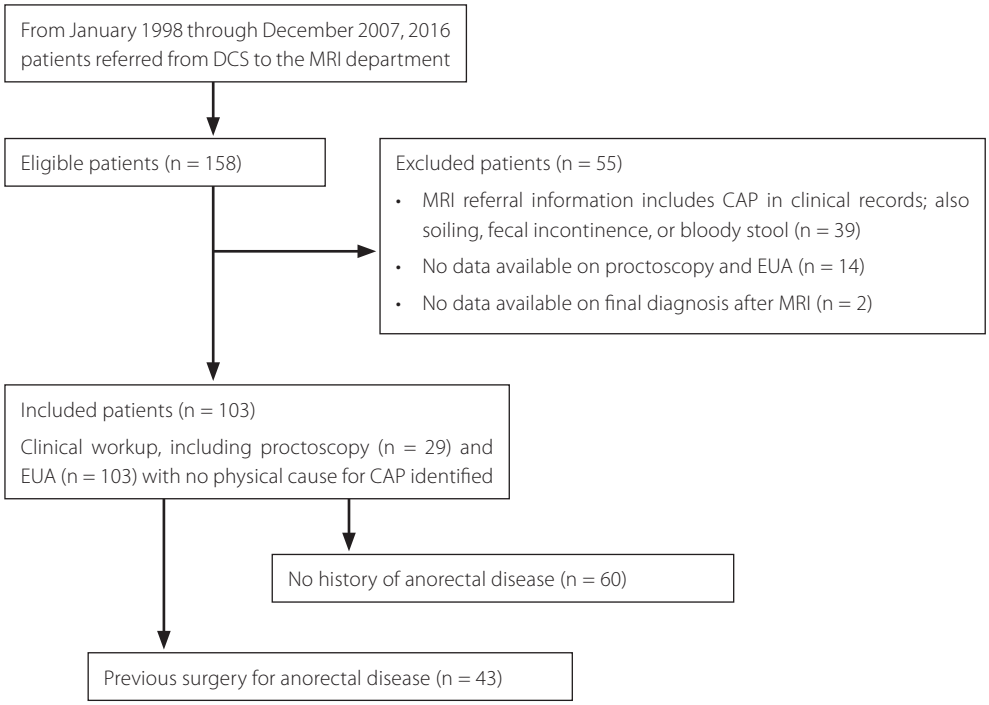

Fig. 1. Flow diagram summarizes patient sampling. DCS = department of colorectal surgery, CAP = chronic anal and perianal pain, EUA = examination under general anesthesia.

Two investigators not involved in image interpretation reviewed the medical records to assess the final clinical diagnosis, treatment method, and follow-up information on the symptoms. The reference standard was surgical confirmation of MRI findings, histologic proof of disease, or clinical assessment of MRI findings, including follow-up data.

Functional gastrointestinal disorders were classified according to the Rome III Diagnostic Criteria for Functional Gastrointestinal Disorders (7-9), which include levator ani syndrome and unspecified functional anorectal pain. Levator ani syndrome is characterized by symptom criteria for chronic proctalgia and tenderness during posterior traction on the puborectalis and levator ani muscles during digital rectal examination. The diagnosis of unspecified functional anorectal pain is based on symptom criteria for chronic proctalgia but without tenderness during posterior traction on the puborectalis and levator ani muscles (10,11).

The follow-up period for the study group ranged from 4 months to 7 years after MRI (median, 18 months; mean, 23 months).

MRI

All examinations were performed with a 1.5- T MR imager (Gyroscan NT Intera 1.5, Philips Healthcare). In 96 cases a rigid endoluminal coil) was inserted into the anal canal. This coil is commercially available and consists of a fixed, rectangular, 60-mm-long rigid receiver coil with a width of 16 mm. The coil is contained in an 80-mm-long cylindric coil holder with a diameter of 19 mm. Before introduction of the coil into the anal canal, a condom was placed over the coil, and ultrasound gel was used as a lubricant. Two patients refused use of the endoluminal coil, and five found it too painful. In these cases imaging was performed with a phased array coil. The phased array coil is a commercially available four-channel coil placed around the pelvis. A standardized imaging protocol of the anus and lower rectum was performed with T2-weighted fast spin-echo sequences in the axial, sagittal, and coronal planes. The protocol included axial T2-weighted images with fat saturation obtained with the endoluminal or phased array coil. Additional imaging of the entire pelvic region in the axial and sagittal planes was followed by imaging with a phased array or body coil.

The parameters for imaging with the endoluminal coil were as follows: TR/TE, 5086/100; FOV, 120 mm; section thickness, 2 mm; gap, 0.2 mm; number of signals acquired, 3; matrix, 186 × 256; flip angle, 90°. The parameters for acquisition with the phased-array coil were as follows:

TR/ TE, 2500/70; FOV, 180 mm; section thickness, 3 mm; gap, 0.3 mm; number of signals acquired, 3; matrix, 512 × 256; flip angle, 60°. The parameters for acquisition with the body coil were as follows: TR/TE, 5075/100; FOV, 250 mm; section thickness, 5 mm; gap, 0.5 mm; number of signals acquired, 2; matrix, 512 × 256.

Image analysis

MRI examinations of patients in the study group were uploaded to a PACS viewing station from digital storage facilities and evaluated by a radiologist with 8 years of experience in pelvic imaging (second reader). This reader was blinded to the original radiologic report and final diagnosis. The second reader recorded the following MRI findings: normal findings; fistulas, including abscesses; abscesses; scarring of anal sphincter muscles; suspicion of malignancy; and other abnormalities. The original readings with prospective image interpretation and reporting were performed by three radiologists with varying levels of experience in MRI of the pelvis (2, 2.5, and 5 years). Agreement between the second reading and the original radiologic report was assessed for type of lesion, location of lesion, and final diagnosis. If the two readings did not indicate the same type and location of lesion, the case was classified as disagreement. If the final diagnosis differed between readings, the case also was classified as disagreement.

Fistulas have a typical appearance on T2- weighted MR images: a central track of high signal intensity surrounded by a wall of relatively low signal intensity (12). This appearance presumably illustrates the true lumen with granulation tissue surrounded by an outer section comprising fibrotic tissue. Any obvious widening of the fistula track is considered a fistulous abscess (13,14). Usually an internal opening of the lesion in the anorectal lumen is present, but this may not be evident on images (15). The second reader located fistulas and abscesses according to the Parks classification (16), which includes lesion site (anterior or posterior), apparent internal opening, and local thinning of the internal sphincter at the site where the lesion is closest to the anorectal lumen. Scarring was defined as a region of

fibrosis of low or intermediate signal intensity on T2-weighted images and adhesion to the muscular structure of the anal sphincters.

Statistical analysis

The study group was stratified into patients without a history of anorectal disease and patients who had undergone surgery for anorectal disease. We calculated 95% CIs for positive predictive value and negative predictive value. Comparisons of percentages between groups were made with chisquare tests. Agreement between readers was assessed for type of lesion, location of lesion, and final diagnosis. Kappa statistics were used to quantify the degrees of agreement between two readers. Analysis was performed with SPSS software (version 11, SPSS). A kappa value of 0.2 or less was generally interpreted as poor agreement; 0.21– 0.40, fair agreement; 0.41–0.60, moderate agreement; 0.61–0.80, substantial agreement; and 0.81 or greater, almost perfect agreement. The limit of significance was set at p = 0.05 (two-sided).

Table 1: Results for Patients Without a History of Anorectal Disease (n = 60)

Final Clinical Diagnosis			MRI Findings	
Diagnosis	No.	%	Finding	No.
Levator ani syndrome	25	42	No abnormality	24
			Scarring of rectovaginal septum	1
Unspecified functional anorectal pain	21	35	No abnormality	21
Perianal suppurative lesions				
Fistula	9	15	Visualized with MRI	9
Fistula with abscess	5	8	Visualized with MRI	5

RESULTS

The study group consisted of 103 patients (54 men, 49 women; mean age, 48.3 years; range, 23–85 years). Figure 1 shows details of patient inclusion and stratification of the study population into the two groups. MRI findings suggested the final diagnoses in 40 patients (39%). Forty-three patients had undergone surgery for anorectal disease. The procedures included sphincterotomy for anal fissure (n = 15), surgery for perianal (n = 8) or anovaginal (n = 1) fistulas, incision and drainage of a perianal abscess (n = 6), anterior anal repair (n = 5), rectocele repair (n = 3), hemorrhoidectomy (n = 2), and proctocolectomy, including ileo-anal anastomosis for ulcerative colitis (n = 2), and low anterior resection with colorectal anastomosis for T2N0 rectal carcinoma (n = 1).

Patients without a history of anorectal disease

Table 1 shows the results for the 60 patients without a history of anorectal disease. Forty-six of these patients (77%) were found to have either levator ani syndrome or unspecified

functional anorectal pain. The other 14 patients (23%) had perianal fistula disease. Scarring of the rectovaginal septum was visualized on MR images of one patient (2%), but clinical assessment revealed that levator ani syndrome was the actual cause of pain. Patients with suppurative lesions (n = 14, 23%) underwent surgery.

Patients with a history of surgery for anorectal disease

The results for the 43 patients with a history of surgery for anorectal disease are shown in Table 2. A morphologic cause of chronic anal and perianal pain was found in 26 of the patients in this group (60%), 14 of whom (54%) had suppurative lesions. Eleven of the 26 patients (42%) had potentially painful scarring of the anus. One patient (2%) had a clinically occult metastasis to the sacrum from an unknown primary tumor. Seventeen patients (40%) underwent surgery, including all 14 patients with suppurative lesions (33%) and three patients (7%) with potentially painful scarring of the sphincter muscles. MRI showed a statistically

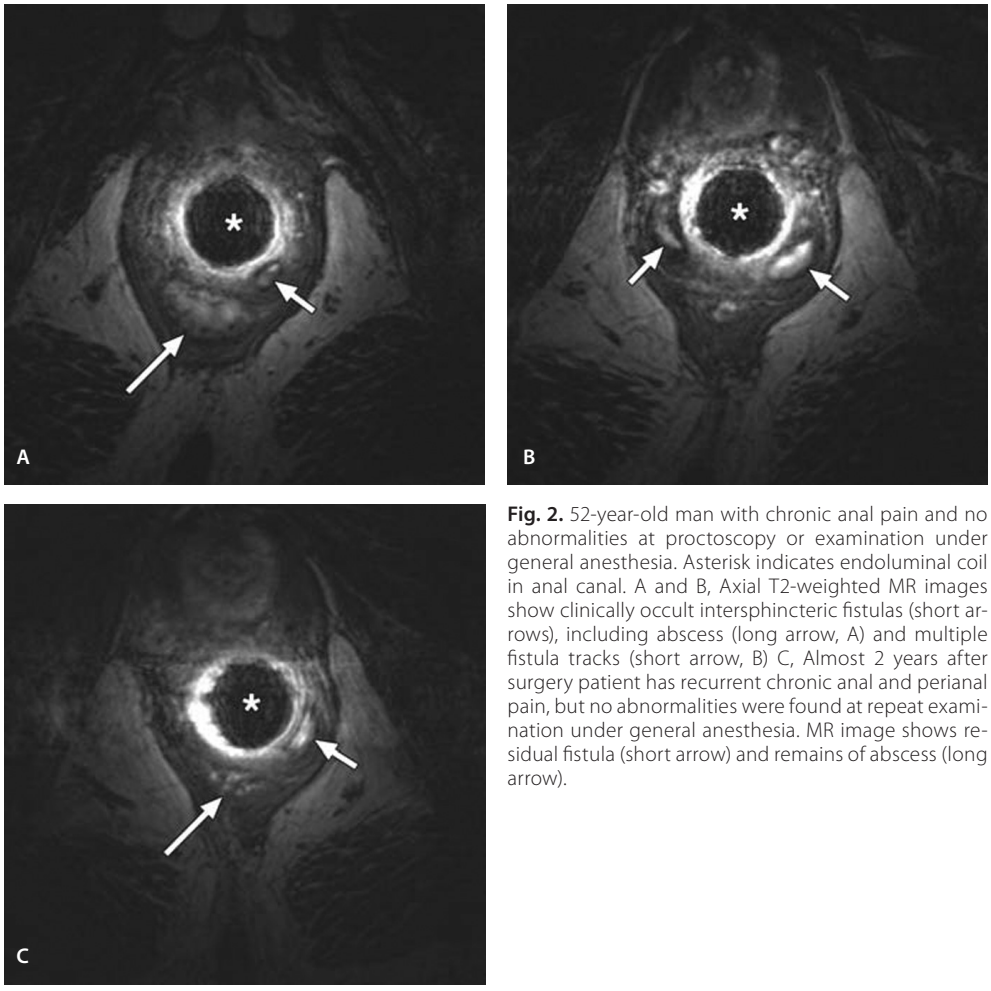

Fig. 2. 52-year-old man with chronic anal pain and no abnormalities at proctoscopy or examination under general anesthesia. Asterisk indicates endoluminal coil in anal canal. A and B, Axial T2-weighted MR images show clinically occult intersphincteric fistulas (short arrows), including abscess (long arrow, A) and multiple fistula tracks (short arrow, B) C, Almost 2 years after surgery patient has recurrent chronic anal and perianal pain, but no abnormalities were found at repeat examination under general anesthesia. MR image shows residual fistula (short arrow) and remains of abscess (long arrow).

significant higher number of abnormalities (26/43, 60%) in the patients with a history of surgery for anorectal disease than in patients without a history of anorectal disease (14/60, 23%) (p = 0.001, chi-square test).

Levator ani syndrome and unspecified functional anorectal pain

In the entire study population of 103 patients, levator ani syndrome and unspecified functional anorectal pain were the most frequently established final diagnoses and were found in 63 patients (61%).

Table 2: Results for Patients With a History of Surgery for Anorectal

Final Clinical Diagnosis			MRI Findings	
Diagnosis	No.	%	Finding	No.
Levator ani syndrome	12	28	No abnormality	9
			Scarring of anal sphincter muscles	3
Unspecified functional anorectal pain	5	12	No abnormality	5
Potential painful scarring anal sphincter muscles	11	26	Scarring anal sphincter muscles	11
Perianal suppurative lesions				
Fistula with abscesses	6	14	Visualized with MRI	6
Recurrent fistulas with abscesses	3	7	Visualized with MRI	3
Recurrent fistulas	2	5	Visualized with MRI	2
Fistulas	1	2	Visualized with MRI	1
Abscess	1	2	Visualized with MRI	1
Recurrent presacral abscess	1	2	Visualized with MRI	1
Sacral metastasis of unknown primary tumor	1	2	Visualized with MRI	1

Table 3: Locations of Anorectal Fistulas and Abscesses in 28 Patients

	Predominant Location of Lesion Site in Relation to Anorectum	
Anatomic Location	Ventral	Dorsal
Intersphincteric	1	14
Transsphincteric	1	5
Perineum and anovaginal septum	3	0
Below the level of sphincter muscles (subsphincteric)	0	3
Presacral	0	1

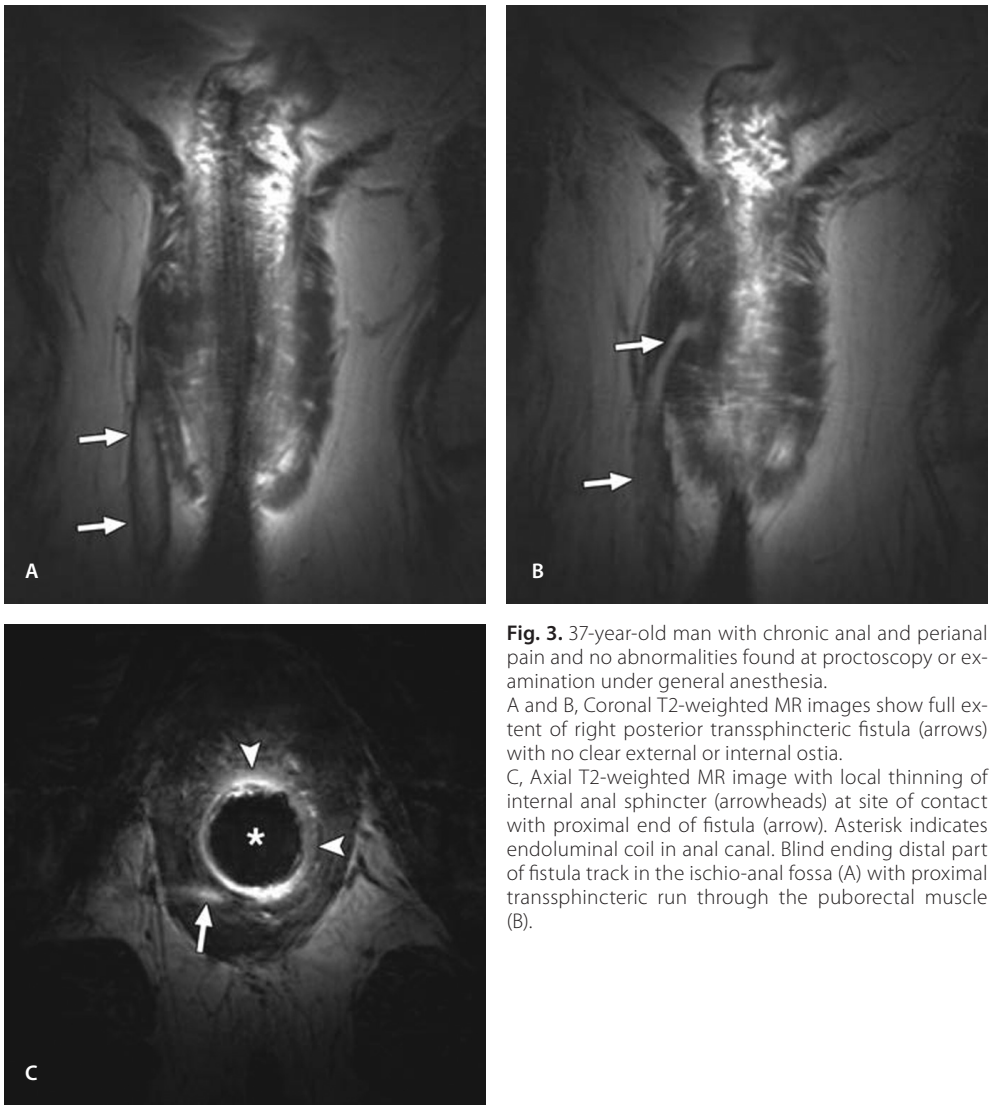

Fig. 3. 37-year-old man with chronic anal and perianal pain and no abnormalities found at proctoscopy or examination under general anesthesia.
A and B, Coronal T2-weighted MR images show full extent of right posterior transsphincteric fistula (arrows) with no clear external or internal ostia.
C, Axial T2-weighted MR image with local thinning of internal anal sphincter (arrowheads) at site of contact with proximal end of fistula (arrow). Asterisk indicates endoluminal coil in anal canal. Blind ending distal part of fistula track in the ischio-anal fossa (A) with proximal transsphincteric run through the puborectal muscle (B).

Anorectal suppurative lesions

In the study population of 103 patients, most abnormalities seen at MRI were fistulas and abscesses in 28 patients (27%). Surgery was performed within 4 months (median, 42 days; mean, 44.9 days) after MRI. MR images served as a roadmap to guide the surgical procedure, and confirmation of fistulas and abscesses was documented in the surgical reports. Patient follow-up data indicated substantial relief of symptoms after surgery.

Significantly more abscesses were seen in the group of patients with a history of surgery for anorectal disease (11/43, 26%) than in the patients without a history of anorectal disease

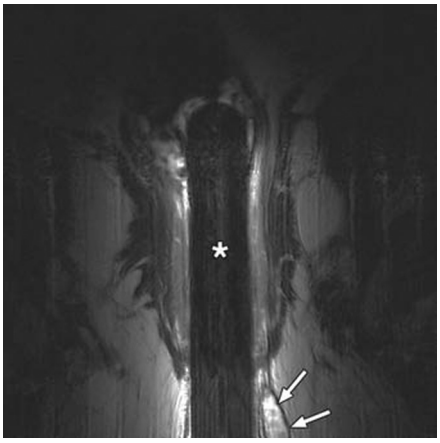

Fig. 4. 43-year-old man with chronic anal and perianal pain radiating anteriorly and in left perianal area 2 years after lateral sphincterotomy for anal fissure.
At examination under general anesthesia no obvious abnormalities were found. Coronal T2-weighted MR image shows small abscess (arrows) in skin below level of anal muscular sphincters (subsphincteric). Asterisk indicates endoluminal coil in anal canal.

(5/60, 8%) (p = 0.035, chi-square test). Most fistulas, including abscesses, were located in the intersphincteric space (n = 15) (Fig. 2). Other locations were transsphincteric (Fig. 3), subsphincteric (Fig. 4), anterior perineal with anovaginal septum (Fig. 5), and presacral (Fig. 6). Table 3 summarizes the abscess locations. In relation to the anorectum, most suppurative lesions (23/28 [82%]; 95% CI, 63– 94%) had a predominantly dorsal, or posterior, location (Figs. 2, 3, and 6) as opposed to a ventral, or anterior, location (Figs. 5 and 7). In the group of patients without a history of anorectal disease, 9 of 14 patients (64%) had fistulas in contact with the internal anal sphincter (IAS), including local thinning of the IAS at the site of contact, but without obvious communication with the anal lumen (Fig. 3). The other five patients had no contact between a fistula and the IAS.

In group of patients with a history of surgery for anorectal disease, 2 of 14 patients (14%) had close contact between a lesion and the IAS (Fig. 5), a significantly lower frequency (p< 0.05) than in patients without a history of anorectal disease.

Two patients with intersphincteric fistulas and an abscess were included in both groups. One patient had clear improvement of the abscess with residual fistulas (Fig. 2). The other had clearance of the initial abscess with a new intersphincteric abscess and persistent fistulas.

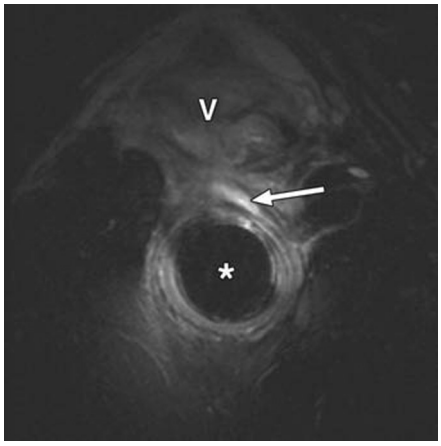

Fig. 5. 29-year-old woman with anterior anal and perianal pain 2.5 years after surgery for rectovaginal fistula. No abnormalities were found at examination under general anesthesia. Axial T2-weighted MR image with fat saturation shows linear structure of high signal intensity (arrow), which suggests presence of active fistula. Lesion extends from anus to perineum. No extension of fistula to vagina (V) is evident; finding was confirmed at surgery. Fistula is in contact with internal anal sphincter, and local thinning of internal anal sphincter at site of contact is evident. Asterisk indicates endoluminal coil in anal canal.

Scarring and pain

Scarring of the anus was assessed as a potential cause of pain in 11 (11%) patients. Surgical exploration (two patients) and resection (one patient) of scar tissue were performed with partial relief of symptoms. In the other eight cases, clinical examination revealed local stiffness with obvious exacerbation of pain when the site of scarring as visualized on MR images was provoked by digital rectal examination. In another four patients (4%), MRI showed scarring of the anus, but clinical examination revealed levator ani syndrome as the actual cause of pain (Fig. 8).

Table 4: Final Clinical Diagnoses by Sex and Age

Final Clinical Diagnosis	Women		Men	
	No. Mean	Age (y)	No. Mean	Age (y)
Levator ani syndrome	23	48.5	14	53
Unspecified functional anorectal pain	14	53.2	12	52
Anorectal sepsis	6	47.6	22	47.3
Scarring	6	49.6	5	45.4
Malignancy of sacrum	0		1	40
Total	49		54	

Malignancy

One patient (1%) was found to have a clinically occult malignant tumor of the sacrum, which was biopsy proven to be adenocarcinoma with an unknown primary lesion (Fig. 9).

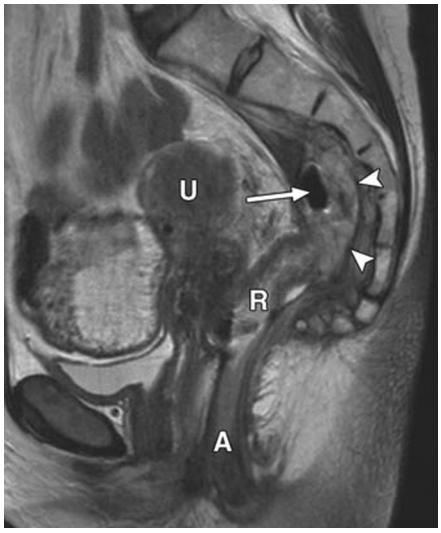

Fig. 6. 55-year-old woman 6 years after radiotherapy and total mesorectal excision for T2N0 rectal carcinoma with colorectal anastomosis and 2 years after surgical drainage of abscess in presacral space with persistent anal and perianal pain after relative pain-free interval. Examination under general anesthesia revealed no obvious abnormalities of perianal region that could explain pain. Sagittal T2-weighted MR image shows complex fluid pocket (arrowheads) with air bubble (arrow) in presacral space in contact with colorectal anastomotic area. Surgical extirpation of rectal remnant, clearing out of fluid pocket, and establishment of permanent ileostomy were performed. Pathologic analysis of resection specimen revealed chronic abscess with fibrotic and inflammatory changes and no malignancy. A = anus, R = rectal remnant, U = uterus.

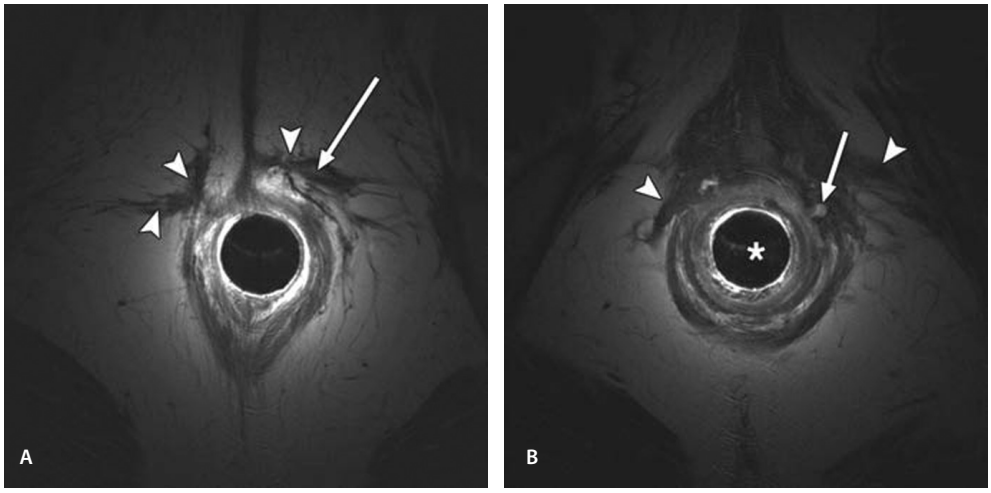

Fig. 7. 35-year-old woman with persistent anal and perianal pain after episiotomy and surgery for perianal fistula at another hospital 6 years earlier. Examination under general anesthesia revealed no obvious history of anorectal disease had significantabnormalities that could explain pain. A and B, Axial T2-weighted images through lower external anal sphincter (A) and at more proximal level (B) show extensive scarring (arrowheads) of anterior aspect of external anal sphincter and perineum and active small fistula (arrows) in scar tissue. Surgery revealed transsphincteric fistula. Asterisk indicates endoluminal coil in anal canal.

3.4

Diagnosis and Sex

There was a significant difference between men and women regarding anorectal suppurative lesions, which had a male preponderance (overall p = 0.009, chi-square test; men, 41%; women, 12%; p = 0.002), and levator ani syndrome, which had a female preponderance (women, 47%; men, 26%; p = 0.044) (Table 4).

Positive and negative predictive values and interobserver agreement

Morphologic alteration was visualized with MRI in 40 of 103 patients (39%). The positive predictive value of MRI was 91% (40/44; 95% CI, 78–95%). The negative predictive value was 100% (59/59; 95% CI, 94–100%). The first and second readers had excellent agreement in the evaluation of MRI examinations, agreeing in 96% of cases (99/103) ($\kappa = 0.92$). One abscess, associated with an intersphincteric fistula, was described in the original radiologic report and confirmed at surgery but was not recorded by the second reader. Three cases were originally reported as having a suggestion of small intersphincteric fistulas; none of these lesions was recorded by the second reader or confirmed at clinical follow-up. All cases of scarring and malignancy were reported by both readers.

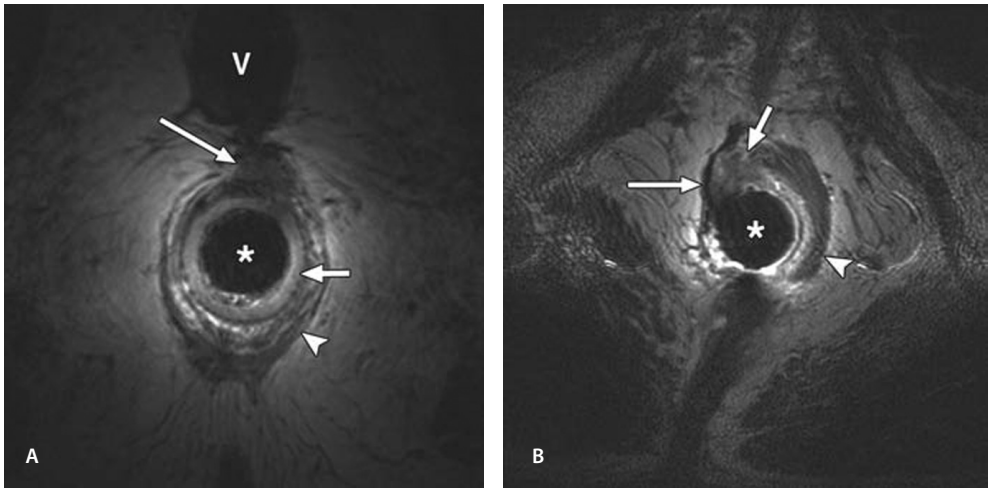

Fig. 8. Examples of cases in which MRI findings suggested scarring of the anus. Asterisk indicates endoluminal coil in anal canal. A, 62-year-old woman 5 years after anterior anal repair for persistent anal and perianal pain that had lasted 1.5 years. Axial T2-weighted MR image shows scarring (long arrow) of anterior aspect of external anal sphincter (arrowhead) and perineum but clinical examination revealed levator ani syndrome as cause of pain. Short arrow indicates internal anal sphincter. V = vagina. B, 59-year-old man 7 years after surgery for perianal fistula disease. Chronic anal and perianal pain had lasted for 2 years with no abnormalities found at proctoscopy or examination under general anesthesia. MR image shows part of intact muscular structure of external anal sphincter (arrowhead) on left side. On right, external anal sphincter is replaced by hypointense linear structure (long arrow) suggestive of fibrotic strand with anterior adjacent area of intermediate signal intensity (short arrow). These abnormalities were interpreted as scarring at MRI, and obvious painful local stiffness was found at clinical evaluation. Final diagnosis was potentially painful scarring.

DISCUSSION

Although chronic anal and perianal pain is a relatively common problem in the general population (1), few studies have focused on this problem. To our knowledge, the current study is the first use of MRI in a cohort of patients with chronic anal and perianal pain. The efficacy of this imaging modality in the evaluation of chronic anal and perianal pain is shown in the identification of suppurative lesions in 27% of all patients. This is an important finding, and these patients will benefit from surgery.

Results of few imaging studies in which the patient cohort had chronic anal and perianal pain have been published (3, 17–19). These ultrasound-based studies showed a common weakness in that a clear clinical reference standard for the reported ultrasound findings was lacking. In addition, the nature of ultrasound as an operator-dependent imaging modality leads to limitations in the reproducibility of findings. On the other hand, the results of these studies indicated that patients with clinically occult chronic anal and perianal pain need further imaging studies before the diagnosis of a functional gastrointestinal disorder can be made.

Although we found lesions in other locations, most suppurative lesions were located dorsally in the intersphincteric space, which may reflect the higher anatomic prevalence of posterior location of anal glands (20). Among 28 patients with suppurative lesions, no ob-

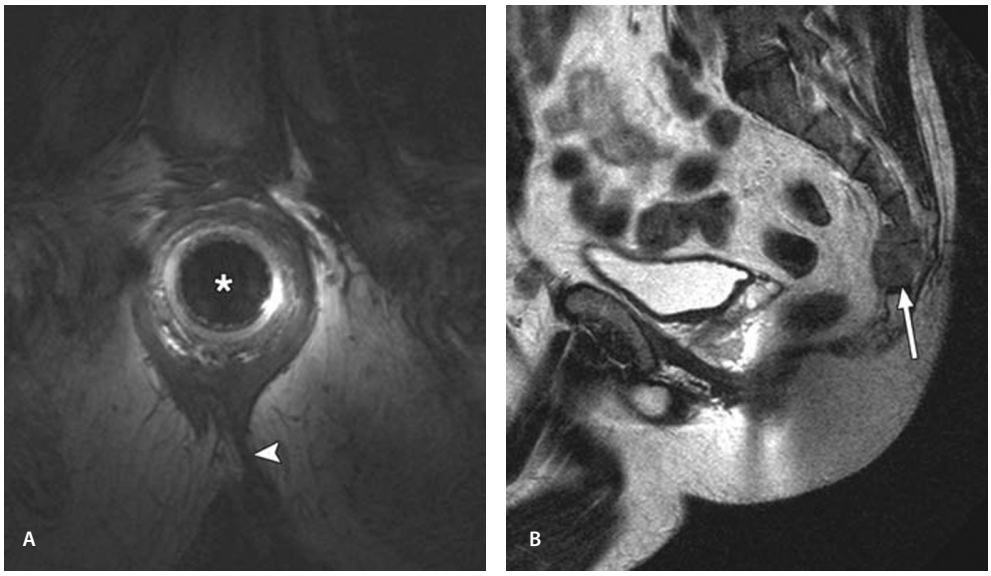

Fig. 9. 40-year-old man 17 years after surgical drainage of perianal abscess with persistent and increasing anal and perianal pain for almost 1 year with no abnormalities at proctoscopy or examination under general anesthesia.
A, Endoanal MR image shows thickened anococcygeus ligament (arrowhead). Asterisk indicates endoluminal coil in anal canal.
B, Whole-pelvis image acquired with body coil shows tumor at sacrococcygeus joint (arrow), which was adenocarcinoma with unknown primary lesion. Patient also had retroperitoneal lymph node and other bone metastasis (not shown).

3.4

vious internal opening of the lesion in the lumen of the anorectum was seen. Previous investigators (14, 21) have described accurate visualization of the internal opening of perianal fistulas with an endoluminal coil similar to that used in this study. In 11 cases in our study close contact was found between the lesion and local thinning of the IAS. It can be assumed that the internal opening of fistulas and abscesses was obstructed, probably by granulation tissue. This may have prohibited drainage of these lesions in the anal lumen, explaining their clinically occult status with pain as the only presentation. Compared with the group of patients who had a history of surgery for anorectal disease, patients without a history of anorectal disease had significantly more suppurative lesions in close contact with the IAS. This finding suggests a different mechanism of infection: patients without a history of anorectal disease had a predominantly cryptoglandular type of fistula disease as opposed to the secondary iatrogenic infections in the group of patients with a history of surgery for anorectal disease (15). In addition, significantly more abscesses were found in the patients with a history of surgery for anorectal disease, which may be explained by the more severe iatrogenic infectious mechanism.

Spatial resolution on MR images can be improved by use of a receiver endoluminal coil in the anal canal itself; however, care should be taken to perform additional imaging of more distant structures with the phased-array or body coil. Focusing on the immediate perianal region in imaging of patients with chronic anal and perianal pain is insufficient, as illustrated by the detection of one case of malignancy of the sacrococcygeal spine in this study (Fig. 9).

The second most common abnormality encountered at MRI was scarring of anal sphincter muscles. Only 3 of 11 patients with scarring as a potential cause of chronic anal and perianal pain had undergone surgery for scar tissue, and they had partial relief of symptoms. In another four patients, clinical assessment revealed levator ani syndrome as the final diagnosis and no perianal scarring, as was found with MRI. This result emphasizes the point that functional gastrointestinal disorders can coexist with morphologic abnormalities and be mainly responsible for pain. In cases of perianal scarring, a thorough physical examination by an experienced gastrointestinal clinician is recommended. Future studies are needed to clarify the role of scarring in the pain experience of patients. In addition, the diagnosis of unspecified functional anorectal pain can be made with considerable certainty when no abnormalities can be established with either clinical workup or MRI. This conclusion was reflected by the finding that no patient with a final diagnosis of levator ani syndrome or unspecified functional anorectal pain was readmitted to the department of colorectal surgery with a change in symptoms that would suggest an occult morphologic cause. Anorectal suppurative lesions were found with significantly higher frequency in men than in women in our study. In contrast, levator ani syndrome was found more often in women, an association that has not been previously reported, to our knowledge.

Our study had limitations, one of which was the retrospective design, which may be prone to selection bias. However, given our strict inclusion criteria and the fact that at our institution performing MRI is standard practice in the care of patients with chronic anal and perianal pain, we believe the study population representative for the aims of this study in a tertiary clinical setting. Another limitation may be the inclusion of patients who had undergone surgery for anorectal disease. Their pain may have been related to their previous disease or treatment. We classified these patients in a separate subgroup and compared their current status with previous findings. Therefore, we believe that the results can be applied to this patient population. Chronic anal and perianal pain due to scarring of the anal sphincter muscles lacks a solid reference standard. In addition, in using MRI to guide the final diagnosis of potentially painful scarring in these patients, we may have overemphasized the roles of both MRI and scar tissue in these patients. We believe this drawback can be alleviated by thorough clinical workups by an experienced colorectal surgeon before and after MRI. The exclusion of other physical and functional disorders makes the current classification acceptable. It might also be helpful to extend clinical follow- up and collect more recent updates on the conditions of patients included in our study, especially those with levator ani syndrome or unspecified functional anorectal pain. This task was beyond the scope of our institutional approval. Because existing follow-up data showed no evidence for a need to reconsider established final diagnoses, we do not consider this a serious weakness of the study.

CONCLUSION

Anorectal MRI is an effective imaging modality for visualization and exclusion of morphologic abnormalities, especially perianal suppurative lesions and scarring. Using MRI, we were able to identify lesions in 39% of patients with chronic anal and perianal pain, for whom a standard clinical workup had failed to reveal abnormalities. MRI is therefore a recommended constituent of the workup of these patients before their symptoms are considered part of a functional gastrointestinal disorder.

REFERENCES

1. Drossman DA, Li Z, Andruzzi E, et al. U.S. householder survey of functional gastrointestinal disorders: prevalence, sociodemography, and health impact. Dig Dis Sci 1993; 38:1569–1580
2. Whitehead WE, Wald A, Diamant NE, Enck P, Pemberton JH, Rao SS. Functional disorders of the anus and rectum. Gut 1999; 45(suppl 2):II55–II59
3. Beer-Gabel M, Carter D, Venturero M, Zmora O, Zbar AP. Ultrasonographic assessment of patients referred with chronic anal pain to a tertiary referral centre. Tech Coloproctol 2010; 14:107–112
4. Henny C, Guenther F, Guex P, Bogousslavsky J, Regli F. Chronic anogenital and perineal pain: clinical and psychopathological characteristics of a syndrome. Rev Med Suisse Romande 1991; 111:27–32
5. Pescatori M. Anal pain? Explore the brain! Dis Colon Rectum 2002; 45:286
6. Greenhalgh R, Cohen CR, Burling D, Taylor SA. Investigating perianal pain of uncertain cause. BMJ 2008; 336:387–389
7. Drossman DA, Dumitrascu DL. Rome III: new standard for functional gastrointestinal disorders. J Gastrointestin Liver Dis 2006; 15:237–241
8. Drossman DA. The functional gastrointestinal disorders and the Rome III process. Gastroenterology 2006; 130:1377–1390
9. Grover M, Drossman DA. Functional abdominal pain. Curr Gastroenterol Rep 2010; 12:391–398
10. Grant SR, Salvati EP, Rubin RJ. Levator syndrome: an analysis of 316 cases. Dis Colon Rectum 1975; 18:161–163
11. Sinaki M, Merritt JL, Stillwell GK. Tension myalgia of the pelvic floor. Mayo Clin Proc 1977; 52:717–722
12. Hussain SM, Stoker J, Schouten WR, Hop WC, Lameris JS. Fistula in ano: endoanal sonography versus endoanal MR imaging in classification. Radiology 1996; 200:475–481
13. Hussain SM, Stoker J, Schutte HE, Lameris JS. Imaging of the anorectal region. Eur J Radiol 1996; 22:116–122
14. Dwarkasing S, Hussain SM, Hop WC, Krestin GP. Anovaginal fistulas: evaluation with endoanal MR imaging. Radiology 2004; 231:123–128
15. Hussain SM, Outwater EK, Joekes EC, et al. Clinical and MR imaging features of cryptoglandular and Crohn's fistulas and abscesses. Abdom Imaging 2000; 25:67–74
16. Parks AG, Gordon PH, Hardcastle JD. A classification of fistula-in-ano. Br J Surg 1976; 63:1–12
17. García-Montes MJ, Argüelles-Arias F, Jiménez- Contreras S, Sánchez-Gey S, Pellicer-Bautista F, Herrerías-Gutiérrez JM. Should anorectal ultrasonography be included as a diagnostic tool for chronic anal pain [in Spanish]? Rev Esp Enferm Dig 2010; 102:7–14
18. Vieira AM, Castro-Pocas F, Lago P, et al. The importance of ultrasound findings in the study of anal pain [in Spanish]. Rev Esp Enferm Dig 2010; 102:308–313
19. Pascual I, Garcia-Olmo D, Martinez-Puente C, Pascual-Montero JA. Ultrasound findings in spontaneous and postoperative anal pain [in Spanish]. Rev Esp Enferm Dig 2008; 100:764–767
20. Gupta PJ. A study of suppurative pathologies associated with chronic anal fissures. Tech Coloproctol 2005; 9:104–107
21. West RL, Zimmerman DD, Dwarkasing S, et al. Prospective comparison of hydrogen peroxide enhanced three-dimensional endoanal ultrasonography and endoanal magnetic resonance imaging of perianal fistulas. Dis Colon Rectum 2003; 46:1407–1415

chapter 4

chapter 4.1

Chronic Lower Urinary Tract Symptoms in Women: Classification of Abnormalities and Value of Dedicated MRI for Diagnosis

Roy S. Dwarkasing
Sylvia I. Verschuuren
Geert J. L. H. Leenders
Maarten G. J. Thomeer
Gerardus R. Dohle
Gabriel P. Krestin

AJR Am J Roentgenol. 2014 Jan;202(1):W59-66. Clinical Perspective.

ABSTRACT

Objective Chronic lower urinary tract symptoms are common in women. We present a classification of abnormalities that can be considered in the differential diagnosis for lower urinary tract symptoms and can show the value of dedicated state-of-the art MRI in the workup of patients.

Conclusion Dedicated MRI tailored to patient symptoms and clinical findings has the potential to map out morphologic causes and categorize dysfunctional conditions from those that are truly non-morphologic.

INTRODUCTION

Lower urinary tract symptoms are a group of symptoms with abnormalities that may be categorized into seven groups: storage problems, voiding problems, postmicturition symptoms, symptoms associated with sexual intercourse or pelvic organ prolapse, lower urinary tract pain, and lower urinary tract dysfunction syndrome [1]. New insights suggest that lower urinary tract symptoms are a non-organ-specific group of symptoms, which are sometimes age related and progressive, affecting up to 26% of women 40 years old and older [2, 3]. The presentation of symptoms can be diverse and the differential diagnoses extensive. It is of importance to differentiate morphologic abnormalities from dysfunctional conditions that are responsible for a patient's complaints. Dedicated MRI and urodynamic studies are important tools in this respect [4]. This article presents a classification of morphologic or functional abnormalities that can be considered in the differential diagnoses of women with chronic lower urinary tract symptoms. This classification is based on common and less-common causes for lower urinary tract symptoms according to the literature and our experience at a tertiary referral center for female genitourinary symptoms and dedicated MRI of the pelvis and pelvic floor. On the basis of this classification, morphologic abnormalities will be described and illustrated on MRI. Important information for clinical management and key features on MRI will be elucidated.

MRI

With its excellent soft-tissue contrast and multiplanar acquisition, MRI has become the imaging modality of choice for diagnosis and preoperative evaluation in female patients with urethral and periurethral disease. Previously, pelvic phased-array coils were applied for female pelvic imaging, including imaging of the urethra and periurethral region. Subsequently, intracavitary MRI coil design (for endovaginal and endorectal placement) made imaging with increased spatial resolution and high signal-to-noise ratio of this anatomic region possible [4–6]. Until 2009, our institute performed pelvic imaging on a 1.5-T MR system (Gyroscan NT Intera 1.5, Philips Healthcare) using a 4-channel pelvic phased-array coil placed around the pelvis or a rigid endoluminal coil placed in the vagina. The endoluminal coil was commercially available and consisted of a fixed rectangular 60-mm-long rigid receiver coil with a width of 16 mm. The coil was contained within an 80-mm-long cylindric coil holder with a diameter of 19 mm. Since 2009, both a 1.5-T system (Discovery MR450, GE Healthcare) and a 3-T system (Discovery MR750, GE Healthcare) have been used. For female pelvic imaging, an 18-channel phased-array multicoil is placed around the pelvis; in addition, an endoluminal coil placed in the vagina is applied for dedicated urethral and periurethral imaging. Both the endoluminal coil for 1.5- T imaging and for 3-T imaging are custom built and consist of a dual coil arrangement orthogonally positioned, with a total length of 195 mm (active region, 90 mm) and a diameter of 20 mm. Before the introduction of the coil into the vagina by the patient herself, a condom is placed over the coil and ultrasound gel is used as a lubricant. It should be noted that this rigid endoluminal coil is not the same as the inflatable rectal coil but is of smaller diameter and is designed to be placed in the anus or vagina.

MRI Protocol

A concise imaging protocol of T2-weighted turbo spin-echo (TSE) sequences with high-resolution slices in three planes (axial, coronal, and sagittal) through the urethra and periurethral region is performed including axial T2-weighted TSE with fat saturation and T1-weighted gradient-echo sequences (Tables 1 and 2). The FOV includes the bladder base and perianal region. With the phased-array multicoils, the FOV can be adjusted to the entire pelvic region. On endoluminal MRI, image volume encompasses the entire sensitive region of the coil. With this concise protocol, scanning times may be limited to an average of 20 minutes per patient. If malignancy is suspected or has to be excluded, a dynamic contrast-enhanced series may be considered. Lesion detection and characterization may be enhanced with diffusion-weighted imaging and apparent diffusion coefficient mapping [7]. To evaluate for prolapse, a dynamic true fast imaging with steady-state free precession (true FISP) or HASTE sequence in the midsagittal plane may be performed [8]. The true FISP sequence is performed as a continuous acquisition with the patient alternating every 5 seconds between rest and maximal strain. The dynamic HASTE sequence is performed with multiple acquisitions per slice alternating between rest and maximal strain. Especially for ectopic ureter, MR urography has proven to be a sensitive diagnostic tool [9].

Table I: Suggested MRI Scan Parameters for High Resolution T2-weighted Imaging of the Female Urethra and Periurethral region using an Endoluminal Coil

Intravaginal Coil Placement	TR/TE (ms)		FOV (mm)		Matrix		Slice Thickness/ Gap (mm)	
MRI system	1.5 T	3 T	1.5 T	3 T	1.5 T	3 T	1.5 T	3 T
Axial T2-weighted TSE	3581/119	5321/116	120	120	384 × 256	256 × 256	2.5/0.3	2/0.2
Axial T2-weighted TSE with fat saturation	5494/82	3366/120	120	120	256 × 224	224 × 224	2.5/0.3	2/0.2
Coronal T2-weighted TSE	3091/113	4182/102	140	120	320 × 224	224 × 224	2.5/0.3	2/0.2
Sagittal T2-weighted TSE	2601/94	4175/101	120	120	320 × 224	224 × 224	2.5/0.3	2/0.2

Note—TSE = turbo spin-echo.

Table 2: Suggested MRI Scan Parameters for Dedicated T2-weighted Imaging of the Female Urethra and Periurethral region using an External Pelvic Coil

Pelvic Phased-Array Coils	TR/TE (ms)		FOV (mm)		Matrix		Slice Thickness/ Gap (mm)	
MRI System	1.5 T	3 T	1.5 T	3 T	1.5 T	3 T	1.5 T	3 T
Axial T2-weighted TSE	5860/121	6010/127	200	200	384 × 256	416 × 384	3.0/0.3	3.0/0.3
Axial T2-weighted TSE with fat saturation	5060/80	5733/121	200	200	256 × 224	224 × 224	3.0/0.3	3.0/0.3
Coronal or sagittal T2-weighted TSE	3360/111	3568/127	200	200	320 × 224	416 × 384	3.0/0.3	3.0/0.3

Note—TSE = turbo spin-echo.

Urodynamic Studies

Urodynamic studies, or urodynamics, include cystometry, urinary flow and urethral pressure studies, stress testing, video-urodynamic studies, and electrophysiological studies. The main indications for urodynamic studies are incontinence and associated voiding problems (lower urinary tract symptoms). In a study of 60 women with clinically evaluated chronic lower urinary tract symptoms, urodynamic studies showed the final diagnosis in 22% of patients, which included dysfunctional voiding (12%) and interstitial cystitis (10%) [4].

CLASSIFICATION

A classification for lower urinary tract symptoms based on the causal substrate may be complicated. However, considering the more common causes for lower urinary tract symptoms, we believe that lower urinary tract symptoms can be subcategorized into morphologic abnormalities of the bladder, urethra, and periurethral region or functional disorders of the lower urinary tract and pelvic floor. We propose the following subclassification, the categories of which will be more fully discussed.

Structural Abnormalities of the Lower Urinary Tract and Periurethral Region

Lesions of the urethra

- Cystic lesions: urethra diverticula, non-communicating submucosal cyst
- Urethritis, inflammatory conditions, and fistulization
- Urethral caruncle
- Neoplastic alterations and malignancy: benign tumors, nephrogenic adenoma, pseudoinflammatory tumor, urethral carcinoma, malignant melanoma

Lesions of the periurethral region

- Cystic lesions: vagina wall inclusion cyst, cyst of urogenital sinus origin (cyst of Skene, cyst of Bartholin), developmental cysts of paramesonephric duct (müllerian cyst) and mesonephric duct origin (Gartner cyst), others
- Benign solid lesions: fibroma, leiomyoma, neurofibroma, lipoma, myoblastoma, hemangioblastoma, others.
- Altered structure of urethra and periurethral region: defects of the urethral supporting structures, periurethral fibrosis.
- Endometriosis
- Locally advanced carcinoma with urethral involvement

Prolapse abnormalities of the lower urinary tract

- Hypermobility of the urethra, urethrocele, cystocele
- Prolapse of the urethra

Miscellaneous

- Ectopic ureter

Functional Abnormalities of the Lower Urinary Tract

- Dysfunctional voiding
- Interstitial cystitis (painful bladder syndrome)
- Others

LESIONS OF THE URETHRA

Cystic Lesions

Urethral diverticula in women are generally thought to be acquired (Fig. 1), most often as a result of obstructed drainage of the periurethral glands, with subsequent cystic dilatation or abscess formation. Other causes are direct or indirect trauma to the urethra mainly from vaginal birth, urethral catheterization (Fig. 2), cystoscopy, urethral dilatation, or surgical pro-

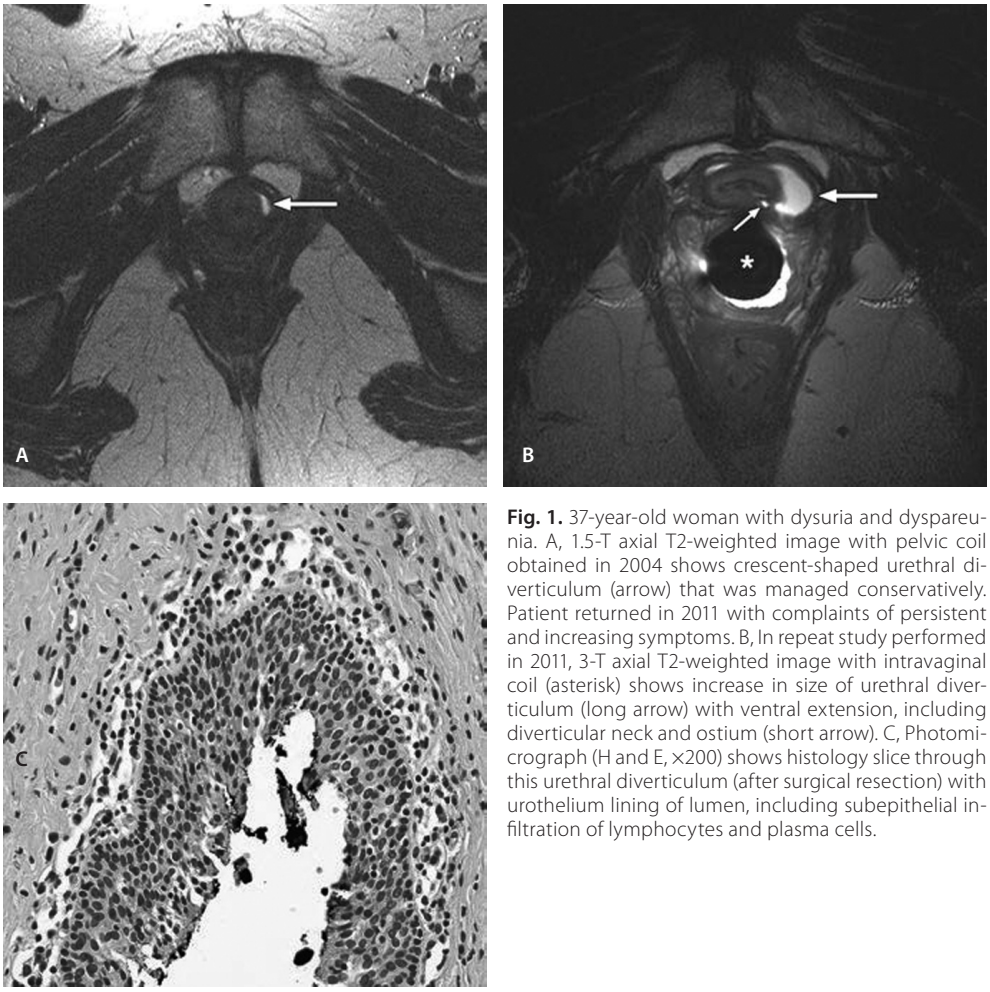

Fig. 1. 37-year-old woman with dysuria and dyspareunia. A, 1.5-T axial T2-weighted image with pelvic coil obtained in 2004 shows crescent-shaped urethral diverticulum (arrow) that was managed conservatively. Patient returned in 2011 with complaints of persistent and increasing symptoms. B, In repeat study performed in 2011, 3-T axial T2-weighted image with intravaginal coil (asterisk) shows increase in size of urethral diverticulum (long arrow) with ventral extension, including diverticular neck and ostium (short arrow). C, Photomicrograph (H and E, ×200) shows histology slice through this urethral diverticulum (after surgical resection) with urothelium lining of lumen, including subepithelial infiltration of lymphocytes and plasma cells.

cedures of the urethra. Dedicated MRI will show the configuration of urethral diverticula, including visualization of the ostium in 84% of cases [4].

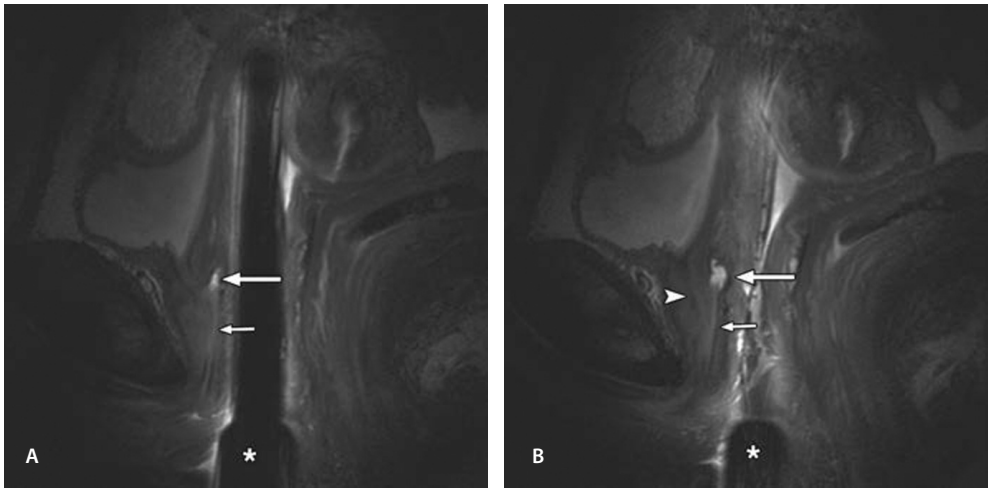

Fig. 2. 26-year-old woman with postmicturition dripping, dyspareunia, recurrent lower urinary tract infections, and inability for bladder catheter insertion. Symptoms originated after painful urethral catheterization at delivery 8 months before imaging. A and B, Midline (A) and off-midline (B) 3-T sagittal T2-weighted images with intravaginal coil (asterisk) show traumatic urethral diverticulum (long arrow). Short arrow indicated new urethral lumen, and arrowhead indicates original lumen.

Fig. 3. 82-year-old woman 3 years after low anterior resection for T3N0M0 rectal cancer and colostomy. Local recurrence (not shown) left pelvic side wall on follow-up MRI after neoadjuvant combined chemoradiotherapy. Patient complained of obstructive urinary symptoms and dysuria. Sagittal T2-weighted 1.5-T image with pelvic coil shows thickened urethra (arrows) with preserved layered structure of wall consistent with radiation-induced inflammatory reaction. Star indicates centrally located thickened mucosal layer surrounded by thickened submucosal layer (arrowheads). A = anus, B = bladder. Compare with normal structure of urethra in Figure 6.

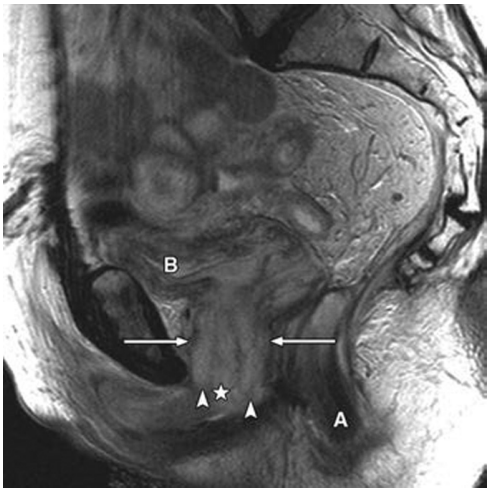

Urethritis, Inflammatory Conditions, and Fistulization

Inflammation of the urethra and periurethral glands can result from bacterial (common: gonorrhea and Chlamydia) infections and noninfectious causes, such as Reiter disease and Crohn disease. Radiation injury can be another cause (Fig. 3). Sometimes, inflammation may

Fig. 4. 34-year-old woman 10 months after cesarean delivery with recurrent lower urinary tract infections, involuntary loss of urine, and dyspareunia. Sagittal T2-weighted 1.5-T image with pelvic coil shows vesicocervical-vaginal fistula (arrow) as high-signalintensity linear structure connecting bladder lumen with cervical lumen.

become extensive and may mimic malignancy. Clinical history and evaluation are important for proper diagnosis. On MRI, urethritis can be seen as a fusiform thickening of the urethra with retained layering structure of the urethral wall (Fig. 3).

Malignancy, however, usually shows a loss of the layered structure of the urethra wall. In equivocal cases, ultimately pathologic analysis may be needed. Fistulization from genital organs to the urethra or bladder may complicate inflammation or local surgery (Fig. 4).

Urethral Caruncle

Urethral caruncle is a common benign exophytic lesion of the urethral meatus usually encountered in postmenopausal women. Urethral caruncle most likely represents ectropion of the dorsal urethral mucosa secondary to postmenopausal regression of the vaginal mucosa. At histologic examination, caruncles exhibit a hyperplastic squamous epithelium with underlying submucosal vascularity, fibrosis, and inflammation. Imaging of urethral caruncle is generally not necessary.

4.1

Fig. 5. 43-year-old woman with obstructive urinary flow symptoms, including painful intralabial lump on physical examination. Sagittal T2-weighted 3-T image with intravaginal coil (asterisk) shows smoothbordered tumor (arrow) with homogeneous high signal intensity (SI). Lesion was initially interpreted (clinically and on imaging) as fibroepithelial polyp because of polypoid appearance, which seems to be in continuity with submucosal layer (arrowhead) of urethra and relative high SI on T2-weighted imaging. Complete surgical resection was performed with leiomyoma proven on pathology analysis. Urethral leiomyoma typically has low or intermediate SI on T2-weighted images (compare with Fig. 11) and paraurethral orientation locating lesion in relation to outer muscle layers of urethral wall.

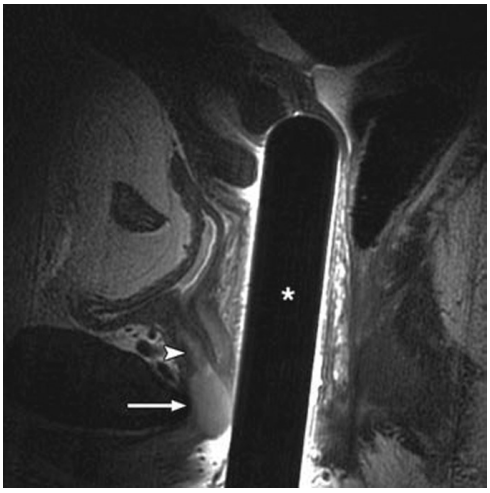

Neoplastic Alterations and Malignancy

Benign tumors—Common benign urethral masses include condyloma, fibroepithelial polyps, hemangioma, and leiomyoma. These may present as an intralabial mass with obstructive symptoms. Urethral involvement by condylomata is reported in 5–31% of patients with genital condylomata caused by human papilloma virus and in 50% of patients with a condyloma at the urethral meatus [10, 11]. Fibroepithelial polyps are rare intraurethral lesions in young women. Urethral hemangiomas are exceedingly rare. They appear as an erythematous inflamed mass surrounding the urethral meatus [12]. Urethral leiomyoma (Fig. 5) usually arises from the circular smooth layer of the urethra. MRI may show the site of origin and extension of the lesion, which may be beneficial for surgery. Imaging features suggestive of benignity are well-defined borders and homogeneous signal intensity (SI) of the lesion (Fig. 5).

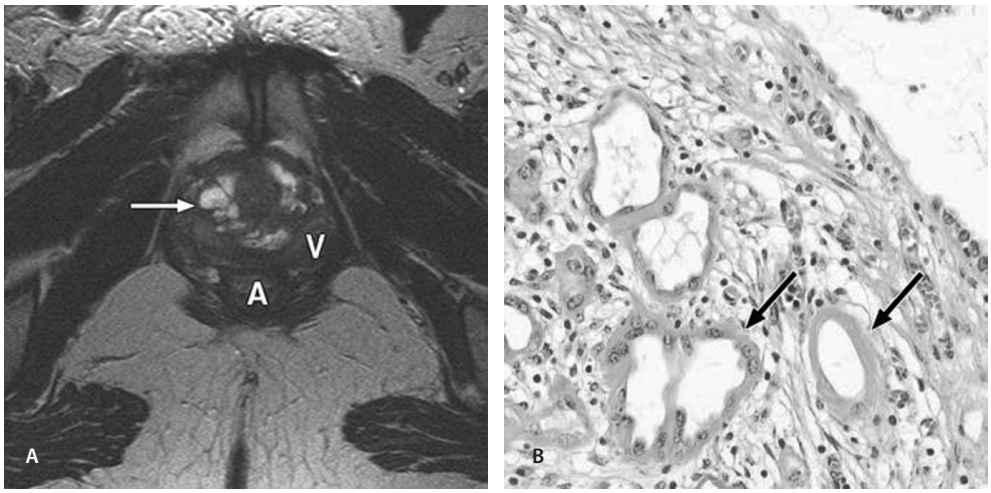

Fig. 6. 45-year-old woman with dysuria, dyspareunia, and postmicturition dripping. A, Axial T2-weighted 1.5-T image with pelvic coil shows multilocular multiseptated cystic lesion (arrow) surrounding midurethra. Surgical resection revealed complicated urethral diverticulum with thickened wall, internal septa, debris, and small calculi. A = anus, V = vagina. B, Photomicrograph (H and E, ×200) at histology analysis shows nephrogenic adenoma composed of small tubules and microcysts embedded in edematous stroma with chronic inflammation within urethral diverticulum. Tubules and microcysts are covered by flat and cubical epithelium and locally hobnail cells encircled by prominent eosinophilic basal membrane (arrows).

Nephrogenic Adenoma

Diverticula are characteristically lined by urothelium (Fig. 1), but squamous and glandular metaplasia commonly occur in response to chronic inflammation [13]. Nephrogenic adenoma is a benign epithelial tumor localized at the level of the urothelium and caused by metaplasia. The lesion may present as thick irregular septa (Fig. 6A) or a mass lesion within a urethral diverticulum on MRI and may be interpreted as carcinoma within the diverticulum. Distinguishing nephrogenic metaplasia (Fig. 6B) from adenocarcinoma on histology can be challenging [13].

Fig. 7. 73-year-old woman with dysuria, nocturia, and obstructive urinary flow. Axial T2-weighted 1.5-T image with pelvic coil shows tumor of urethra (long arrow) with expansion into vaginal wall (short arrows). Biopsy of lesion revealed inflammatory pseudotumor with extensive inflammation consisting of lymphocytes, plasma cells, histiocytes, and eosinophilic and neutrophilic granulocytes within subepithelial connective tissue, together with necrosis. Additional histochemical staining (periodic acid and Ziehl-Neelsen) did not reveal fungi or mycobacteria. After treatment with corticosteroids, tumor reduced significantly in size.

Pseudoinflammatory Tumor of the Urethra

Clinically and radiologically, inflammatory pseudotumors resemble malignant tumors with extension into adjacent structures and organs, including heterogeneous SI and contrast enhancement on MRI (Fig. 7). Histopathology examination reveals the presence of spindle cells, myofibroblasts, plasma cells, lymphocytes, and histiocytes.

4.1

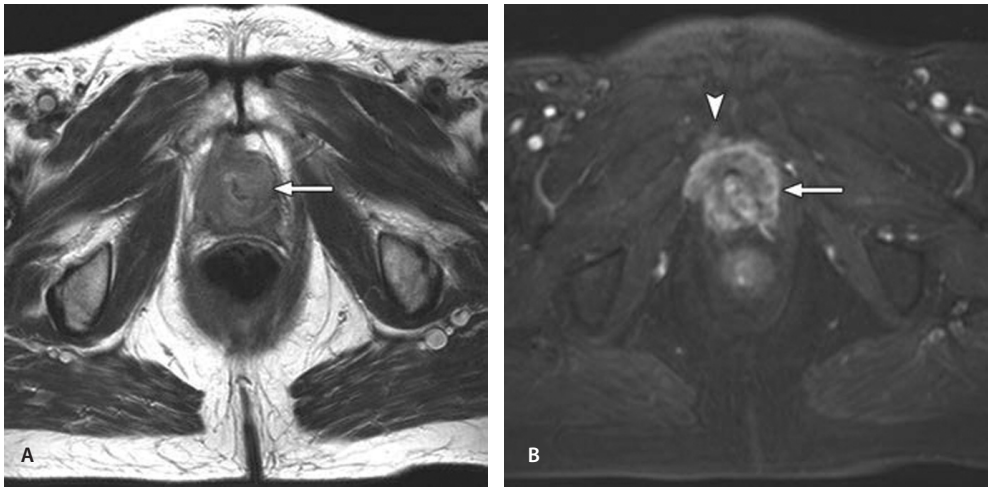

Fig. 8. 56-year-old woman with initial symptoms of painful and obstructive urinary flow. Imaging took place almost 6 weeks after surgical intervention in another hospital because of urethral stenosis with proven squamous cell carcinoma, probably arising within urethral diverticulum. Symptoms at time of imaging were fast-growing extremely painful mass at urethral meatus and vaginal wall. A and B, Axial T2-weighted 1.5-T image with pelvic coil (A) and axial T1-weighted image with fat saturation after IV administration of gadolinium chelate (B) show locally advanced tumor of distal urethra extending to os pubis on right (arrow). Gadolinium-enhanced image (B) reveals invasion of right pubic bone (arrowhead), finding that is not clear on A.

Fig. 9. 79-year-old woman with painful mass at urethral meatus, dysuria, and obstructive urinary symptoms. Sagittal T2-weighted 1.5-T imagewith pelvic coil shows pathology-proven primary melanoma (arrow) located in dorsal urethral meatus with extension in perineum and involvement of ventral vaginal wall. Note cystocele of dorsal bladder wall (arrowhead) with position below pubococcygeal line (dashed line).

Urethral Carcinoma

Approximately 10% of surgically resected diverticula show atypical glandular findings, including invasive adenocarcinoma [14]. Adenocarcinoma accounts for up to 70% of carcinomas arising in urethral diverticula. Squamous cell carcinoma usually affects the distal urethra (Fig. 8); adenocarcinoma and transitional cell carcinoma occur in the proximal urethra. Pelvic examination (under anesthesia) combined with cystourethroscopy and biopsy of the lesion is required. MRI can be used for proper local staging (Fig. 8).

Malignant Melanoma

Malignant melanoma may rarely include the urethra as either a primary (Fig. 9) or a metastatic site. Initially, the lesion may present as a well-defined polypoid mass lesion with homogeneous SI (Fig. 9) and may resemble a benign lesion on MRI. Final diagnosis is usually assessed by pathology.

LESIONS OF THE PERIURETHRAL REGION

Periurethral masses may be cystic or solid. The clinical presentation correlates with the position of the mass in relation to the urethra. Centrally located masses may lead to dysuria, frequency, dyspareunia, hematuria,

and obstructive symptoms. Imaging may be considered to confirm the cystic or solid nature and to assess the depth and extent of the lesion before surgery.

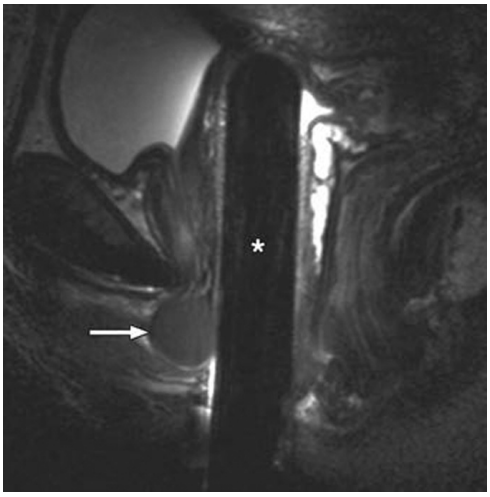

Fig. 10. 32-year-old woman with increasingly painful lump behind urethral orifice with obstructed urinary flow and dyspareunia. Sagittal T2-weighted 1.5-T image with intravaginal coil (asterisk) shows surgically confirmed infected cyst of Skene (arrow). Lesion has typical location in floor of distal urethra (left-sided) with low-signal-intensity content, which is suggestive of infected cyst of Skene.

Cystic Lesions

Benign vaginal and periurethral cystic lesions are frequently encountered in gynecologic and female urologic practices. These may be congenital or acquired. Preexistent asymptomatic cystic lesions may become symptomatic after intralesional hemorrhage or infection. Symptomatic lesions will therefore often display atypical SI characteristics of the content of the lesion. Hemorrhagic cysts may show low SI on T2-weighted and high SI on T1-weighted imaging. Infected cysts may show debris (sedimentation layer) within the cyst and a thick enhancing border. Vaginal wall inclusion cysts are small, often asymptomatic, and more common in the anterior wall [15]. Surgical treatment in which a vaginal mucosa island is buried leads to a risk of epithelial inclusion cyst formation. The cyst of Skene is thought to result from inflammation of the glands and ducts of Skene with subsequent obstruction at its urethral connection (Fig. 10). Complete surgical excision is effective [16–18]. The cyst of Bartholin is typically located in the lateral introitus medial to the labia minora. Pain may herald infection of the cyst and may require surgical attention. Clinically, the distinction between müllerian cysts and Gartner duct cysts is of little importance. Müllerian cysts represent vaginal cysts of paramesonephric duct origin that are lined with stratified squamous epithelium and originate anywhere in the proximal four fifths of the vagina. Gartner cysts are lined with cuboid or low columnar epithelium and are located on the anterolateral aspects of the vagina. Gartner duct cysts can also be associated with abnormalities of the metanephric urinary system (ectopic ureter, unilateral renal agenesis, and renal hypoplasia) [19].

Fig. 11. 36-year-old woman with pollakisuria, urge-complaints with no incontinence, dysuria at end micturition, and dyspareunia. Unclear mass lesion was seen at bladder base on clinical examination with endovaginal ultrasound. Sagittal T2-weighted 1.5-T image with pelvic coil shows rounded tumor (T) with low signal intensity below bladder base that cannot be clearly discriminated from bladder wall. Complete laparoscopic resection of lesion was performed and proved to be hyalinized leiomyoma of Retzius space.

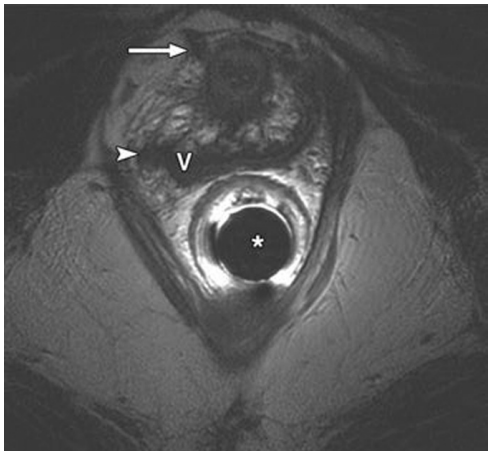

Fig. 12. 59-year-old woman with stress-urinary incontinence and dysuria. Axial T2-weighted 3-T MR image with endoluminal coil (asterisk) in anus shows disruption of periurethral ligament (arrow) and loss of vaginolevator attachment (arrowhead) on right with dorsal displacement of vagina (V).

Benign Solid Lesions

Primary lesions are usually evident on physical examination and include fibroma, leiomyoma, neurofibroma, lipoma, myo-

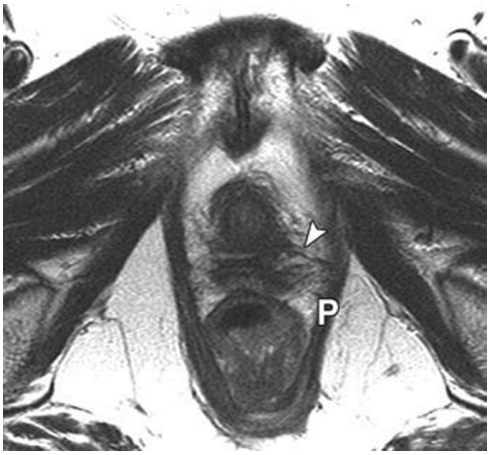

Fig. 13. 69-year-old woman with clinical occult pain in vagina and retropubic region and dysuria (painful and obstructive micturition). Axial T2-weighted 1.5-T image with pelvic coil shows fibrous strands (arrowhead) with adhesions of urethra, vagina, and puborectal muscle (P) on left. Patient was treated conservatively with repeated local infiltration of anesthetic on left side of urethra and vagina, with significant relief of symptoms. Patient refused surgery. In this case, MRI served as road map to guide local therapy.

blastoma, and hemangioblastoma. Once biopsy establishes the diagnosis, surgical resection is performed for symptomatic relief. Periurethral leiomyoma (Fig. 11) commonly arises from the anterior vaginal smooth muscle or vesicovaginal septum. These are rare benign tumors representing about 4% of periurethral masses in women between 30 and 50 years old [20].

Altered Structure of Urethra and Periurethral Region; Defects of the Urethral Supporting Structures, Periurethral Fibrosis

Although the periurethral ligaments may not be clearly shown on MRI without an endovaginal coil, wherever possible the symmetry and integrity of the periurethral ligaments should be analyzed, especially in women with symptoms of urinary incontinence [21].

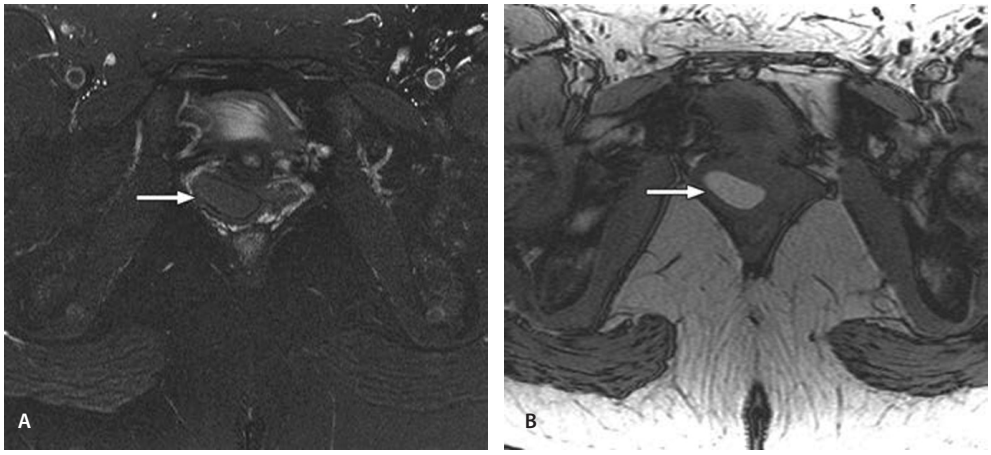

Fig. 14. 40-year-old woman with medical history of pelvic surgery for endometriosis with intractable pain in pelvic region and dyspareunia, including painful lump in vaginal wall. A and B, Axial 3-T images with pelvic coil show endometrioma (surgically and histologically confirmed) in vaginal wall (arrows). Note low signal intensity (SI) on T2-weighted image (A) and high SI on T1-weighted image (B), suggestive of bloody content of lesion. Local symptoms improved significantly after surgical clearance of lesion.

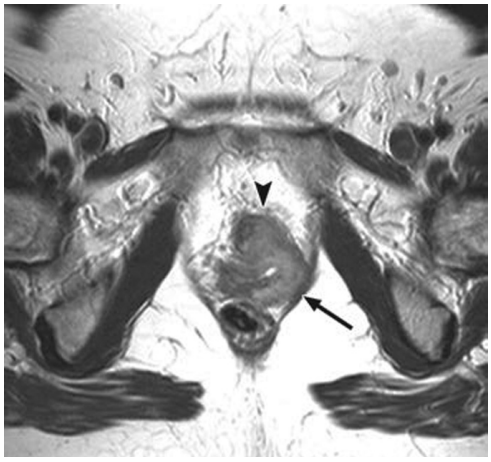

Fig. 15. 56-year-old woman with newly diagnosed vaginal carcinoma (cT4aN0M0). Symptoms include vaginal blood spotting with dyspareunia and dysuria. Axial T2-weighted 1.5-T image with pelvic coil shows vaginal carcinoma on left with extension to puborectal muscle (arrow) and tumor invasion of urethra (arrowhead).

Stress urinary incontinence may be associated with defects of the urethral supporting structures [22] (Fig. 12).

Periurethral fibrosis is not rare in women with lower urinary tract symptoms and urodynamic evidence of obstruction [4, 6]. Periurethral fibrosis may be treated surgically with transvaginal ureterolysis [6]. Periurethral fibrosis may be recognized on MRI as a non-mass-forming lesion with strands of low SI adhesive to adjacent structures (Fig. 13).

Endometriosis

4.1

Primary occurrence of endometriosis in the periurethral region is rare and usually represents a secondary manifestation of pelvic disease. Endometriosis should be considered in patients with a history of pelvic pain who present with lower urinary tract symptoms and a periurethral lesion [23]. Typically, the lesion will display high SI on T1-weighted imaging, which is indicative of the hemorrhagic content (Fig. 14).

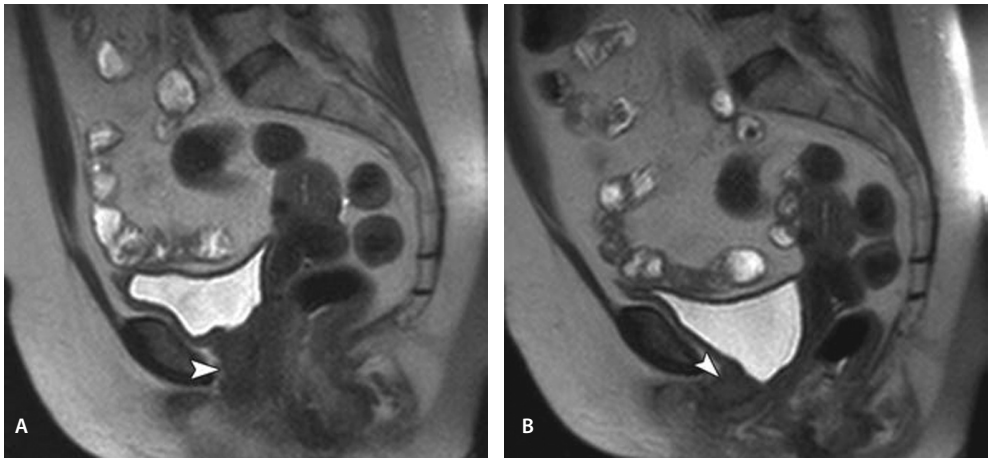

Fig. 16. 74-year-old woman with obstructive micturition and dysuria.
A and B, Midline sagittal HASTE 1.5-T images with body coil obtained at rest (A) and maximal strain (B) reveal urethral hypermobility. Note horizontal translation (B) of urethra away from normal vertical oriented axis (A) during strain, which is consistent with hypermobility of urethra (arrowhead).

Locally Advanced Carcinoma With Urethral Involvement

Locally advanced carcinoma with urethral involvement may include stage IV bladder, vagina, vulva, cervix, and anorectal carcinoma. Tumor extension to the urethra with loss of the normal layered structure of the urethra may be discerned (Fig. 15).

Prolapse Abnormalities of the Lower Urinary Tract

Pelvic organ prolapse results when the support mechanisms to individual organs are disrupted. Symptoms may range from mild vaginal pressure to urinary incontinence or retention. Urodynamics and anorectal manometry are useful in localizing the problems to the anterior (bladder and urethra), middle (vagina, cervix, uterus, and adnexa), and posterior (anus and rectum) compartments [24].

Hypermobility of the Urethra, Urethrocele, Cystocele

Cystocele or urethrocele forms when the bladder base or urethra descends below the pubococcygeal line (extends from the most inferior portion of the symphysis pubis to the last coccygeal joint and defines the level of the pelvic floor) (Fig. 9). This results from a loss of the normal fascial supports [25].

Hypermobility of the urethra is defined as a horizontal translation of the urethra away from the normal vertically oriented axis, with strain at an angle greater than 30° [8] (Fig. 16).

Prolapse of the Urethra

Urethral prolapse presents as a circular mucosal eversion of the distal urethra from the external meatus (in contrast to a caruncula, which usually presents with a partial eversion of the dorsal urethra). Diagnosis is usually certain on physical examination and no imaging is necessary.

Ectopic Ureter

An ectopic ureter (Fig. 17) may present as incontinence in an older girl or young woman in combination with recurrent uri-

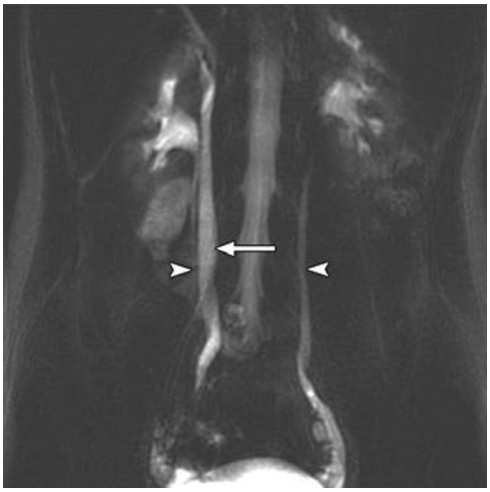

Fig. 17. 13-year-old girl with recurrent intractable drop incontinence (day and night), including recurrent lower urinary tract infection. Clinical evaluation, including urethrocystoscopy showed no abnormalities. Repeated ultrasound examinations revealed no abnormalities. MR urography at 1.5 T with body coil (coronal 3D, thick slab, heavily T2-weighted fast spin-echo with fat saturation) shows duplicature of collecting system of right kidney with dysplastic upper pole, including dilated ureter with ectopic termination in upper vagina on right. Surgical resection was performed of upper pole, including associated ureter, with histology-confirmed segmental tubulointerstitial nephritis and atrophy. Clearance of symptoms was observed after surgery. Note medial position of dilated right-sided upper pole ureter (arrow) compared with normal lateral position of lower pole ureter and left ureter (arrowheads). Normal termination of these at ureteral meatus was confirmed at cystoscopy.

nary tract infections. MR urography (Fig. 17) has proven to be a sensitive tool for diagnosis [9].

CONCLUSION

We have presented a subclassification of morphologic abnormalities based on anatomic region that can be considered in the differential diagnoses for chronic lower urinary tract symptoms in women. In addition, we have shown the power of dedicated state-of-the-art MRI for diagnosis. Dedicated MRI tailored to patient symptoms and clinical findings has the potential to map morphologic causes and facilitate appropriate treatment.

REFERENCES

1. Al-Hayek S, Abrams P. Women's lower urinary tract function and dysfunction: definitions and epidemiology. Minerva Ginecol 2004;56:311-325
2. Chapple CR, Wein AJ, Abrams P, et al. Lower urinary tract symptoms revisited: a broader clinical perspective. Eur Urol 2008;54:563-569
3. Coyne KS, Sexton CC, Thompson CL, et al. The prevalence of lower urinary tract symptoms (LUTS) in the USA, the UK and Sweden: results from the Epidemiology of LUTS (EpiLUTS) study. BJU Int 2009;104:352-360
4. Dwarkasing RS, Dinkelaar W, Hop WC, Steensma AB, Dohle GR, Krestin GP. MRI evaluation of urethral diverticula and differential diagnosis in symptomatic women. AJR Am J Roentgenol 2011;197:676-682
5. Elsayes KM, Mukundan G, Narra VR, Abou El Abbass HA, Prasad SR, Brown JJ. Endovaginal magnetic resonance imaging of the female urethra. J Comput Assist Tomogr 2006;30:1-6
6. Lorenzo AJ, Zimmern P, Lemack GE, Nurenberg P. Endorectal coil magnetic resonance imaging for diagnosis of urethral and periurethral pathologic findings in women. Urology 2003;61:1129-1133; discussion 1133-1124
7. Padhani AR, Koh DM, Collins DJ. Whole-body diffusion-weighted MR imaging in cancer: current status and research directions. Radiology 2011;261:700-718
8. Bennett GL, Hecht EM, Tanpitukpongse TP, et al. MRI of the urethra in women with lower urinary tract symptoms: spectrum of findings at static and dynamic imaging. AJR Am J Roentgenol 2009;193:1708-1715
9. Payabvash S, Kajbafzadeh AM, Saeedi P, Sadeghi Z, Elmi A, Mehdizadeh M. Application of magnetic resonance urography in diagnosis of congenital urogenital anomalies in children. Pediatr Surg Int 2008;24:979-986
10. Fletcher SG, Lemack GE. Benign masses of the female periurethral tissues and anterior vaginal wall. Curr Urol Rep 2008;9:389-396
11. Dupin N. Genital warts. Clin Dermatol 2004;22:481-486
12. Uchida K, Fukuta F, Ando M, Miyake M. Female urethral hemangioma. J Urol 2001;166:1008
13. Cocco AE, MacLennan GT. Unusual female suburethral mass lesions. J Urol 2005;174:1106
14. Thomas AA, Rackley RR, Lee U, Goldman HB, Vasavada SP, Hansel DE. Urethral diverticula in 90 female patients: a study with emphasis on neoplastic alterations. J Urol 2008;180:2463-2467
15. Pradhan S, Tobon H. Vaginal cysts: a clinicopathological study of 41 cases. Int J Gynecol Pathol 1986;5:35-46
16. Sharifi-Aghdas F, Ghaderian N. Female paraurethral cysts: experience of 25 cases. BJU Int 2004;93:353-356
17. Lucioni A, Rapp DE, Gong EM, Fedunok P, Bales GT. Diagnosis and management of periurethral cysts. Urol Int 2007;78:121-125
18. Isen K, Utku V, Atilgan I, Kutun Y. Experience with the diagnosis and management of paraurethral cysts in adult women. Can J Urol 2008;15:4169-4173
19. Eilber KS, Raz S. Benign cystic lesions of the vagina: a literature review. J Urol 2003;170:717-722
20. Blaivas JG, Flisser AJ, Bleustein CB, Panagopoulos G. Periurethral masses: etiology and diagnosis in a large series of women. Obstet Gynecol 2004;103:842-847
21. Law YM, Fielding JR. MRI of pelvic floor dysfunction: review. AJR Am J Roentgenol 2008;191:S45-53
22. El Sayed RF, El Mashed S, Farag A, Morsy MM, Abdel Azim MS. Pelvic floor dysfunction: assessment with combined analysis of static and dynamic MR imaging findings. Radiology 2008;248:518-530
23. Chowdhry AA, Miller FH, Hammer RA. Endometriosis presenting as a urethral diverticulum: a case report. J Reprod Med 2004;49:321-323
24. Boyadzhyan L, Raman SS, Raz S. Role of static and dynamic MR imaging in surgical pelvic floor dysfunction. Radiographics 2008;28:949-967
25. Macura KJ, Genadry RR, Bluemke DA. MR imaging of the female urethra and supporting ligaments in assessment of urinary incontinence: spectrum of abnormalities. Radiographics 2006;26:1135-1149

chapter 4.2

MRI Evaluation of Urethral Diverticula and Differential Diagnosis in Symptomatic Women

Roy S. Dwarkasing
Wouter Dinkelaar
Wim C. J. Hop
Anneke B. Steensma
Gert R. Dohle
Gabriel P. Krestin

AJR Am J Roentgenol. 2011 Sep;197(3):676-82.

ABSTRACT

Objective The purpose of this study was to evaluate the role of MRI in the diagnosis and differential diagnosis of urethral diverticula in symptomatic women.

Materials and methods Women referred for MRI at a single institution because of suspicion of urethral diverticula were included. All MRI examinations were independently evaluated by two radiologists and compared with patients' follow-up data. Sensitivity and specificity of MRI for urethral diverticula were calculated using surgery and clinical confirmation as the reference standards. Image quality of the urethra and periurethral region performed with the endoluminal coil was compared with the pelvic phased-array coil.

Results From a study group of 60 patients (mean age, 44 years), 20 patients (33%) had urethral diverticula and 28 (47%) had an alternative diagnosis, of which 13 (46%) were visualized with MRI. In the remaining 12 patients (20%) no abnormalities were found. For urethral diverticula, MRI had both sensitivity and specificity of 100%. Twenty patients had a total of 27 diverticula; these were mostly locally round (n = 12) with sharp margins (n = 25) and high (n = 19) homogeneous (n = 16) signal intensity on T2- weighted sequences. The ostium of urethral diverticula was identified in 23 diverticula (85%) by both readers. Agreement was 93% with $\kappa = 0.72$. Endoluminal coil placement in the vagina showed the best image quality of the urethra and periurethral region.

Conclusion Dedicated MRI is an excellent imaging modality for urethral diverticula; furthermore, MRI will show the alternative diagnosis in almost one half of the remaining patients.

INTRODUCTION

Female urethral diverticulum is often overlooked and frequently misdiagnosed because of unawareness of the condition. Urethral diverticula are estimated to occur in 1–6% of women. Although usually diagnosed between the third and fifth decade of life, it can affect all age groups [1–3]. Usually, an array of nonspecific genitourinary symptoms predominate. The most frequent symptoms described are frequency and urgency (40–100%), dysuria (30–70%), recurrent urinary tract infection (30–50%), postmicturition dribble (10–30%), dyspareunia (10–25%), and hematuria (10–25%) [4, 5]. It may also present with a tender mass (35%), urinary incontinence (32%), stones (1–10%), discharge of pus from the urethra (12%), and retention (4%) [6]. This condition should always be considered in women with unexplained lower urinary tract ymptoms. In addition to interstitial cystitis, urethral syndrome, and urgency-frequency syndrome, the clinician should include urethral diverticula in the differential diagnosis [7]. Appropriate investigations play an important role in the diagnosis of urethral diverticula and ideally should provide the surgeon with information regarding location, number, size, configuration, and communication of the urethral diverticula [8]. MRI has now become the imaging study of choice [8]. The purpose of this study was to evaluate the role of MRI in the diagnosis of urethral diverticula and differential diagnosis for this condition in symptomatic women.

MATERIALS AND METHODS

This study was performed without financial support, and the authors had exclusive control of the data and information presented in this article.

Patient Population

Institutional review board approval was obtained for this retrospective study, and informed consent was waived. Women referred for MRI at a single institution because of clinical suspicion of urethral diverticula were included in the study. Patients were electronically identified using a department database. All patients had two or more lower urinary tract symptoms, including pain, urinary incontinence, dyspareunia, and frequency or urgency. Patients were excluded when no convincing information for suspicion of urethral diverticula was presented. From hospital- and department-based digital information systems, a search was performed to assess the specific diagnosis for the complaints for which the patient was referred to the MRI unit. The reference standard was surgery or, in case no surgery was performed, confirmation of MRI findings with a second imaging modality, including video urodynamic studies and voiding cystourethrography and clinical examination.

MRI Technique

All examinations were performed using a 1.5-T MR imager (Gyroscan NT Intera 1.5, Philips Healthcare) with application of a rigid endoluminal coil placed in the vagina (n = 17) or in the anus (n = 2) or with a pelvic phased-array coil (n = 6). The endoluminal coil is commercially available and consists of a fixed, rectangular, 60-mm-long rigid receiver coil with a width of 16 mm. The coil is contained within an 80-mm-long cylindric coil holder with a

diameter of 19 mm. Before the introduction of the coil into the vagina or anus, a condom was placed over the coil and ultrasound gel was used as a lubricant. It should be noted that this rigid endoluminal coil is not the same as the inflatable rectal coil but is of smaller diameter and is designed to be placed in the vagina or anus. The phased-array coil is a commercially available four-channel coil (Synergy, Philips Healthcare) placed around the pelvis. A standardized imaging protocol of T2-weighted turbo spin-echo and gradient-echo sequences with and without fat saturation was performed in all cases, with high-resolution slices in three planes (axial, coronal, and sagittal) through the urethra and periurethral region. The FOV included the bladder base and perianal region. At endoluminal MRI, image volume encompassed the entire sensitive region of coil. For the endoluminal coil, parameters were transverse T2-weighted fast-field echo imaging (TR/TE, 23/14; matrix, 205 × 256; flip angle, 60°; FOV, 140 mm; thickness, 2 mm with no gaps; and two signals acquired). Transverse T2-weighted fast spin-echo MRI was performed with and without fat saturation (TR/TE, 5086/100; matrix, 186 × 256; flip angle, 90°; FOV, 120 mm; section thickness, 4 mm with a 0.4-mm gap; and three signals acquired). Coronal and sagittal T2-weighted fast spin-echo MRI was performed without fat saturation (TR/ TE, 2454/100; matrix, 186 × 256; flip angle, 90°; FOV, 120 mm; section thickness, 4 mm with a 0.4-mm gap; and four signals acquired). For the pelvic phased-array coils, parameters were transverse, coronal, and sagittal T2-weighted fast spin-echo sequences without fat suppression (TR/TE, 2500/70; matrix, 512 × 256; flip angle, 60°; FOV, 300 mm; section thickness and gap, 3 mm and 0.3 mm, respectively; and two signals acquired) and transverse T2-weighted fast spin-echo with fat suppression (TR/TE, 4000/85; matrix, 512 × 256; flip angle, 60°; FOV, 300 mm; section thickness and gap, 3 mm and 0.3 mm, respectively; and two signals acquired). Transverse fat-saturated T1-weighted fast spin-echo imaging after IV gadolinium chelate administration (0.2 mL/kg of 0.5 mmol/mL of gadopentetate dimeglumine [Magnevist, Schering]) was performed in few (n = 6) cases (TR/TE, 3.61/1.4; matrix, 512 × 256; flip angle, 15°; FOV, 300 mm; section thickness and gap, 4 mm and 0.4 mm, respectively; and one signal acquired).

4.2 *Image Analysis*

All MRI examinations were loaded in a PACS viewing station from digital storage facilities and were examined by two observers with experience in reading approximately 2500 and 500 pelvic MR examinations, respectively. The observers were blinded to the patient history, findings in the clinical workup, or other imaging studies and to each other's results. The following items were evaluated separately by both observers: MRI examination technique using the pelvic phased-array or endoluminal coil placed in the vagina or in the anal canal; number of urethral diverticula; size of urethral diverticula on three axes: anteroposterior, transverse, and craniocaudal measured in mm; shape of urethral diverticula (locally round, oval shaped, circumferential, or elongated); identification of the ostium of urethral diverticula in the urethra; localization of the ostium with "uncertain" added as a separate category; distance of the ostium to the bladder neck measured in mm; signal intensity of urethral diverticula on T2-weighted images; borders of urethral diverticula (well-defined or ill-defined); important remarks, such as stones or suggestion of other solid components within urethral diverticula; added value of T1-weighted sequences with IV gadolinium chelate administration; and alternative diagnoses. The ostium of urethral diverticula was defined as a beaklike linear extension of the diverticular neck through the muscular and submucosal layers of the urethra with high signal intensity on T2-weighted images. Image quality of the urethra and periurethral region with the pelvic phased-array or endoluminal coil was evaluated by both observers. Every examination was scored independently by both observers

using a 3-point scale (fair, satisfactory, and excellent), indicating the best detailed anatomy of the urethra and periurethral region in the perception of the observer.

Statistical Analysis

Ninety-five percent confidence intervals were calculated for sensitivity and specificity. Comparisons of percentages between groups were performed using Fisher's exact test. The limit of significance was set at $p = 0.05$ (two-sided). Kappa statistics were used to quantify degrees of agreement between readers for identifying the ostium of the diverticulum in the urethra. The classification "uncertain" was included in the latter calculation as a separate category. A kappa value ≤ 0.20 was interpreted as slight agreement; 0.21–0.40, fair agreement; 0.41–0.60, moderate agreement; 0.61–0.80, substantial agreement; and ≥ 0.81, almost perfect agreement.

RESULTS

Between January 1995 and December 2006, 1541 women underwent MRI of the pelvis and pelvic floor for a variety of reasons. We identified 60 patients (all women; mean age, 44 years; age range, 18–80 years) who fulfilled the criteria for inclusion in the study population. In total, 20 patients had 27 urethral diverticula on 25 different MRI examinations. This included three patients with follow-up MRI examinations after surgery because of persistent complaints and proved residual or recurrent urethral diverticula. Two patients underwent control MRI before surgery because of a long delay of 19 and 26 months, respectively, between the first MRI examination and surgery. Two patients had two separate urethral diverticula with separate outlines and diverticular necks on a single MRI examination (Fig. 1). In 16 patients, urethral diverticula were surgically proven. Surgery was performed between 2 and 10 weeks after MRI. These patients had a total of 19 surgical procedures for urethral diverticula, including three patients with recurrent or residual urethral diverticula. In 17 cases, urethrocystoscopy was performed as a preoperative tool, with visualization of the ostium of urethral diverticula in eight cases. The location of the ostium described in the surgical report was in agreement with MRI. In the remaining nine surgical cases, identifi-

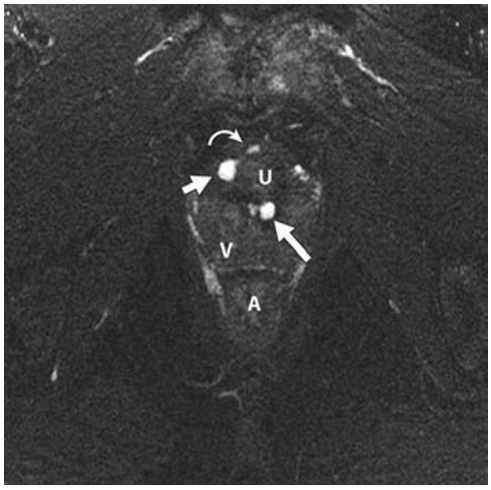

Fig. 1. 43-year-old-woman with multiple urethral diverticula. Axial T2-weighted image with fat saturation performed with pelvic phased-array coil shows urethral diverticulum in 9-o'clock position (short arrow), including diverticular neck (curved arrow). Ostium (not shown) was located in midline anteriorly (12-o'clock position). Separate urethral diverticulum is seen posteriorly (long arrow) with ostium in midline posteriorly (6-o'clock position). Both urethral diverticula, including diverticular neck and ostia, were confirmed surgically. U = urethra, V = vagina, A = anus.

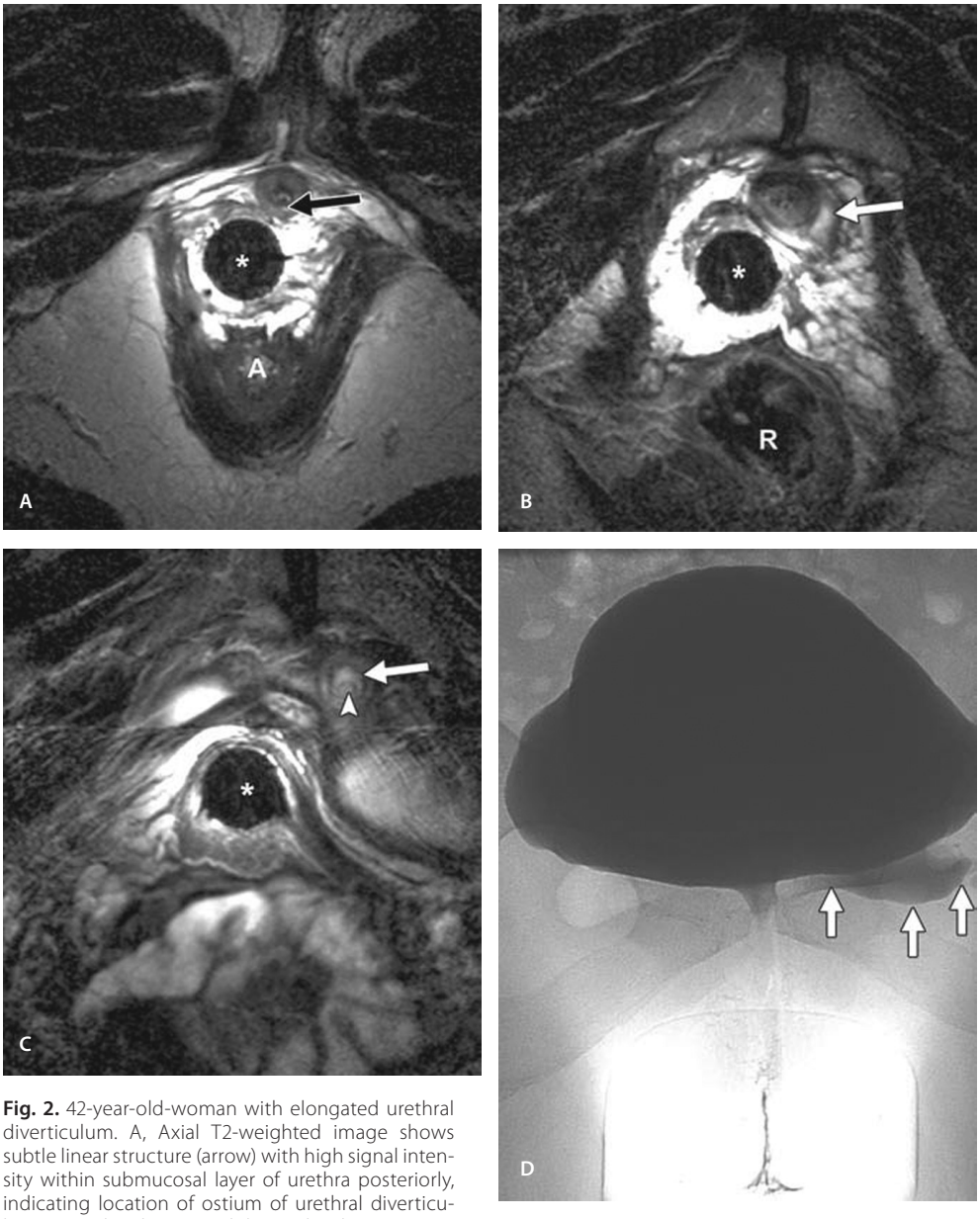

Fig. 2. 42-year-old-woman with elongated urethral diverticulum. A, Axial T2-weighted image shows subtle linear structure (arrow) with high signal intensity within submucosal layer of urethra posteriorly, indicating location of ostium of urethral diverticulum. Asterisk indicates endoluminal coil, A = anus.
B and C, Axial T2-weighted images show track of this elongated urethral diverticulum (arrow). Arrowhead in C indicates debris in apex of urethral diverticulum. Asterisk indicates endoluminal coil, R = rectum.
D, Voiding cystoureterogram shows same urethral diverticulum (arrows) with good correlation with MRI appearance. To our knowledge, this type of urethral diverticula with its elongated nature has not been described before. Patient had no additional abnormalities of kidneys, ureters, and lower urinary tract.

cation and excision of urethral diverticula, including the diverticular neck, was documented. In these cases, MRI had good correlation concerning the orientation of urethral diverticula, including the diverticular neck, as was described in the surgical report. Four patients either refused surgery or preferred expectant management for urethral diverticula. In the patients with no surgery (n = 4), MRI findings of urethral diverticula were confirmed with follow-up video urodynamics within 3 months after MRI (n= 4), including visualization of urethral diverticula on an initial voiding cystourethrography (n = 2), which was performed 4 and 5 months before MRI (Fig. 2). In the clinical workup, which included palpation and massage of the urethra through the vagina, the diagnosis of urethral diverticula was considered confirmed and proved by the urologist as was documented in patients' records. We searched for the clinically confirmed final diagnoses in the rest of the study group (Fig. 3). Twenty-eight of 60 patients (47%) had an alternative diagnosis. Thirteen (46%) were correctly diagnosed with MRI. Periurethral scarring, urethrovaginal fistula, infected cyst of Skene, cystocele, and endometriosis of the vaginal vault were confirmed by surgery. Periurethritis and inflammatory pseudotumor of the urethra were proved by biopsy. Dysfunctional voiding and interstitial cystitis were confirmed by clinical evaluation, including video urodynamics, with no abnormalities found on MRI. Urethritis and vaginitis by Candida species was proved by specific laboratory findings and response to specific therapy, with no abnormalities found on MRI. In the remaining 12 patients (20%), no abnormalities were found on MRI and in the clinical follow-up. The follow-up period was at least 18 months and ranged from 1.5 to 8 years (mean, 5 years). MRI showed the final diagnosis (urethral diverticula or alternative diagnosis) in 33 of 60 patients (55%). On the basis of MRI; clinical evaluation, including video urodynamics; and clinical data, 80% of patients were diagnosed with an abnormality that was responsible for their complaints. For the diagnosis of urethral diverticula, MRI had sensitivity of 100% (20 of 20 patients; 95% CI, 83–100%) and specificity of 100% (40 of 40 patients; 95% CI, 91–100%). Of 25 MRI examinations with findings of urethral diverticula, 19 were performed with the endoluminal coil placed in the vagina (n = 17) or anal canal (n = 2), and 6 examinations were performed with the pelvic phased-array coil (Table 1). Imaging

Table 1: Quality of Images of the Urethra and Periurethral Region Using Different MRI Coils

Quality	Rigid Endoluminal Coil in Vagina	Phased-Array Coil	Rigid Endoluminal Coil in Anus
Fair	0	0	2
Satisfactory	0	6	0
Excellent	17	0	0

Table 2: Shape of 27 Urethral Diverticula on 25 MRI Examinations in 20 Women

Shape	No. of Diverticula	Largest Axis Range (mm)
Circumferential (100%)	4	26–33
Circumferential (50–99%)	8	
Locally round or oval shaped	12	4–22
Locally crescent shaped	2	7–21
Truncated or fistulalike	1	25

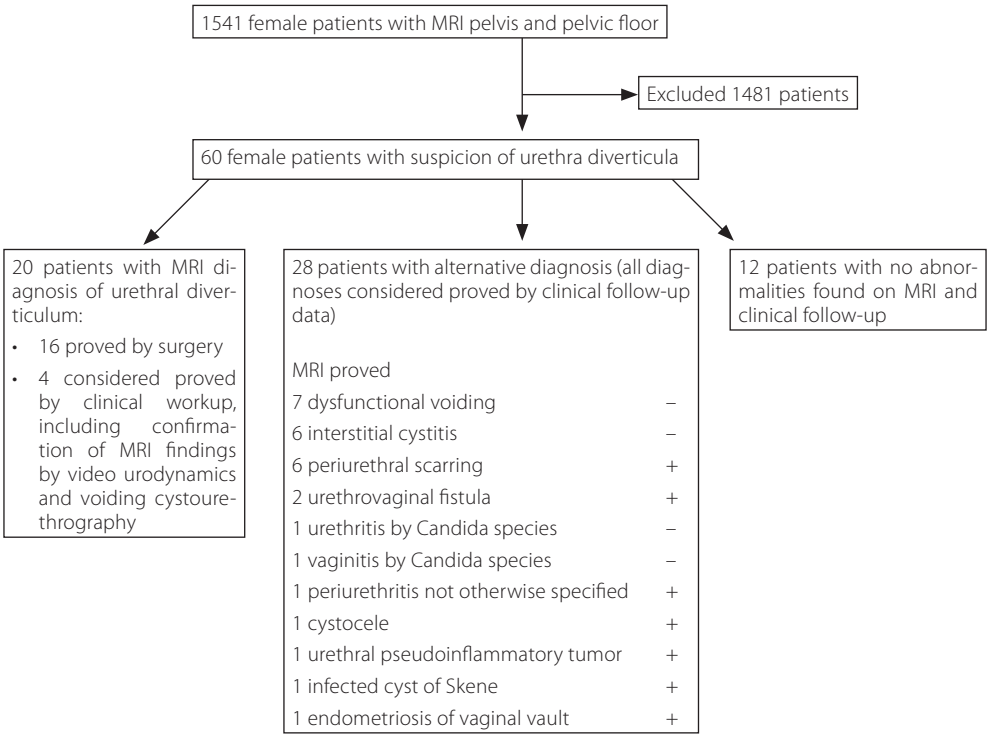

Fig. 3. Flow diagram summarizes patient sampling.

4.2

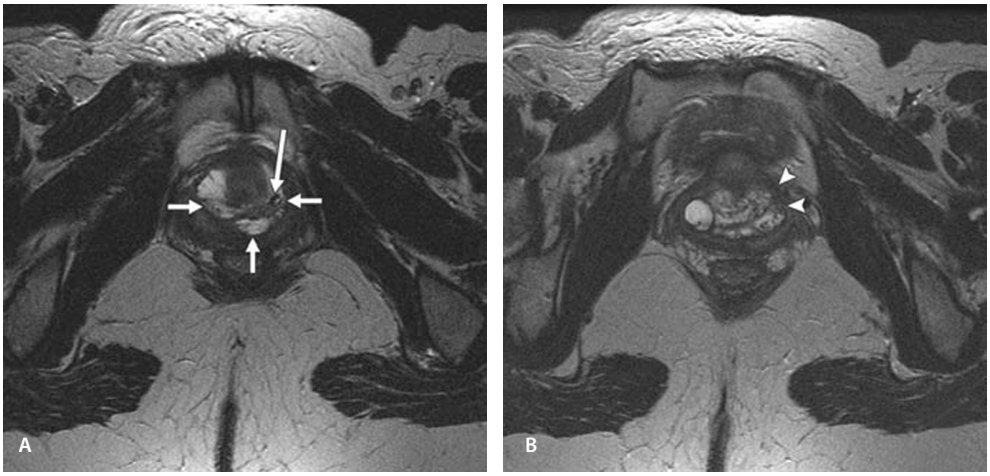

Fig. 4. 39-year-old-woman with urethral diverticulum imaged with pelvic phased-array coil. A, Axial T2-weighted image shows circumferential urethral diverticulum (short arrows) with internal inhomogeneity as a result of debris, septa, and stone (long arrow).
B, Axial T2-weighted image shows unsharp margins of diverticulum, best seen on left (arrowheads), which is caused by perilesional inflammation (pathology proven). Ostium of this complicated urethral diverticulum was considered by two observers as "not identified" and "uncertain," respectively.

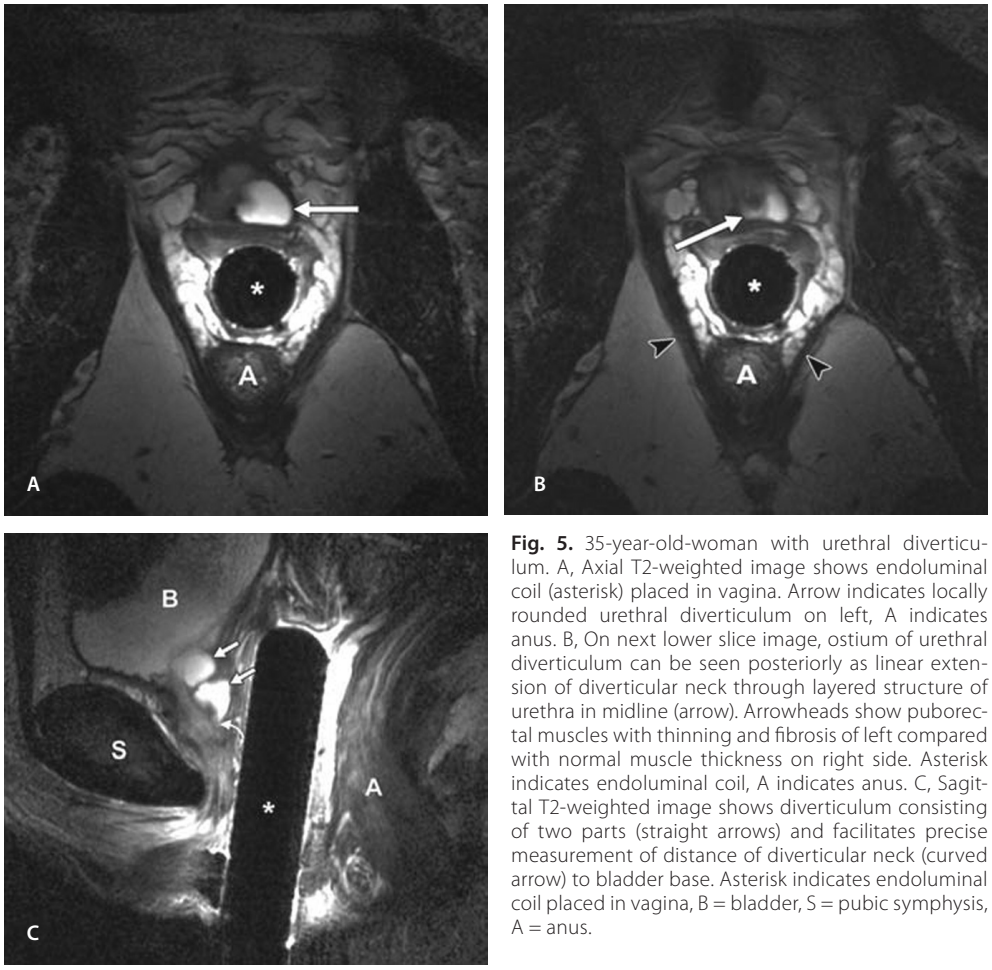

Fig. 5. 35-year-old-woman with urethral diverticulum. A, Axial T2-weighted image shows endoluminal coil (asterisk) placed in vagina. Arrow indicates locally rounded urethral diverticulum on left, A indicates anus. B, On next lower slice image, ostium of urethral diverticulum can be seen posteriorly as linear extension of diverticular neck through layered structure of urethra in midline (arrow). Arrowheads show puborectal muscles with thinning and fibrosis of left compared with normal muscle thickness on right side. Asterisk indicates endoluminal coil, A indicates anus. C, Sagittal T2-weighted image shows diverticulum consisting of two parts (straight arrows) and facilitates precise measurement of distance of diverticular neck (curved arrow) to bladder base. Asterisk indicates endoluminal coil placed in vagina, B = bladder, S = pubic symphysis, A = anus.

with the endoluminal coil placed in the vagina had 17 of 17 graded excellent versus 0 of 6 with phased-array imaging ($p < 0.001$, Fisher's exact test). Too few patients (n = 2) were imaged with the endoluminal coil placed in the anus to evaluate the results statistically. Both observers fully agreed in each of the gradings displayed in Table 1 that visualization of the best image quality of the urethra and periurethral region occurred with the endoluminal coil placed in the vagina. Urethral diverticula had different shapes (Table 2). The most frequent shape was locally round or oval. When considering the borders of the urethral diverticula, most cases showed well-defined margins (n = 25). Two urethral diverticula showed partly sharp and partly ill-defined margins. This was caused by perilesional inflammation, which was proved by histology (Fig. 4). The ostia of urethral diverticula could be identified in 23 of 27 cases (85%) by both observers. Observer 2 could not identify the ostium in two diverticula and, in another two diverticula, considered this to be uncertain. Observer 1 scored the same four diverticula as uncertain. The agreement was 93% (25/27) with $\kappa = 0.72$. Twenty-three identified ostia of urethral diverticula by both observers were located in the midline anterior (12-o'clock position) (n = 1); left lower quadrant (between 3-o'clock and 6-o'clock positions) (n = 11); midline posterior (6-o'clock position) (n = 4); and right lower

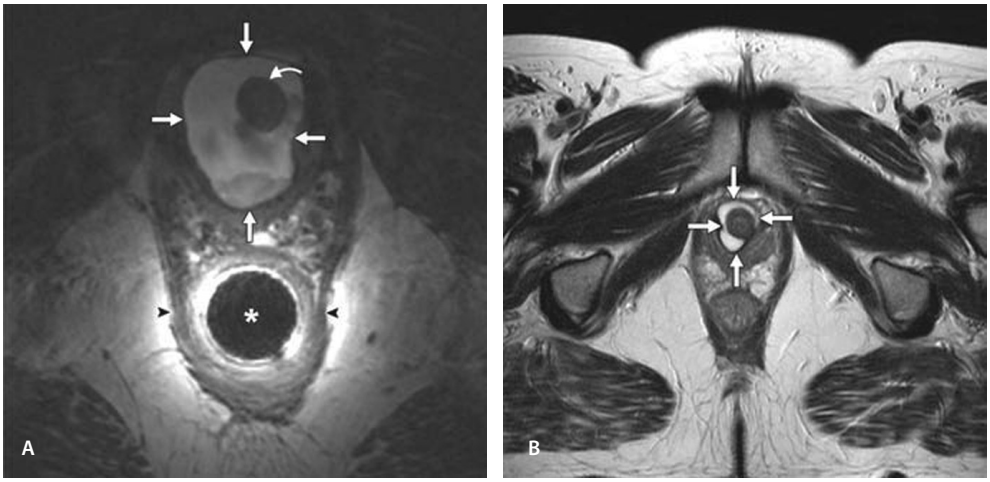

Fig. 6. 42-year-old-woman with circumferential urethral diverticulum. A, Axial T2-weighted image shows sharp borders (straight arrows) of urethral diverticulum with high inhomogeneous signal intensity containing debris on dependent side. Endoluminal coil (asterisk) is placed in anal canal. Curved arrow indicates urethra, and arrowheads indicate puborectal muscles. B, Axial T2-weighted image acquired almost 1.5 years after surgery shows recurrent or residual urethral diverticulum (arrows). Image was acquired with four-channel phased-array pelvic coil. For optimal imaging results of urethral diverticula, smaller FOV is recommended (see also Figure 5).

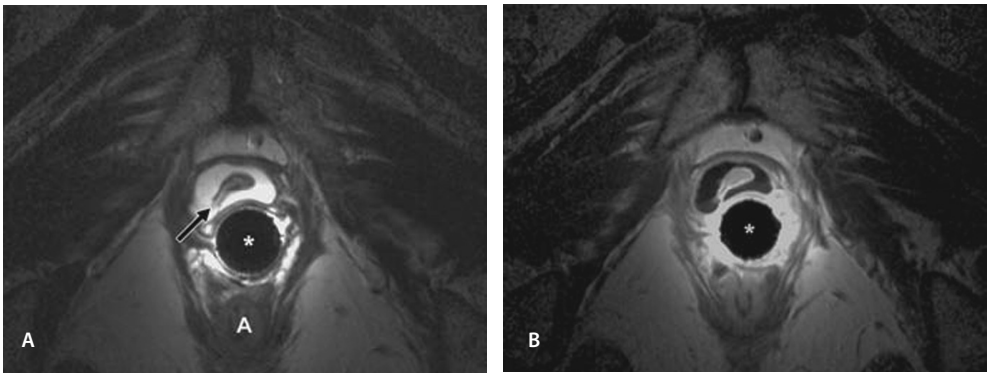

Fig. 7. 47-year-old-woman with circumferential urethra diverticulum. A, Axial T2-weighted image shows endoluminal coil (asterisk) placement in vagina results in better image quality of urethra and periurethral region compared with Figure 2. Urethral diverticulum with sharp borders, homogeneous hyperintense signal intensity, and identification of ostium in right lower quadrant (arrow) are visualized. A indicates anus. B, Contrast-enhanced axial T1-weighted turbo spinecho image with fat saturation after IV gadolinium chelate administration image obtained at same level as A shows no enhancing components within urethral diverticula. Asterisk indicates endoluminal coil.

quadrant (between 6-o'clock and 9-o'clock positions) (n = 7) with the patient in the supine position. The mean distance of the ostia to the bladder neck was 12 mm (range, 7–36 mm) (Fig. 5). Twenty-three identified ostia of urethral diverticula by both observers were imaged with the endoluminal coil placed in the vagina (17 of 18 diverticula), or anal canal (2 of 2 diverticula), or with the pelvic phased-array coil (4 of 7 diverticula). These findings tended toward significance regarding the identification of the ostium of urethral diverticula with the endoluminal coil placed in the vagina compared with the phased-array coil (p = 0.053,

Fisher's exact test). On T2-weighted images, urethral diverticula had high signal intensity similar (n = 19) or slightly lower (n = 8) than the signal intensity of urine in the bladder. Signal intensity on T2-weighted sequences was homogeneous (n = 16) (Fig. 5) or inhomogeneous (n = 11) (Figs. 4 and 6A). Inhomogeneous signal intensity was found in diverticula containing debris (n = 9) (Fig. 6A) or debris, septa, and stone (n = 2) (Fig. 4). In six MRI examinations, gadolinium enhanced T1-weighted series were performed in addition to the T2-weighted sequences. Both observers were of opinion that contrast enhanced studies had no additional value for the diagnosis of urethral diverticula (Fig. 7).

DISCUSSION

In our study, urethral diverticula were diagnosed in 20 of 60 symptomatic women (33%) referred for MRI. Other studies reported urethral diverticula in 10% of patients examined with endorectal coil MRI or 74% of patients examined with a combination of transvaginal, transperineal, and urethral sonography (using a catheter-based transducer) [9, 10]. Previous MRI studies of symptomatic female urethral and periurethral diseases were based on the use of the pelvic phased array coil or the inflatable endoluminal coil placed in the vagina or in the rectum. To our knowledge, our study is the first with application of the rigid endoluminal coil in these patients. The rigid endoluminal coil can be inserted into the vagina by the patient herself, and there is no need for administration of glucagon or butylbromide to prevent rectal spasm, which could be the case when using the inflatable endoluminal coil [9]. Although a limited number of patients in our study was examined with the endoluminal coil placed in the anal canal or with the pelvic phased- array coil, a qualitative comparison suggests better image quality of the urethra and periurethral region with the endoluminal coil placed in the vagina (Table 1 and Figs. 4, 6A, and 7A). With intraanal placement of the endoluminal coil, the urethra falls slightly outside the sensitive region of the coil, whereas the perianal region is displayed in great detail (Fig. 6A). According to data in the literature and our experience, care should be taken to use the right scanning parameters. With the pelvic phased-array coil, a slice thickness of 3 mm and the use of axial T2-weighted turbo spin-echo sequences from the bladder base through the entire urethra has been recommended [11] with no need for T1-weighted sequences or contrast-enhanced series for the diagnosis of urethral diverticula [8] (Fig. 7). With this dedicated imaging protocol, imaging times can be limited to an average of 15 minutes [8]. Contrast-enhanced studies, however, may improve visualization of granulation tissue or carcinoma within urethral diverticula and tumor spread to adjacent adipose tissue [12, 13]. Malignancy arising from a diverticulum can be visualized as enhancing soft tissue within the diverticulum [14]. Cancer within urethral diverticula that is still small may be overlooked with torso phased-array MRI including gadolinium-enhanced sequences [15]. In our study, among 19 resected and pathology-proven urethral diverticula, no carcinoma was found. Few studies have focused on the differential diagnosis of patients with urethral diverticula. In the differential diagnosis, one should also consider other regional cystic lesions. Visualization of communication between the lesion and the urethra confirms urethral diverticula [16]. The differentiation between a communicating or non-communicating cystic lesion with the urethra is important because the surgical approach for the two entities differs. Both lesions are resected; however, a diverticulum may require urethral reconstruction procedures [16–18]. To our knowledge, our study is the first to identify the ostium of urethral diverticula in the majority of cases (85%) on MRI with improved confidence using the rigid endoluminal coil rather than the pelvic phased-array coil. Kim et al. [19] could not identify the ostium of urethral diverticula on MRI

with application of the body or pelvic coil. Blander et al. [20] identified the diverticular neck (ostium) in 11 of 27 patients (41%) on MRI with the inflatable endoluminal coil. In our study, urethrocystoscopy showed the ostium of urethral diverticula in 47% of cases. Other studies have reported 52% accuracy of urethrocystoscopy in identifying the ostium of urethral diverticula [20]. This warrants accurate preoperative imaging to assess the precise location of urethral diverticula, including the diverticular neck and ostium with additional information regarding size, extent, content, and complexity of the lesion. This practice may shorten the duration and improve the outcome of the surgical procedure. The only study we found to clearly identify the ostium of urethral diverticula in the majority of cases used a combination of transvaginal, transperineal, and urethral sonography (using a catheter-based transducer) in 19 women with urethral symptoms [10]. The neck was precisely seen in 13 of 15 diverticula on sonography, especially via the transurethral approach. The disadvantages of this modality are that most diverticular necks were identified using the transurethral approach, which is not as convenient for the patient and is not as readily available as transvaginal and transperineal sonography [10]. Furthermore, transurethral sonography requires a dedicated intravascular sonographic unit as well as a catheter-based transducer [10]. In our study, MRI showed the final diagnosis (urethral diverticula or alternative diagnosis) in 33 of 60 patients (55%). On the basis of MRI; clinical workup, including functional urodynamic studies; and clinical data, 80% of patients were diagnosed with an abnormality that was responsible for their complaints. According to these findings, in the diagnostic workup of women with suspicion of urethral diverticula, both MRI and urodynamic studies can be considered. After clinical evaluation, MRI can be considered to assess a physical cause. In addition, urodynamic studies may be used to evaluate associated urinary incontinence and for planning additional incontinence surgery to obtain the best postoperative results for urethral diverticula [8, 18, 21]. Bennett et al. [22] advocated that addition of a sagittal dynamic sequence to the MRI protocol will permit detection of pelvic organ prolapse that may not be evident on static at-rest images and that may also go undetected at physical examination. In 20% of our study group, no clear diagnosis could be established. No physical abnormalities were found on MRI and in the clinical follow-up. We believe that functional aspects of the pelvic floor and supporting ligaments of the bladder base and urethra may be a cause for the complaints in these patients. Follow-up studies, including dynamic MRI and functional urodynamic studies, may be needed to evaluate these patients thoroughly. There were limitations to this study. First, our study was retrospective and included a relatively small number of urethral diverticula. Second, two control MRI examinations (because of a long delay of 19 and 26 months between the first MRI examination and surgery) were included for analysis of specific imaging features of urethral diverticula. This may have led to selection bias; however, we believe that the morphology of urethral diverticula may change in time depending on the state of filling and secondary inflammation. This may justify the inclusion of both examinations per patient. Third, we found that sensitivity and specificity of MRI for urethral diverticula were both 100%, using surgery and clinical confirmation as the reference standards. Not all 60 patients had the same additional evaluation for urethral diverticula, and thus the true sensitivity may not be 100%. Finally, there was no uniform reference standard. We consider surgery as the reference standard for urethral diverticula. Surgery was performed in the majority of patients (80%), with urethral diverticula proved. In the remaining patients, MRI findings of urethral diverticula were confirmed with a second imaging modality (video urodynamic studies and voiding cystourethrography) and considered proved by clinical examination and evaluation by the urologist. Furthermore, no reports were found in the hospital-based long-term follow-up data of these patients for whom the MRI findings of urethral diverticula were clinically in doubt. Nevertheless, we believe that adequate imaging and clinical follow-up information was available for

all patients, and therefore we consider our conclusions valid. In conclusion, there is an expanding role for dedicated MRI in women with suspicion of urethral diverticula. MRI will show the diagnosis in more than one half of all patients. On the basis of MRI, functional urodynamic studies, and clinical evaluation, 80% of patients will be diagnosed with an abnormality that is responsible for their complaints. Additional studies should follow to clarify the reason for complaints in the remaining 20% of patients.

REFERENCES

1. Davis BL, Robinson DG. Diverticula of the female urethra: assay of 120 cases. J Urol 1970; 104:850–853
2. Foster RT, Amundsen CL, Webster GD. The utility of magnetic resonance imaging for diagnosis and surgical planning before transvaginal periurethral diverticulectomy in women. Int Urogynecol J Pelvic Floor Dysfunct 2007; 18:315–319
3. Rufford J, Cardozo L. Urethral diverticula: a diagnostic dilemma. BJU Int 2004; 94:1044–1047
4. Romanzi LJ, Groutz A, Blaivas JG. Urethral diverticulum in women: diverse presentations resulting in diagnostic delay and mismanagement. J Urol 2000; 164:428–433
5. Bennett SJ. Urethral diverticula. Eur J Obstet Gynecol Reprod Biol 2000; 89:135–139
6. Ganabathi K, Leach GE, Zimmern PE, Dmochowski R. Experience with the management of urethral diverticulum in 63 women. J Urol 1994; 152: 1445–1452
7. Aspera AM, Rackley RR, Vasavada SP. Contemporary evaluation and management of the female urethral diverticulum. Urol Clin North Am 2002; 29:617–624
8. Patel AK, Chapple CR. Female urethral diverticula. Curr Opin Urol 2006; 16:248–254
9. Lorenzo AJ, Zimmern P, Lemack GE, Nurenberg P. Endorectal coil magnetic resonance imaging for diagnosis of urethral and periurethral pathologic findings in women. Urology 2003; 61:1129–1133; discussion, 1133–1134
10. Siegel CL, Middleton WD, Teefey SA, Wainstein MA, McDougall EM, Klutke CG. Sonography of the female urethra. AJR 1998; 170:1269–1274
11. Neitlich JD, Foster HE Jr, Glickman MG, Smith RC. Detection of urethral diverticula in women: comparison of a high resolution fast spin echo technique with double balloon urethrography. J Urol 1998; 159:408–410
12. Hricak H, Secaf E, Buckley DW, Brown JJ, Tanagho EA, McAninch JW. Female urethra: MR imaging. Radiology 1991; 178:527–535
13. Elsayes KM, Mukundan G, Narra VR, Abou El Abbass HA, Prasad SR, Brown JJ. Endovaginal magnetic resonance imaging of the female urethra. J Comput Assist Tomogr 2006; 30:1–6
14. Chou CP, Levenson RB, Elsayes KM, et al. Imaging of female urethral diverticulum: an update. RadioGraphics 2008; 28:1917–1930
15. Chung DE, Purohit RS, Girshman J, Blaivas JG. Urethral diverticula in women: discrepancies between magnetic resonance imaging and surgical findings. J Urol 2010; 183:2265–2269
16. Hahn WY, Israel GM, Lee VS. MRI of female urethral and periurethral disorders. AJR 2004; 182:677–682
17. Rovner ES, Wein AJ. Diagnosis and reconstruction of the dorsal or circumferential urethral diverticulum. J Urol 2003; 170:82–86; discussion, 86 18. Fortunato P, Schettini M, Gallucci M. Diagnosis and therapy of the female urethral diverticula. Int Urogynecol J Pelvic Floor Dysfunct 2001; 12:51–57
19. Kim B, Hricak H, Tanagho EA. Diagnosis of urethral diverticula in women: value of MR imaging. AJR 1993; 161:809–815
20. Blander DS, Rovner ES, Schnall MD, et al. Endoluminal magnetic resonance imaging in the evaluation of urethral diverticula in women. Urology 2001; 57:660–665
21. Porten S, Kielb S. Diagnosis of female diverticula using magnetic resonance imaging. Adv Urol 2008; 213516
22. Bennett GL, Hecht EM, Tanpitukpongse TP, et al. MRI of the urethra in women with lower urinary tract symptoms: spectrum of findings at static and dynamic imaging. AJR 2009; 193:1708–1715

chapter 5

chapter 5.1

Value of MRI for Diagnosis and Local Staging of Recurrent Rectal Cancer: Correlation with Surgery and Histopathology of Resected Specimen

Roy S. Dwarkasing
Ruben M. van Waardhuizen
Wijnand J. Alberda
Michael Doukas
Maria de Ridder
Joost J. Nuyttens
Cornelis Verhoef
François E. J. A. Willemssen

Submitted

ABSTRACT

Objective To assess the value of MRI for predicting surgical outcome of locally recurrent rectal cancer (LRRC). In addition, patterns for diagnosis of LRRC on MRI using T2- weighted sequences (T2W) and contrast enhanced series (CE MRI) were evaluated.

Methods Surgically resected LRRC with curative intent were included. MR image analysis, using T2W and CEMRI of LRRC was done through visual interpretation by an experienced observer (reader 1) and compared with post processing image evaluation by an inexperienced observer (reader 2). MRI findings of LRRC were correlated with surgery and histopathology (PA) of the resected specimen.

Results A total of 51 lesions (47 patient) were included. Thirty (59%) tumors were radically resected (R0), 21 (41%) tumors were incompletely resected (R1). Lesions fixed to the pelvic side walls or presacral fascia (n=28) had 36% R0; non-fixed lesions (n=23) had 87% R0 (p=0.001). Tumor measurements on CE MRI had better agreement with PA than T2W. Imaging characteristics of LRRC on CE MRI include: arterial enhancement (100 %), persistent enhancement (100 %), dominant peripheral rim enhancement (59%), heterogeneous mosaic enhancement (21%).

Conclusions Tumor fixation to the pelvic side walls or presacral fascia yield incomplete resection margins in 64%, whereas non- fixed tumors were completely resected in 87%. CE MRI has typical imaging characteristics for LRRC and is more accurate for tumor assessment than T2W.

INTRODUCTION

Colorectal cancer is a common malignancy and rectal cancer accounts for approximately one third of the colorectal malignancies [1]. Developments in the treatment of rectal cancer, such as neo-adjuvant (chemo) radiotherapy and total mesorectal excision, have significantly reduced local recurrence rate over the last decades. Currently, the local recurrence rate after rectal surgery amounts 5-10 % [2]. Locally recurrent rectal cancer (LRRC) often occurs within the first 2 years after treatment of the primary tumor and has often disabling and difficult to treat symptoms, such as severe pain, fistulating and bleeding tumors [3; 4]. Radical surgical resection of the local recurrence offers the highest chance of cure and leads to survival rates ranging between 14 % and 30 % [5; 6]. On the contrary, without surgical intervention LRRC is associated with a dismal 5-year survival rate of less than 4% (4). Early detection of LRRC may facilitate radical resection and thus achieve a better survival [6; 7].

Magnetic Resonance imaging (MRI) is widely used for diagnosis and surgical planning of LRRC [8]. The diagnosis is challenging due to difficulty of differentiating actual recurrent disease from fibrosis and scarring [4; 7; 8]. This hinders the detection of local recurrences and also poses a problem in defining the exact tumor extent [8]. In addition to conventional MRI sequences (T1- and T2- weighted MRI), contrast enhancement (CE MRI) has the potential to increase lesion visibility and conspicuity and thus may be of additional value in distinguishing malignant from non-malignant tissue. CE MRI effects are based on the principle of increased tumoral neovascularization with vascular permeability will display earlier and higher contrast enhancement than surrounding fibrosis or normal tissue [7; 9; 10].

The aim of this study was to evaluate the additional value of CE MRI, using image post processing tools and compare with visual image interpretation, for the assessment of LRRC. In addition, the value of MRI for predicting surgical outcome (radical or involved resection margins) was assessed.

MATERIAL AND METHODS

Institutional approval was obtained for this retrospective analysis and informed consent was waived.

Patient selection

From a prospectively collected database we selected all patients with histologically proven LRRCs who were treated by intentionally curative surgery between January 2003 and December 2012 in a tertiary referral center. All patients were discussed in a multidisciplinary tumor board which included a specialized surgeon, radiologist, oncologist and radiotherapist to determine the optimal treatment strategy. During this period all patients were staged by a standard MRI protocol, which included T1-, T2- weighted sequences and CE MRI series.

MR Imaging protocol

MRI examinations were performed on a 1.5 T system (General Electric Medical systems, Milwaukee, USA) using a pelvic coil (8- or 16-channel phased array multicoil). A standardized imaging protocol of rectum and anus was performed with T2-weighted (T2W) fast spin-echo (FSE) sequences in axial, sagittal, and coronal planes. The scan parameters were: TR/ TE, 4570 / 80-85; FOV, 24,0 cm; slice thickness, 3 mm; gap, 0.3 mm; matrix, 320x256; 512-x 275; flip angle, 90°-150°; NSA, 2. In all patients, an additional axial T2W FSE sequence with fat saturation was performed (TR/TE, 5090/85). Transverse fat-saturated T1-weighted (T1W) gradient echo (GRE) imaging unenhanced and after intravenous gadolinium chelate administration (bolus of 0.2 mL/kg of 0.5 mmol/mL of gadopentetate dimeglumine [Magnevist, Schering], power injected at a rate of 2 ml/s) followed by a 20- ml saline flush was performed. The scan parameters were: TR/TE, 3.61/1.4; matrix, 256 x 224; flip angle, 15°; FOV, 300 mm; section thickness and gap, 4 mm and 0.4 mm, respectively; and one signal acquired. After intravenous contrast administration 10 scans were acquired within a time frame of 200 seconds, starting with an early arterial phase 6 seconds after contrast infusion. Every scan was executed at regular time intervals of 20 seconds after the previous scan with data sets acquired during 8.0 seconds of breath hold at expiration. Five minutes after gadolinium administration, sagittal and coronal T1-weighted GRE images were obtained using identical imaging parameters to those used for the pre- contrast T1W sequences. No special rectal preparation and no spasmolytic medication was used. With this contrast series arterial, venous, parenchymal and late dominant phases were obtained.

Image post- processing

MR images were exported in DICOM format from the picture archiving and communications system (PACS) to a viewing workstation (AW Server 2.0 from GE Healthcare, 2012). Fusion images were produced as an overlay of axial T2W images and last CE MRI scan. The field of view and slice level of the CE MRI images were automatically attuned to exactly match the T2W MRI. The CE MRI images were converted to a red-to-yellow color scale and semi-automatically adjusted to a blue-to-red color scale if an overexposed picture was generated (Fig. 1). Subtraction CE MRI (SCE MRI) images were digitally performed for the arterial-dominant phase (first or second scan after intravenous contrast infusion) (Fig. 2) and the late phase (last scan of the CE MRI series) (Fig. 2,3). To perform time intensity curves (TICs), regions of interest (ROIs) were selected and manually encircled with a cursor on the display screen of the last scan. Several (3, 5, or 7) ROI samples of variable size (20 – 40 mm2) were drawn, depending on the tumor size. These ROIs were placed well within the confines of the tumor and distributed evenly within the tumor volume. The workstation generated TICs automatically after ROI placement (Fig. 3). The TIC per lesion was recorded.

MRI Evaluation

All MRI examinations were available in a PACS viewing station and were evaluated visually by a radiologist with ten years of experience in pelvic MRI (reader 1). This reader used a standard form to register the following items: number and location of the recurrences. For tumor site a subdivision was made into lesions fixed to the pelvic side walls or presacral fascia (subgroup A) and lesions that were not fixed to the pelvic inner surroundings (subgroup B). Tumor fixation was defined as firm contact of tumor, with no fat interface, to the pelvic inner surfaces. Furthermore, the tumor outline facing the pelvic inner surface had to

be fixed for a significant portion (visual estimate of at least a quarter of the tumor circumference) to the pelvis. Additional items registered include: invasion of adjacent organs, pelvic floor, perineum; maximum tumor size measured on T2W and CE MRI separately and contrast enhancement characteristics: no enhancement; initial enhancement in arterial, venous or late dominant phase; persistent contrast pooling or wash-out; any obvious enhancement pattern in the perception of the reader. Reader 2, a medical student in his master degree, with no experience in reading pelvic MRI, did a separate assessment using a post processing workstation. In the preparation stage, reader 2 was trained by reader 1 in MRI of pelvic anatomy, MRI sequences, including demonstration of recurrent rectal carcinoma. The required post-processing skills at a dedicated viewing workstation were trained by a member of our PACS maintenance team. The examinations were transferred to this workstation without reports and with no access to the digital hospital information system. Reader 2 gave a confident level score to T2W, CE MRI and fusion images for detection and delineation of the lesion (1, not confident; 2, probably but not sure; 3, confident). Reader 2 measured the maximum tumor size on T2W, CE MRI and on fusion images using post processing tools. Additionally, Reader 2 acquired SCE MRI images and created TICs for all lesions. The additional images were uploaded in PACS. Based on this execution an interpretation was given to the following items per lesion: initial enhancement (arterial, venous, late phase), persistent enhancement or wash out, most frequent TIC. A radiologist with 8 years of experience in abdominal and pelvic imaging and an experienced surgeon in surgical oncology, both not involved with image interpretation, did an assessment of local tumor staging based on the surgical reports and of tumor size based on reports from PA of the resected specimen.

Reference standard

MRI findings were correlated with surgical findings and histopathology analysis (PA) of the resected specimens. Surgical findings as documented in the surgical reports served as reference for tumor localization, fixation to the pelvic side walls or presacral fascia and invasion in adjacent organs, pelvic floor or perineum. PA reports of the resected specimens served as the reference for completeness of resection: R0 (resection margins are microscopically free of tumor) or R1 (tumor cells in resection margins) and for maximum tumor size of R0 resected lesions.

Statistical analysis

Data analysis was done with SPSS software (IBM SPSS statistics 20 for windows, SPSS, Chicago). Bland and Altman plots (11) were used to determine the limits of agreement for the measurements between two readers, performed on T2W and CE MRI. Bland and Altman plots were also used to assess agreement between measurements on T2W and CE MRI of LRRC and histopathology analysis (11, 12). To determine actual tumor size, only R0 resected lesions were included for comparison between MRI and PA. Categorical variables were compared using Chi-square test. A 2-sided significance level of 0.05 was used.

RESULTS

Patient characteristics

During the study period, a total of 47 patients (32 men, 15 women, mean age 63 years, range 39-80 years) were eligible for analysis. One patient had tumors at two separate locations in the pelvis, three patients developed a re-recurrence and underwent re-resection. A total of 51 lesions and resected specimen were available for evaluation.

Time interval MRI, neo- adjuvant (chemo) radiotherapy and surgery

In 40 patients MRI was performed after completion of neo- adjuvant (chemo) radiotherapy within a mean time interval of 3 weeks (range 3-5 weeks) and prior to surgery (mean 6 weeks, range 4-7 weeks). Six patients had MRI prior to neo- adjuvant therapy (mean 6 weeks,

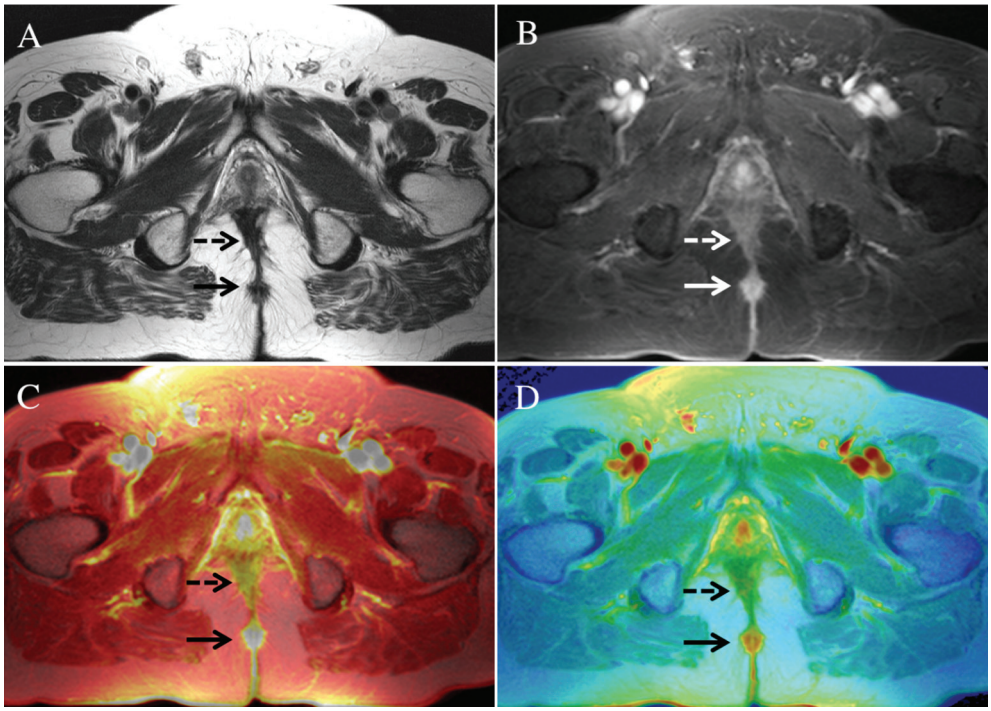

Figure 1. Recurrent rectal carcinoma in the perineum: Value of contrast enhanced MRI and fusion with T2-weighted images for tumor identification and delineation
68- years old man, 3.5 years after rectal resection for rectal cancer (T2N0M0; R0). Local recurrence within perineal scar tissue. Pre- operative MRI (after 30 Gy radiotherapy on pelvis): T2-weighted MR image (A) shows two masses in the perineum (arrows) within scar tissue. Both lesions appear to enhance after gadolinium administration on the CE MR image (B). The red-to-yellow color fusion image (C) displays an overexposed image that hinders an obvious conclusion, the blue-to-red color scaled fusion image (D) makes clear that the ventral lesion (dashed arrow) does not demonstrate intense enhancement, while the dorsally located lesion (arrow) demonstrates intense enhancement in a dominant rim pattern. Pathology analysis of the ventral lesion demonstrated fibrotic tissue with no tumor cells, the dorsal lesion corresponded with active local tumor recurrent. The lesion was completely resected (R0).

range 6-7 weeks) and prior to surgery (mean 15 weeks, range 13-15 weeks). One patient did not receive neo-adjuvant therapy with MRI performed 7 weeks prior to surgery.

Table 1: Association of Locally Recurrent Rectal Cancer Fixed to the Pelvic Side Walls or Presacral Fascia and Resection Status

Tumor Site	R1 resection	R0 resection	Total
	n (%)	n (%)	(n)
Fixed to the pelvic walls or presacral fascia	18 (64 %)	10 (36%)	28
Pelvic side walls (n = 16)			
Presacral fascia (n = 12)			
Not fixed to the pelvic side walls or presacral fascia	3 (13 %)	20 (87%)	23
Anastomotic, genitourinary organs (n = 15)			
Pelvic floor (n = 4)			
Perineum (n = 4)			
Total	21	30	51

Site is based on the predominant site of tumor tissue in case of extended lesions; (n), number of lesions

Tumor site and resection status

There was agreement for tumor site, fixation to the pelvic side walls or presacral fascia, invasion of adjacent organs, pelvic floor or perineum as described by reader 1 and surgical findings for all lesions. Thirty lesions (59%) were radically resected (R0). In the remaining 21 lesions (41%) no radical resection was achieved (R1). On MRI, 28 lesions (55%) demonstrated attachment to the pelvic side walls (Fig. 2) or presacral fascia (Fig. 4) (subgroup A), the remaining 23 lesions (45 %) were not attached to the pelvic inner surroundings (Fig. 1, 3) (subgroup B). Subgroup A resulted in 64 % R1 resections compared to 13 % R1 resections in subgroup B. (p = 0.001, table 1).

Tumor size measured by reader 1 and reader 2: all lesions

Maximum tumor size by reader 1: median 25 mm (IQR 19 – 40) for T2W; median 28 mm (IQR 20 - 40) for CE MRI. Corresponding measurements performed by reader 2 were: median 26 mm (IQR 20 - 40) for T2W; median 28 mm (IQR 23 - 45) for CE MRI and median 27 mm (IQR 21 - 41) for T2W/CE MRI fusion images. See figure 5, measurements performed on CE MRI

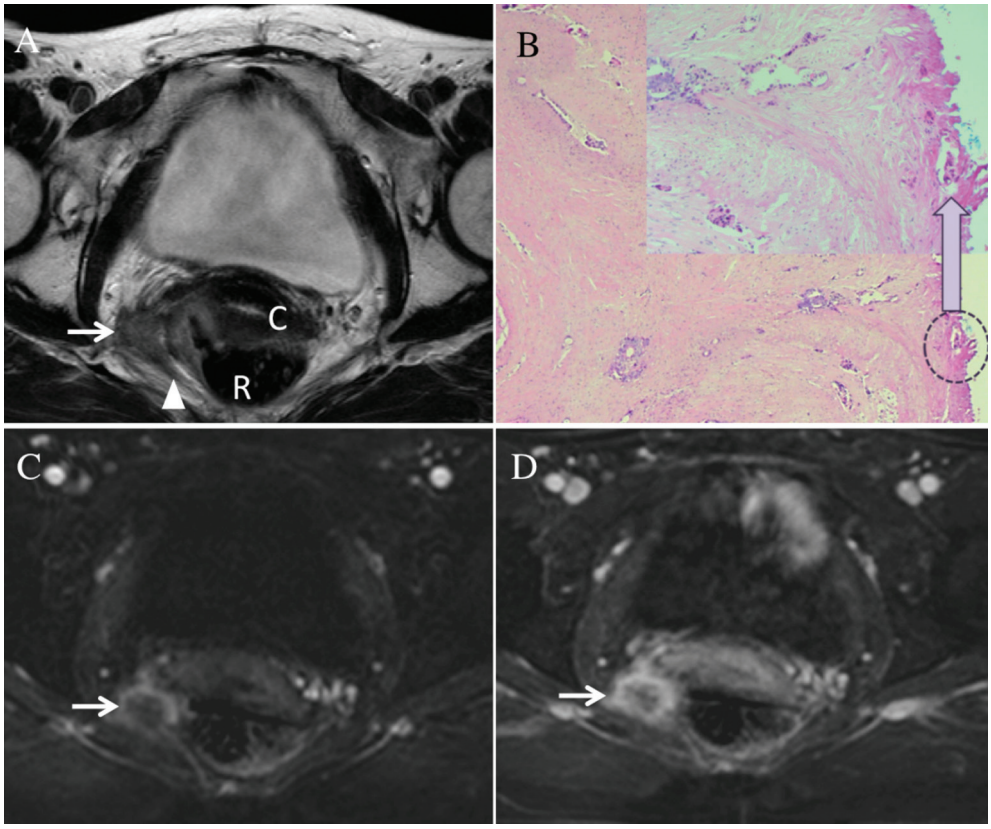

Figure 2. Recurrent rectal cancer located in the rectal wall with transmural tumor extension and fixed to the pelvic side wall
43- years old woman, 3 years after low anterior resection for rectal cancer (T3N2M0; R0) with local recurrence in the rectal wall including mesorectum and fixation to the right dorsolateral pelvic wall. Pre- operative MRI after 50 Gy radiotherapy on the pelvis. Axial T2-weighted MR images (A) shows the tumor (arrow) located within the rectal wall, adjacent mesorectum and fixed to the sacrospinous ligaments (arrowhead). Low anterior resection was performed of the tumor, including rectum, dorsal vagina wall, cervix, uterus and right ovary, followed by ileostomy and reconstructive surgery with a colo-anal pouch. The lesion was incompletely resected (R1) at the pelvic side wall with 10 Gy intra-operative radiotherapy on the resected surface during operation. B) Adenocarcinoma was located in the surgical resection margin (H-E 100x, encircled area 200X). Characteristic peripheral enhancement pattern of the lesion is seen on the contrast enhanced subtraction images (SCE MRI; C, arterial dominant phase; D, late phase). On D a persistent enhancement (no wash-out) is demonstrated. Close contact is seen with the posterior vagina and cervix on T2W without evidence of invasion on DCES as was proven by histopathology. C, cervix; R, rectum.

images show smaller limits of agreement than measurements performed on T2W images, thus the degree of conformity is higher on measurements performed on CE MRI images. The subjective interpretation of reader 2 for tumor identification and delineation was: For T2W: not confident 55 %, probably 33% and confident 12 %. Using CE MRI, including fusion with T2W images, these figures were respectively 6 %, 18 % and 76 %.

Tumor size determined by histopathology analysis (PA) and MRI: R0 lesions

Of R0 lesions (n=30), 27 lesions were documented with an accurate maximum size of vital tumor tissue on PA. Based on these 27 lesions, mean tumor size on PA was 20 mm (IQR 30-17 = 13 mm). All lesions were evaluated on MRI after neo-adjuvant (chemo) radiotherapy.

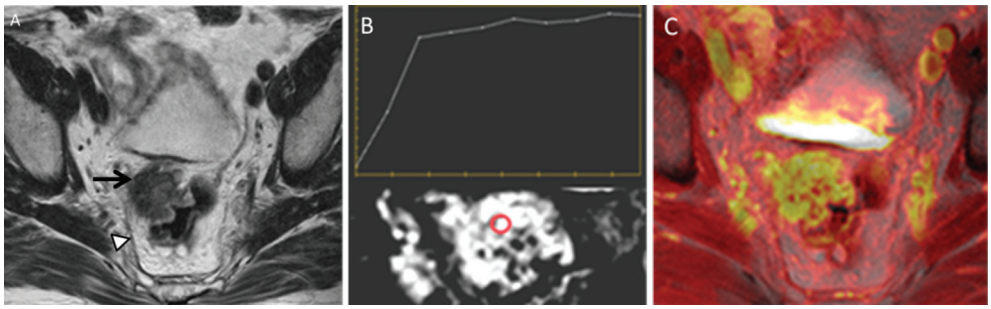

Figure 3. Local recurrent rectal cancer, located at the anastomotic level of the rectal wall with extension in the mesorectum, not fixed to the pelvic walls
66- years old man, 5 years after low anterior resection for rectal cancer (pT3N1M0; R0). Pre- operative MRI, after 45 Gy radiotherapy on the pelvis. Axial (a) T2W image demonstrates the tumor (arrow) at the anastomotic level in the rectal wall with extension in the mesorectum and invasion of the right seminal vesicle (not shown). No fixation to the adjacent pelvic wall (arrowhead: peritoneal surface pelvic wall). The dynamic contrast- enhanced image (late dominant phase) with region of interest (red ring) and corresponding time intensity curve (TIC) demonstrates arterial enhancement with no wash out (TIC, Type 3). Fusion image of DCE and T2W demonstrates a heterogenous mosaic enhancement pattern of the lesion. Total excenterative surgery was performed with clean resection margins (R0).

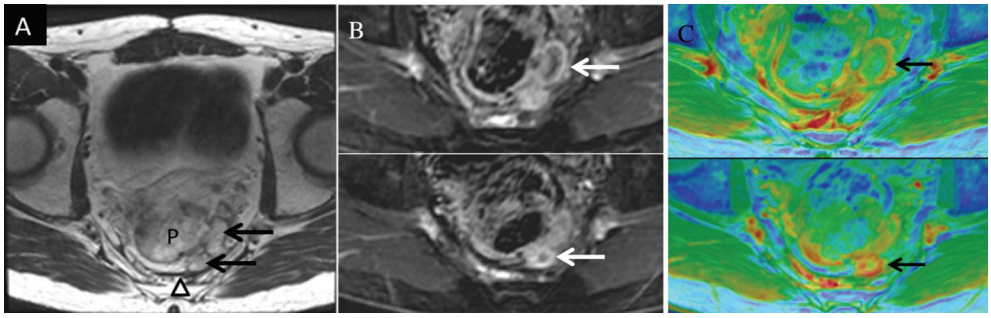

Figure 4. Re-recurrent rectal carcinoma (mucinous type adenocarcinoma) fixed to the presacral fascia
42- years old man, with local re-recurrent rectal carcinoma, 2 years after resection of the first local recurrence (T3N0M0; R0). Previous total mesorectal extirpation and proctocolectomy with ileo-anal J-pouch. A) Pre- operative MRI (after concomitant chemo- radiotherapy (Capacitabine, 50 Gy on pelvis) with active lesions (arrows) fixed to the presacral fascia (arrowhead). Note the high signal intensity content on T2W image which reflects the mucinous content of the tumor and makes it difficult to discern and discriminate from the pouch (P). On SCE MR images (late phase) typical rim- enhancement can be appreciated on consecutive slices (composite image of a more proximal and distal level with corresponding T2W/CE MRI fusion image (C). The lesions were incompletely resected (abdominal peritoneal resection of the pouch, R1, with 10 Gy intra- operative radiotherapy on the resected presacral surface).

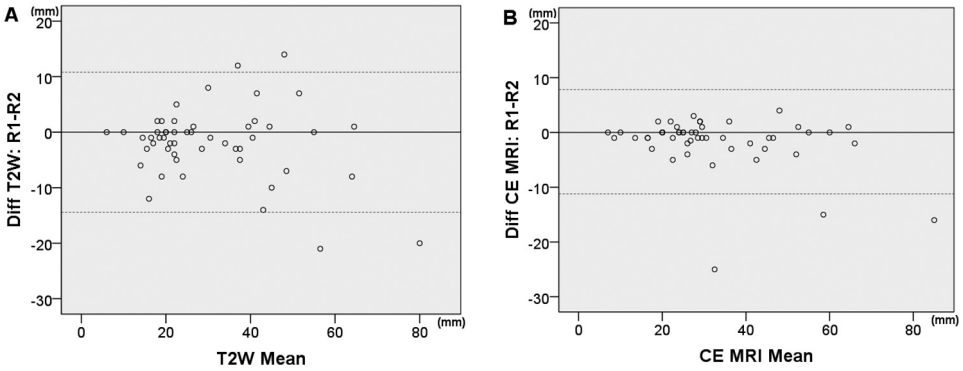

Figure 5. Agreement of vital tumor measurement by 2 readers for T2W (A) and CE MRI (B) on 51 lesions. Diff, difference.

For reader 1, average tumor size on T2W, mean 20 mm (IQR 36-19 = 17 mm); CE MRI, mean 24 mm (IQR 35-20 = 15 mm). For reader 2, mean tumor size on T2W, 22 mm (IQR 39-18 = 21 mm); CE MRI, mean 25 mm (IQR 35-20 = 15 mm); T2W/CE MRI fusion, mean 23 mm (IQR 35-19 = 16 mm). Figure 6 shows Bland-Altman plots with difference between MRI and PA measurements plotted against PA (reference standard). The solid (base) lines represent agreement between PA and MRI with the dashed lines representing the upper and lower 95 % limits of agreement. For reader 1, CE MRI shows better agreement with PA than T2W. For reader 2, best agreement with PA is found for T2W/CE MRI fusion.

Contrast enhancement pattern

Reader 1 reported arterial visual contrast enhancement after gadolinium administration with no wash-out of all lesions (100 %) (Fig 3). This finding was confirmed by reader 2, using SCE MRI (Fig 2) images and TICs. The flow volume curves of lesions showed fast (steep angle) and persisting plateau contrast enhancement, without wash out (TIC, type 3) (Fig 3). Two main contrast enhancement patterns were distinguishable: dominant peripheral rim enhancement (n=30, 59%) (Fig 1,2,4) or heterogeneous mosaic enhancement (n=11, 21%) (Fig. 3). In the remaining cases no clear enhancement pattern was observed (n=10, 20%). See table 2.

5.1

Table 2: Characteristics of Locally Recurrent Rectal Cancer on Contrast Enhanced MRI based on Analysis of 51 Tumors

Characteristic feature	n (%)
Arterial dominant enhancement	51 (100)
Contrast pooling; no wash- out	51 (100)
Dominant peripheral rim enhancement	30 (59)
Heterogeneous mosaic enhancement	11 (21)

n, number of lesions.

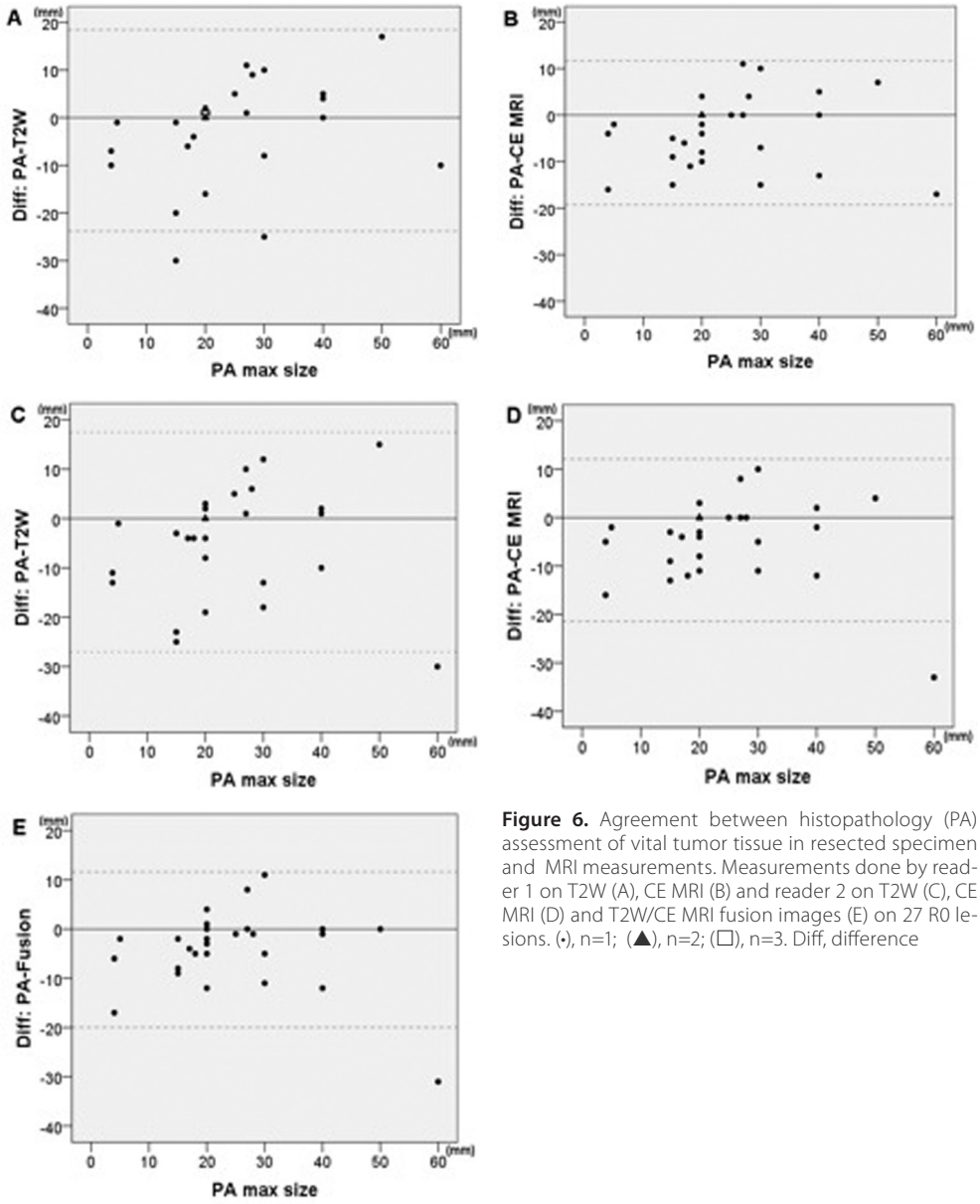

Figure 6. Agreement between histopathology (PA) assessment of vital tumor tissue in resected specimen and MRI measurements. Measurements done by reader 1 on T2W (A), CE MRI (B) and reader 2 on T2W (C), CE MRI (D) and T2W/CE MRI fusion images (E) on 27 R0 lesions. (•), n=1; (▲), n=2; (□), n=3. Diff, difference

DISCUSSION

The aim of this study was to assess the additional value of CE MRI for diagnosis and pre-operative assessment of LRRC. Furthermore, the value of MRI for predicting surgical outcome was evaluated. We found that compared with T2W, there is better agreement between both readers of measurements performed on CE MRI images. In addition, CE is more accurate than T2W in measuring the size of vital tumor tissue in R0 resected lesions. We found a combination of contrast enhancement characteristics (Table 2). It should be noted that immature fibrosis and inflammation may demonstrate high signal intensity on T2W, and may demonstrate contrast enhancement [11]. However, the CE MRI enhancement characteristics found in this our study may be supportive to diagnose LRRC and differentiate from fibrosis (Fig 1). Messiou et al. described that rectal tumor recurrences may exhibit rim enhancement patterns on CE MRI [4]. To our knowledge, our study is the first to assess a combination of typical CE MRI characteristics, including dominant peripheral rim- or heterogeneous mosaic enhancement pattern, in a cohort of patients. Diffusion weighted MR imaging (DWI) may increase confidence for the detection of LRRC [12; 13]. However, the application of DWI to the abdomen and pelvis has proved to be challenging due to artifacts which may cause image distortion [14]. Furthermore, adding DWI to T2 weighted MRI, does not significantly improve performance of MRI for diagnosis, but will increase specificity and interobserver agreement [15]. CE MRI not only increases confidence in detection, but is more accurate than T2W to assess vital tumor dimensions, and thus seems especially valuable for pre-operative assessment and surgical planning. Another potential for CE MRI in the management of LRRC is monitoring of local image guided therapies like radio frequency ablation. In our experience CE MRI is less effected by post procedural effects than T2W and DWI to confidently demonstrate local residual or recurrent disease. Future studies are needed to present evidence for this. Our results show that tumor fixation to the pelvic side walls or presacral fascia is of importance to predict surgical outcome, with an incomplete resection margin in the majority of cases (64%), in contrary to non-fixed lesions (13%). A clinical study by Moore et al. [16] reported that pelvic recurrences of rectal and colon cancer in the axial and anterior locations, are more likely to be completely resectable than those involving the pelvic sidewall. To our knowledge, our study is the first MRI based study for LRRC that endorses these clinical results. In our center intra-operative radiotherapy will be applied on the resected surface in case of tumor fixation to the pelvic side walls or presacral fascia [17; 18]. Although our study explored especially morphologic criteria of LRRC using CE MRI, a recent study suggests that quantitative DCE-MRI measures of flow and permeability into and out of the tumor mass may be used to predict resection status, chance of re- recurrence and survival [19]. Our study has some limitations. First, because of the retrospective design. Furthermore, the reading of MRI examinations of the study population was done by one radiologist and the post processing evaluation by a master degree medical student. In the contemplations of our study design we focused on the additional value of CE MRI and invited a non- radiologist as the second reader for post processing image evaluation. The post processing could therefore be performed without being influenced by the own frame of reference based on experience with T2W and CE MRI reading. We believe that the second reader had a decisive role in our study design by objectifying patterns of enhancement using post- processing tools. Another point of consideration is that our study design was not based on direct comparison between LRRC and surrounding fibrosis. This was technically not feasible because the surgical resection specimen was aimed at the LRRC and some, but not all, of the surrounding fibrosis. Thus, the only acceptable reference was maximum tumor size in R0 resected lesions and not the amount of fibrosis. Another point to stress is that our study population is a retrospective analysis in a cohort of patients with a well- known final diagnosis. It is not sure what the additional value of CE MRI is in patients

with follow up MRI for screening or clinical suspicion of LRRC. Lambregt et al. [15] found that T2W MRI, on its own, has a high accuracy for the diagnosis of local recurrent rectal cancer in 42 patients with clinical suspicion of LRRC. Based on our results in table 2, CE MRI has the potential to confidently diagnose LRRC in a screening population. The results of our study are promising and warrant further study in a prospective fashion to confirm this.

In conclusion, our study has demonstrated that CE MRI is a valuable supplement in the MRI protocol for diagnosis and pre-operative evaluation of LRRC. LRRC has typical CE MRI findings of arterial and persistent enhancement (100%), dominant peripheral rim- or heterogeneous mosaic enhancement pattern (80%), and is more consistent for assessment of vital tumor dimensions than T2W. For surgical outcome, tumor fixation to pelvic side walls or presacral fascia will result in incomplete resection margins in 64% of cases, whereas non-fixed tumors will be completely resected in 87%.

REFERENCES

1 Jemal A, Siegel R, Xu J, Ward E (2010) Cancer statistics, 2010. CA Cancer J Clin, 60:277-300

2 Bakx R, Visser O, Josso J, Meijer S, Slors JF, van Lanschot JJ (2008) Management of recurrent rectal cancer: a population based study in greater Amsterdam. World J Gastroenterol, 14:6018-6023

3 Kusters M, Marijnen CA, van de Velde CJ, et al. (2010) Patterns of local recurrence in rectal cancer; a study of the Dutch TME trial. European Journal of Surgical Oncology, 36:470-476

4 Messiou C, Chalmers A, Boyle K, Sagar P (2006) Surgery for recurrent rectal carcinoma: The role of preoperative magnetic resonance imaging. Clin Radiol, 61:250-258

5 Shoup M, Guillem JG, Alektiar KM, et al. (2002) Predictors of survival in recurrent rectal cancer after resection and intraoperative radiotherapy. Dis Colon Rectum, 45:585-592

6 Hahnloser D, Haddock MG, Nelson H Intraoperative radiotherapy in the multimodality approach to colorectal cancer. Surgical Oncology Clinics of North America, 12:993-1013

7 Krestin GP, Steinbrich W, Friedmann G (1988) Recurrent rectal cancer: diagnosis with MR imaging versus CT. Radiology, 168:307-311

8 Dresen RC, Kusters M, Daniels-Gooszen AW, et al. (2010) Absence of tumor invasion into pelvic structures in locally recurrent rectal cancer: prediction with preoperative MR imaging. Radiology, 256:143-150

9 Muller-Schimpfle M, Brix G, Layer G, et al. (1993) Recurrent rectal cancer: diagnosis with dynamic MR imaging. Radiology, 189:881-889

10 Goh V, Padhani AR, Rasheed S (2007) Functional imaging of colorectal cancer angiogenesis. Lancet Oncol, 8:245-255

11 Lavini C, de Jonge MC, van de Sande MG, Tak PP, Nederveen AJ, Maas M (2007) Pixel-by-pixel analysis of DCE MRI curve patterns and an illustration of its application to the imaging of the musculoskeletal system. Magn Reson Imaging, 25:604-612

12 Koh DM, Collins DJ (2007) Diffusion-weighted MRI in the body: applications and challenges in oncology. AJR. American Journal of Roentgenology, 188:1622-1635

13 Rao SX, Zeng MS, Chen CZ, et al. (2008) The value of diffusion-weighted imaging in combination with T2-weighted imaging for rectal cancer detection. Eur J Radiol, 65:299-303

14 Nishie A, Stolpen AH, Obuchi M, Kuehn DM, Dagit A, Andresen K (2008) Evaluation of locally recurrent pelvic malignancy: performance of T2- and diffusion-weighted MRI with image fusion. J Magn Reson Imaging, 28:705-713. 15 Lambregts DM, Cappendijk VC, Maas M, Beets GL, Beets-Tan RG (2011) Value of MRI and diffusion-weighted MRI for the diagnosis of locally recurrent rectal cancer. Eur Radiol, 21:1250-1258

16 Moore HG, Shoup M, Riedel E, et al. (2004) Colorectal cancer pelvic recurrences: determinants of resectability. Dis Colon Rectum, 47:1599-1606

17 Ferenschild FT, Vermaas M, Nuyttens JJ, et al. (2006) Value of intraoperative radiotherapy in locally advanced rectal cancer. Dis Colon Rectum, 49:1257-1265

18 Rodriguez-Bigas MA, Chang GJ, Skibber JM (2010) Multidisciplinary approach to recurrent/unresectable rectal cancer: how to prepare for the extent of resection. Surgical Oncology Clinics of North America, 19:847-85919

19 Gollub MJ, Cao K, Gultekin DH, et al. (2013) Prognostic Aspects of DCE-MRI in Recurrent Rectal Cancer. Eur Radiol, 23:3336-3344

chapter 5.2

Primary Cystic Lesions of the Retrorectal Space: MRI Evaluation, Histopathology Confirmation and Clinical Assessment

Roy S. Dwarkasing
Sylvia I. Verschuuren
Geert J.L.H. Leenders
Loes M.M. Braun
Gabriel P. Krestin
W. Rudolf Schouten

Submitted

ABSTRACT

Purpose To assess the a priori chance that primary cystic lesions of the retrorectal space (RCL) are malignant and investigate MRI characteristics which indicate malignancy.

Materials and Methods Patients referred to a center for colorectal surgery were recruited from 2000-2014.
Lesions were proven by clinical assessment and histopathology. MRI was performed on 1.5 T with examinations evaluated by two radiologists. Interobserver agreement was assessed (Cohen's Kappa) and differences between malignant and benign lesions calculated (Fisher's exact test).

Results Twenty eight patients (22 female, 6 male, 18-70 years) with 31 lesions were included. Lesions were subdivided into: tailgut cyst (n=16, 52 %), epidermoid and dermoid cyst (n=6, 19%), colorectal (n=4, 13%), teratoma (n=3, 10%), neurogenic (n=2, 6%). Five patients (18%) had malignancy. Colorectal lesions had the highest percentage of malignancy (3/4, 75%). Solid tissue component was found in all 5 (100 %) malignant lesions, and 2 (8%) of benign lesions, both teratoma's ($p < 0.05$). For unilocularity, multilocularity, debris, septa and wall thickening, differences were not significant. Interobserver agreement was excellent (kappa = 1) for all characteristics except debris (kappa = 0.795).

Conclusion Eighteen percent of patients with RCL display malignancy, with MRI findings of solid tissue component indicative of a malignant lesion.

INTRODUCTION

The retrorectal space, also known as the presacral space, is a space bounded anteriorly by the posterior wall of the rectum, posteriorly by the sacrum and coccyx, superiorly by the peritoneal reflection, and inferiorly by the pelvic floor muscles. Laterally, the space is bounded by the iliac vessels and ureters. This space contains remnants derived from embryonic neuro-ectoderm, notochord, and hindgut, and hence may result in a wide variety of congenital lesions herein (1-4). Malignancy is more common in the pediatric population, and solid lesions are more likely to be malignant than are cystic lesions (5). Retrorectal cystic lesions (RCL) in adults are rare with little literature available and an unknown prevalence. Often the basic clinical problem is whether a RCL should be considered a malignant lesion.

The purpose of this study was to assess the a priori chance that RCL are malignant and identify MR imaging characteristics which indicate malignancy.

MATERIALS AND METHODS

Institutional ethical committee approved this retrospective study and informed consent was waved.

Patient selection and inclusion criteria

Patients were referred to a tertiary center for colorectal surgery between January 2000 and October 2014 and were recruited from prospective collected databases from the departments of surgery and radiology. Criteria for inclusion were: minimum patient age 18 years; lesion found at first referral consultation at our center with no surgery of the pelvis and pelvic floor for at least 3 years prior to referral; histology proven lesion; MRI performed within 3 months of histology; at initial prospective evaluation lesion characterization was "cystic" clinically and on MRI.

MRI and MR Imaging protocol

MRI was performed in all patients on 1.5 T (General Electric Medical systems, Milwaukee, USA) using a 8 or 16- channel phased array multicoil. In all cases T2- weighted (T2W) fast spin-echo (FSE) images were acquired in axial, sagittal, and coronal planes through the entire pelvis and pelvic floor: TR/TE, 4570/80-85; FOV, 24.0 cm; slice thickness, 3 mm; gap, 0.3 mm; matrix, 320x256; 512x275; flip angle, 90°-150°; NSA, 2. Axial T2W FSE with fat saturation: TR/TE, 5090/85. Axial T1W gradient echo (GRE) imaging with and without fat saturation: TR/TE, 3.61-7.0 /1.4-3.0; matrix, 256 x 224; flip angle, 15°; FOV, 300 mm; slice thickness and gap, 4 mm and 0.4 mm; NSA, 1. Contrast enhanced series were available in all but one case. Axial T1W GRE fat saturated imaging unenhanced and after intravenous gadolinium chelate administration (bolus of 0.2 mL/kg of 0.5 mmol/ml of gadopentetate dimeglumine [Magnevist, Schering].

MRI reading

MRI examinations were evaluated by a radiologist with 10 years of experience in MRI of the pelvis and pelvic floor (reader 1). Second reader was a radiologist with one year of professional experience (reader 2). All examinations were evaluated separately by both readers who were blinded to the final diagnosis. A standard form was used to record: number of lesions; lesion composition (solid, cystic, mixed); lesion size (largest axis in 3 planes (mm)); configuration (lobulated or smooth); unilocular or multilocular; containing septa; measurement of thickest septa (mm); debris; solid tissue component; site according to the level of the sacral vertebral body (SL) and coccygeal level (CL) in sagittal plane; attached to the presacral fascia; confinement within the mesorectal compartment; infralevatoir extension; epicenter: (median or paramedian orientation in the axial plane); erosion or destruction of the sacrococcygeal spine, signal intensity (SI) on T1W and T2W MRI; additional remarks. Cases were discussed between both readers, in case of disagreement and consensus was reached. Histopathology assessment, clinical management and follow-up information were obtained from patients' records in the digital hospital information system.

Definitions

See figure 1 below for an illustration of the definitions.

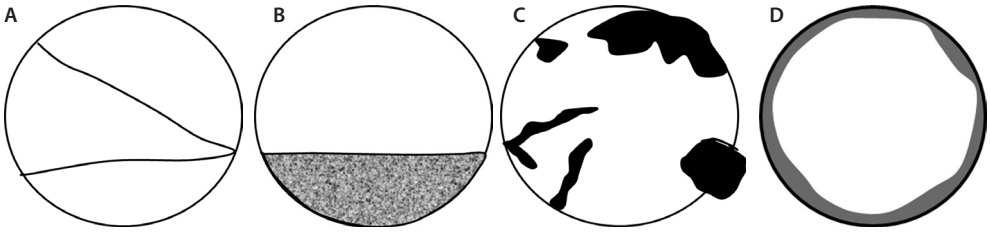

Figure 1. Illustration of septa (A), debris (B), solid components (C), wall thickening (D)

Reference standard

All lesions were pathology proven. This assessment was done after surgical resection (n=24) or thick needle biopsies of the lesion (n= 3). One case of Curanino syndrome was assessed by typical MRI findings and clinical confirmation of an alteration of the HLXB9- gene at patient' genomic analysis. Lesion characteristics on MRI were matched with reports from surgery and histopathology.

Statistical analysis

Interobserver agreement for both readers was assessed by calculating Cohen's Kappa value for each lesion characteristic separately. Significance of differences between malignant and benign lesions was calculated with a 95% confidence level, using a two-sided Fisher's exact test. All calculations were performed with SPSS Statistics, version 21.

RESULTS

A total of 28 patients were included. See figure 2 for patients sampling and table 1 for characteristics of the study population, including final diagnoses.

Table 1. Included patients with diagnosis, patient characteristics and number of lesions

Diagnosis	**Patients**				**Lesions**
	(n)	F	M	Age (years) m, mean; r, range	(n)
Tailgut cyst	13	11	2	m 60, r 40-70	16
Epidermoid cyst	5	4	1	m 47, r 28-56	5
Recurrent mature dermoid cyst with carcinoid	1	1	0	18	1
Mature cystic teratoma	2	1	1	20, 34	2
Recurrent mature cystic teratoma with abscess	1	1	0	44	1
Rectal duplication cyst	1	0	1	34	1
Rectal duplication cyst with mucinous adenocarcinoma	1	1	0	57	1
Mucinous adenocarcinoma of rectum primary	1	0	1	59	1
Subperitoneal pelvic mucinous adenocarcinoma from colorectal origin	1	1	0	50	1
Anterior sacral meningomyelocoele (Curanino Syndrome)	1	1	0	22	1
Differentiating neuroblastoma	1	1	0	40	1

Twenty eight patients (22 female, 6 male, 18-70 years) with 31 lesions were included.

Lesions were subdivided into: tailgut cyst (n=16, 52 %), epidermoid and dermoid cyst (n=6, 19%), colorectal origin (n=4, 13%), teratoma (n=3, 10%), neurogenic (n=2, 6%). Tailgut cysts (TGC) were the most prevalent lesion, consisting of 13/28 (46 %) patients or 16/31(52%) lesions. On patient level, 5 of 28 patients had malignancy (18%); on lesion level 5 out of 31 were malignant (16%). The subgroup of lesions from colorectal origin had the highest percentage of malignancy (3 of 4, 75%). Age of patients with malignancy ranged from 18 to 59 years, median 50 years, with 2 patients younger or equal to 40 years. Solid tissue component was found in all 5 (100 %) malignant lesions, whereas 2 (8%) benign lesions demonstrated solid components. This is a significant finding ($p < 0.05$), with a difference of 92.3% (95% CI = [82.1% – 102.6%]).

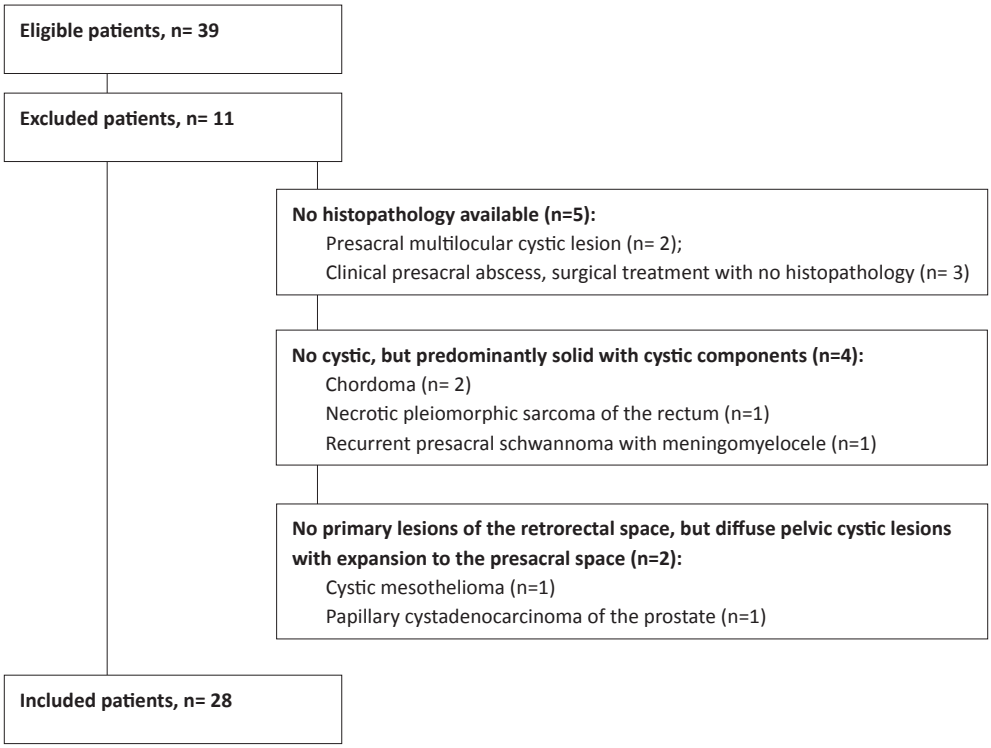

Figure 2. Flow diagram summarizes patient sampling

For unilocularity, multilocularity, debris, septa and wall thickening, differences were not significant between malignant and benign lesions. Interobserver agreement between both readers was perfect (kappa = 1) for all items except debris. In two lesions reader 2 interpreted initially debris and reader 1 heterogeneous signal intensity (SI). After consensus reading this finding was assessed as inhomogeneous SI. For debris, kappa = 0.795, which is considered substantial agreement. The different subgroups of lesions will be more fully discussed.

5.2 *Tailgut cysts*

Primary lesions in 11 patients (total of 13 lesions) and recurrent lesions in 2 patients (total of 3 lesions). Recurrent lesions at 6 and 32 years post- surgery respectively.

In 8 (62 %) patients lesions were incidentally detected on previous imaging (Fig 3A). Five patients (38 %) were symptomatic, including two patients with non- specific pelvic pain, two patients with obstructed defecation (Fig 3 B) and one patient who presented with chronic perianal fistulas and pararectal abscesses. This patient had undergone 3 surgical procedures for fistula disease with 10 repeat MRI, including T1W and T2W sequences (no contrast administration). Fifteen (94 %) lesions were attached to the presacral fascia with a midline (n=8) or paramedian (n=7) orientation, including 14 lesions above the pelvic floor (supralevatoir) and one lesion above and below the pelvic floor (supra- and infralevatoir)

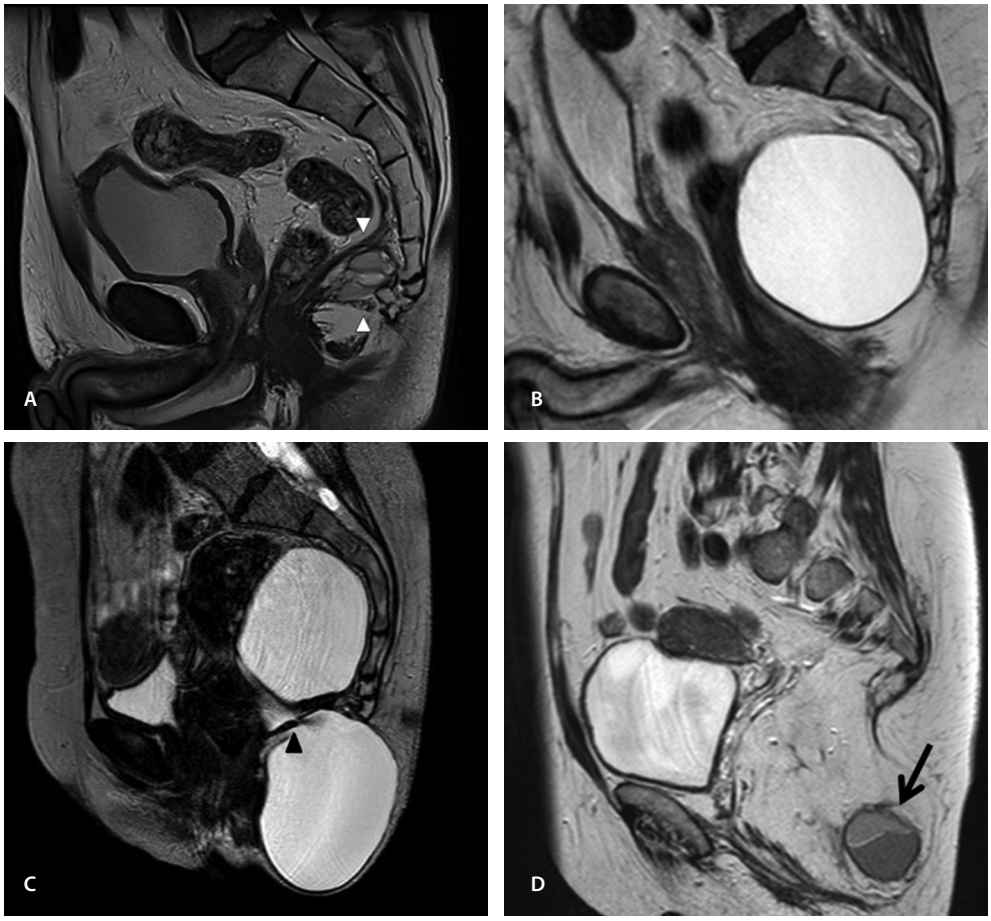

Figure 3. A) 44-year-old man with multilocular tailgut cyst (TGC) at the coccygeal level. Note different shades of high signal intensity within the lesion. Thickened peritoneal reflection from the rectum (upper arrowhead) indicates the upper border of the retrorectal space (RRS), with the levator ani muscle (lower arrowhead) at the level of the lower border of the RRS. The lesion was an incidental finding on previous imaging. B) 64-year-old man with a recurrent unilocular TGC, 10 years after incomplete resection. Note homogeneous high signal intensity and thin wall of the lesion. The lesion was symptomatic with obstructed defecation through compression on the rectum. C) 52-year-old woman with a large TGC at first presentation, hourglass appearance, located partly above and partly below the pelvic floor. Arrowhead indicates the level of the pelvic floor. Patient had a painfull perianal swelling with obstructed defecation. D) 65-year-old woman with recurrent TGC, 32 years after sacrococcygectomy. Two lesions locally presacral (not shown) and in the left ischio-rectal space (arrow). Note intermediate to low SI of the lesion, including debris. All images T2W TSE in the mid-sagittal (A-C) and left paramedian (D) plane.

(Fig 3 C). One patient had 2 recurrent lesions, including one lesion in the left ischiorectal fossa (Fig 3D). Lesion location with respect to the sacrococcygeal spine: first sacral vertebral body (SL 1) – coccygeal level (CL) (n=1), SL 1 - SL 4 (n=1), SL 4 – SL 5 (n=5), SL 4 - CL (n=5), CL (n=3), left ischiorectal fossa (n=1).

Table 2. MRI Findings of Primary Cystic Lesions of the Retrorectal Space

Diagnosis	**Unilocular** (Uni) **Multilocular** (Multi) **Max size** (range, cm)	**Debris, Septa** (mm), **Solid components,** **Wall thickening** (mm)	**T1W/T2W**	**Remarks**
Tailgut Cyst (n=16)	Uni 4, Multi 12, (217 cm)	Debris 2, Septa 12 (2 -5 mm), Solid 0, Wall 0	↓/↑9 ↑/↑5 ↑/↓ 2	Different shades SI 3 Erosion sacrum 1
Epidermoid cyst (n=5)	Uni 5, Multi 0 (2,5-9,5 cm)	Debris 0, Septa 0, Solid 0, Wall 1 (5mm)	↓/↑ 2 ↑/↑ 1 ↑/↓ 2	Heterogeous SI 5
Recurrent mature cystic dermoid with carcinoid (n=1)	Uni 1 (9.5 cm)	Debris 0, Septa 0, Solid 1, Wall 0	↓/↑ 1	Heterogenous SI
Mature cystic teratoma (n=2)	Uni 0, Multi 2, (5 cm, 7 cm)	Debris 1, Septa 2 (3 mm); solid 1; Wall 2 (5 mm, 8mm)	↓/↑ 2	Heterogenous SI 1 Different shades SI 1
Recurrent mature cystic teratoma with abscess	Multi 1 (including abscess with fluidair level)	Debris in abscess 1, Septa 1 (2 mm), Solid 1, Wall 0	↑/↓ 1	Different shades SI Abscess with air-fluid level (↓/↑)
Retal duplication cyst	Uni 1 (5 cm)	Debris 0, Septa 0, Solid 0 Wall 0	↓/↑ 1	No internal ostium
Rectal duplication cyst with adenocarcinoma	Uni 1 (5.5 cm)	Debris 0, Septa 1 (2 mm), Solid 1, Wall 1 (10 mm)	↓/↑ 1	Heterogenous SI 1 internal ostium
Mucinous adenocarcinoma Rectum primary	Uni 1 (6 cm)	Debris 0, Septa 0, Solid 1, Wall 0	↓/↑ 1	
Subperitoneal pelvic mucinous adenocarcinoma (colorectal origin)	Multi 1 (13.5 cm)	Debris 0, Septa 1 (6mm), Solid 1, Wall 1 (7 mm)	↓/↑ 1	
Meningomyelocele (Curanino Sdm)	Multi 1 (5 cm)	Debris 0, Septa 0 (2mm), Solid 0, Wall 0	↓/↑ 1	Different shades SI Sacral aplasia
Differentiating Neuroblastoma	Multi 1 (10 cm)	Debris 1, Septa 0, Solid 1, Wall 0	↑/↑ 1	Different shades SI

SI, signal intensity; ↓, low signal intensity; ↑, high signal intensity

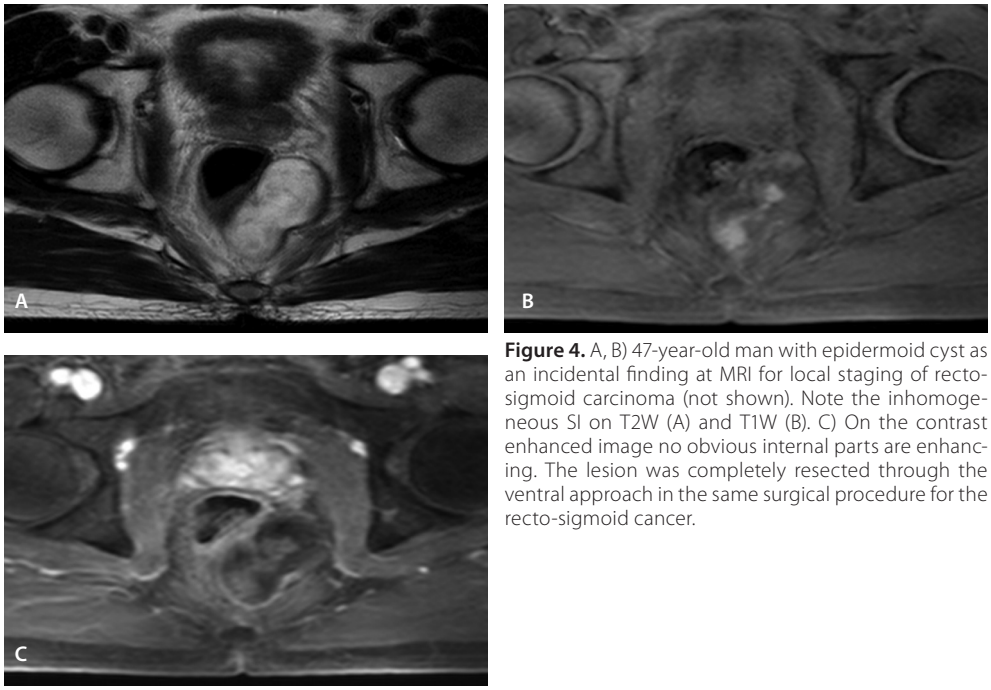

Figure 4. A, B) 47-year-old man with epidermoid cyst as an incidental finding at MRI for local staging of recto-sigmoid carcinoma (not shown). Note the inhomogeneous SI on T2W (A) and T1W (B). C) On the contrast enhanced image no obvious internal parts are enhancing. The lesion was completely resected through the ventral approach in the same surgical procedure for the recto-sigmoid cancer.

See table 2 for imaging findings. Only one lesion was found with erosion of the sacrococyygeal bone. Management: 12 patients (15 lesions) had undergone surgery. One patient was managed conservatively with follow up MRI. Clinical follow up for all lesions ranged 1 to 6 years: two patients had a local recurrence after surgery. Patient with conservative management (n=1) demonstrated unchanged lesion at 3 years follow up MRI.

Epidermoid and dermoid cysts

There were 5 patients (18%) with epidermoid cysts; 4 cases were incidental findings on previous imaging and one case was referred with a recurrent lesion 4 years after surgical drainage. Lesion level according to the sacrococcygeal spine was SL 4 - CL (n=1), CL (n=4). Four lesions were attached to the presacral fascia and located in the midline above the levator ani muscle. One lesion was attached to the distal tip of coccygeal bone with a proximal paramedian extension within the mesorectum. All lesions were unilocular with heterogeneous SI (Fig 4). Management: 3 patients had undergone surgery and 2 patients were managed conservatively. Clinical follow up was 1 to 6 years with no recurrence after surgery and unchanged lesions (conservative management).

Another patient had a recurrent mature cystic dermoid with carcinoid, 10 years after resection of a pelvic dermoid cyst (Fig 5 A,B). This lesion was detected on screening ultrasound with no specific symptoms. The lesion was attached to the presacral fascia, located in the midline at SL 1 – SL 4 level. Surgical resection was radical. Five years after surgery a solitary liver metastasis was found. Two years after liver metasectomy no recurrence (pelvic or liver) and no metastasis were found.

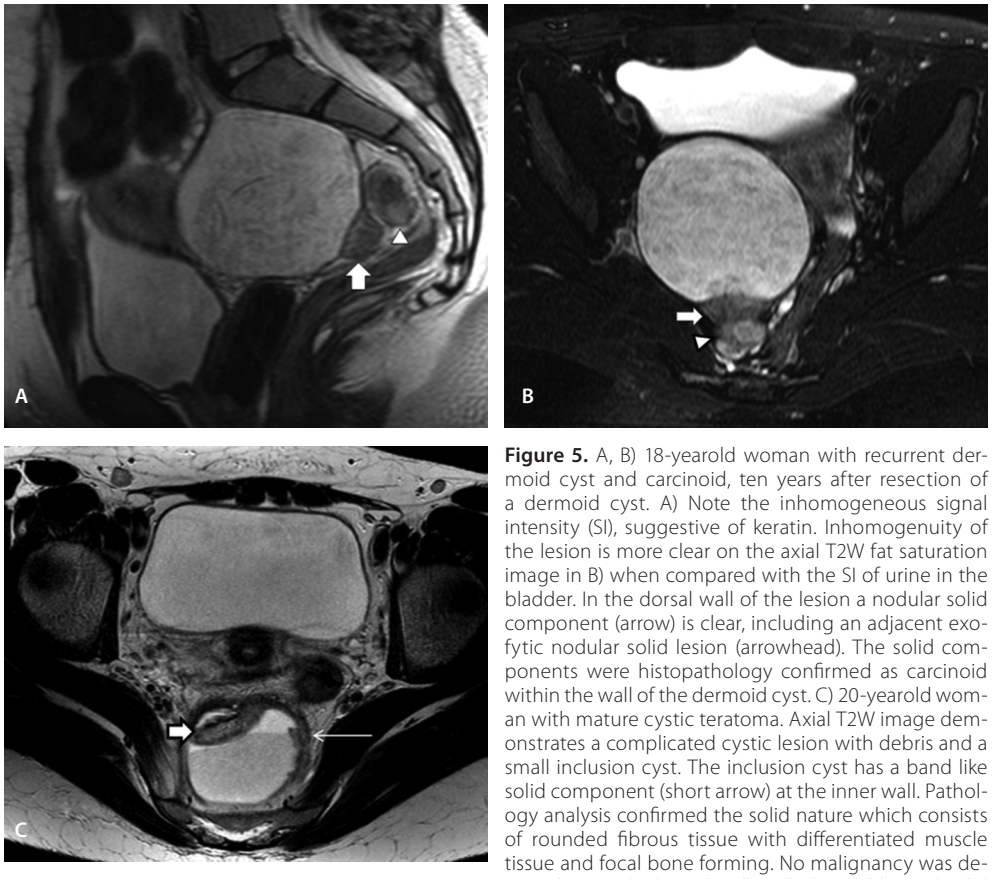

Figure 5. A, B) 18-yearold woman with recurrent dermoid cyst and carcinoid, ten years after resection of a dermoid cyst. A) Note the inhomogeneous signal intensity (SI), suggestive of keratin. Inhomogenuity of the lesion is more clear on the axial T2W fat saturation image in B) when compared with the SI of urine in the bladder. In the dorsal wall of the lesion a nodular solid component (arrow) is clear, including an adjacent exofytic nodular solid lesion (arrowhead). The solid components were histopathology confirmed as carcinoid within the wall of the dermoid cyst. C) 20-yearold woman with mature cystic teratoma. Axial T2W image demonstrates a complicated cystic lesion with debris and a small inclusion cyst. The inclusion cyst has a band like solid component (short arrow) at the inner wall. Pathology analysis confirmed the solid nature which consists of rounded fibrous tissue with differentiated muscle tissue and focal bone forming. No malignancy was detected. Note thickened wall, including additional solid components at de inner wall on the left (long arrow).

Teratoma

We found two patients (7%) with benign mature cystic teratomas. One lesion was initially clinically suspected of a presacral abscess (Fig 5 C). The other lesion was an incidental finding at MRI for local staging of rectal carcinoma. Both lesions were surgically resected. Lesion level: SL 2 - CL and SL 4 - CL. Both lesions were attached to the presacral fascia and located in the midline supralevatoir. Follow up MRI at respectively 2 and 5 years post- surgery revealed no local recurrence. Another patient (4%) presented with a presacral abscess, including a recurrent mature cystic teratoma. This patient had undergone resection of a teratoma in another hospital 10 years earlier. After successful percutaneous drainage of the current abscess, CT- guided targeted biopsies aimed at the wall and solid tissue component followed. Patient refused surgery and agreed to biopsy to exclude malignancy. Lesion level: SL 3 - CL; attached to the presacral fascia and located in the midline supralevatoir. The lesion was stable for 7 years when compared with a previous MRI.

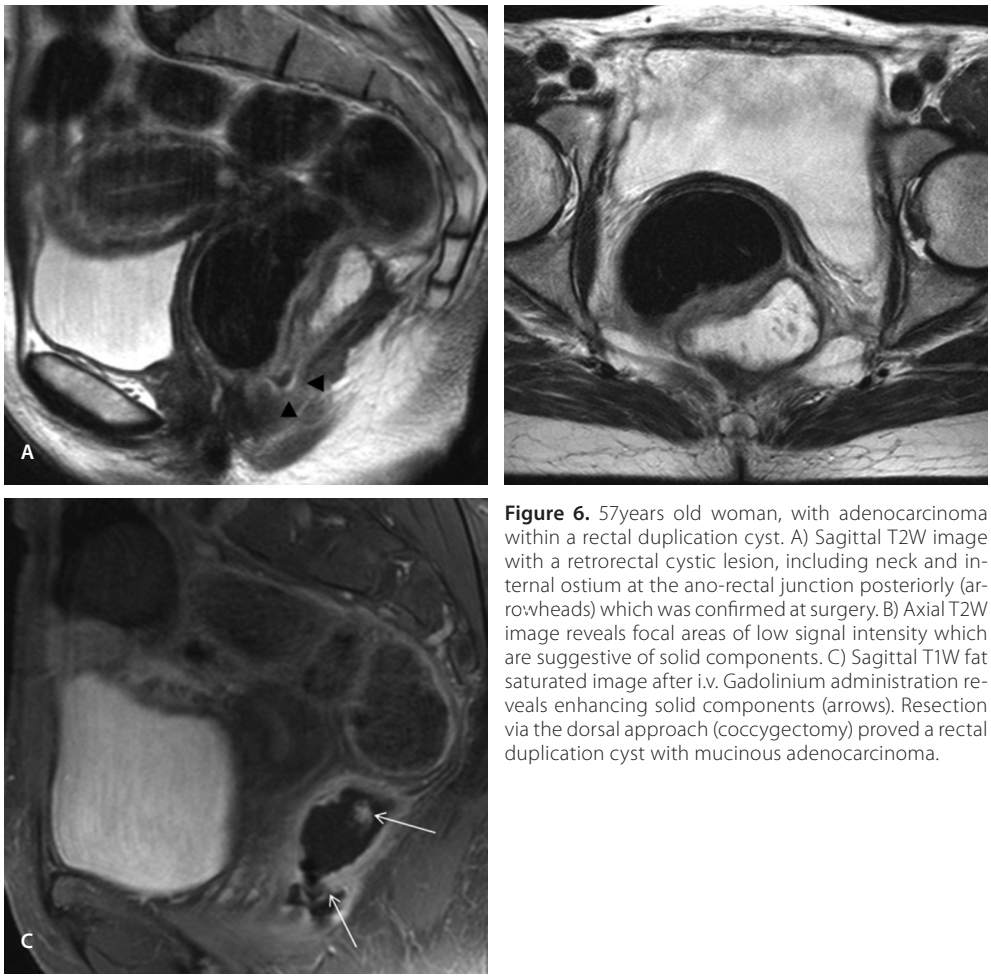

Figure 6. 57years old woman, with adenocarcinoma within a rectal duplication cyst. A) Sagittal T2W image with a retrorectal cystic lesion, including neck and internal ostium at the ano-rectal junction posteriorly (arrowheads) which was confirmed at surgery. B) Axial T2W image reveals focal areas of low signal intensity which are suggestive of solid components. C) Sagittal T1W fat saturated image after i.v. Gadolinium administration reveals enhancing solid components (arrows). Resection via the dorsal approach (coccygectomy) proved a rectal duplication cyst with mucinous adenocarcinoma.

Colorectal lesions

We found two patients (7 %) with rectal duplication cyst, one benign and one with mucinous adenocarcinoma. Both lesions were incidental findings on previous imaging and were located within the mesorectum, with a median orientation at the coccygeal level. Both lesions were resected. The benign lesion showed no recurrence for 2 years. The malignant lesion was incompletely resected with additional radiotherapy (50 Gy) on the pelvis (Fig 6). Follow up MRI at 6 months interval revealed no local recurrence for 8 years. Another patient had a mucinous adenocarcinoma of rectal origin (Fig 7). At screening colonoscopy an asymptomatic ulcerated lesion was found in the lower rectum. Biopsy revealed a mucinous adenocarcinoma. MRI demonstrated a retrorectal cystic lesion with substantial growth after neo-adjuvant chemo radiotherapy. The lesion was resected with additional intra-operative radiotherapy on resected surfaces. Histopathology confirmed a cT3N0M0 mucinous type adenocarcinoma of rectal origin. Lesion level: SL 4 – CL with a median orientation. Follow up one year after surgery revealed no local recurrence and no distant metastasis. A fourth

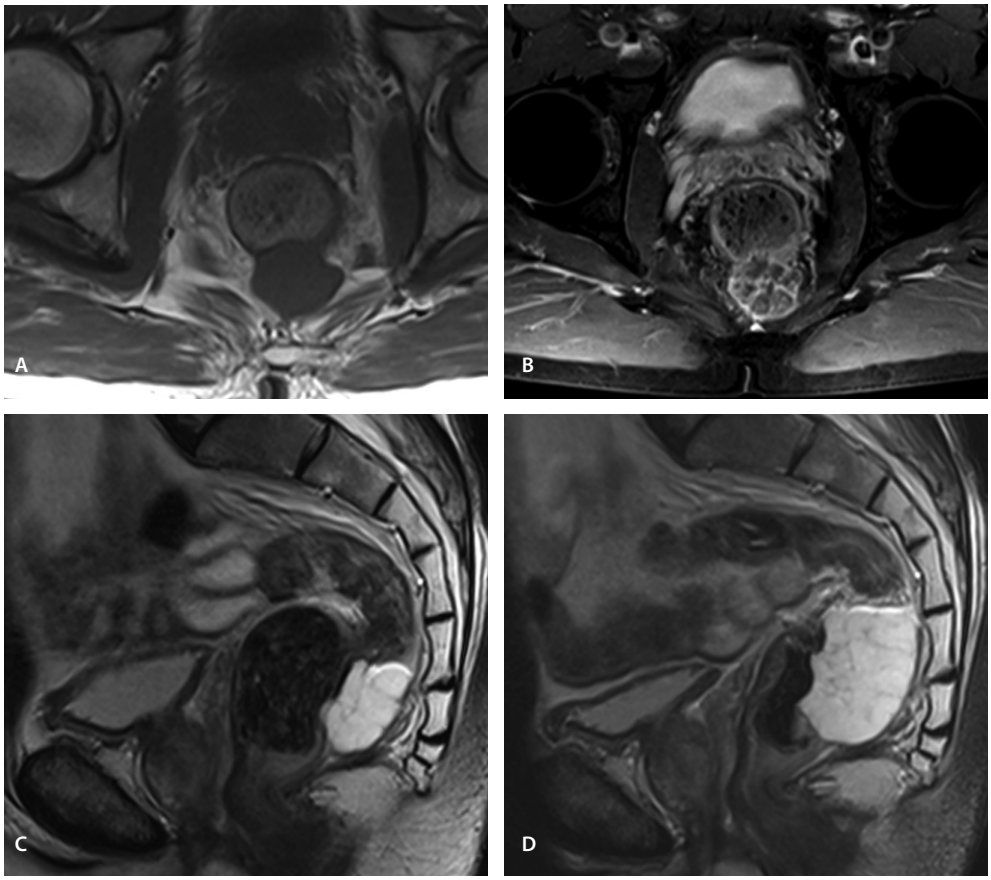

Figure 7. 59year-old man with a mucinous type adenocarcinoma of the lower rectum. A-C) A, axial T1W image; B, axial T1W fat saturation image after i.v. Gadolinium administration; C) Sagittal T2W image. At initial presentation the lesion has a cystic aspect with thick enhancing strands (B). D) Sagittal T2W image after 10 months. The lesions showed progressive increase in size with involved circumferential resection margins dorsally after neo adjuvant chemoradiotherapy.

5.2

patient had a subperitoneal mucinous adenocarcinoma from colorectal origin (Fig 8). This patient had Hirschsprung's disease and was operated at the age of 3 years with repeat surgery at age 26 (rectum resection and ano-colic anastomosis). Lesion level: SL 4 – CL, above the pelvic floor (supralevatoir) with a rounded orientation. The lesion was incompletely resected with no malignancy found. Follow up MRI at16 months demonstrated a growing recurrence. Re- resection, including frozen section pathology analysis, demonstrated a mucinous adenocarcinoma probably originating from the distal colonic stump. Patient was referred initially with obstructed defecation (Fig 8A) and died 18 months after repeat surgery and palliative treatment.

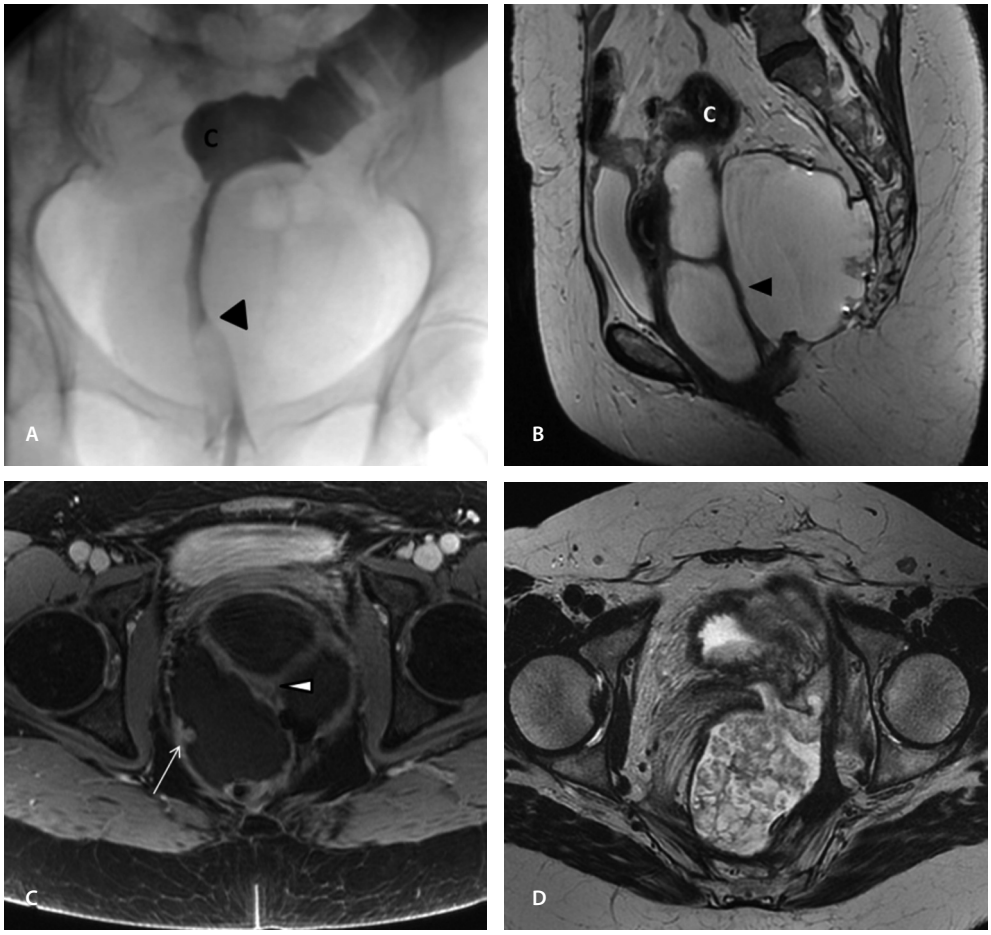

Figure 8. 50-yearold woman with subperitoneal mucinous adenocarcinoma from colorectal origin, after rectum resection and colonic-anal anastomosis 25 years ago. A) Barium enema image for evaluation of obstructed defeacation reveals an elongated stenotic aspect at the anastomotic level (arrowhead). B) Sagittal T2W MR image demonstrates a large multiloculated cystic lesion wrapped around the elongated stenotic anastomosis (arrowhead), including suggestion of solid nodular component in the dorsal wall of the lesion. C) Axial T1W fat saturated image after iv Gadolinium administration reveals the central position of compressed lumen (arrowhead), including solid enhancing nodular component in the wall (arrow). D) Axial T2W FSE: Local recurrence with increased solid content within the cyst proved a mucinous adenocarcinoma originating from the stump of the colonic-anal anastomosis. C: colon (most distal part).

Neurogenic lesions

We found one patient with anterior sacral meningocoele and Curanino syndrome. The lesion was an incidental finding. Lesion level: SL 2 – CL, including hemi-aplasia of the sacral bone below the S2 level. Curanino Syndrome was clinically confirmed. Clinical follow up 3 years after MRI revealed no indication for repeat imaging or specific treatment.

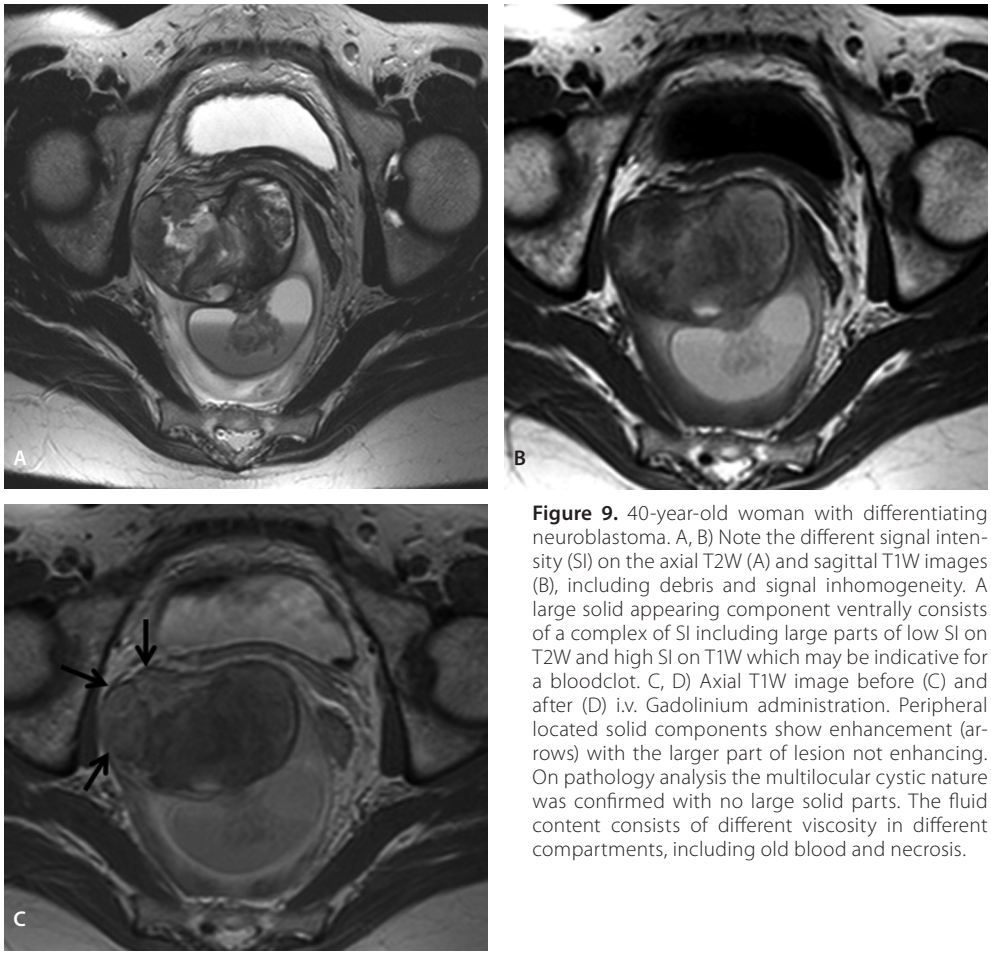

Figure 9. 40-year-old woman with differentiating neuroblastoma. A, B) Note the different signal intensity (SI) on the axial T2W (A) and sagittal T1W images (B), including debris and signal inhomogeneity. A large solid appearing component ventrally consists of a complex of SI including large parts of low SI on T2W and high SI on T1W which may be indicative for a bloodclot. C, D) Axial T1W image before (C) and after (D) i.v. Gadolinium administration. Peripheral located solid components show enhancement (arrows) with the larger part of lesion not enhancing. On pathology analysis the multilocular cystic nature was confirmed with no large solid parts. The fluid content consists of different viscosity in different compartments, including old blood and necrosis.

Another patient had differentiating neuroblastoma (Fig 9). This patient presented with acute abdominal pain in the lower abdomen at the emergency ward. Initial CT scan and subsequent MRI revealed a complicated cystic tumor, including findings suggested of intracystic hemorrhage. The lesion was attached to the presacral fascia with a median orientation from SL 2 – CL. Surgery followed with marginal resection margins. Two years post- surgery local recurrence and metastases to the lumbosacral spine were evident on MRI. Palliative treatment with chemotherapy and consolidation radiotherapy followed. Five years later marginal growth of the metastases was seen.

DISCUSSION

In the current literature retrorectal cystic lesions (RCL) are often categorized into congenital, inflammatory, neurogenic, osseous, and miscellaneous (6,7). The basic clinical problem, however, is whether a RCL is to be considered malignant and what are the imaging characteristics that suggest malignancy. Our study tries to answer these questions. We found 18 % of the patients to present with a malignant lesion. Other studies that evaluated all (solid and cystic) primary lesions in the retrorectal space reported 43 % in 120 patients, 48 % in 45 patients and 50 % in 42 patients to be malignant (1,6,8). These relative high percentages of malignancy are obviously due to the contribution of solid lesions. To the best of our knowledge, our study is the first to evaluate exclusively RCL with MRI. Hjermstad et al. found 1 malignant lesion in 53 patients with tailgut cysts (TGC) (9). Mathis et al. found 4 malignant lesions (13 %) in 31 patients with TGC (10). Although in our series no malignancy was found in 16 TGC, case reports of malignancy in TGC are consistent with findings of solid tissue component in the wall of the lesion on MRI (11-13).

Key findings on MRI for the differentiation between malignant and benign lesions are described in table 3. The most important finding to suggest malignancy is solid tissue component. We found solid tissue components in all (100%) malignant lesions. Only 2 (8%) of benign lesions had solid components, both teratomas. Teratoma may exhibit solid components, but without malignancy (Fig 5). On the other hand, teratomas are real neoplasms and should be considered and approached as malignant lesions (14). Wall thickening was found in 2 (40 %) malignant and in 3 (12%) of benign lesions. A thickened wall may also be a sign of secondary inflammation and a cause for pain symptoms and not exclusively associated with malignancy (9). The subgroup from colorectal origin had the highest percentage (3 of 4, 75 %) of malignancy. Few case reports of rectal duplication cyst with malignancy were found in the literature (15). In addition, we found one case of mucinous adenocarci-

Table 3 MRI Findings of Primary Cystic lesions of the Retrorectal Space Subdivided into Malignant and Benign Lesions

MRI feature	malignant (n=5)	benign (n=26)
Unilocular	4 (80%)	10 (38%)
Multilocular	1 (20%)	16 (62%)
Max size (range)	5.5-13.5 cm	2-17 cm
Debris	1 (20%)	4 (15 %)
Septa	2 (40%)	15 (58 %)
Solid component	5 (100 %)	2 (8%)
Wall Thickening (> 5 mm)	2 (40 %)	3 (12 %)
SI T1W/T2W	↓/↑ 4 (80 %)	↓/↑ 15 (58 %)
	↑/↑ 1 (20 %)	↑/↑ 7 (27 %)
		↑/↓ 4 (15 %)

SI, signal intensity; ↓, low signal intensity; ↑, high signal intensity

noma of the rectum, presenting as a retrorectal cystic lesion (Fig 7). This is an extra-ordinary presentation of rectal carcinoma of which no separate reports were found in de literature. Furthermore, one case of subperitoneal pelvic mucinous adenocarcinoma was found. To our knowledge, only one similar case was described in the literature so far of subperitoneal pelvic adenomucinosis (16). Our case, however, is a mucinous adenocarcinoma that was confirmed at repeat surgery. The difference in imaging features of the initial and the recurrent lesion are striking and may reflect the pathology findings (Fig 8). MR imaging of the remaining malignant lesions (dermoid with carcinoid) and differentiating neuroblastoma were not reported in the literature to our knowledge. Another point to stress is that malignancy can occur in RCL at relative young age. In five patients with malignancy, two were respectively 18 and 40 years. Most patients in our study group were asymptomatic, this is consistent with reports from the literature (5). Symptoms are often due to mechanical problems from large lesions or secondary infection (7). Treatment of choice is surgery. This can be through the ventral, posterior or combined approach. Lusanoff et al. presented a practical classification of RCL to guide proper surgery (17). The multiplanar capabilities of MRI enables the lesion to be demonstrated in relation to the surgical plane. On the other hand, surgery of the retrorectal space is prone to complications (8,18). We believe that whenever surgery is relatively contraindicated, then regular follow up MRI is the best approach. Evolution of the lesion with emerging solid tissue component and wall thickening may be a way to reconsider treatment.

Our study has some limitations; first because of the retrospective analysis. Second, because of the relative small number of patients. We are, however, dealing with rare lesions of which some were not previously described in the literature using MRI. Not all patients were imaged with a uniform MRI protocol, still we believe that all necessary imaging sequences were available, including contrast enhanced series in all but one lesion for a decent morphological analysis. Furthermore, it would be interesting to see whether diffusion weighted imaging (DWI) and apparent diffusion coefficient (ADC) can differentiate between benign and malignant lesions. Not all patients in our study group had DWI so this was left out of evaluation. DWI and ADC seem especially important to differentiate cystic from non-cystic lesions as the SI from RCL may be variable as was indicated in table 2. Future studies may be needed to evaluate the added value of DWI and ADC for characterizing RCL.

In conclusion, retrorectal cystic lesions (RCL) represent a broad diversity of lesions. Our study has demonstrated that 18 % of patients with RCL have a malignant lesion with MRI findings of solid tissue component indicative of malignancy.

5.2

REFERENCES

1. Lev-Chelouche D, Gutman M, Goldman G, et al. Presacral tumors: a practical classification and treatment of a unique and heterogeneous group of diseases. Surgery 2003;133(5):473-478.
2. Neale JA. Retrorectal tumors. Clin Colon Rectal Surg 2011;24(3):149-160.
3. Glasgow SC, Dietz DW. Retrorectal tumors. Clin Colon Rectal Surg 2006;19(2):61-68.
4. Chen N, Min PQ, Liu ZY, Wu B, Yang KQ, Lu CY. Radiologic and anatomic study of the extraperitoneal space associated with the rectum. AJR American Journal of Roentgenology 2010;194(3):642-652.
5. Bullard Dunn K. Retrorectal tumors. Surg Clin North Am 2010;90(1):163-171, Table of Contents.
6. Hobson KG, Ghaemmaghami V, Roe JP, Goodnight JE, Khatri VP. Tumors of the retrorectal space. Dis Colon Rectum 2005;48(10):1964-1974.
7. Singer MA, Cintron JR, Martz JE, Schoetz DJ, Abcarian H. Retrorectal cyst: a rare tumor frequently misdiagnosed. Journal of the American College of Surgeons 2003;196(6):880-886.
8. Wang JY, Hsu CH, Changchien CR, et al. Presacral tumor: a review of forty-five cases. Am Surg 1995;61(4):310-315.
9. Hjermstad BM, Helwig EB. Tailgut cysts. Report of 53 cases. Am J Clin Pathol 1988;89(2):139-147.
10. Mathis KL, Dozois EJ, Grewal MS, Metzger P, Larson DW, Devine RM. Malignant risk and surgical outcomes of presacral tailgut cysts. Br J Surg 2010;97(4):575-579.
11. Tampi C, Lotwala V, Lakdawala M, Coelho K. Retrorectal cyst hamartoma (tailgut cyst) with malignant transformation. Gynecol Oncol 2007;105(1):266-268.
12. Lim KE, Hsu WC, Wang CR. Tailgut cyst with malignancy: MR imaging findings. AJR American Journal of Roentgenology 1998;170(6):1488-1490.
13. Prasad AR, Amin MB, Randolph TL, Lee CS, Ma CK. Retrorectal cystic hamartoma: report of 5 cases with malignancy arising in 2. Arch Pathol Lab Med 2000;124(5):725-729.
14. Miles RM, Stewart GS, Jr. Sacrococcygeal teratomas in adult. Ann Surg 1974;179(5):676-683.
15. Springall RG, Griffiths JD. Malignant change in rectal duplication. J R Soc Med 1990;83(3):185-187.
16. Dahan H, Arrive L, Wendum D, Docou le Pointe H, Djouhri H, Tubiana JM. Retrorectal developmental cysts in adults: clinical and radiologic-histopathologic review, differential diagnosis, and treatment. Radiographics 2001;21(3):575-584.
17. Losanoff JE, Sauter ER. Retrorectal cysts. Journal of the American College of Surgeons 2003;197(5):879-880.
18. Bohm B, Milsom JW, Fazio VW, Lavery IC, Church JM, Oakley JR. Our approach to the management of congenital presacral tumors in adults. Int J Colorectal Dis 1993;8(3):134-138.

chapter 6

Interlude

El Tatio Geiser Valley, Atacama Desert, Chile.
Photography: Roy Dwarkasing©

chapter 7

General Discussion & Summary

Samenvatting

SUMMARY & GENERAL DISCUSSION

Studies have shown that preoperative MR imaging revealed important additional information compared with surgery alone and better predicts clinical outcome of patients with fistula-in-ano than initial surgical exploration (1). Anovaginal fistula is a socially disabling disease in which patients pass gas and feces through the vagina and experience recurrent vaginal infections. In our study of 20 patients, anovaginal fistulas were identified on T2-weighted MR images as predominantly high-signal-intensity linear abnormalities extending between the anal canal and the vagina. The internal opening in the anal canal was detected in all patients. The internal opening in the vagina was detected in 19 (95%) patients. In seven (35%) patients, additional abnormalities were found, including abscesses within the rectovaginal septum, additional perianal fistulas and defects of the external anal sphincter. History of obstetric trauma, pelvic floor surgery, or Crohn disease was present in 10 (50%) patients. These patients had more complex fistulas compared with patients without relevant medical history. Previously, other authors stated that obstetric injury and Crohn disease are important causes for anovaginal fistula(2, 3). In all patients, the anovaginal fistulas were depicted to their full extent. Complete mapping of the fistula with extensions, abscesses, and sphincter damage is important in the preoperative work-up of the patient and may improve treatment (1), (4).

The treatment of cryptoglandular fistulas is mainly surgical, with a number of options. Preservation of fecal continence is a paramount consideration, and treatment strategies aim to preserve the integrity of the external sphincter. Fistulotomy, fistulectomy, drain placement, advancement flap closure, and fecal deviating colostomy are common techniques for fistula surgery (5). Perianal fistulas passing through the upper or middle third of the external anal sphincter present a challenge to many surgeons. Transanal advancement flap repair provides a useful tool in the treatment of these fistulas. It enables the healing of the fistula without damage of the external sphincter and consequent fecal incontinence. Initially, the reported healing rates varied between 84 and 100% (6, 7). However, during the past decade it has become clear that transanal advancement flap repair fails in 1 of 3 patients (8, 9). In our study of 157 patients who had undergone transanal advancement flap repair, posterior fistulas were identified in 119 patients (76%). Anterior fistulas were observed in 23% of the patients. Associated abscesses were found in 47% of the posterior fistulas and in 5% of the anterior fistulas. The healing rate of fistulas with a direct course (traversing the external anal sphincter in a direct course to the external opening) was significantly lower than the healing rate of fistulas with a classic or intersphincteric horseshoe extension. Once adequately drained, the abscesses did not affect the outcome of transanal advancement flap repair. Concordance between surgical findings and MR images was very high. The most striking finding of our study is the poor outcome after flap repair in patients with a high transsphincteric fistula, and a direct course to the external opening. This finding is difficult to explain and has not been described before. It might be possible that both anterior and posterior fistulas with a direct course represent a more aggressive form of perianal fistulous disease. Another finding of the present study is the high prevalence of associated abscesses, especially in high transsphincteric fistulas with their internal opening at the posterior midline. Most of these abscesses could not be detected by physical examination. Although some of these abscesses presented a rather complex and bizarre course above the pelvic floor, they all could be detected and drained because of preoperative MR imaging. Endoanal MR imaging provides a useful tool for the visualization of these abscesses, enabling adequate drainage.

The efficacy of MRI in the evaluation of chronic anal and perianal pain is shown in the identification of suppurative lesions in 27% of all (n=103) patients in our study. This is an important finding, and these patients will benefit from surgery. Although we found lesions in other locations, most suppurative lesions were located dorsally in the intersphincteric space, which may reflect the higher anatomic prevalence of posterior location of anal glands (10). It can be assumed that the internal opening of fistulas and abscesses was obstructed, probably by granulation tissue. This may have prohibited drainage of these lesions in the anal lumen, explaining their clinically occult status with pain as the only presentation. In addition, significantly more abscesses were found in patients with a history of surgery for anorectal disease, which may be explained by the more severe iatrogenic infectious mechanism. The second most common abnormality encountered at MRI was scarring of anal sphincter muscles. In addition, the diagnosis of unspecified functional anorectal pain can be made with considerable certainty when no abnormalities can be established with either clinical workup or MRI. Using MRI, we were able to identify lesions in 39% of patients with chronic anal and perianal pain, for whom a standard clinical workup had failed to reveal abnormalities. MRI is therefore a recommended constituent of the workup of these patients before their symptoms are considered part of a functional gastrointestinal disorder.

Dedicated MRI tailored to patient symptoms and clinical findings has the potential to map morphologic alterations and facilitate appropriate treatment in female patients with lower urinary tract symptoms (LUTS). In our cohort of 60 clinical patients with LUTS, 20 patients (33%) had urethral diverticula and 28 (47%) had an alternative diagnosis, of which 13 (46%) were visualized with MRI. In the remaining 12 patients (20%) no abnormalities were found. Other studies reported urethral diverticula in 10% of patients examined with endorectal coil MRI. The rigid endoluminal coil, that was used in our study, can be inserted into the vagina by the patient herself, and there is no need for administration of glucagon or butylbromide to prevent rectal spasm, which could be the case when using the inflatable endoluminal coil (11). Few studies have focused on the differential diagnosis of patients with urethral diverticula. In the differential diagnosis, one should also consider other regional cystic lesions. Visualization of communication between the lesion and the urethra confirms urethral diverticula (12). The differentiation between a communicating or non- communicating cystic lesion with the urethra is important because the surgical approach for the two entities differs. Both lesions are resected; however, a diverticulum may require urethral reconstruction procedures (12-14). To our knowledge, our study is the first to identify the ostium of urethral diverticula in the majority of cases (85%) on MRI with improved confidence using the rigid endoluminal coil rather than the pelvic phased-array coil. In our study, MRI showed the final diagnosis (urethral diverticula or alternative diagnosis) in 33 of 60 patients (55%). Based on MRI, clinical workup, including functional urodynamic studies, and clinical data, 80% of patients were diagnosed with an abnormality that was responsible for their complaints. According to these findings, in the diagnostic workup of women with suspicion of urethral diverticula, both MRI and urodynamic studies, should be considered.

In our study of 47 patients with locally recurrent rectal cancer (LRRC), a total of 51 lesions were evaluated. The results show that contrast enhanced MRI (CEMRI) is a valuable supplement in the MRI protocol for diagnosis and pre- operative evaluation of LRRC. LRRC has typical CEMRI findings of arterial and persistent enhancement (100%), dominant peripheral rim- or heterogeneous mosaic enhancement pattern (80%), and is more consistent for evaluation of tumor dimension than T2W MRI. For surgical outcome, tumor fixation to pelvic walls or presacral fascia will result in incomplete resection margins in 64% of cases, whereas non fixed tumors will be completely resected in 87%. It should be noted that immature

fibrosis and inflammation may demonstrate high signal intensity on T2W, and may demonstrate contrast enhancement (15). However, the CEMRI characteristics found in our study may be supportive to diagnose LRRC and differentiate from fibrosis. To our knowledge, our study is the first to assess a combination of typical CEMRI characteristics. Another potential for CEMRI in the management of LRRC is monitoring of local image guided therapies like radio frequency ablation. In our experience CEMRI is less effected by post procedural effects than T2W and DWI to confidently demonstrate local residual or recurrent disease. Future studies are needed to present evidence for this. Our results show that tumor fixation to the pelvic walls or presacral fascia is of importance to predict surgical outcome, with an incomplete resection margin in the majority of cases (64%), in contrary to non-fixed lesions (13%). To our knowledge, our study is the first MRI based study for LRRC that endorses these clinical results. In our center intra-operative radiotherapy will be applied on the resected surface in case of tumor fixation to the pelvic walls or presacral fascia (16, 17).

We evaluated 28 patients with 31 retrorectal cystic lesions (RCL). Lesions were subdivided into 5 groups: tailgut cyst, epidermoid and dermoid cyst, teratoma, colorectal origin, neurogenic origin. Tailgut cyst was the most prevalent (16/31, 52 %) lesion. Five patients had malignancy (18%); on lesion level 5 out of 31 were malignant (16%) with MRI findings of solid tissue components (100 %) most suggestive of malignancy. To the best of our knowledge, our study is the first to evaluate RCL as a separate group of lesions with MRI. We found solid tissue components in all (100%) of malignant lesions. Only 2 (8%) of benign lesions had solid tissue components, both teratomas. Teratoma may exhibit solid tissue components, but without malignancy. On the other hand, teratoma are real neoplasms and should be considered and approached as a malignant lesion (18). Wall thickening was found in 2 (40 %) malignant lesions. A thickened wall may also be a sign of secondary inflammation and a cause for pain symptoms (19). Another point to stress is that malignancy can occur in RCL at relative young age. In the five patients with malignancy, two were respectively 18 and 40 years. Most patients in our study group were asymptomatic, this is consistent with reports from the literature (20). Symptoms are often due to mechanical problems from large lesions or secondary infection (21). The treatment of choice is surgery. This can be through the ventral, posterior or combined approach. The multiplanar capabilities of MRI enables the lesion to be demonstrated in relation to the surgical plane. On the other hand, surgery of the retrorectal space is prone to complications (22, 23). We believe that whenever surgery is relatively contra- indicated, then regular follow up MRI is the best approach. Evolution of the lesion with emerging solid tissue component and wall thickening may be a way to reconsider treatment.

Future perspective

In theory, a further increase in SNR of the current endoluminal coil applied in some of studies may be achieved by applying four loops rather than two of the current generation of the endoluminal pelvic coil. By arranging the four elements two by two in series the SNR could be increased without suffering loss of field homogeneity in the radial direction. Less decrease in SNR at increasing distance from the coil could also be expected when compared to the dual loop configuration. Currently a version is being studied for endorectal application, including use of flexible material to adjust for the anorectal angle. Coupling of the endoluminal coil to an external receiver coil array may further increases the volume to be imaged. For this configuration proper matching and tuning of all components (endoluminal-, external coil and MR system) is required. For prostate imaging this configuration, using a single loop coil, resulted in significant improvement of anatomic details, extracapsular extension accuracy and specificity (24). We believe that stepwise technical improvements should be pursued based on clinical need.

With the emergence of novel surgical treatments for perianal fistula disease like MRI-guided surgery, laser, and adhesive treatments, MR imaging is a mainstay for preprocedural and intraoperative evaluation to ensure the adequacy of the procedure. The use of laser ablation or fibrin glue to treat fistula seems attractive, especially in more complex fistulas (25, 26). There are promising reports of human granulocyte colony-stimulating factor, as an alternative to fibrin glue in the treatment of perianal Crohn's fistula (27). MRI-guided surgery for anal fistula is feasible. Pre-procedural and intraoperative MRI techniques can be used to identify the extent of the fistula tracts and septic foci and to ensure the adequacy of the surgical procedure.

Dedicated MRI of the pelvis and pelvic floor should play an important role in the work up of patents with clinical occult pelvic pain. Currently, eligible patients undergo an adapted MRI protocol based on clinical presentation and findings and are discussed within the institutional board for Diseases of the Pelvis and Pelvic Floor. In addition, new developments in functional and molecular imaging are promising to identify specific biomarkers of pain and may indicate the precise focus and possible cause for pain. A joint effort with collaborating clinical partners should lead to a build- up of expertise and insights in pelvic pain and guide proper management.

Conclusion

This thesis demonstrates the value of dedicated MRI, mostly with application of a rigid endoluminal coil, for these complex, often disabling and difficult to diagnose diseases. Dedicated MRI of the pelvis and pelvic floor will facilitate accurate diagnosis, map lesions in relation to anatomic structures and guide appropriate treatment. In case of surgery, MRI is therefore a recommended tool for pre- surgical planning and prevention of recurring disease.

REFERENCES

1. Lunniss PJ, Armstrong P, Barker PG, Reznek RH, Phillips RK. Magnetic resonance imaging of anal fistulae. Lancet 1992; 340:394-396.
2. Hull TL, Fazio VW. Surgical approaches to low anovaginal fistula in Crohn's disease. Am J Surg 1997; 173:95-98.
3. Senatore PJ, Jr. Anovaginal fistulae. Surg Clin North Am 1994; 74:1361-1375.
4. Beets-Tan RG, Beets GL, van der Hoop AG, et al. Preoperative MR imaging of anal fistulas: Does it really help the surgeon? Radiology 2001; 218:75-84.
5. Seow C, Phillips RK. Insights gained from the management of problematical anal fistulae at St. Mark's Hospital, 1984-88. Br J Surg 1991; 78:539-541.
6. Wedell J, Meier zu Eissen P, Banzhaf G, Kleine L. Sliding flap advancement for the treatment of high level fistulae. Br J Surg 1987; 74:390-391.
7. Aguilar PS, Plasencia G, Hardy TG, Jr., Hartmann RF, Stewart WR. Mucosal advancement in the treatment of anal fistula. Dis Colon Rectum 1985; 28:496-498.
8. van Koperen PJ, Wind J, Bemelman WA, Bakx R, Reitsma JB, Slors JF. Long-term functional outcome and risk factors for recurrence after surgical treatment for low and high perianal fistulas of cryptoglandular origin. Dis Colon Rectum 2008; 51:1475-1481.
9. Zimmerman DD, Delemarre JB, Gosselink MP, Hop WC, Briel JW, Schouten WR. Smoking affects the outcome of transanal mucosal advancement flap repair of trans-sphincteric fistulas. Br J Surg 2003; 90:351-354.
10. Gupta PJ. A study of suppurative pathologies associated with chronic anal fissures. Tech Coloproctol 2005; 9:104-107.
11. Lorenzo AJ, Zimmern P, Lemack GE, Nurenberg P. Endorectal coil magnetic resonance imaging for diagnosis of urethral and periurethral pathologic findings in women. Urology 2003; 61:1129-1133; discussion 1133-1124.
12. Hahn WY, Israel GM, Lee VS. MRI of female urethral and periurethral disorders. AJR Am J Roentgenol 2004; 182:677-682.
13. Rovner ES, Wein AJ. Diagnosis and reconstruction of the dorsal or circumferential urethral diverticulum. J Urol 2003; 170:82-86; discussion 86.
14. Fortunato P, Schettini M, Gallucci M. Diagnosis and therapy of the female urethral diverticula. Int Urogynecol J Pelvic Floor Dysfunct 2001; 12:51-57.
15. Lavini C, de Jonge MC, van de Sande MG, Tak PP, Nederveen AJ, Maas M. Pixel-by-pixel analysis of DCE MRI curve patterns and an illustration of its application to the imaging of the musculoskeletal system. Magn Reson Imaging 2007; 25:604-612.
16. Ferenschild FT, Vermaas M, Nuyttens JJ, et al. Value of intraoperative radiotherapy in locally advanced rectal cancer. Dis Colon Rectum 2006; 49:1257-1265.
17. Rodriguez-Bigas MA, Chang GJ, Skibber JM. Multidisciplinary approach to recurrent/unresectable rectal cancer: how to prepare for the extent of resection. Surg Oncol Clin N Am 2010; 19:847-859.
18. Miles RM, Stewart GS, Jr. Sacrococcygeal teratomas in adult. Ann Surg 1974; 179:676-683.
19. Hjermstad BM, Helwig EB. Tailgut cysts. Report of 53 cases. Am J Clin Pathol 1988; 89:139-147.
20. Bullard Dunn K. Retrorectal tumors. Surg Clin North Am 2010; 90:163-171, Table of Contents.
21. Singer MA, Cintron JR, Martz JE, Schoetz DJ, Abcarian H. Retrorectal cyst: a rare tumor frequently misdiagnosed. J Am Coll Surg 2003; 196:880-886.
22. Bohm B, Milsom JW, Fazio VW, Lavery IC, Church JM, Oakley JR. Our approach to the management of congenital presacral tumors in adults. Int J Colorectal Dis 1993; 8:134-138.
23. Wang JY, Hsu CH, Changchien CR, et al. Presacral tumor: a review of forty-five cases. Am Surg 1995; 61:310-315.
24. Futterer JJ, Engelbrecht MR, Jager GJ, et al. Prostate cancer: comparison of local staging accuracy of pelvic phased-array coil alone versus integrated endorectal-pelvic phased-array coils. Local staging accuracy of prostate cancer using endorectal coil MR imaging. Eur Radiol 2007; 17:1055-1065.

25. Bodzin JH. Laser ablation of complex perianal fistulas preserves continence and is a rectum-sparing alternative in Crohn's disease patients. Am Surg 1998; 64:627-631; discussion 632.
26. Lindsey I, Smilgin-Humphreys MM, Cunningham C, Mortensen NJ, George BD. A randomized, controlled trial of fibrin glue vs. conventional treatment for anal fistula. Dis Colon Rectum 2002; 45:1608-1615.
27. Vaughan D, Drumm B. Treatment of fistulas with granulocyte colony-stimulating factor in a patient with Crohn's disease. N Engl J Med 1999; 340:239-240.

SAMENVATTING

MRI spoelen in het kleine bekken

Er zijn 2 soorten MRI signaal ontvang spoelen voor het klein bekken; de uitwendige spoel (phased array) en de inwendige (endoluminale) spoel. De endoluminale type kent een opblaasbare en een rigide variant. In ons centrum gebruiken we de rigide variant naar tevredenheid. Deze wordt toegepast in de anus of in de vagina. Deze spoel heeft een technische verbetering ondergaan door het "dual loop" concept. De vorige generatie inwendige spoelen waren gebaseerd op het "single loop" concept. De nieuwe versie heeft een betere signal-ruis-verhouding dan de vorige generatie en kan aldus scherpere afbeeldingen maken zonder dat de duur van het onderzoek verlengd wordt. Dit betekent een winst voor de diagnostiek in ons vak.

MRI onderzoek van fistelgangen en pijn rond de anus

Bij fistelgangen blijkt MRI van grote waarde en laat meer afwijkingen zien dan de chirurg zou vermoeden op basis van het klinische onderzoek alleen. Dit is dan van groot belang voor de chirurgische behandeling. Anovaginale fistels zijn fistels tussen de anus en vagina die verlies van faeces via de vagina en steeds terugkerende ontstekingen van de vagina kan veroorzaken. In een analyse van 20 patienten liet MRI alle anovaginale fistels zien en additionele afwijkingen z.a. abcessen, fistelgangen op andere locaties en defecten van het sphincter complex (steunende spierweefsel) van de anus. De opening van fistelgangen in de anus werd aangetoond in alle gevallen en de opening in de vagina werd gezien in 19 gevallen. De helft van de patienten had een onderliggende aandoening of eerdere operatie in het bekkenbodem gebied ondergaan wat indirect geleid heeft tot deze fistels. In deze patienten werd vaker complexe anovaginale fistels met abcessen aangetroffen bij vergelijking met patienten die geen duidelijke onderliggende oorzaak voor de fistels hadden.

De behandeling van fistels is voornamelijk chirurgisch. Hiervoor zijn een aantal technieken beschikbaar. Een specifieke operatie techniek die veel toegepast wordt voor lange fistels die hoog in de anus communiceren is de "advancement flap closure". Deze techniek is gebaseerd op behoud van het continentie mechanisme na de operatie. We hebben 157 patienten geevalueerd die deze operatie techniek hebben ondergaan. Het blijkt dat de genezing van fistels die behandeld zijn met deze operatie minder gunstig is wanneer de fistels een rechtlijnige verloop hebben. Bovendien werden vaker abcessen bij de fistels gevonden wanneer deze aan de achterkant van de anus gelegen waren. Deze abcessen konden alleen met de MRI goed worden vastgesteld en indien goed gedraineerd, hadden deze geen verdere invloed op de operatie. Er was een hoge mate van overeenkomst tussen de MRI beelden en de bevindingen tijdens de operatie

Aanhoudende langdurige pijn de anus komt niet zelden voor. Wanneer het klinische onderzoek door de behandelende arts geen duidelijke oorzaak laat zien is afbeeldend onderzoek belangrijk. MRI liet bij 103 patienten die verwezen waren naar een gespecialiseerde centrum, in 27 % verborgen fistels en/of abcessen zien. Deze patienten hebben baat bij een operatieve behandeling van de fistels met afname van hun pijnklachten. Een tweede afwijking die redelijk vaak gezien wordt is verlittekening van de anus. MRI is aldus een belangrijke gereedschap in de diagnostiek bij deze patienten en dient overwogen te worden voordat de klacht als 'psychisch' wordt afgedaan.

MRI op maat bij de vrouw met afwijkingen van de plasbuis en omgeving

MRI kan een belangrijke rol spelen bij het onderzoek van vrouwen met chronische blaas- en plas klachten. In een groep van 60 vrouwelijke patienten die MRI ondergingen met dergelijke klachten, werd door de MRI in 20 patienten (33%) een uitstulping van de plasbuis (divertikel van de urethra) vastgesteld. In 28 patienten werd een andere diagnose uiteindelijk vastgesteld waarvan 13 gevallen (46 %) door de MRI werd ontdekt. De MRI werd in de meeste gevallen uitgevoerd met een MRI spoel in de vagina. Deze spoel ontvangt de MRI signalen van de plasbuis en directe omgeving en kan aldus hele scherpe afbeeldingen maken. Deze spoel is een rigide spoel die door de patient zelf wordt ingebracht in de vagina. Door de haarscherpe afbeeldingen komen belangrijke detailles van de afwijking goed in beeld. Bijvoorbeeld het vaststellen van de positie van de interne opening van het divertikel naar is plasbuis wordt in 85 % van de gevallen duidelijk. Dit is niet eerder met andere afbeeldingstechnieken gelukt. Dit kan van belang zijn bij de chirurgische behandeling.

MRI van het achterste compartiment in het kleine bekken.

Het recidief rectum (endeldarm) carcinoom.

Het recidief rectum carcinoom wordt in 5- 10 % gezien en veelal binnen 2 jaar na operatie van het eerste rectum carcinoom. Complete chirurgische verwijdering van het recidief biedt de beste kans op genezing. We hebben de MRI kenmerken van het local recidief rectum carcinoom (LRRC) onderzocht in 47 patienten met in totaal 51 tumoren en tevens gekeken naar bevindingen op MRI die belangrijk zijn voor de uitkomst van de chirurgische behandeling (compleet verwijderd of microscopische tumor rest achter latend). We hebben aangetoond dat het LRRC typische kenmerken heeft op MRI na toediening van MRI contrast middel (gadolinium). Deze zijn vroege en aanhoudende aankleuring (100%) met een ringvormige of heterogene mozaiek patroon (80%). Voor de uitkomst van de chirurgie is van belang dat de meeste tumoren die gefixeerd zijn aan de bekkenwand niet volledig verwijderd kunnen worden met achterlating van een microscopische tumor rest (64%). Niet- gefixeerde tumoren worden in de meeste gevallen compleet verwijderd (87 %).

Vochthoudende gezwellen van het achterste compartiment in het kleine bekken.

Vochthoudende gezwellen van het achterste compartiment in het kleine bekken (Retrorectal cystic lesions (RCL)) zijn zeldzaam in de volwassen leeftijd en met weinig literatuur hierover. Vaak is de grote vraag of een dergelijke gezwel gerekend moet worden tot de kwaadaardige of goedaardige gezwellen. We hebben een analyse gedaan van 28 patienten met in totaal 31 soortgelijke vochthoudende gezwellen. De afwijkingen werden in 5 subgroepen verdeeld met de "Tailgut cyst" als groep met de meeste gezwellen (16/31, 52 %). In 5 patienten betrof het kwaadaardige gezwel (18%) of (5/31, 16% van alle gezwellen). We vonden dat vast weefsel component in het gezwel (100%) een belangrijke aanwijzing is voor een kwaadaardige gezwel. Een andere bevinding die kan wijzen op een kwaadaardig gezwel is een verdikte wand welke in 40 % van de kwaadaardige gezwellen werd gevonden. Van belang is verder te weten dat de kwaardige gezwellen ook op relatieve jonge leeftijd kunnen voorkomen en dat de meeste afwijkingen geen specifieke klachten geven, maar vaak per toeval ontdekt worden bij onderzoek van de patient om andere redenen.

Toekomst perspectief

Verdere technische verbetering van de bestaande inwendige MRI spoelen is mogelijk. Denk aan extra (4) loops in plaats van de huidige dual (2) loops. Andere voorbeelden zijn het technisch koppelen van de inwendige spoel met de uitwendige spoel voor het scherp afbeelden van een ruimer gebied. Studies hebben laten zien dat dit veelbelovend en haalbaar is. We zijn van mening dat de technische verbeteringen stapsgewijs moet geschieden naar gelang de noodzaak voor betere afbeeldingen.

Nieuwe behandeltechnieken, z.a. gebruik van laser, voor fistels rond de anus zijn in ontwikkeling. MRI is hierbij van belang voor de planning en begeleiding van de procedure. De operatie vindt plaats in de MRI kamer in een speciale "open MRI" apparaat door de chirurg en radioloog. De eerste rapportages zijn veelbelovend en laten zien dat een d.g. opstelling haalbaar.

Nieuwe ontwikkelingen in beeldvormende technieken kunnen een belangrijke rol spelen in de diagnostiek en behandeling bij patiënten met klinisch onbegrepen en vaak invaliderende pijnen in het kleine bekken gebied.

chapter 8

List of Publications
PhD Portfolio
Acknowledgements
About the author

LIST OF PUBLICATIONS

West RL, Zimmerman DD, **Dwarkasing S**, Hussain SM, Hop WC, Schouten WR, Kuipers EJ, Felt-Bersma RJ. Prospective comparison of hydrogen peroxide-enhanced three-dimensional endoanal ultrasonography and endoanal magnetic resonance imaging of perianal fistulas. Dis Colon Rectum. 2003 Oct;46(10):1407-15.

Dwarkasing S, Hussain SM, Hop WC, Krestin GP. Anovaginal fistulas: evaluation with endoanal MR imaging. Radiology. 2004 Apr;231(1):123-8.

West RL, **Dwarkasing S**, Felt-Bersma RJ, Schouten WR, Hop WC, Hussain SM, Kuipers EJ. Hydrogen peroxide-enhanced three-dimensional endoanal ultrasonography and endoanal magnetic resonance imaging in evaluating perianal fistulas: agreement and patient preference.
Eur J Gastroenterol Hepatol. 2004 Nov;16(12):1319-24.

West RL, **Dwarkasing S**, Briel JW, Hansen BE, Hussain SM, Schouten WR, Kuipers EJ.
Can three-dimensional endoanal ultrasonography detect external anal sphincter atrophy? A comparison with endoanal magnetic resonance imaging.
Int J Colorectal Dis. 2005 Jul;20(4):328-33.

Hussain SM, De Becker J, Hop WC, **Dwarkasing S**, Wielopolski PA. Can a single-shot black-blood T2-weighted spin-echo echo-planar imaging sequence with sensitivity encoding replace the respiratory-triggered turbo spin-echo sequence for the liver? An optimization and feasibility study. J Magn Reson Imaging. 2005 Mar;21(3):219-29.

Dwarkasing S, Hussain SM, Krestin GP. Magnetic resonance imaging of perianal fistulas. Semin Ultrasound CT MR. 2005 Aug;26(4):247-58. Review.

Hussain SM, van den Bos IC, **Dwarkasing RS**, Kuiper JW, den Hollander J. Hepatocellular adenoma: findings at state-of-the-art magnetic resonance imaging, ultrasound, computed tomography and pathologic analysis. Eur Radiol. 2006 Sep;16(9):1873-86. Review.

van Veen RN, de Baat P, Heijboer MP, Kazemier G, Punt BJ, **Dwarkasing RS**, Bonjer HJ, van Eijck CH. Successful endoscopic treatment of chronic groin pain in athletes.
Surg Endosc. 2007 Feb;21(2):189-93.

van den Bos IC, Hussain SM, **Dwarkasing RS**, Hop WC, Zondervan PE, de Man RA, IJzermans JN, Walker CW, Krestin GP. MR imaging of hepatocellular carcinoma: relationship between lesion size and imaging findings, including signal intensity and dynamic enhancement patterns. J Magn Reson Imaging. 2007 Dec;26(6):1548-55.

van den Bos IC, Hussain SM, **Dwarkasing RS**, Stoop H, Zondervan PE, Krestin GP, de Man RA. Hepatoid adenocarcinoma of the gallbladder: a mimicker of hepatocellular carcinoma. Br J Radiol. 2007 Dec;80(960):e317-20.

Witjes CD, de Man RA, Eskens FA, **Dwarkasing RS**, Zondervan PE, Verhoef C, Ijzermans JN. Hepatocellular carcinoma: the significance of cirrhosis for treatment and prognosis- retrospective study. Ned Tijdschr Geneeskd. 2010;154:A1747

Dols LF, Verhoef C, Eskens FA, Schouten O, Nonner J, Hop WC, Méndez Romero A, de Man RA, van der Linden E, **Dwarkasing RS**, IJzermans JN. Improvement of 5 year survival rate after liver resection for colorectal metastases between 1984-2006. Ned Tijdschr Geneeskd. 2009 Mar 14;153(11):490-5.

Ferenschild FT, Vermaas M, Verhoef C, **Dwarkasing RS**, Eggermont AM, de Wilt JH. Abdominosacral resection for locally advanced and recurrent rectal cancer. Br J Surg. 2009 Nov;96(11):1341-7.

Tilanus AM, de Geus HR, Rijnders BJ, **Dwarkasing RS**, van der Hoven B, Bakker J. Severe group A streptococcal toxic shock syndrome presenting as primary peritonitis: a case report and brief review of the literature. Int J Infect Dis. 2010 Sep;14 Suppl 3:e208-12. Review.

Kekelidze M, **Dwarkasing RS**, Dijkshoorn ML, Sikorska K, Verhagen PC, Krestin GP. Kidney and urinary tract imaging: triple-bolus multidetector CT urography as a one-stop shop--protocol design, opacification, and image quality analysis. Radiology. 2010 May;255(2):508-16.

van Aalten SM, Terkivatan T, de Man RA, van der Windt DJ, Kok NF, **Dwarkasing R**, Ijzermans JN. Diagnosis and treatment of hepatocellular adenoma in the Netherlands: similarities and differences. Dig Surg. 2010;27(1):61-7.

van Aalten SM, Verheij J, Terkivatan T, **Dwarkasing RS**, de Man RA, Ijzermans JN. Validation of a liver adenoma classification system in a tertiary referral centre: implications for clinical practice. J Hepatol. 2011 Jul;55(1):120-5.

Liedenbaum MH, Bipat S, Bossuyt PM, **Dwarkasing RS**, de Haan MC, Jansen RJ, Kauffman D, van der Leij C, de Lijster MS, Lute CC, van der Paardt MP, Thomeer MG, Zijlstra IA, Stoker J. Evaluation of a standardized CT colonography training program for novice readers. Radiology. 2011 Feb;258(2):477-87.

Méndez Romero A, Verheij J, **Dwarkasing RS**, Seppenwoolde Y, Redekop WK, Zondervan PE, Nowak PJ, Ijzermans JN, Levendag PC, Heijmen BJ, Verhoef C. Comparison of macroscopic pathology measurements with magnetic resonance imaging and assessment of microscopic pathology extension for colorectal liver metastases. Int J Radiat Oncol Biol Phys. 2012 Jan 1;82(1):159-66.

Marsman HA, van der Pool AE, Verheij J, Padmos J, Ten Kate FJ, **Dwarkasing RS**, van Gulik TM, Ijzermans JN, Verhoef C. Hepatic steatosis assessment with CT or MRI in patients with colorectal liver metastases after neoadjuvant chemotherapy. J Surg Oncol. 2011 Jul 1;104(1):10-6.

Mitalas LE, **Dwarkasing RS**, Verhaaren R, Zimmerman DD, Schouten WR. Is the outcome of transanal advancement flap repair affected by the complexity of high transsphincteric fistulas? Dis Colon Rectum. 2011 Jul;54(7):857-62.

Dwarkasing RS, Dinkelaar W, Hop WC, Steensma AB, Dohle GR, Krestin GP. MRI evaluation of urethral diverticula and differential diagnosis in symptomatic women. AJR Am J Roentgenol. 2011 Sep;197(3):676-82.

van Aalten SM, Thomeer MG, Terkivatan T, **Dwarkasing RS**, Verheij J, de Man RA, Ijzermans JN. Hepatocellular adenomas: correlation of MR imaging findings with pathologic subtype classification. Radiology. 2011 Oct;261(1):172-81.

Bökkerink GM, de Graaf EJ, Punt CJ, Nagtegaal ID, Rütten H, Nuyttens JJ, van Meerten E, Doornebosch PG, Tanis PJ, Derksen EJ, **Dwarkasing RS**, Marijnen CA, Cats A, Tollenaar RA, de Hingh IH, Rutten HJ, van der Schelling GP, Ten Tije AJ, Leijtens JW, Lammering G, Beets GL, Aufenacker TJ, Pronk A, Manusama ER, Hoff C, Bremers AJ, Verhoef C, de Wilt JH.
The CARTS study: Chemoradiation therapy for rectal cancer in the distal rectum followed by organ-sparing transanal endoscopic microsurgery. BMC Surg. 2011 Dec 15;11:34.

Witjes CD, Ten Kate FJ, van Aalten SM, **Dwarkasing RS**, Willemssen FE, Verhoef C, de Man RA, Ijzermans JN. Hepatocellular adenoma as a risk factor for hepatocellular carcinoma in a non-cirrhotic liver: a plea against. Gut. 2012 Nov;61(11):1645-6.

Witjes CD, Verhoef C, Kwekkeboom DJ, **Dwarkasing RS**, de Man RA, Ijzermans JN.
Is bone scintigraphy indicated in surgical work-up for hepatocellular carcinoma patients?
J Surg Res. 2013 May;181(2):256-61.

Ayez N, Alberda WJ, Burger JW, Eggermont AM, Nuyttens JJ, **Dwarkasing RS**, Willemssen FE, Verhoef C. Is restaging with chest and abdominal CT scan after neoadjuvant chemoradiotherapy for locally advanced rectal cancer necessary? Ann Surg Oncol. 2013 Jan;20(1):155-60.

Hepatocellular adenomas and pregnancy.
Bröker ME, van Aalten SM, Ijzermans JN, **Dwarkasing RS**, Steegers EA, de Man RA.
Ned Tijdschr Geneeskd. 2012;156(38):A5102.

Alberda WJ, Dassen HP, **Dwarkasing RS**, Willemssen FE, van der Pool AE, de Wilt JH, Burger JW, Verhoef C. Prediction of tumor stage and lymph node involvement with dynamic contrast-enhanced MRI after chemoradiotherapy for locally advanced rectal cancer. Int J Colorectal Dis. 2013 Apr;28(4):573-80.

Witjes CD, Polak WG, Verhoef C, Eskens FA, **Dwarkasing RS**, Verheij J, de Man RA, Ijzermans JN. Increased alpha-fetoprotein serum level is predictive for survival and recurrence of hepatocellular carcinoma in non-cirrhotic livers. Dig Surg. 2012;29(6):522-8.

Dwarkasing RS, Schouten WR, Geeraedts TE, Mitalas LE, Hop WC, Krestin GP.
Chronic anal and perianal pain resolved with MRI. AJR Am J Roentgenol. 2013 May;200(5):1034-41.

Thomeer MG, Willemssen FE, Biermann KK, El Addouli H, de Man RA, Ijzermans JN, **Dwarkasing RS**. MRI features of inflammatory hepatocellular adenomas on hepatocyte phase imaging with liver-specific contrast agents. J Magn Reson Imaging. 2014 May;39(5):1259-64.

Dwarkasing RS, Verschuuren SI, Leenders GJ, Thomeer MG, Dohle GR, Krestin GP.
Chronic lower urinary tract symptoms in women: classification of abnormalities and value of dedicated MRI for diagnosis. AJR Am J Roentgenol. 2014 Jan;202(1):W59-66.

Thomeer MG, E Bröker ME, de Lussanet Q, Biermann K, **Dwarkasing RS**, de Man R, Ijzermans JN, de Vries M. Genotype-phenotype correlations in hepatocellular adenoma: an update of MRI findings. Diagn Interv Radiol. 2014 May-Jun;20(3):193-9.

Bax HI, van Ingen J, **Dwarkasing RS**, Verbon A. Lipotourism, not without risks: a complication of cosmetic surgery abroad. Ned Tijdschr Geneeskd. 2014;158:A7926.

Van der Deure WM, Lugtenburg EP, **Dwarkasing RS**, Biermann K, Tjwa ET. Malignancy presenting as multiple lesions in a cirrhotic liver: not always hepatocellular carcinoma. J Gastrointestin Liver Dis. 2015 Mar;24(1):7.

Verseveld M, de Graaf EJ, Verhoef C, van Meerten E, Punt CJ, de Hingh IH, Nagtegaal ID, Nuyttens JJ, Marijnen CA, de Wilt JH; CARTS Study Group (Tanis PJ, Bökkerink GM, Rütten H, Doornebosch PG, Derksen EJ, **Dwarkasing RS**, Cats A, Tollenaar RA, Rutten HJ, Leijtens JW, van der Schelling GP, Ten Tije AJ, Lammering G, Beets GL, Aufenacker TJ, Pronk A, Manusama ER, Hoff C, Bremers AJ.). Chemoradiation therapy for rectal cancer in the distal rectum followed by organ-sparing transanal endoscopic microsurgery (CARTS study). Br J Surg. 2015 Jun;102(7):853-60.

Ten Berge JC, Suker M, Bruno MJ, Poley JW, **Dwarkasing RS**, Biermann K, van Eijck CH. Are a Double Duct Sign or Endoscopic Biopsies Reliable Predictors of Malignancy in Periampullary Lesions? Dig Surg. 2015 Jul 2;32(4):306-311.

Deerenberg EB, Harlaar JJ, Steyerberg EW, Lont HE, van Doorn HC, Heisterkamp J, Wijnhoven BP, Schouten WR, Cense HA, Stockmann HB, Berends FJ, Dijkhuizen FP, **Dwarkasing RS**, Jairam AP, van Ramshorst GH, Kleinrensink GJ, Jeekel J, Lange JF. Small bites versus large bites for closure of abdominal midline incisions (STITCH): a double-blind, multicentre, randomised controlled trial. Lancet. 2015 Jul 15. pii: S0140-6736(15)60459-7.

Submitted

Dwarkasing RS, Flick H, Krestin GP. Endoluminal Receiver Coil for Endoanal and Intravaginal Application on 1.5 and 3.0 T MRI Systems; Technical Aspects, Design and Clinical Value

Dwarkasing RS, Verschuuren SI, Leenders GJLH, Braun LMM, Krestin GP, Schouten W.R. Primary Cystic Lesions of the Retrorectal Space: MRI evaluation, Histopathology Confirmation and Clinical Assessment.

PHD PORTFOLIO

Invited Lectures (thesis related topics)

ESMRMB 2002 (European Society for Magnetic Resonance in Medicine and Biology)
19th Annual Scientific Meeting
August 22 - 25, Cannes, France
Invited speaker Clinical Focus Session Gastrointestinal and Pelvis,
"MRI of perianal fistula disease"

ESMRMB 2003 (European Society for Magnetic Resonance in Medicine and Biology)
20th Annual Scientific Meeting
September 18 - 21, Rotterdam, The Netherlands Invited Speaker, Advanced MR Imaging of the Abdomen,
"MR Imaging of the Anorectal Diseases"

ESMRMB 2004 (European Society for Magnetic Resonance in Medicine and Biology)
21st Annual Scientific Meeting
September 9 - 12, Copenhagen, Denmark
Invited Speaker, Teaching Session, "MR imaging of the anorectum"
Moderator "MRI and MRS of abdomen and pelvis"

ESGAR 2005 (European Society for GastroIntestinal and Abdominal Radiology)
16-th annual scientific meeting
May 28-31, Florence, Italy
Invited Speaker, Teaching Session and workshop
"MRI of the anorectum, fistula disease and pelvic sepsis"

ESMRMB 2006 (European Society for Magnetic Resonance in Medicine and Biology)
23-rd annual scientific meeting
September 21-23, Warsaw, Poland
Invited Speaker, School of MRI, Teaching Session, "MRI of the anorectum".

Externe Refereeravond 2011, afdeling Urologie, Erasmus MC
March 7, Rotterdam.
Invited Speaker, "State of the art MRI bij diagnostiek van uretrale en peri-uretrale pathologie in symptomatische vrouwelijke patiënten"

ISMRM 2013 (The International Society for Magnetic Resonance in Medicine)
21-st Annual Meeting & Exhibition
April 20-26, Salt lake City, UT/USA
Invited Speaker, Body MRI educational program
"MR Imaging of Anal Pain and Perianal Fistula Disease"

Externe Refereeravond 2015, afdeling Radiologie, Erasmus MC
April 23, 2015, Rotterdam
"Dedicated MRI of the Lower Pelvis: Do We Need an Endoluminal Coil ?"

Selected (Inter)national Conferences, Seminars, Workshops, including scientific and teaching presentations

Radiological Society of North America (RSNA), Chicago, USA
Annual Scientific Meeting: 2001, 2002, 2003, 2004, 2007, 2008, 2009, 2011, 2012, 2013, 2014
2009, scientific podium presentation.
R.S. Dwarkasing, W. Dinkelaar, W. Hop, G. Dohle, GP. Krestin.
MRI evaluation of urethral diverticula and differential diagnosis in female patients with chronic lower urinary tract symptoms.

2011, scientific poster presentation.
R.S. Dwarkasing, T. Geeraerdts, W. Hop, R. Schouten, GP Krestin.
MRI Evaluation of Patients with Anal and Perianal Pain Referred to a Tertiary Colorectal Surgical Department.

2011, teaching exhibit poster presentation.
R.S. Dwarkasing, S. Verschuuren, G.R. Dohle, G.P. Krestin.
MR Imaging and Urodynamic Findings in Female Patients with Chronic Lower Urinary Tract Symptoms (LUTS).

2012, scientific podium presentation.
R. Elias, K. Biermann, G. P. Krestin, R.S. Dwarkasing.
Can Inflammatory Myofibroblastic Tumor of the Hepatobiliary System be Differentiated from Cholangiocarcinoma on Imaging?

2012, scientific poster presentation.
R. Dikkers, R. Devos, G. P. Krestin, R.S. Dwarkasing.
Pediatric Primary Liver Tumors: Imaging Appearances and Pathologic Correlation.

2012, teaching exhibit poster presentation.
R. Elias, F. Willemssen, K. Biermann, G.P. Krestin, R.S. Dwarkasing.
Inflammatory Myofibroblastic Tumor of the Hepatobiliary System: Imaging Characteristics with Histopathology Correlation and Differential Diagnosis.

2012, teaching exhibit poster presentation.
S. Verschuuren, R.S. Dwarkasing, G. van Leenders, R.W. Schouten, G.P. Krestin.
MRI of Primary Cystic Lesions of the Retrorectal Space.

2013, teaching exhibit poster presentation.
R.S. Dwarkasing, H. Flick, G. Kotek, G.P. Krestin.
Endoluminal Receiver Coil for Endoanal and Intravaginal Application on 1.5 and 3.0 T MRI Systems. Design, technical Aspects and Clinical Application. Proposal for a New Rigid Endorectal Coil Design For Dedicated Prostate Imaging.

2015, scientific podium presentation.
K. Ramsaransing, R.S. Dwarkasing, F. Willemssen, M. de Vries.
Is Contrast-Enhanced Ultrasound Comparable to MRI with Liver-Specific Contrast Agent for Diagnosis of Focal Nodular Hyperplasia and Hepatocellular Adenoma?

2015, scientific poster presentation.
R.S. Dwarkasing, R. van Waardhuizen, W.J. Alberda, M. Doukas, M. de Vries, C. Verhoef, F. Willemssen.
Value of MRI for Diagnosis and Local Staging of Recurrent Rectal Cancer: Correlation with Surgery and Histopathology of Resected Specimen.

2015, teaching exhibit poster presentation.
M.L. Dijkshoorn, F. Willemssen, D. van der Velden, M. van Straten, R.S. Dwarkasing.
State-of-the-art CT Imaging Techniques of the Abdomen with 3rd Generation Dual Source CT.

2015, teaching exhibit poster presentation.
R.S. Dwarkasing, R.N. Boxhoorn, G.P. Krestin, C.H. van Eijck.
Dedicated Imaging of Inguino-femoral and Lower Abdominal Wall Hernias.

2015, teaching exhibit poster presentation.
V. Lai Nguyen, M. Rossius, P. Wielopolsky, G. Dohle, G.P. Krestin, R.S. Dwarkasing.
Magnetic Resonance Imaging of Penile Diseases.

European Society for Magnetic Resonance in Medicine and Biology (ESMRMB)
Annual Scientific Meeting
2002, August 22-25, Cannes, France.
2003, September 18 - 21, Rotterdam, The Netherlands.
2004, September 9 - 12, Copenhagen, Denmark.
2006, September 21-23, Warsaw, Poland.

European Society of Gastrointestinal and Abdominal radiology (ESGAR)
Annual Scientific Meeting
2005, May 28-31, Florence, Italy
2012, June 12–15, Edinburgh, UK.
2014, June 18 – 21, Salzburg, Austria.
2015, June 9-12, Paris, France.

European Society of Radiology (ECR)
Annual Scientific Meeting.
2010, March 4-8, Vienna, Austria

2010, scientific poster presentation.
F. Willemssen, R.S. Dwarkasing.
Imaging Features of Hepatobiliary Cystadenoma.

2015, scientific podium presentation.
R.S. Dwarkasing, S. Verschuuren, G. van Leenders, L.M.M. Braun, W.R. Schouten, G.P. Krestin.
Primary Cystic Lesions of the Retrorectal Space: MRI evaluation, Histopathology Confirmation and Clinical Assessment

2015, scientific podium presentation.
M.G. Thomeer, F. Willemssen, K. Biermann, R. de Man, J. IJzermans, R.S. Dwarkasing.
MRI features of inflammatory hepatocellular adenomas on hepatocyte phase imaging with liver-specific contrast agents.

2015, educational poster presentation.
F. Willemssen, R.S. Dwarkasing.
Practical Guide to Differentiate Cystic Lesions of the Liver

International Diagnostic Course in Davos (IDKD).
Abdominal and Pelvic Imaging.
2006, April 1-7, Switzerland.

ESOR, European School of Radiology, Brussles, Belgium
Advanced Untrasound and Contrast Enhanced Ultrasound
2011, May 12-13.

The International Society for Magnetic Resonance in Medicine (ISMRM)
Annual Scientific Meeting
2013, April 20-26, Salt Lake City, USA

Radiologen Dagen, The Netherlands
2007, 2008, 2009, 2012, 2013
2007, scientific podium presentation.
M. Kekelidze, R. Dwarkasing, M. Dijkshoorn, P. Verhagen, G.P. Krestin.
Optimizing MDCT of Kidneys and Urinary Tract with Triple - bolus Contrast Injection Technique.

2009, scientific podium presentation.
R.S. Dwarkasing, S.I. Verschuuren, W. Dinkelaar, W. Hop, G. Dohle, G.P. Krestin.
MRI evaluation of Urethral Diverticula and differential Diagnosis in Female Patients with Chronic Lower Urinary Tract Symptoms.

2010, scientific podium presentation.
T.E.A. Geeraedts, R.S. Dwarkasing, W. Hop, R. Schouten, G.P. Krestin.
MRI Evaluation of Patients with anal and perianal pain referred to a tertiary colorectal surgical department

2012, scientific podium presentation.
R. Elias, K. Biermann, G.P. Krestin, R.S. Dwarkasing. Can Inflammatory Myofibroblastic Tumor of the Hepatobiliary System Be Differentiated from Cholangiocarcinoma on Imaging?

2012, educational podium presentation.
R. Dikkers, A. Devos, G.P. Krestin, R.S. Dwarkasing. Pediatric Primary Liver Tumors: Imaging Appearances and Pathologic Correlation.

2012, educational podium presentation.
S.I. Verschuuren, R. S. Dwarkasing, G. J.L.H. van Leenders, G. R. Dohle, G. P. Krestin.
MR Imaging and Urodynamic Findings in Female Patients with Chronic Lower Urinary Tract Symptoms (LUTS).

2012, educational podium presentation
S.I. Verschuuren, R. S. Dwarkasing, G. J.L.H. van Leenders, W. R. Schouten, G.P. Krestin.
MRI of Primary Cystic Lesions of the Retrorectal Space

2013, scientific podium presentation
I.J.S.M.L Vanhooymissen, R. Atzei, R.S. Dwarkasing, F.E.J.A. Willemssen.
Validity of One Stop Triple-Bolus Multidetector CT Urography in Detecting renal and urothelial malignancy

2013, educational podium presentation
M. de Vries, M.G.J. Thomeer, R.S. Dwarkasing.
Adenomen in de Lever: Alles wat een Radioloog moet weten.

2014, scientific podium presentation; Winner Travel Grant Award
R.M. van Waardhuizen, R.S. Dwarkasing, W.J. Alberda, M. Doekas, M.A.J. de Ridder, J.J.M.E. Nuyttens, C. Verhoef, F.E.J.A. Willemssen.
Value of Dynamic Contrast Enhanced MRI and Fusion with T2-weighted Imaging for Local Staging of Recurrent Rectal Cancer: Correlation with Surgery and Histopathology of Resected Specimen.

2015, educational podium presentation
V. Lai Nguyen, M. Rossius, P. Wielopolsky, G. Dohle, G.P. Krestin, R.S. Dwarkasing.
Dedicated Magnetic Resonance Imaging of Penile Disorders.

2015, educational podium presentation
R.N. Boxhoorn, R.S. Dwarkasing, C. van Eijck, G.P. Krestin.
Dedicated Imaging of Inguino-femoral and lower abdominal wall hernias.

2015, scientific podium presentation.
L.M.M. Braun R.S. Dwarkasing, S. Verschuuren, G. van Leenders, W. Schouten, G. Krestin.
Primary Cystic Lesions of the Retrorectal Space: MRI evaluation, Histopathology Confirmation and Clinical Assessment.

Others

2006, Recht in de Medische Praktijk, 29 mei, Pfizer partners in Practice.

2007, Teach the Teacher, Erasmus MC, Rotterdam.

2008, Invited Lecture, Cursus Klinische Hepatologie 29-30 mei 2008, Nederlandse Vereniging voor Hepatologie. "Beeldvorming van focale leverhaarden, MRI en CT".

2008, October 9, Moderator, Scientific Session, Abdominal Oncology Imaging, Radiologen Dagen, Rotterdam, The Netherlands.

2010, October 12-15, Moderator, NVvR Sandwichcursus Abdomen, Ede.

2010, April 26, Training: Implementatie Modernisering Medische Vervolgopleidingen voor Medische Specialisten en Arts Assistenten in Opleiding tot Medisch Specialist. Desiderius School, Erasmus MC, OORZWN.

2011, Persoonlijk Leiderschapsprogramma. Sector Organisatie Advies en – Ontwikkeling, EMC, Rotterdam.

2011, Organisor, Landelijke Sectiedag Abdomen, NVvR, April 27, de Euromast, Rotterdam.

2014, February 6, Roadshow Wetenschappelijke Integriteit, Erasmus MC, Rotterdam.

2014, March 25, Workshop Postdoc Network Erasmus MC Meeting: Presenting yourself and your work.

2016, June 8,9. Course leader, SWC Abdomen, NVvR.

2017, February 7-10. Course leader, Teaching In Holland, AIRP, SWC Abdomen, NVvR.

Teaching

Supervisor Master Research, Medical Faculty, Erasmus MC

Completion of the following projects

2011, E.C. Boer, C.P Raaijmakers. CT imaging of Complications Related to Major Abdominal Surgery.

2011, F. Dahbi, J. Makhkash. Contrast Enhanced MRI in the surveillance, therapy and monitoring of Therapeutic Effects in Patients with Recurrent Rectal Carcinoma.

2012, N. Haverkamp. The value of CT in the Detection or Confirmation of Acute Pyelonephritis.

2013, H. Fares. Clinical aspects and Imaging of Primary Malignant Liver Tumors in Children.

2013, R.M. van Waardhuizen. The value of T2-weighted, Dynamic Contrast Enhanced (DCE) MRI and Fusion Imaging for Pre-operative Assessment of Local Recurrent Rectal Carcinoma, Correlation with Histopathology Analysis of Resected Specimen.

2014, K. Ramsaransing. Is Contrast- Enhanced Ultrasound Equivalent to MRI with Liver-specific Contrast Agent for the Diagnosis of Hepatocellular Adenoma and Focal Nodular Hyperplasia?

Work in progress

C. Spanjer. Imaging and Clinical Aspects of Uncommon Primary Liver Lesions, Analysis of Cases Referred to a Tertiary Referral Center for Hepatobiliary Diseases.

S. Tajjiou. Atypical and Suspect- Symptomatic Liver Hemangiomas: Cross-sectional Imaging with Pathology Confirmation and Surgical Outcome.

Reviewer radiology journals

Reviewer for European Radiology, 2009 – current.
Referee for papers on "Hepatobiliary Imaging" and "Pelvic Imaging"

ACKNOWLEDGEMENTS

This thesis is the result of a long learning process during which I was supported by several people. Contributing authors (in alphabetical order):

Wijnand J. Alberda, MD
Loes M.M. Braun, MD, PhD
Wouter Dinkelaar, MD
Gerardus R. Dohle, MD, PhD
Michael Doukas, MD, PhD
Herman Flick, BSEE
Tychon E. A. Geeraedts, MD
Wim C. J. Hop, PhD
Shahid M. Hussain, MD, PhD
Gabriel P. Krestin, MD, PhD
Geert J. L. H. Leenders, MD, PhD
Litza E. Mitalas, MD, PhD
Joost J. Nuyttens, MD, PhD
Maria de Ridder, PhD
W. Rudolf Schouten, MD, PhD
Anneke B. Steensma, MD, PhD
Maarten G. J. Thomeer, MD
Cornelis Verhoef, MD, PhD
Sylvia I. Verschuuren, MD
Ruben M. van Waardhuizen, MD
François E. J. A. Willemssen, MD

Thank you all for your significant contribution to the chapters of this thesis.

I wish to express my most sincere gratitude to:
Shahid M. Hussain, MD, PhD, current Prof. in Abdominal Imaging, Department of Radiology, University of Nebraska Medical Center, USA. Dear Shahid, you were very important at the beginning of my thesis. You awakened my interest in research and taught me the basics of imaging based clinical research.

Prof. Gabriel P. Krestin, my supervisor and promotor. Dear Gabriel, thanks for your support, advice and guidance throughout this project. I admire your efforts of transforming our department into an internationally acclaimed top level imaging center.

Other Supporting People:
Research Bureau, Department of Radiology, Erasmus MC.
Especially Laurens Groenendijk (Trial Bureau), Ton Everaers (graphic designer), Jolanda Meijer, Msc BA (unit manager Research & Education) and Linda Everse, PhD (Research Coordinator). Many, many thanks for your assistance in all the logistics concerning my research. You certainly made it all possible.

Secretary Office Radiology Department, Erasmus MC.
All the ladies at the Secretary Office of our department. Esther, Marjolein, Brenda, Dianne, Roos, Annelise, Desiree, Haydee and Astrid. You were always willing to assist in any way pos-

sible. Astrid, you made life easier for me in helping out with administrative- and planning duties.

My colleagues of section abdominal imaging, Erasmus MC.
François Willemssen, Marianne de Vries, Maarten Thomeer, Ivo Schoots, Nanda Krak.
Thanks for your support. There is a lot of work, both in clinic and research, to be done!

I would like to thank my mom, brothers, sisters and friends who encouraged me along the way.

Hilmar, my "lonely planet", thanks.

And to all the persons who have contributed to this thesis and have not been mentioned, THANK YOU SO VERY MUCH!

ABOUT THE AUTHOR

Roy Dwarkasing grew up in Paramaribo, Suriname. After obtaining his medical degree at the Academic Hospital Paramaribo, University of Suriname, in 1994, he worked subsequently as a general practitioner, fellow in internal medicine, emergency room doctor and fellow at the radiology department of the Diaconessen Hospital Paramaribo. His supervising radiologist Dr. R. Hofwijk recognized his motivation and talent for imaging and proposed his further training as a radiologist at the Dijkzigt Hospital in Rotterdam, where he started his training in 1997 under the supervision of Prof. J. S. Laméris. Roy finished his training as a radiologist in 2002 under the supervision of Prof. G.P. Krestin. From 2002 to 2004 he completed a fellowship in pediatric radiology and abdominal radiology in Rotterdam. In 2003 he became staff radiologist with special focus on Abdominal and Pelvic imaging. From 2008 to 2013 he was chief of the section Abdominal Imaging and is currently chief radiologist in the institutional multidisciplinary boards for Hepatobiliary Diseases, Colorectal Cancer, and Diseases of the Pelvis and Pelvic Floor. He is director of abdominal imaging fellowship program at the Erasmus MC in Rotterdam. After his first publication in 2004, he slowly but steadily worked on his thesis, beside his busy work in the clinic. He is regarded as an esteemed senior radiologist in Abdominal and Pelvic Imaging.

In his personal life, he lives happily together with Hilmar and their sons Martijn en Pascal.

ISBN: